MODULATION OF T CELL RESPONSE IN TUBERCULOSIS GRANULOMAS

by

Eileen A. Wong

B.S., University of California, Berkeley, 2008

M.S., University of Washington, 2010

Submitted to the Graduate Faculty of

School of Medicine in partial fulfillment

of the requirements for the degree of

Doctor of Philosophy

University of Pittsburgh

2018

UNIVERSITY OF PITTSBURGH

SCHOOL OF MEDICINE

This dissertation was presented

by

Eileen A. Wong

It was defended on

May 15, 2018

and approved by

Jennifer Bomberger, PhD, Microbiology and Molecular Genetics

Robert L. Hendricks, PhD, Microbiology and Molecular Genetics

Dario A. Vignali, PhD, Immunology

John V. Williams, MD, Pediatrics

Dissertation Advisor: JoAnne L. Flynn, PhD, Microbiology and Molecular Genetics

MODULATION OF T CELL RESPONSE IN TUBERCULOSIS GRANULOMAS

Eileen A. Wong, M.S.

University of Pittsburgh, 2018

Tuberculosis (TB) remains a major threat to global health. When an individual is infected with *M. tuberculosis* (Mtb), the causative agent of TB, host immune cells form highly organized structures, granulomas, around the bacteria. Granulomas contain Mtb and prevent dissemination, but can also serve as a niche for persistence. While host control of Mtb infection involves an interplay of innate and adaptive immune cells in the granulomas, T cells have been demonstrated to be a critical component. The goal of this dissertation was to define facets of the host immune system that modulate the T cell cytokine response in TB granulomas and ways to alter the T cell cytokine responses to improve protection through vaccination, by using a non-human primate (NHP) model that recapitulates human TB disease and granuloma formation. In the first aim, the role of IL-10 in downregulating T cell responses in granulomas was investigated by neutralization of IL-10 in Mtb-infected NHPs. Although lack of IL-10 had a transiently increased the immune response early in Mtb infection (4 weeks), the presence or absence of IL-10 did not affect the overall inflammation, bacterial burden, or disease pathology up to 8 weeks post-infection. The second aim examined T cell exhaustion in TB granulomas by characterizing expression of the inhibitory receptors PD-1, CTLA-4, and LAG-3 on T cells. Low levels of expression of the inhibitory receptors suggested few exhausted T cells in granulomas. Moreover, T cells expressing inhibitory receptors were still functional and capable of proliferation, indicating that these inhibitory receptors may not be a marker of exhaustion in TB. Finally, the third aim investigated vaccination strategies to alter granuloma T cell response and confer

protection from TB disease. While none of the experimental vaccination strategies were more protective than the current vaccine BCG, some of the strategies increased T cell cytokine response in granulomas. In summary, the factors investigated in this dissertation were not significant contributors to the modulation of T cell responses or Mtb control in TB granulomas, but these results further inform the field of the immune response to Mtb for potential future vaccines and therapeutics.

TABLE OF CONTENTS

LIST OF TABLES

LIST OF FIGURES

PREFACE

I would like to thank my parents, Boon and Carrie Wong for their endless support throughout this process. Their encouragement pushed me to pursue my goals. I would also like to thank my sister, Wendy Wong, for being my editor and general advisor over the years. To James, thank you for being there to support me and bounce ideas around.

This work could not have been possible without my incredible mentor, JoAnne Flynn, who has always provided me with honest guidance and wise advice. Thank you for always pushing me to improve and for teaching me to become a critical thinker, a better presenter, and a responsible scientist.

I would also like to thank my project collaborators at University of Massachusetts Medical School (Keith Reimann and Carolyn Kraus), University of Michigan (Denise Kirschner and Louis Joslyn), and Statens Serum Institut (Peter Andersen, Thomas Lindenstrom, Rasmus Mortensen, and Else Marie Agger) for providing critical reagents and insightful scientific advice. The members of the Flynn lab and the rest of our TB lab consortium at University of Pittsburgh were vital to the completion of this dissertation. Thank you to the vet techs and lab techs who were indispensable for these projects, to Hannah Gideon, Josh Mattila, Ling Lin, Chuck Scanga, and Pauline Maiello for their expertise and advice, and to the rest of my graduate student and post-doctoral associate lab mates for always being there to lend a hand and make lab more

enjoyable. A special shout-out to Nicole Grant and Amy Fraser, who were tremendously helpful for the last stages of these projects, especially on T cell exhaustion and experimental vaccines.

1.0 INTRODUCTION

1.1 TUBERCULOSIS: A MAJOR GLOBAL HEALTH PROBLEM

Tuberculosis, or TB, is one of the leading causes of death worldwide. In 2016 alone, 1.7 million people died from TB. While TB is found all over the world, it currently disproportionately affects low- to middle-income countries. The World Health Organization estimates that 87% of the new cases of TB arise within just 30 countries, and more than 95% of TB-related deaths occur in developing countries [1]. While the United States does not bear the majority of TB cases or death with a total of 9,272 cases reported to the Centers for Disease Control in 2016, complete elimination of TB in the U.S. or the world with current prevention and treatment strategies is not feasible within the foreseeable future [2]. Clinically, TB presents as primary active disease about 4-14% of the time, characterized by coughing, chest pains, weight loss, weakness and night sweats. The remaining infected majority are considered to be "latently infected," and contain their infection, are asymptomatic and non-infectious [1, 3, 4]. About 5-10% of those latently infected individuals reactivate at some point in their lifetime, and the risk is higher (~50%) in those who are immunosuppressed [5-7].

Despite the continuous obstacles presented by TB, the incidence of TB has fallen significantly over its long history, with an estimated decrease of 2% every year [1]. A global effort has emerged to eliminate TB, through the Stop TB Partnership established in 2000 and the

WHO End TB Strategy, adapted by the World Health Assembly in 2014. However, TB remains a major global health problem in spite of these renewed and continued efforts.

There are many reasons for the difficulty in eliminating TB and reducing the morbidity and mortality. The addition of another major global health problem, HIV, greatly increases the mortality of TB. TB is the major cause of death in HIV+ individuals, accounting for ~40% of HIV deaths. 1.4 million new cases of TB were reported in HIV-positive populations in 2016 [1]. Furthermore, the emergence of drug resistant strains of *Mycobacterium tuberculosis* (Mtb), the causative agent of TB, has further complicated the problem of TB. Although drug-susceptible cases of TB can usually be treated with a 6-month multi-drug regimen consisting of isoniazid, rifampicin, pyrazinamide, and ethambutol, resistance to these drugs have emerged. Resistance to at least isoniazid and rifampicin (multidrug-resistant TB, MDR-TB) has been reported in nearly all countries, but mostly occurs within China, India, and the Russian Federation. MDR-TB that is also resistant to second-line TB drugs (extensively drug-resistant TB disease, XDR-TB) has also emerged, accounting for 6.2% of MDR-TB cases in 2016 [1]. Further compounding the burdens of TB, there is currently no fully protective TB vaccine. The only currently approved vaccine for TB, BCG (Bacille-Calmette Guérin), has efficacy as variable as 0-80%, with geographic and strain differences affecting efficacy [8].

The difficulty in preventing or treating TB has been suggested to be a result of the long history of TB evolving along with humankind, the particular characteristics of the bacterium that causes TB, and the difficulties in elucidating immunological correlates of protection. These aspects of TB will be further expanded upon below.

1.1.1 A brief summary of the long history of TB

TB has affected and evolved with mankind for millennia [9, 10]. Genomic evidence of TB in humans has been suggested to have started as early as 70,000 years ago, originating in Africa and expanding along with human migration patterns [11]. Global evidence of TB-related disease has been found in human cultures as varied and old as Egyptian mummies (2400BC), the writings of Ancient Greeks (~174AD), descriptions of TB in India and China, and pre-Columbian Peruvian mummies (~1000 AD) [9, 12]. TB remained a common affliction through the Middle Ages in Europe and well into the 19th century, causing devastating numbers of deaths across the continent, particularly among the younger population [9].

Throughout history, TB has had numerous names, including phthisis, "the king's touch," and consumption, until Johann Lukas Schönlein first coined the current term "tuberculosis" in the mid-19th century [9]. During this time, physicians puzzled over many aspects of the disease, including the causes of the disease, with hereditary, moral, or spontaneous causes as the most common theories [10]. Additionally, the many pulmonary and extrapulmonary manifestations of TB caused confusion over whether TB was a single disease with multiple clinical symptoms or multiple diseases. René Théophile Hyacinthe Laennec was the first to unify the many different forms of TB under a single disease, describing the physical signs of pulmonary TB and establishing the modern concepts of TB in his book, *D'Auscultation Mediate* in 1819 [13]. Although some conjectured that TB was caused by a particle of contagious nature early on, exemplified by Italy passing a law of quarantining anyone with symptoms of TB starting in 1700s, the contagious nature of TB was not established until Jean-Antoine Villemin. In 1865, Villemin demonstrated the transmissibility of TB by inoculating a rabbit with an extract from a lesion from an infected patient [13].

In the 1880s, Robert Koch isolated the causative agent of TB, a rod-shaped bacterium that was very difficult to stain. He was able to cultivate the bacterium in animal serum and on solid culture media, and show that it indeed could reproduce the disease in guinea pigs when they were inoculated with his bacterial culture. By observing that these bacteria were in TB lesions only and not associated with other diseases; that these bacteria could be cultured *in vitro* outside of animal or man; and that these *in vitro* bacteria could be grown and then reinfect an uninfected animal and cause the same TB lesions, Robert Koch definitively showed *Mycobacterium tuberculosis* (Mtb) as the infectious cause of TB. The results were reported in his seminal paper to the Berlin Society of Physiology in 1882 [10]. With Koch's work and conclusions, the idea that diseases could be caused by microscopic infectious agents was established, including the concept of Koch's postulates. The era of research into ways to combat Mtb had begun.

1.1.2 Transmission and detection of Mtb

Mtb is primarily transmitted by inhalation of aerosolized droplets containing the bacteria produced by people with active TB disease coughing, sneezing, or spitting [14]. The airborne transmission of Mtb was confirmed in a series of experiments exposing susceptible guinea pigs to air from TB wards, which led to Mtb infection in the guinea pigs [15-17]. Fennelly et al. observed 25% of their patients with pulmonary TB generated culture-positive cough aerosols, with most of the particle sizes within the respirable range [18]. Thus, there is a high chance of exposure to Mtb, particularly within enclosed spaces. A systematic review of all TB contact studies found 3.1% of exposed contacts had active TB, while 51.5% had latent infections [19]. In general, children tend to be at the most risk of Mtb infection from their contacts [20]. A meta-

analysis of household contact studies concluded that children exposed to TB in their households were more likely to be infected than their community counterparts, and this was higher in children under 4 years of age compared to children 10-14 years [21]. However, the locations with the greatest risk of Mtb exposure may be age-dependent. For young adults, the majority of the transmission likely occur outside of the household, with 50% occurring in schools, and for people across all ages public transportation poses a significant risk for Mtb transmission [22, 23]. Andrews et al. estimated the annual risk of Mtb infection among daily commuters in South Africa to be 3.5-5% [24]. The risk of TB disease tends to be the greatest within the first year of Mtb exposure, but remains high for the next five years after exposure [19].

Classically, the disease outcomes of Mtb infection were separated into two major outcomes, active disease or latent infection, but increasingly a spectrum of TB disease has been recognized (Figure 1). Exposure to Mtb does not always lead to infection, as Mtb is less successful at establishing infection compared to other infectious microorganisms, but leads to much longer durations of infections. The infection could be quickly cleared by the innate or adaptive immune system, or could lead to latent infection, classified by positive tuberculin skin test (TST) but no clinical symptoms [25]. There is evidence in humans and animal models that within the clinical classification of latent TB, there is substantial heterogeneity, possibly influencing the risk of reactivation [26, 27]. At the other end of the spectrum, active TB presents with clinical symptoms, and in the absence of treatment, can lead to fatality in about 70% of active TB patients in approximately 3 years [28]. Between latent infection and active TB disease are the subclinical TB disease patients who may exhibit some symptoms of TB, but do not have overt illness [29]. Only those with subclinical or active TB disease are infectious, although because subclinical patients likely have lower bacterial burdens, they have lower risks of

transmission [25, 29]. Previous infections may also impart some protection against Mtb reinfection [4, 30].

Mtb infection is primarily confirmed by tuberculin skin tests (TST), which consists of an intradermal injection of a purified protein derivative (PPD) of mycobacteria. Mtb-infected individuals with a cell-mediated immune response to Mtb can then be identified by a delayed-type hypersensitivity reaction that occurs between 48 and 72 hours after test placement. However, BCG vaccination or NTM exposure can confound the results. An alternative to TSTs are blood tests, such as the Interferon Gamma Release Assay (IGRA), which measures the cellular immune response in blood to antigens from the RD-1 region of Mtb, which is not present in BCG or most NTMs. Both TSTs and IGRAs have reduced sensitivity in immunocompromised patients and have low predictive value for whether a patient may be latently infected or their likelihood to develop active TB [14, 25].

Active TB disease is defined by clinical symptoms and confirmed by microbiological assays. Initial screening for active TB can consist of chest X-rays or CT imaging. Since abnormalities on chest x-rays are non-specific, microbiological assays are still needed to confirm. Sputum smear microscopy is one of the most common methods to confirm the disease state of an individual, although cultures of samples are the gold standard. However, sputum smears are not always accurate as patients do not always have Mtb present in their sputum, or in sufficient quantities, and culturing of samples takes weeks before a result. Countries are increasingly using molecular based assays, such as Xpert MTB/RIF, to more accurately diagnose patients [14, 25]. By nucleic acid amplification of sputum samples, Xpert MTB/RIF is not only more accurate and rapid than sputum smear microscopy, it also detects the HIV-positive individuals that are typically missed by sputum assays and quickly identifies drug-resistant Mtb

strains. However, it is more expensive and requires more technical expertise [31, 32]. More research has also been devoted to finding biomarkers that distinguish between the different clinical outcomes of Mtb infection, especially to predict those with latent or subclinical infections that may progress to active disease [33, 34]. These improved detection methods may help identify high-risk patients for treatment and prevent further transmission.

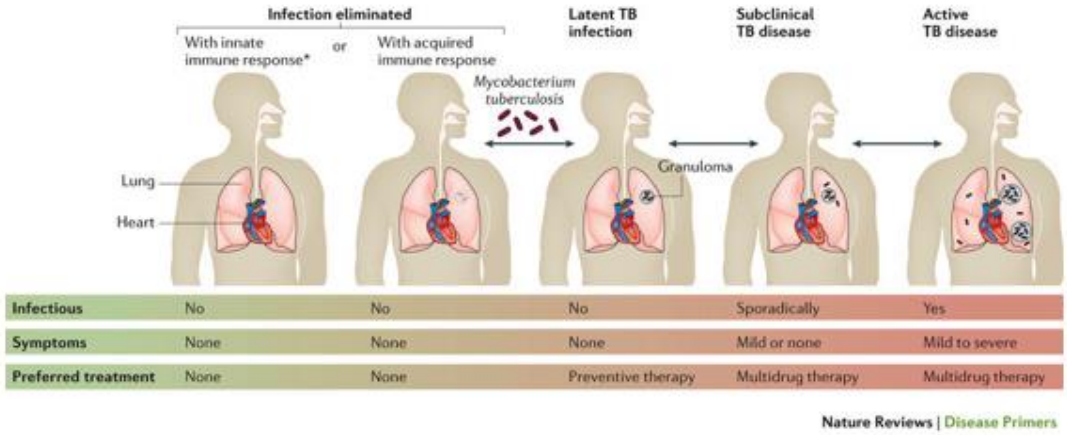

Figure 1. Spectrum of outcomes during Mtb infections.

Exposure to Mtb can lead to many different outcomes, from complete elimination of the infection by the innate and/or adaptive immune response to fully active TB disease with clinical symptoms. Adapted by permission from Springer Nature: Springer Nature, Nature Reviews Disease Primers, Tuberculosis, Pai et al., 2016 [25].

1.2 M. TUBERCULOSIS: THE CAUSATIVE AGENT OF TB

Mtb is an aerobic, facultative intracellular, non-motile and non-spore forming bacillus that grows best in high oxygen environments, such as the lungs. The unique lipid-rich cell wall composed of mycolic acids makes Mtb less permeable relative to other bacteria, which makes drug treatment more challenging. Mtb is not considered to be Gram-positive or Gram-negative, but is categorized as acid-fast because of its impermeability to basic dyes. Mtb also replicates slowly, dividing only every ~24 hours, making drug treatments longer in duration [35]. Mtb is a human obligate pathogen with no known environmental reservoirs [11].

Mtb is one species within the larger Mtb complex of mycobacteria, which includes *M. africanum*, *M. bovis*, *M. microti*, and *M. canetti*. All species of the Mtb complex can cause human disease [35]. Genomic studies have shown that Mtb and *M. bovis* (the progenitor of BCG vaccine) evolved into separate lineages, and that the deletion of one sequence TbD1 in modern Mtb strains suggests a major bottleneck occurred approximately 15,000-20,000 years ago before spreading around the world [36]. Mtb has been distinguished by genomic data into six main geographical lineages that are closely associated with specific human populations [37]. While the differences between these Mtb strains are still being studied, some of the strains, particularly the Beijing strain that originated in Asia, have shown distinct characteristics of increased virulence, mortality, and drug resistance [38].

There are approximately 4000 genes in the Mtb genome [39]. Mtb secretes approximately 200 proteins during culturing process, which are collectively referred to as culture filtrate proteins (CFP) [40]. CFP contains proteins, particularly the critical virulence factors ESAT-6 and CFP-10, that stimulate host immune responses [41, 42]. ESAT-6 and CFP-10 are part of and secreted by the ESX-1 system of mycobacteria, a type VII secretion system [43]. Notably, the

genes for ESAT-6 and CFP-10 and the rest of the ESX-1 proteins lie in the RD1 deletion region, which is found in all virulent Mtb and *M. bovis* strains, but not in the TB vaccine BCG, which suggests its role in the virulence of Mtb [36]. Indeed, deletion of the RD1 region from virulent Mtb resulted in attenuated virulence, while complementation of the RD1 region in BCG increased virulence during infections in mice [44, 45]. The mechanism of ESAT-6 and CFP-10 virulence have not been determined, but ESAT-6 has been demonstrated to restrict TLR responses in innate cells and assist in dissemination by promoting cell lysis and pore formation [46-48]. While Mtb has many more virulence factors that have been identified, not all of their mechanisms and immunogenic properties have been characterized, however some of the more immunogenic ones have been incorporated into diagnostics and vaccines [49].

1.3 THE HOST IMMUNE RESPONSE TO M. TUBERCULOSIS

1.3.1 Initial events in Mtb infection: bacterial containment and persistence in granulomas

When aerosolized droplets containing Mtb are inhaled, alveolar macrophages phagocytose Mtb in the lung alveoli before invading the epithelial layer. The host innate immune system brings in the first Mtb responders: macrophages, including epithelioid macrophages, giant cells, and foamy macrophages, myeloid dendritic cells and neutrophils [50]. Within the first 4 weeks of infection, a complex orchestration of all of the various innate immune cells occur within the lungs, with their individual roles and contributions to the containment and control of Mtb [51-53]. Macrophages have been shown to be particularly crucial for containing mycobacteria during the initial days of infection [54]. Dendritic cells, however, are the crucial infected cell subset to

transport Mtb to the lymph nodes, and without their trafficking of live Mtb to the mediastinal lymph nodes, the T cell response to Mtb is not initiated [53, 55]. The adaptive immune response cells, CD4 and CD8 T cells and B cells, are recruited to the cluster of infected and uninfected cells in the lung. Delayed measurable T cell responses by TSTs in humans (6-8 weeks post-infection) and NHPs (4-6 weeks post-infection) or in the lungs of mice (2-3 weeks post-infection) suggest that the adaptive T cell response is quite slow [55-57].

As more cells are recruited to the site of infection, a granuloma, the hallmark of Mtb infection, is formed. Typically, TB granulomas are highly structured, with the center of a granuloma containing caseous necrosis, surrounded by a ring of epithelioid macrophages, and an outer ring of lymphocytes and macrophages, sometimes with a fibrotic cuff (Figure 2) [58-60]. As demonstrated in the NHP model, the onset of the adaptive immune response in the granulomas assists with Mtb killing and clearance between 4 and 11 weeks of infection [61].

The granuloma serves to contain Mtb, but may be advantageous for the bacterium to shield itself from host defense mechanisms. Mtb has been suggested to manipulate the granuloma environment to promote subsistence [50]. Studies from the zebrafish model of mycobacterial granulomas has indicated that infected macrophages recruited to early granulomas by mycobacteria are also motile and may assist in dissemination [54, 62]. Mtb also persists within macrophages by blocking phagosome maturation and phagolysosomal fusion [63, 64]. Mtb can also alter the macrophage balance of LXA4 and PGE2 signals to promote necrosis and impede dendritic cell cross-priming of T cells [65]. Mtb infection may actively inhibit dendritic cell maturation [66]. Additionally, Wolf et al. found that Mtb-infected dendritic cells in a mouse model may actively inhibit MHC II antigen presentation to CD4 T cells [53]. T cell priming in the lymph nodes may also be delayed because of Mtb-specific expansion of regulatory T cell

populations [67]. The early events in Mtb infection are critical to the outcome of infection, yet are difficult to study, particularly in humans [68].

Although the clinical manifestations are strikingly different between active disease and latent infection, there is much overlap in granuloma pathology and bacterial burden per granuloma between the disease states [61, 69]. On the individual granuloma level, in Mtb-infected NHPs, mineralized and caseous granulomas are found in across the spectrum of infection outcomes [69]. Both sterile and non-sterile granulomas are found in active TB, subclinical TB, and latent infection, but there are usually more granulomas and complex pathologies with higher overall bacterial burden in the lungs and lymph nodes in active TB [61].

The differences in the immune responses that lead to controlled infections versus active disease are not known. Much of the evidence thus far supports that T cell responses are a crucial factor in the control and clearance of Mtb, particularly from the extreme susceptibility of murine knock-out animals and humans with T cell deficiencies [70-73]. Human studies of active and latent TB have also shown significant differences in their Th1 responses [74-76]. Despite its critical role in the progression of TB, much about the granuloma remains unknown due to technical and logistical challenges. It is challenging to obtain granulomas from Mtb-infected patients, the commonly used mouse models do not form granulomas that accurately resemble human granulomas, and there are fewer immunological reagents available to study them in rabbits and guinea pigs [59]. Instead, much of what is known and researched in the granuloma is in the *M. marinum*-infected zebrafish and Mtb-infected non-human primate (NHP) model, as the granulomas from the latter recapitulate those of human infection [59, 77].

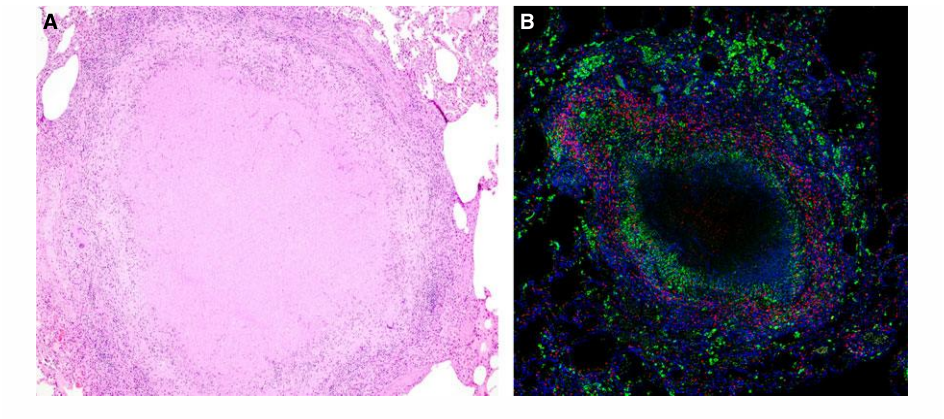

Figure 2. Classic caseous granuloma structure.

(A) Hematoxylin and eosin stained section of necrotic lung granuloma with caseous necrosis (10x magnification) and (B) immunohistochemical staining of necrotic lung granuloma with a dark center of caseous necrosis with no visible cell nuclei (blue). CD68+ macrophages (green) line the edge of the necrosis and CD3+ T cells (red) form lymphocytic cuff (20x magnification). Other clusters of CD68+ (green) macrophages are in the outer edge of the granuloma and in the surrounding tissue. Reproduced by permission from John Wiley and Sons, Immunological Reviews, Immunology studies in non-human primate models of tuberculosis, Flynn et al., 2015 [78].

1.3.2 The adaptive immune response to Mtb

The primary adaptive immune actors in Mtb infections are T cells. Both CD4 and CD8 T cells are involved in the host adaptive immune response to Mtb infections, but the CD4 response to Mtb has been studied more extensively [79]. The necessity of CD4 T cells has been illustrated by

the increased susceptibility in HIV patients [80, 81]. The importance of CD4 T cells has also been demonstrated in murine and NHP models of TB [82-84]. An important component in control of Mtb infection is the inflammatory response, mediated by Th1 cells which produce cytokines like IFN-γ, TNF, and IL-2 [85]. The importance of IFN-γ has been illustrated with IFN–γ deficient mice, which are extremely susceptible to even low doses of Mtb [72, 86]. Humans with genetic defects in their Th1 IFN-γ-and IL-12 signaling pathways (Mendelian susceptibility to mycobacterial diseases, MSMD) also are more susceptible to mycobacterial infections [71]. TNF is essential for control of Mtb infection, as mice, NHPs, and patients with rheumatoid arthritis treated with anti-TNF antibodies have increased risk of TB [73, 87, 88]. The role of IL-2 in Mtb infections is more contentious, but IL-2 may have an interplay with IFN- γ and higher levels of IL-2 are associated with better disease outcome [89, 90]. Mtb infections induce IL-17 production in humans and mice, but the function of IL-17 during Mtb infections less clear [91-93]. CD8 T cells in Mtb infections have been shown to be crucial for protection from TB, as knock-outs of the MHCI pathway in mice and CD8 depletion in NHPs result in increased lung pathology and decreased control of Mtb [94-96].

Although most studies have focused on the effect of the immune response on the whole animal disease outcome, there is evidence of the importance of the local T cell response on granuloma formation at the local site of infection. The loss of CD4 T cells, IFN-γ, and TNF can cause dysfunctional granulomas [85, 97]. Mice and humans with defects in IFN-γ or TNF pathways have disseminated disease [71, 86]. Neutralization of TNF in NHPs results in poor control of initial infection and increased reactivation of latent TB [88, 98]. Furthermore, studies in mice without TNF have deficiencies in granuloma formation, excessive neutrophil infiltration and tissue destruction [73, 99, 100]. TNF may be necessary for chemokine expression and cell

recruitment in granuloma formation and maintenance [101]. A balanced T cell response in granulomas, such as inhibitory IL-10 and a pro-inflammatory cytokine, is associated with increased bacterial killing in lung granulomas [102].

Since Mtb is an intracellular pathogen, much of the research in the adaptive immune response has emphasized the cellular response, rather than the humoral response. Thus, much less is known about B cells than T cells during Mtb infection. Activated B cells have been characterized in clusters within the lymphocytic cuff of TB granulomas in a NHP model, with higher concentrations of Mtb-specific IgG in granulomas as opposed to uninfected tissue samples [103]. The presence of inducible lymphoid follicles, or inducible BALT (iBALT), in lungs is associated with better disease outcomes [104]. Furthermore, antibody signatures may be distinct between patients with latent Mtb infections compared to active disease. The antibodies from latently infected patients also induced more macrophage activation and killing of Mtb, suggesting that antibodies may be critical for bacterial control [105]. B cell-deficient mice had more immunopathology and susceptibility when challenged with Mtb, but B cell-depleted NHPs had similar disease outcomes and bacterial loads compared to controls after Mtb challenge, although they had altered granuloma cytokine responses [106]. Although the humoral response may not be critical for host control of Mtb infection, other studies have shown that B cells and antibodies may be adjunctive or synergistic for Mtb control by interacting and enhancing other immune cells [107].

1.4 MODULATORS OF THE T CELL RESPONSE IN TB GRANULOMAS

As reviewed above, many different immune cell types contribute to the containment and control of Mtb during infection, with the T cell response noted as a crucial component. Besides the local inflammatory response, an effective immune response requires a balance between pro- and anti-inflammatory factors, as an imbalance will provoke excessive tissue damage or ineffective bacterial clearance. Several modulators of pro-inflammatory T cell responses have been suggested and investigated as potentially significant in Mtb infections, including regulatory T cells (Tregs), immunoregulatory cytokines, and exhausted T cells.

1.4.1 Regulatory T cells

Tregs may have an immunosuppressive role in TB; mice depleted of Foxp3-expressing Tregs and infected with Mtb had significantly lower bacterial burden, although they also had multi-organ inflammation [108]. Tregs have been suggested to migrate to the local sites of Mtb infection, with Tregs accumulating in the lungs of mice, and frequencies of peripheral Tregs decreasing during early Mtb infection in humans and NHPs, but increasing in the airways of Mtb-infected NHPs [108-110]. Treg populations also expand in response to Mtb antigens, and may inhibit the priming of effector T cells in the lymph nodes [67]. A study in the PBMCs of TST reactors found that Treg expansion in the presence of Mtb also required the expression of PD-1 [111]. Tregs can suppress other immune cells through inhibitory cytokines, cytolysis, metabolic disruption, or modulation of dendritic cells. In particular, the inhibitory cytokines IL-10 and TGF-β are induced by Tregs as one of their main mechanisms of suppression, which will be discussed in further detail below [112]. Interestingly, Tregs have been known to express

inhibitory receptors CTLA-4 and LAG-3, and there is growing evidence that they may also express PD-1 [111-114]. These inhibitory receptors in the context of T cell exhaustion will also be further discussed below.

1.4.2 Inhibitory cytokines: IL-10 and TGF-β

Levels of IL-10 and TGF-β are higher in active TB patients, suggesting these inhibitory cytokines may be associated with increased disease [115-118]. Fewer studies of TGF-β in TB are available, but TGF-β exacerbated pulmonary TB through T cell suppression in guinea pigs [119], and inhibition of TGF- β during BCG vaccination enhanced immune response [120]. In human studies, higher levels of TGF-β associated with active TB, and suppressed lymphocyte proliferation and IFN-γ production *in vitro* [118, 121]. A study suggested IL-10 and TGF-β together have synergistic immunosuppressive effects on Mtb-infected cells [117].

The more well-studied of the two cytokines, IL-10, still has a debated role during Mtb infections. In addition to being produced by Tregs, IL-10 is produced by nearly all immune cells, including monocytes, macrophages, dendritic cells, B cells, NK cells, mast cells, and nearly all T cell subsets [122]. IL-10 downregulates Th1 responses by inhibiting antigen presentation from macrophages and DCs and IL-12 production [123-125]. IL-10 can also inhibit macrophage function, reducing macrophage killing, and nitric oxide and TNF production [125]. The balance of IL-10 response during infections and autoinflammatory conditions is critical, as it is associated with many negative disease outcomes [125-127]. In patients with TB disease, IL-10 is elevated and may downregulate the Th1 response [115, 128-131]. The downregulation of

beneficial Th1 responses by IL-10 during Mtb infection is further supported by mouse studies, in which eliminating IL-10 enhances protection, IFN- γ production, and T cell recruitment without negatively increasing pathology [132-136]. Conversely, excessive IL-10 in the murine model increased bacterial burden and exacerbation of the disease [137, 138]. However, other studies in mice found loss of IL-10 increased IFN-γ production and inflammatory responses, but had a negative or no effect on protection from TB [139-142]. Although the available studies do not definitively demonstrate that IL-10 detrimentally downregulates Th1 responses or prevents immunopathology during Mtb infections, recent studies suggest that IL-10 may have more specific roles during particular points of Mtb infection. In mice, lack of IL-10 early in Mtb infection, during the first month of infection had significant improved the long-term control of Mtb infection [136], while blocking IL-10 later in Mtb infection, after 3 months, only partially reduced bacterial loads [134]. Additionally, in NHPs, at the local site of infection (granulomas), IL-10 expressed in the same granuloma as a pro-inflammatory cytokine was associated with increased sterilization [102]. Thus, the role of IL-10 within Mtb infections is unsettled, and will be clarified through the studies described in Chapter 2.

1.4.3 Exhaustion of T cells during chronic diseases

T cell exhaustion has been characterized in other chronic infections, such as HIV, LCMV, and hepatitis B, and in cancer, in which T cells lose functionality and proliferation capabilities in response to chronic antigenic stimulation [143-148]. Considering that Mtb can persist in humans for years until death and antigen load (bacterial burden) was associated with decreased T cell responses in patients, T cell exhaustion has also been hypothesized to contribute to the immune response during TB [75]. Exhausted T cells are characterized by low cytokine production, low

proliferation, and expression of one or more inhibitory receptors, including PD-1, CTLA-4, and LAG-3. These inhibitory receptors interact with their corresponding ligands on antigen presenting cells to activate negative regulatory pathways [149, 150]. While T cell exhaustion in CD8 T cells has been well studied in a variety of disease models, the phenomenon of exhaustion in CD4 T cells has more recently emerged, although exhausted CD8 and CD4 T cells appear to differ transcriptionally [151, 152]. As demonstrated in other diseases, blocking inhibitory receptors rescues T cell function and may lead to improved disease outcomes [153-158]. However, although inhibitory receptors and their regulatory pathways may help prevent chronic inflammation and tissue destruction, they may also prevent necessary T cell functions for complete clearance of infections or tumor cells.

The question of whether T cell exhaustion occurs or is important during Mtb infection has been examined by characterization of the inhibitory receptors PD-1, CTLA-4, and LAG-3. TB patients had increased PD-1 expressing T cells in their peripheral blood mononuclear cells (PBMC) compared to healthy controls, and blockade of inhibitory receptors *in vitro* enhanced T cell function [159-161]. In a mouse model, PD-1+ T cells accumulated in the lungs and lymph nodes during Mtb infection [162]. Relatedly, the ligand for PD-1, PD-L1, has also been shown to be upregulated on neutrophils in active TB patients, and downregulated after TB treatment [163]. Dendritic cells from chronic (10 week) liver granulomas in a mouse model of mycobacterial infection also tended to express higher levels of PD-L1 than in acute (3 week) liver granulomas [164]. CTLA-4 has been less well-characterized in Mtb, but two studies in different populations indicate that polymorphisms in gene for CTLA-4 may be associated with more pulmonary TB or more severe pulmonary TB [165, 166]. A study in PBMCs of active TB patients associated CTLA-4 expression with activation in T cells [115]. In a murine model, blockade of CTLA-4

during mycobacterial infection increased lymphocyte proliferation and IFN-γ production in lymph nodes, but did not reduce the bacterial loads or lung pathology [167]. LAG-3 on T cells in a NHP model was associated with active or reactivated TB compared to clinically latent NHPs [168]. Although studies use these inhibitory receptors, especially PD-1, as markers of T cell exhaustion, and thus reduction in protective T cell activity, some mouse studies have suggested that T cells expressing PD-1 may be necessary to maintain antigen-specific effector T cells during Mtb infections [169, 170]. Importantly, mice developed extreme inflammation and poor outcome in the absence of PD-1 during Mtb infection [171-173]. When Einarsdottir et al. specifically blocked PD-1 and PD-L1 during chronic Mtb infection in mice, they found no detectable change in T cell function or bacterial load [162].

The majority of the current published literature on T cell exhaustion in TB have identified exhausted T cells based on the expression of a single inhibitory receptor. However, inhibitory receptors can also be upregulated during activation, and T cells can simultaneously express both inhibitory and activation markers [150, 174-177]. Since increasing co-expression of multiple inhibitory receptors on T cells may reveal increasing T cell exhaustion, characterization of inhibitory receptor co-expression may be more accurate [178]. T cells co-expressing inhibitory receptors during Mtb infections have not been studied as thoroughly, although PD-1 expression was found to correlate with CTLA-4 expression on CD4+ T cells from tissues of Mtb-infected NHPs [179]. Gideon et al. found low frequencies of PD-1+ T cells co-expressing CTLA-4, with significantly higher PD-1+CTLA-4- T cells [102]. Mtb infections in mice increased the expression of PD-1 and LAG-3 as the infection progressed, and this was associated with increased T cell impairment. However, PD-1+ T cells co-expressing TIM-3, another inhibitory receptor, had an even more dysfunctional exhausted phenotype during Mtb infection [180].

These PD-1+TIM-3+ cells also had upregulation of genes associated with other inhibitory receptors, including TIGIT, Blimp1, LAG-3. And CTLA-4. While there are other inhibitory receptors that may mark T cell exhaustion, the study presented in Chapter 3 will focus on the expression of PD-1, CTLA-4, and LAG-3.

1.5 MODULATION OF IMMUNE RESPONSES IN TB BY VACCINATION

Since correlates of protection against TB are currently still unknown, development of an effective vaccine has been stymied for the past century, almost since the initial identification and isolation of Mtb by Robert Koch. Initially, in 1890, Koch claimed to have isolated a substance from Mtb that when injected could treat tuberculosis. This substance, which was subsequently named tuberculin, was soon proved to be ineffective as a treatment and actually harmful in some cases, but it became useful as a diagnostic tool for infection and the basis for the current standardized test for Mtb. Following tuberculin, in 1921, Albert Calmette and Camille Guérin introduced their vaccine, BCG (Bacille Calmette-Guérin) to combat TB. BCG was eventually widely accepted, and has been and continues to be the only licensed vaccine for TB in the world [13]. As further described below, BCG has its drawbacks with variable efficacy, but a new and more effective vaccine has yet to be developed.

1.5.1 History and current status of BCG

Initially, attempts to make a vaccine against TB by boiling or chemically treating Mtb failed. Although tuberculin was not effective as a vaccine against TB, Albert Calmette suspected that

the sensitivity following injection was a sign of an immune reaction. Combined with the previous observation that patients with tuberculous glands in their necks tended to not also have pulmonary tuberculosis, Calmette began a long journey in 1900 to find a live, avirulent vaccine that would artificially stimulate the immune response to Mtb and prevent TB. He and Camille Guérin, they first began culturing tubercle bacilli on glycerin and potato media, but because they could not create a homogeneous suspension of the bacteria, they added ox bile to their media to reduce clumping. After realizing the addition of ox bile during subculturing reduced the virulence of the bacteria, they began serially subculturing a virulent bovine strain related to Mtb, *M. bovis* in 1908. Calmette and Guérin continued to subculture even through World War I, despite the difficulty of acquiring the supplies necessary to make the medium. Finally, in 1919, after over 200 subcultures over 11 years, their culture did not cause progressive tuberculosis in guinea pigs or other animal models. They named their culture Bacille Calmette-Guérin (BCG) [8, 13, 181, 182].

The first trial of BCG in humans was in 1921, when BCG was administered by oral route to an infant born to a tuberculous mother with no complications. By 1928, over 100,000 doses of BCG were given to infants and it began to be administered to infants in other European countries. Although Calmette and Guérin published a reduction in infant mortality from TB after BCG vaccination, it was still met with skepticism in other parts of the world, with strong criticisms of their claims [8, 182, 183]. In 1930, an accidental contamination of the BCG vaccine with virulent Mtb that was administered to over 200 children in “the Lubeck disaster” caused a further setback in the confidence in BCG. However, when World War II caused epidemics of TB throughout Europe and Asia, BCG began to be used on a global scale [8, 182]. Under the International Tuberculosis Campaign, nearly 30 million people were tested for TB, and almost

14 million were vaccinated in 22 countries by 1951 [184]. Despite the increased global use of BCG, the United States resisted adoption of BCG vaccination, citing low levels of TB in the U.S., the benefits of tuberculin testing, and prophylactic chemotherapy of tuberculin-positive patients to be sufficient to prevent TB in the U.S. [185, 186].

Even during the early decades of BCG vaccinations, there were contradictory reports in the efficacy of BCG. Most reports agree that BCG has been shown to be protective in infants against severe TB disease, preventing TB meningitis and military disease, however, the efficacy of BCG against pulmonary TB remains inconsistent [187-189]. Protection against pulmonary TB varies from 0-80%, depending on the clinical trial [188, 190-194]. One potential cause is the variability in immunogenicity between the strains of BCG currently in use worldwide, with phenotypic and molecular differences between the strains, likely due to divergence in production methods over the years [8, 195]. Geographical differences and exposure to other non-tuberculous mycobacteria NTM) is widely believed to affect BCG vaccine efficacy, called the North-South effect [8, 188, 194]. Further confusing the benefits of BCG, the administration of BCG has been suggested to prevent infant mortality beyond simply protecting from TB, continuing the need for administration of BCG in endemic areas despite doubts of its efficacy against pulmonary TB [196].

The mechanisms by which BCG provides protection are currently unknown. Genomic studies have shown many regions of difference (RD) between virulent Mtb and BCG, where genes present in Mtb are no longer in the present passage of BCG [197]. Notably, these genomic changes may affect T cell epitopes in BCG compared to Mtb [198]. Vaccination with BCG has been shown to induce robust T cell response from both CD4 and CD8 T cells [199-201]. However, these responses have been shown to be mostly of the effector T cell type, primarily

producing IFN-γ, rather than of a long-lived central memory T cell. The peak BCG T cell response is typically within 10 weeks of vaccination, and protection appeared to wane over time, likely due to the lack of central memory T cell response [200, 202, 203]. Additionally, comprehensive studies of infants vaccinated with BCG failed to identify any immunological correlates of risk for developing TB disease [204, 205]. The unidentified factors of BCG that confer partial protection to TB have made it difficult to improve upon BCG and to produce a fully protective vaccine.

1.5.2 Strategies for protective TB vaccines

Considering the waning immune response to BCG, the simplest strategy of extending protection is by revaccination using BCG. Unfortunately, repeated vaccination with BCG has not shown substantial additional protection [206-208]. By studying the variability in response to revaccination depending on the geographical site (19% in Salvador vs. 1% in Manaus), Barreto et al. proposed that exposure to NTM before BCG vaccination may block the protection conferred by BCG, and may be overcome or bypassed by new TB vaccines [208]. Novel vaccines strategies aim to protect against TB at three stages of disease: pre-exposure to Mtb to prevent infection or TB disease, post-exposure to Mtb to prevent TB disease, and therapeutic to cure TB disease. The underlying mechanism of the current proposed vaccines is to induce and alter the T cell response, particularly of memory T cells that produce IFN-γ, TNF, and IL-2, since the T cell response has been shown to be crucial for protection [209].

Currently, 12 new vaccine candidates have been developed and are in various stages of pre-clinical and clinical trials [14]. These vaccines arise from two main approaches – to either improve BCG by genetic recombination or by boosting BCG through additional subunit vaccines

using protein or viral vectors [210]. Of the vaccines currently in clinical trials, MTBVAC and VPM1002 are live mycobacterial vaccines designed to replace BCG [14]. MTBVAC is a live clinical isolate of Mtb containing deletions of *phoP* and *fadD26* genes, which encode two genes that control major virulence factors [211]. On the other hand, VPM1002 is a live recombinant BCG vaccine that contains the listeriolysin encoding gene from *Listeria monocytogenes* to promote rapid phagosome acidification and phagolysosome fusion [212]. RUTI, Vaccae, and DAR-901 are all inactivated vaccines derived from whole or fragmented mycobacteria. RUTI and Vaccae were designed as therapeutic vaccines to shorten TB drug treatment [14]. RUTI consists of detoxified and liposomed cellular fragments of Mtb, while Vaccae consists of a nonpathogenic NTM vector, *M. vaccae*, expressing a 19kDa fragment of Mtb to stimulate T cell responses [213, 214]. DAR-901 is the scalable vaccine based on SRL172, an inactivated, whole-cell vaccine from NTM that is meant to boost BCG vaccine responses [215].

Subunit vaccines consist of one or more immunogenic antigens expressed by a viral vector or formulated in an antigen designed to boost the efficacy of BCG [210]. Ag85A, a mycolyl transferase in mycobacteria that contains several CD4 and CD8 T cell epitopes, has been incorporated into multiple vaccines, including the viral vectored vaccines Ad5 85A (adenovirus), ChAdOx185A-MVA85A (adenovirus and vaccinia virus), and TB/FLU-04L (influenza virus) [14, 210, 216]. MVA85A, modified vaccinia Ankara-expressing Ag85A, had formerly been the most advanced vaccine in the TB vaccine pipeline, until it was shown to lack any efficacy against TB or Mtb infection in a randomized, placebo-controlled phase 2b trial [217]. Alternatively, TB subunit vaccines with non-viral adjuvants currently in clinical trials are H56:IC31, H4:IC31, ID93+GLA-SE, and M72/AS01E [14]. H4, which is designed for pre-exposure vaccination includes antigens produced by Mtb during active replication, while H56,

ID93, and M72 incorporate larger combinations of antigens to cover all stages of Mtb infection for post-exposure use [210]. ID93, which consists of the mycobacterial antigens associated with virulence, Rv2608, Rv3619, Rv3620, and latency, Rv1813, combined with a stable oil-in-water-emulsion adjuvant GLA-SE has been shown to induce Th1 responses [218]. M72 is a recombinant fusion protein vaccine composed of Mtb32A and Mtb39A proteins in a liposomal adjuvant containing TLR4 ligand 3-O-desacyl-4'-monophosphoryl lipid A (MPL) and immunostimulant *Quillaja saponaria* fraction 1 (QS21) to promote antigen-specific CD4 T cells [219]. H56 and H4 fusion protein vaccines in clinical trials are administered via IC31, an adjuvant that combines immunostimulatory oligodeoxynucleotide containing deoxy-Inosine/deoxy-Cytosine (ODN1a) and the antimicrobial peptide $KLKL_5KLK$, which signals through the TLR9 pathway to induce Th1 and humoral responses [220]. Protein subunit vaccines, including H56, will be discussed in further detail below.

1.5.2.1 Protein subunit vaccines with liposomal adjuvants

Subunit vaccine H4 and H56 are protein fusion vaccines currently in clinical trials that have shown a strong immune response and protection in animal models and were developed by our collaborators at the Statens Serum Institute (SSI) [221, 222]. Both H4 and H56 contain Ag85B, an abundant and strongly immunogenic protein part of the Ag85 protein complex of mycolyl transferases [221, 223]. Ag85B, which is produced in Mtb and BCG, is recognized by Th1 cells and triggers strong cytokine responses, including IL-2, IFN-γ, and TNF [224, 225]. Besides Ag85B, H4 also contains the immunodominant Mtb antigen, Mtb10.4, which is also present in Mtb and BCG, and stimulated the greatest responses of its subfamily within the *esat-6* gene family [223, 226]. In H56, in addition to Ag85B, the protein vaccine also includes ESAT-6, a highly immunogenic protein secreted by Mtb but not BCG or environmental mycobacteria, and

Rv2660c, a latency associated protein up-regulated by Mtb under nutrient starved and hypoxic conditions to mimic antigen from Mtb entering the persistent stage of infection *in vivo* [221, 222, 227, 228]. H56 induced vaccine-specific immune responses in mice, non-human primates (NHPs), and humans, and reduced bacterial burden in mice, while preventing reactivation in NHPs [221, 222, 229, 230]. Additionally, SSI has since developed a new related fusion protein vaccine, H74. H74 is composed of the strongly immunogenic Mtb antigens ESAT-6, Rv3881c (EspB), Rv3614c (EspD), Rv3615c (EspC), Rv3616c (EspA), and Rv3849 (EspR), which are co-regulated and secreted through the ESX-1 secretion system of Mtb throughout the course of Mtb infection [231-241]. H74 has been demonstrated to cause strong immunogenic response and decrease bacterial burden in the mouse model of Mtb infection (SSI, data not published).

These vaccines have also been tested with a variety of adjuvants to try to induce the protective immune response, even though the parameters of this immune response, especially at the local level, is still unclear, but are suspected to include a strong Th1/Th17 cytokine response, particularly IFN-γ. Besides IC31, which is currently being used with H4 and H56 in clinical trials, SSI has formulated a series of novel liposome-based cationic adjuvant formulations (CAF) [14, 242], including CAF09 and CAF01. CAF09 is composed of monomycoloyl glycerol (MMG)-1, a synthetic analogue of a mycobacterial cell wall lipid, and Poly(I:C), a synthetic dsRNA and TLR3 agonist, and demonstrated to induce robust CD4 and CD8 T cell responses [243, 244]. In contrast, CAF01 has trehalose 6,6-dibehenate (TDB) glycolipids, a synthetic variant of a mycobacterial cell wall cord factor, as a stabilizer and immunomodulatory, and has been demonstrated to trigger long-lasting Th1 and Th17 immune responses [242, 245-248]. Chapter 4 of this dissertation will investigate the efficacy of the H56 and H74 protein fusion vaccines with the adjuvants CAF01 and CAF09.

1.5.2.2 Vaccination routes

The route of vaccination can also greatly affect the modulation of immune response by vaccines. For example, BCG, which was originally given as an oral vaccination, but is currently given as an intradermal injection, can have very different immunogenic effects and levels of protection depending on the route of vaccination. Mouse studies have suggested that aerosolized BCG may confer the most protection compared to oral or intradermal administration [249]. Similarly, Lagranderie et al. also found improved protection to Mtb challenge in aerosol vaccinated guinea pigs compared to intradermal vaccinated animals [250]. Although systemic intravenous vaccination of BCG in mice led to higher levels of BCG and CD4 T cells in tissues, Mittrucker et al. found that these higher immune responses in intravenous vaccination did not improve protection against Mtb challenge compared to oral BCG vaccination [251]. Surprisingly, intravenous administered BCG in rhesus macaques vastly improved protection during Mtb challenge compared to intradermal vaccination [252-254]. Thus, vaccination routes can greatly affect the efficacy of a vaccine and may need to be optimized for each vaccine. As BCG boosting protein subunit vaccines must be used in conjunction with current intradermal vaccination practices, optimization of the vaccination route and strategy of these novel vaccines must be tested with BCG [14, 255-257].

Since TB primarily is a pulmonary disease, vaccination that targets the site of infection for a mucosal pathogen, such as Mtb may increase the efficacy of a TB vaccine [258-263]. Additionally, studies have shown that booster vaccines given simultaneously as BCG toward the same draining lymph node can boost immune response [264]. The studies described in Chapter 4 will investigate whether various routes and strategies of protein subunit boost vaccination

improve protection from TB, particularly focusing on the administration of vaccines via the mucosal route.

1.6 NON-HUMAN PRIMATE MODEL OF TB

Many animal models have been adapted for TB studies. The earliest landmark studies of TB transmission used the highly susceptible models of rabbits and guinea pigs. A variety of strains of mice are commonly used for TB, and although they are a tractable model of TB, mice are relatively resistant to Mtb and they do not reproduce the same type of disease as in humans, with high levels of bacterial burden and uncircumscribed lung granulomas. In contrast, NHPs are naturally susceptible to Mtb, develop TB that resembles that of humans, have similar immune responses to Mtb, and have similar levels of protection with BCG vaccination. However, they are more expensive, and more difficult to maintain under Biosafety Level 3 conditions, and are outbred, leading to substantial variability in infection outcome and immune responses, similar to humans [265, 266].

Our lab previously developed a low dose (≤ 25 CFU) cynomolgus macaque (*Macacca fasicularis*) model that recapitulates the spectrum of human Mtb infection in both disease progression (clinically active disease to latent infection) and pathology (granuloma formation and more complex pathologies) [57, 77, 267, 268]. In particular, the histopathology of granulomas in the NHP model fully represents the range of granulomas in human disease, with identifiable caseous, non-necrotizing, suppurative, fibrotic, and mineralized granulomas, and TB pneumonia [57, 77]. A number of immunological and physical monitoring tools have also been developed along with the NHP model to further track disease progression and address specific

questions about Mtb infection, including PET-CT imaging and intracellular cytokine staining of tissues, including granulomas and lymph nodes [77, 269, 270]. Our NHP model has several advantages: (1) recapitulates the spectrum of human TB; (2) ability to modulate immune responses with vaccinations, including adjuvants, host-directed therapies, or antibodies; (3) ability to manipulate timing of infection and observe the earliest events of infection; (4) ability to extract and characterize individual lung granulomas by bacterial burden, pathology, and immunology; (5) ability to track Mtb infection in lung and lymph nodes non-invasively by using ^{18}F-FDG in PET-CT imaging [78]. Thus, the NHP model of TB serves as the ideal model to examine the modulation of immune responses at the local site of Mtb infection, within individual granulomas, while also observing the relation of the local response on the overall disease outcomes and bacterial loads within animals.

1.7 STATEMENT OF THE PROBLEM

Each year, TB is responsible for well over a million deaths around the world. Despite continued efforts to reduce the global burden of TB and nearly a century of vaccination with the TB vaccine BCG, an additional 10.4 million people become infected every year [14]. Part of the roadblock to TB eradication is that the immune response during Mtb infections is not fully understood, and thus immune correlates of protection have not been identified. Additionally, the only available vaccine for TB, BCG, has variable efficacy, particularly in preventing pulmonary TB in adolescents and adults. While the host immune response involves many innate and adaptive immune cells working in concert, T cells have been identified as a crucial component in the control of Mtb. Gideon et al. demonstrated a balance of pro- and anti-inflammatory T cell

cytokines in the granulomas is associated with bacterial clearance. Despite this need for a balanced T cell response in the granulomas, low frequencies of pro-inflammatory cytokine response (IFN-γ, IL-2, TNF, IL-17) in T cells from TB granulomas were observed [102]. These low cytokine responses in T cells may be caused by a variety of factors, including (1) high levels of immunomodulatory soluble factors and regulatory cells, such as anti-inflammatory cytokines IL-10, TGF-β, or regulatory T cells; (2) decreased response from increased numbers of exhausted T cells during chronic antigen exposure; (3) influx of non-specific T cells; or (4) downregulation of T cell response by Mtb. This dissertation aimed to address two of these potential causes – the anti-inflammatory cytokine, IL-10 and T cell exhaustion. Due to the difficulty of isolating individual lung granulomas in patients and most animal models, much of the known aspects of the T cell response during Mtb infections originate from studies of the systemic (blood) response rather than the local (granuloma) response. This dissertation uses the NHP model of TB, which recapitulates the spectrum of disease, granuloma structure and formation, and immune response observed in humans. Using the NHP model, the goals of this dissertation were to answer the questions: (1) Does IL-10 downregulate the T cell response in TB granulomas? (2) Does T cell exhaustion contribute to the modulation of T cell response in TB granulomas? (3) Can different vaccination strategies alter the T cell response in TB granulomas for increased control and overall better disease outcomes?

These data will contribute to the understanding of the factors modulating T cell response in TB granulomas to take a step toward identifying the correlates of protection needed for successful prevention of TB disease.

2.0 THE ROLE OF IL-10 DURING EARLY MTB INFECTION IN A NHP MODEL

2.1 ABSTRACT

Tuberculosis (TB), caused by the bacterium *M. tuberculosis* (Mtb), continues to be a major global health problem. Lung granulomas, organized structures of host immune cells to contain Mtb, are the pathologic hallmark of TB. The host cytokine response plays a major role in containment of Mtb infection within these granulomas. While the importance of pro-inflammatory cytokines IFN-γ and TNF in controlling Mtb infections has been established, the effects of immunomodulatory cytokines, such as IL-10, in Mtb infections are less well understood. We used cynomolgus macaques, a non-human primate (NHP) model that recapitulates human TB to investigate the role of IL-10 early in Mtb infection. A cross-reactive, rhesus recombinant anti-IL-10 antibody was used to neutralize IL-10 in vivo in NHPs prior to and during the early course of Mtb infection. Disease progression was monitored by PET-CT scans, and local immune responses in the granulomas and lymph nodes assessed at necropsy. Our data indicate transient differences in innate cell response early in infection between anti-IL-10-treated and control animals. Surprisingly, there was less inflammation and more fibrosis in lung granulomas and earlier lymph node effacement from IL-10 neutralized animals at 3-4 weeks post-infection, compared to control animals. Overall, this unique dataset provides important

insight into the contribution of IL-10 to the immunological balance necessary for granulomas to control bacterial burden and disease pathology in Mtb infections.

2.2 INTRODUCTION

Tuberculosis (TB) continues to be a major cause of death worldwide, with 1.7 million deaths from TB in 2016 alone [1]. Despite decades of research, the nuances of the complex relationship between the host response and the bacterial cause of TB, *M. tuberculosis (*Mtb), remains unclear. For the best-case scenario, host immune cells coordinate their responses to contain the bacteria, in a delicate balance of halting bacterial spread without causing excessive disease pathology. When Mtb bacilli are initially inhaled, they are phagocytosed by alveolar macrophages, followed by an influx of other innate immune cells, such as neutrophils and dendritic cells, to the site of infection to assist in containment of Mtb. Later in infection, the adaptive immune response, including T cells and B cells, arrive to assist innate immune responses. Together, these host immune cells form the organized structure of a granuloma around the Mtb to contain the bacteria and prevent further bacterial spread. Both innate and adaptive immune cells and their cytokine responses have been established to be critical for control and clearance of Mtb (reviewed in [60, 68, 85, 271]).

These events and the host immune response early in infection are critical for the disease outcome. Subjects infected with Mtb have early initial inflammatory response and lymph node involvement, usually within the first two months of infection (reviewed in [68]). Studies in non-human primates (NHPs) have also indicated the importance of these early immune events on the eventual disease outcome [61, 270]. As reviewed by Cadena et al. [68], many host immune cells

and their cytokine responses are necessary for clearance of the bacteria. In particular, pro-inflammatory cytokines such as IFN-γ, TNF, and IL-17 have been shown in humans, non-human primates (NHPs), and mice to be critical for optimal control of Mtb [60, 71-73, 85, 86, 88, 92, 93, 98, 100, 101, 272, 273]. However, uncontrolled inflammatory cytokine response from these immune cells can also cause damage to the tissues.

The immune response has many checks and balances to counter a pro-inflammatory response and prevent damage. One major factor that can prevent tissue damage is IL-10, a cytokine that has been identified with anti-inflammatory properties. IL-10 can be produced by nearly all immune cells, including monocytes, macrophages, dendritic cells, B cells, NK cells, mast cells, and nearly all T cell subsets [122]. Dysregulation of IL-10 (increase or decrease) has been associated with many negative disease outcomes, including against bacterial and viral infections and autoimmune or inflammatory diseases [125-127].

Many studies have investigated the role of IL-10 in Mtb infections, but the cumulative results have been inconclusive. Elevated levels of IL-10 in patients have been suggested to be associated with more active or severe cases of TB [130, 131, 274]. In patients with Mtb infections, Th1 function increased when IL-10 was blocked during *in vitro* PBMC studies [115]. In the murine model, IL-10 has been observed to prevent control of the bacteria. Mice with IL-10 function blocked or knocked-out are better at controlling their bacterial burdens and enhancing survival during Mtb infections [132-136]. Overexpressing IL-10 in the murine model increased bacterial burden and exacerbation of the disease [137, 138]. In contrast, other studies using the murine model of TB indicated that IL-10 had insignificant effects on the bacterial burden during Mtb infections, with sometimes detrimental immunopathology and decreased survival [139-142]. While many of these studies indicate that IL-10 during Mtb infection may be decreasing Th1

function and preventing a sufficient immune response to reduce bacterial burden, some of these studies also implicate IL-10 in preventing immunopathology. Further contributing to these contradictory results, some studies suggest the timing of IL-10 may have differential effects during the course of Mtb infection. While blocking IL-10 later in infection (after 3 months) partially reduced bacterial burden [134], transiently blocking IL-10 during the first month of infection had even greater effects on the long-term control of Mtb infection [136]. Most of these studies were based on whole organ or whole animal outcomes, there are fewer studies of individual TB granulomas. By computational modeling of TB granulomas, IL-10 within the granulomas was necessary to reduce bacterial loads [275]. Granulomas from NHP-infected macaques expressing IL-10 in conjunction with pro-inflammatory cytokines, such as IL-17, were associated with better clearance [102].

To conclusively address the role of IL-10 during Mtb infections for the host immune response to contain Mtb, we used our NHP model and a macaque-specific anti-IL-10 neutralizing antibody to manipulate the levels of IL-10 *in vivo* during Mtb infection. Our NHP model recapitulates the spectrum of disease and pathology in human Mtb infections. Since we have the advantage of knowing exactly when the NHPs are infected, we can address the role of IL-10 at critical, early time points after infection, as the immune cells establish in the lungs and form granulomas. Using our NHP model, we can examine the effect of IL-10 on TB outcome on a systemic level, as well as probe the effects in the individual TB granulomas. When IL-10 was neutralized in our model, certain cytokine responses in lung granulomas and thoracic lymph nodes increased early on, 4 weeks after the onset of Mtb infection. However, by 8 weeks post-infection, these effects on lung granulomas and lymph nodes decreased or stabilized. Our study indicated that while IL-10 impairs the cytokine response in lung granulomas and lymph nodes

early in infection, IL-10 does not affect the short-term overall bacterial burden or disease outcome during Mtb infection.

2.3 RESULTS

2.3.1 Anti-IL-10 antibody neutralizes activity of macaque IL-10

The role of IL-10 in Mtb infections has been difficult to discern due to model variability and technical difficulties in studying IL-10 at the local sites of infection in TB patients. To better understand IL-10 at the primary site of infection, TB lung granulomas, we used our NHP cynomolgus macaque model of Mtb infections, which recapitulates the granuloma structure and disease pathology observed in humans. While TB granulomas are independent entities, and not all have detectable levels of IL-10, we aimed to understand how those granulomas with IL-10 differed in their control of the bacterial burden and disease pathology from those lacking IL-10.

Collaborators at MassBiologics (Dr. Keith Reimann, University of Massachusetts Medical School) created an antibody to specifically bind to macaque IL-10, which neutralizes active IL-10 activity (Figure 3A). D36 mouse mast cells are IL-10 dependent, thus the addition of 20ng/ml rhesus macaque IL-10 increased cell proliferation. The anti-macaque-IL-10 antibody was added at varying concentrations to the rhesus macaque IL-10, and reduced D36 mast cell proliferation to baseline levels. This demonstrated neutralization of macaque IL-10 by this antibody. We used this anti-IL-10 antibody in the rest of this study to investigate whether IL-10 had an effect on T cell function in TB granulomas.

Using excised and homogenized TB granulomas from Mtb-infected cynomolgus macaques, we treated one half of a granuloma sample with the anti-IL-10 antibody, while treating the other half as a media control, and then looked at the effects of neutralizing IL-10 on cytokines by flow cytometry. In TB granulomas with detectable levels of IL-10 by ELISA, treatment of TB granuloma T cells with anti-IL-10 antibody increased the frequency of CD3 T cells producing IL-2 compared to the media control (i.e., delta IL-2% = anti-IL-10 IL-2% – media IL-2% > 0). Granulomas with detectable levels of IL-10 had greater increase in IL-2 response after anti-IL-10 antibody treatment (Figure 3B), suggesting that IL-10 in TB granulomas, when present, may be suppressing the IL-2 response in T cells.

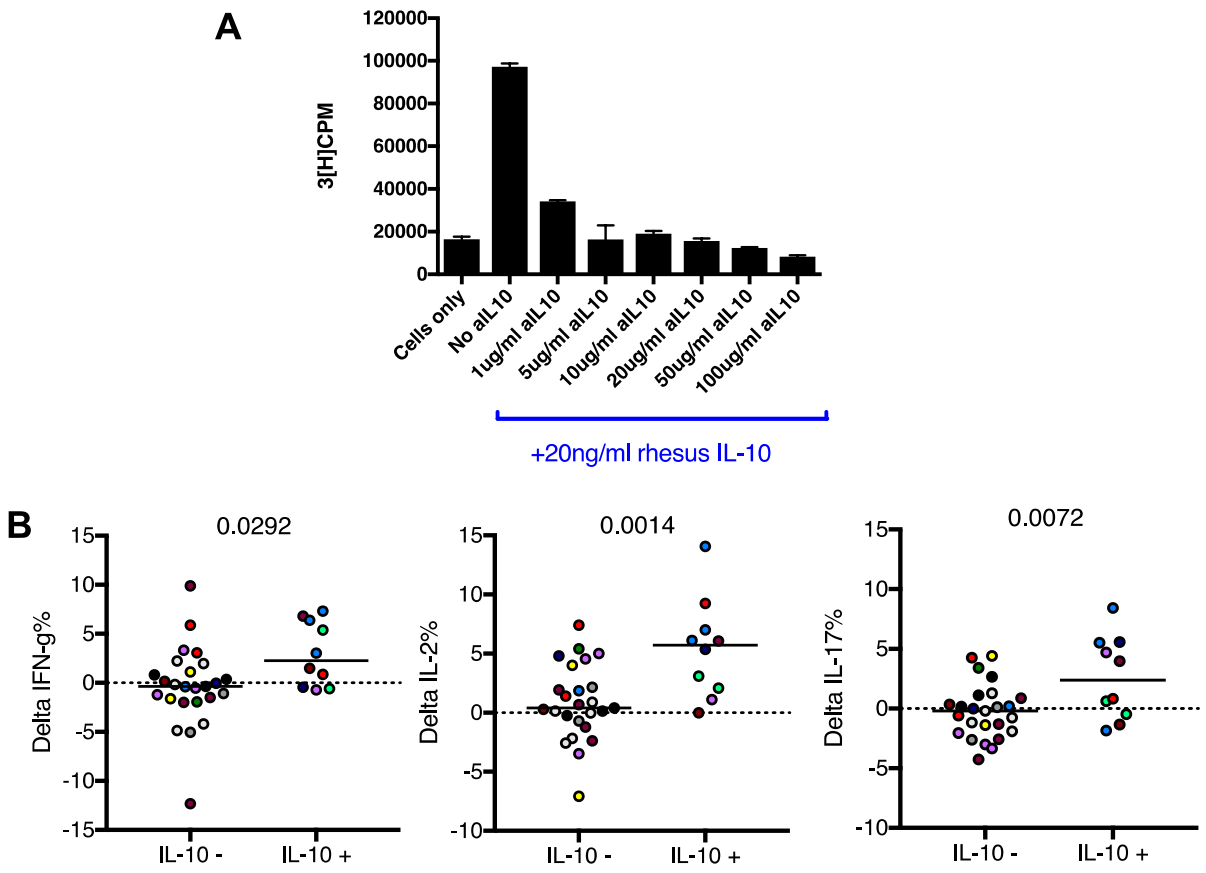

Figure 3. Anti-IL-10 antibody neutralizes macaque IL-10.

(A) D36 mouse mast cells are IL-10 dependent for cell proliferation. Mast cells supplemented with 20ng/ml rhesus IL-10 proliferate, while mast cells and rhesus IL-10, plus varying concentrations of anti-IL-10 antibody have reduced proliferation, as measured by tritiated-thymidine levels. (B) Changes in frequency of T cells (comparing *ex vivo* anti-IL-10-antibody-treated to the same untreated excised granulomas) producing IFN-γ (Delta IFN-γ%), IL-2 (Delta IL-2%), and IL-17 (Delta 1L-17%) by flow cytometry according to whether there were detectable levels of IL-10 in the granulomas. IL-10- indicates granulomas with no detectable IL-10 by ELISA, IL-10+ indicates granulomas with detectable IL-10 by ELISA.

2.3.2 *In vivo* assessment of IL-10 effects on M. tuberculosis infection

Immune responses in individual granulomas, even from the same macaque, are extremely variable. This was true of IL-10 levels in granulomas as well (Figure 3B) [102]. Although not every TB granuloma has detectable levels of IL-10, those that do are more likely to experience IL-10 modulation. Previously, we have observed that granulomas with strong T cell-mediated IL-10 production balanced with a pro-inflammatory cytokine response, such as IL-17, are associated with sterilization [102]. However, the timing of the IL-10 response in TB granulomas is not well understood [134, 136, 137]. To examine whether IL-10 in TB granulomas early in infection may prevent a robust T cell response and thus sterilization, we planned an *in vivo* IL-10 depletion study (Figure 4). The adaptive immune response to Mtb is initiated between 3-4 weeks post-infection, but robust bacterial killing in granulomas is only observed after 8 weeks. This study looked specifically at 4 weeks and 8 weeks post-infection, with IL-10 depletion throughout the course of infection, beginning one day before Mtb infection. We maintained IL-10 depletion throughout the study by infusions with the anti-IL-10 antibody approximately every 10 days. A dose of 15mg/kg was chosen based on unpublished data from a similar human antibody in cynomolgus macaques, which indicated effectiveness without side effects. Lack of IL-10 has been shown to cause intestinal inflammation and colitis in both human genetic studies and animal models [276-278]. Our collaborators confirmed that this dose of anti-IL-10 antibody in our cynomolgus macaque model did not cause adverse side effects and colitis in uninfected cynomolgus macaques (data not shown).

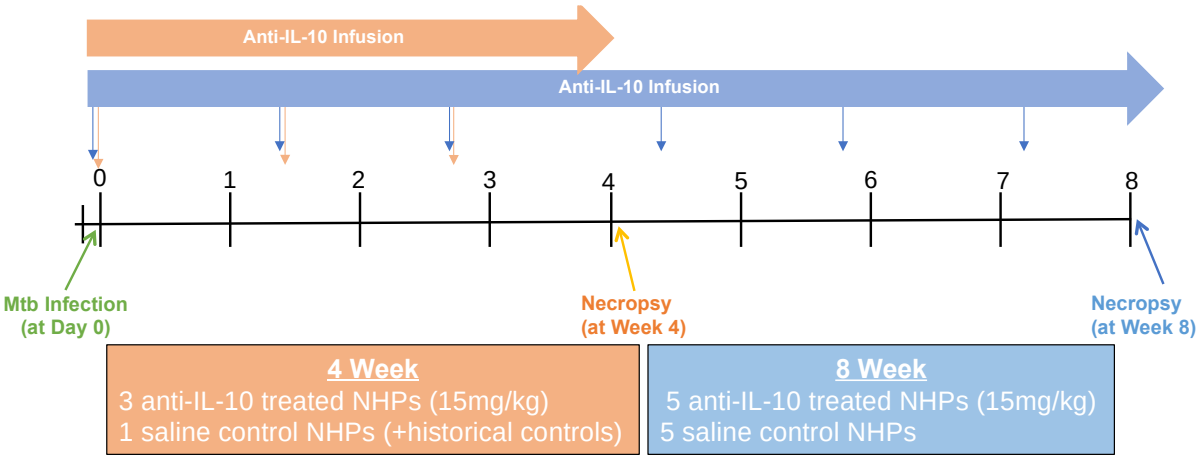

Figure 4. Experimental setup for study of IL-10 neutralization in vivo in cynomolgus macaques for 4 weeks and 8 weeks.

In each study, anti-IL-10 antibody infusions began one day before Mtb infection and continued throughout the course of infection, for every 10 days (+/-3 days).

2.3.3 Early peripheral and tissue-specific response to IL-10 neutralization

During the course of the study, we tracked the peripheral effects of IL-10 neutralization on the immune response to Mtb infection. Since IL-10 can affect many immune cell types in addition to lymphocytes, we tested the peripheral immune cell response to Mtb by stimulating whole blood from critical time points during the course of infection (Figure 5A) and measuring IL-10 by multiplex immunoassay (Luminex). Since this assay does not distinguish between active and inactive IL-10, the cytokines detected could be bound by the anti-IL-10 antibody. While unstimulated (media only) whole blood cells had undetectable levels of IL-10 throughout the Mtb infection, the neutralization of IL-10 led to sustained peripheral IL-10 responses to Mtb

stimulation in whole blood through 4 weeks. In comparison, control animals peaked in their response to Mtb at 2 weeks. This suggests the host immune response produces IL-10 in response to Mtb early in infection (2 weeks), and in the absence of functional IL-10, this response may continue for an additional 2 weeks before additional immune response factors compensate for IL-10 by 8 weeks post-infection.

We also followed the inflammatory response in the lungs over the course of Mtb infection using PET-CT imaging of ^{18}F-FDG uptake as a marker of inflammation. Overall lung inflammation was similar between the anti-IL-10 treated animals and the saline control animals (Figure 5B). But when we further examined the FDG avidity within individual granulomas, we found a subset of granulomas in anti-IL-10 treated animals had much lower levels of inflammation, particularly early in infection, at 3 and 4 weeks post-infection (Figure 5C). Although there was a range of FDG activity in granulomas in both groups, a subset of the granulomas from IL-10 neutralized animals were extremely low, which was not seen in saline-treated animals. Granulomas from anti-IL-10 treated animals tended to have low inflammation through the 8 weeks of infection, while granulomas from saline animals started with higher inflammation, peaking at 4 weeks post-infection, and then decreasing to similar levels as anti-IL-10 granulomas by 8 weeks. The reduction in inflammation after neutralizing an anti-inflammatory cytokine, IL-10, in TB granulomas was a surprising result. Since ^{18}F-FDG is a marker of metabolic activity, and a general indicator of inflammation, these results suggest that IL-10 may be indirectly or directly acting on the inflammation in a granuloma.

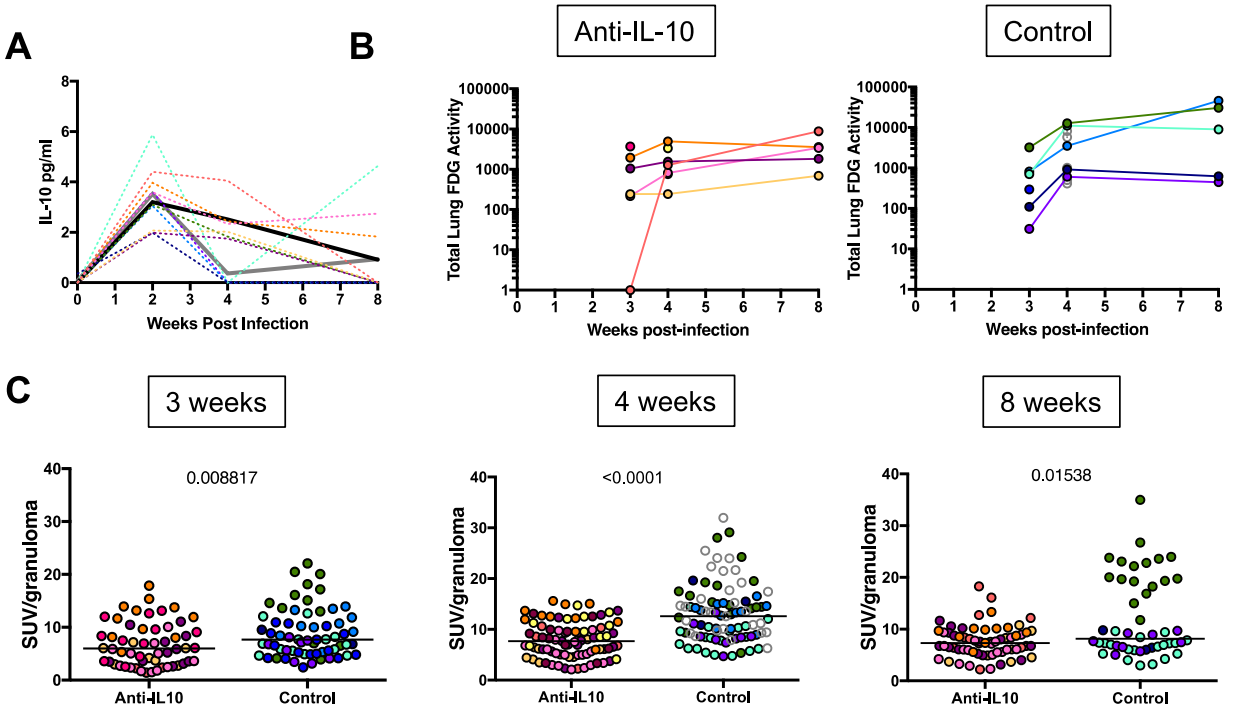

Figure 5. Early peripheral and lung response to anti-IL-10 treatment.

(A) Whole blood IL-10 response to gamma-irradiated Mtb over the course of Mtb infection (p = 0.02 at 4 Weeks post-infection, Mann-Whitney test). Each dotted line/color indicates a NHP, solid black line indicates average of anti-IL-10 NHPs, solid gray line indicates average of control NHPs. (B) Total lung inflammation (total 18F-FDG uptake) during the course of infection, anti-IL-10 treated and saline control. Each color indicates a NHP. Gray points indicate historical controls. (C) ^{18}F-FDG-uptake in individual lung granulomas during the course of infection, as measured by standard uptake value normalized to muscle (SUV) Each point is a granuloma identified from PET-CT scans, each color is a NHP. Lines at medians. Numbers indicate p-values from Mann-Whitney test.

2.3.4 Neutralization of IL-10 does not affect early disease outcome

The differences in early peripheral response and granuloma inflammation did not translate to overall disease outcome. Anti-IL-10 treated animals had similar disease pathology at the end of 4 and 8 weeks of infection as untreated animals (Figure 6). Their total thoracic (lung plus lymph node) bacterial burden, as well as bacterial burden within individual granulomas, was also similar between the two groups at both 4 and 8 weeks post-infection. Few animals had evidence of extrapulmonary disease, and there were no differences between the anti-IL-10 and control groups (data not shown). Lower inflammation in granulomas at 4 weeks did not seem to lead to less disease pathology or bacterial burden.

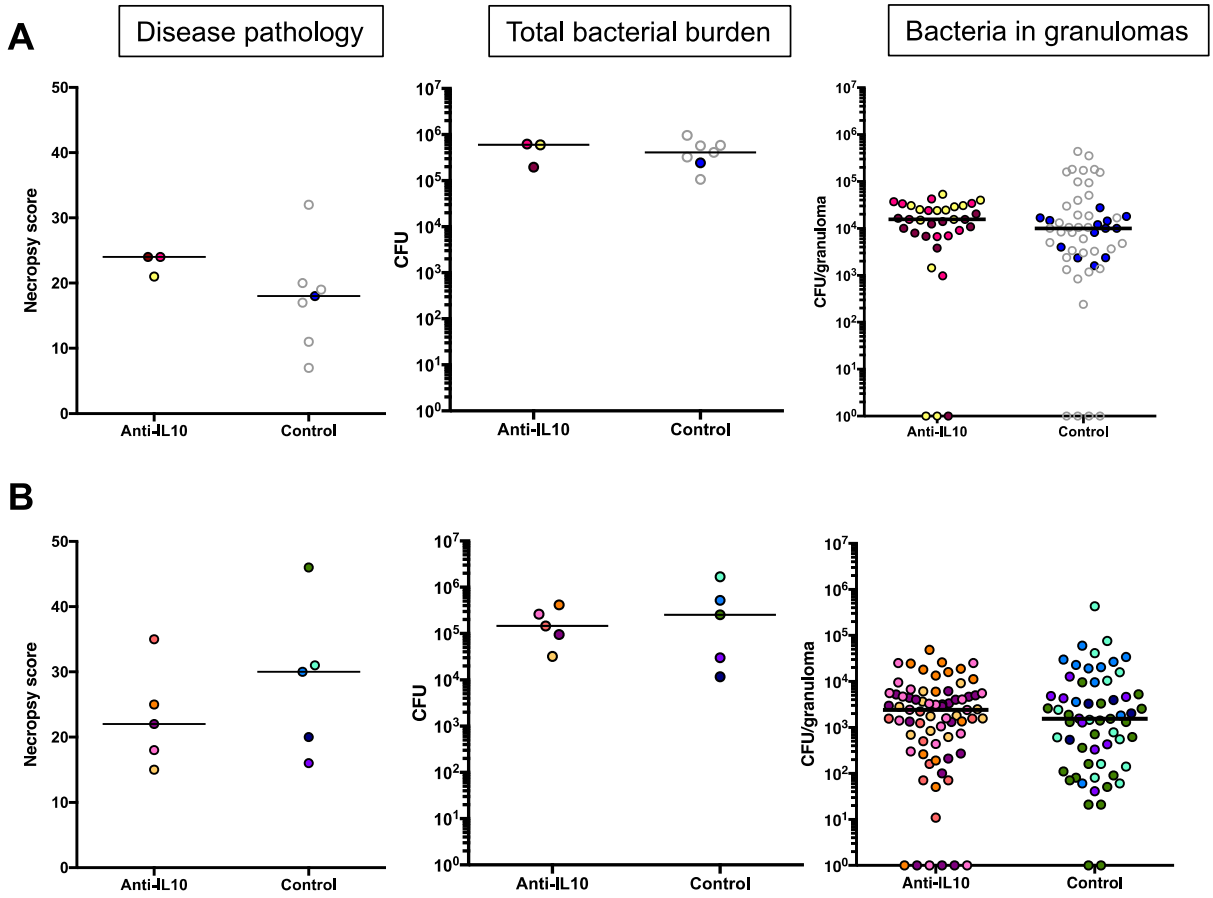

Figure 6. Disease pathology and bacterial burdens.

Similar disease outcomes between anti-IL-10 treated animals compared to untreated animals at (A) 4 weeks and (B) 8 weeks post-infection. Disease pathology quantified by necropsy scores, which measures amount of disease pathology in lungs, lymph nodes, and extrapulmonary sites. Bacterial burden measured by colony forming units (CFU) in all lung and lymph node samples for total bacterial burden, and in individual excised granulomas for bacteria in granulomas. Each point/color in disease pathology and total bacterial burden graphs indicate a NHP, gray indicates historical controls. Each point in bacteria in granulomas graph indicate a granuloma, each color indicates a monkey, gray indicates samples from historical controls. Lines at medians.

2.3.5 IL-10 neutralization does not affect lung granuloma cell composition or T cell function

To further assess the effects of anti-IL-10 treatment on the immune cells in lung granulomas and granuloma clusters, we looked at the frequencies of cell populations by flow cytometry (Figure 7). Although some granulomas in anti-IL-10 treated animals had higher frequencies of some cell populations than granulomas from saline controls, overall the cell populations within granulomas were similar between the two groups at 4 and 8 weeks post-infection (Figure 8A and 8B). We further investigated T cell populations in unstimulated granulomas by flow cytometry, looking at regulatory T cell populations (CD4+FOXP3+), activated T cells (CD69+), and Th1 cells (IFN-γ+TNF+) (Figure 9). We could not discern a difference in T cell populations between the anti-IL-10-treated and untreated animals.

Since we observed neutralization of IL-10 in TB granulomas *ex vivo* increased IL-2 response, we asked whether the anti-IL-10 antibody infusions *in vivo* also increased T cell IL-2 responses. As we had observed *ex vivo*, some of the granulomas from anti-IL-10 treated animals had higher IL-2 responses from the T cells compared to granulomas from the saline control animals, but it was not consistent (Figure 9). Perhaps only a subset of the granulomas in the anti-IL-10 animals were IL-10 responsive, and thus had differential response with IL-10 neutralization.

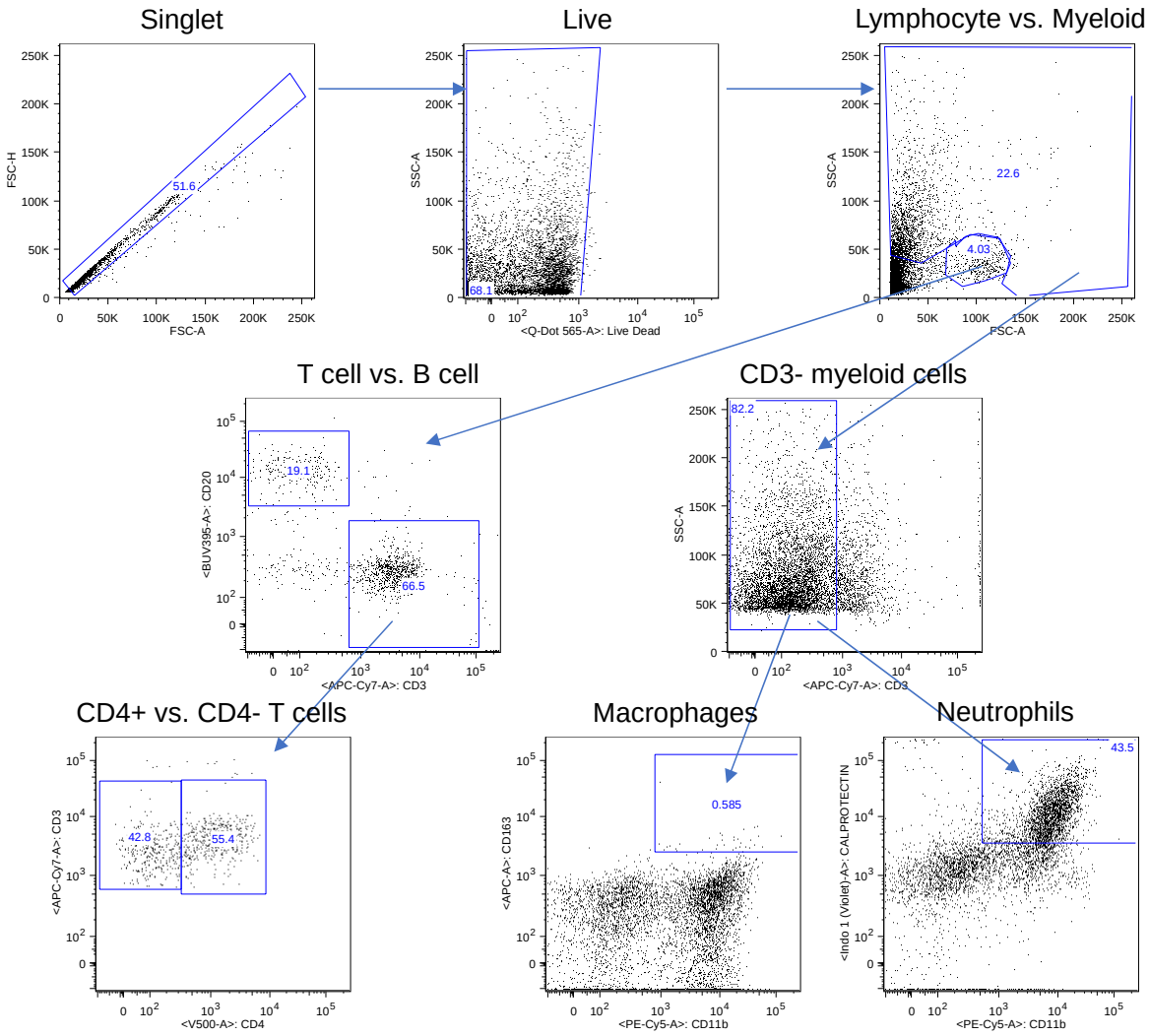

Figure 7. Flow cytometry gating strategy for cell populations.

Gating strategy from representative lung granuloma used to distinguish different cell populations, using CD3 as a T cell marker, CD20 as a B cell marker, CD11b and CD163 as macrophage markers, and CD11b and calprotectin as neutrophil makers. CD3 T cell population further separated into CD4+ and CD4- populations, with CD4- cells used to approximate the CD8 T cell population.

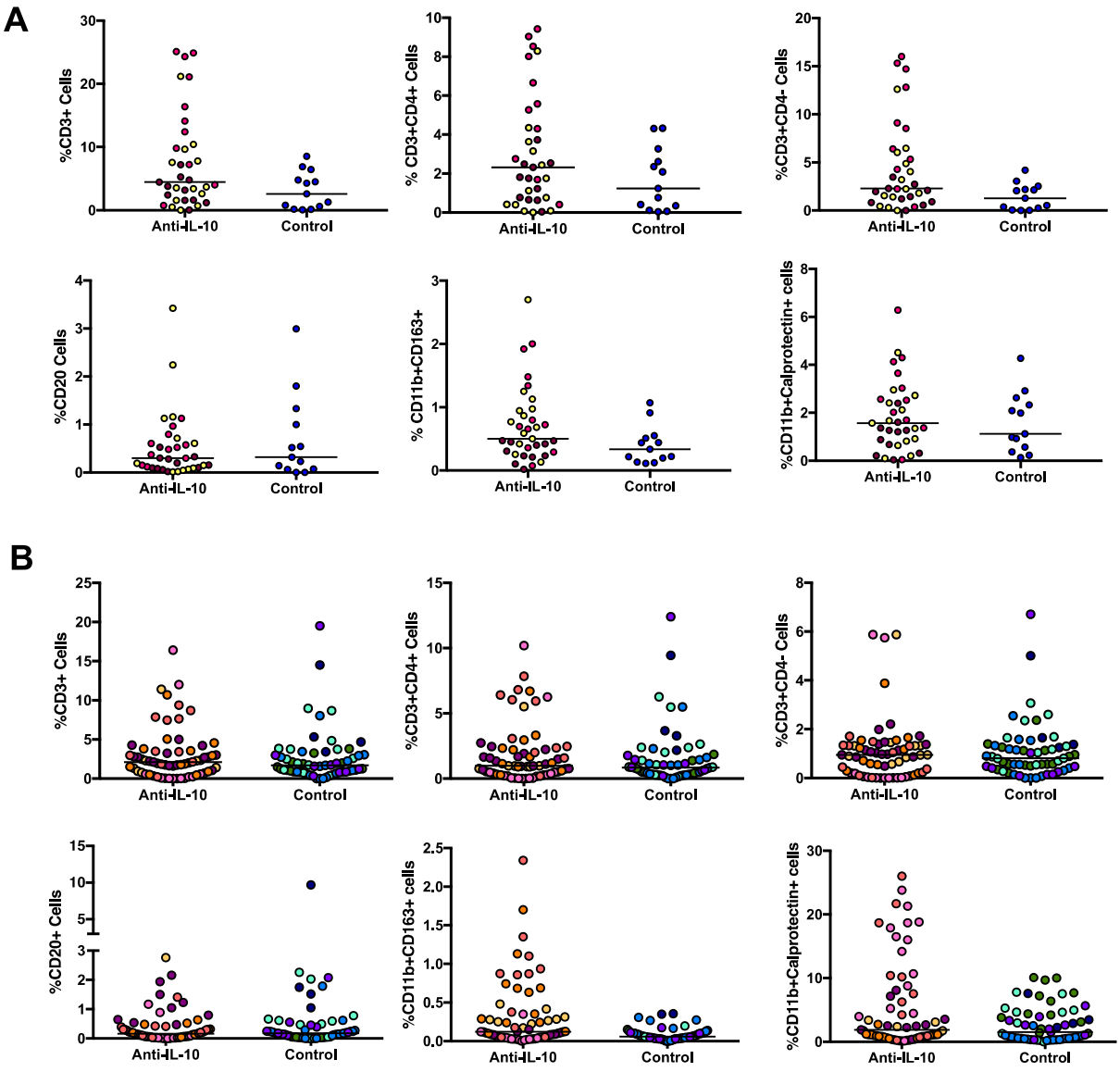

Figure 8. Immune cell populations in lung granulomas and lung clusters.

Similar frequencies of immune cell populations in lung granulomas and granuloma clusters between anti-IL-10 treated and untreated animals at (A) 4 weeks and (B) 8 weeks of infection. CD3 is used as a marker of T cells, CD4 is used as a marker of CD4 T cells, CD4- is used as an approximation of CD8 T cells, CD20 is used as a marker of B cells, CD11b+CD163+ is used as a marker of macrophages, CD11b+Calprotectin+ is used as a marker of neutrophils. Each point represents a lung granuloma or cluster of granulomas, each color is a NHP. Lines are at medians.

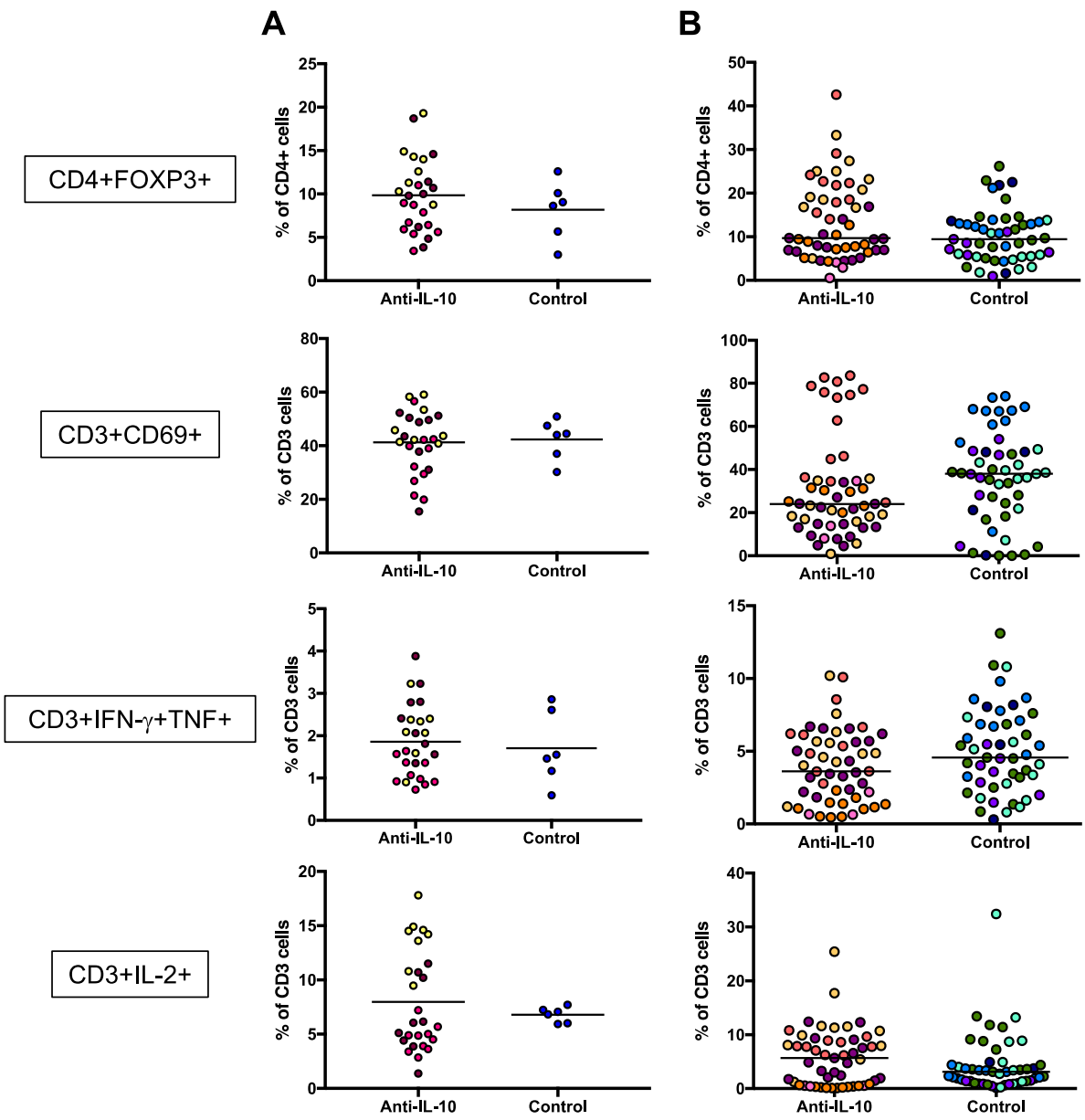

Figure 9. T cell populations in lung granulomas and granuloma clusters.

Similar T cell population frequencies between anti-IL-10 treated and untreated controls at (A) 4 weeks and (B) 8 weeks of infection. CD4+FOXP3+ is used as a marker of regulatory T cells, CD3+CD69+ is used as a marker of T cell activation, CD3+IFN-g+TNF+ is used as a marker of Th1 cells, and CD3+IL-2+ is used as a marker of T cells producing IL-2. Each point represents a lung granuloma or cluster of granulomas, each color is a NHP. Lines are at medians.

2.3.6 IL-10 receptor is most commonly expressed on non-T cells in TB granulomas

Since we did not observe many differences in the T cell populations or their cytokine responses in lung granulomas despite our initial results *ex vivo* IL-10 neutralization results (Figure 3B), we sought to measure the number and types of cells in TB granulomas that would be responsive to IL-10. By immunohistochemistry, we determined that the majority of cells in TB granulomas expressing IL-10 receptor (IL-10R) were not CD3+ at either 4 weeks or 8 weeks (Figure 10A and 10B). Instead, IL-10R co-localized more with CD11c+ macrophage clusters on the outer edge of the granuloma macrophage region and with CD20+ B cells in the lymphocyte cuff (Figure 10B and 10C). A few CD3 cells co-expressed IL-10R, but most of the IL-10R signal was not on CD3 cells (Figure 10 insets). Although IL-10 has immunosuppressive effects on T cells (which may be indirect), perhaps the T cells in TB granulomas were not as affected by the absence of IL-10 during anti-IL-10 neutralization because they tend to be the minor IL-10R-expressing immune cell in the granuloma. Thus, IL-10 neutralization may have a more significant role on the immune response of non-T cells in TB granulomas, such as macrophages and B cells.

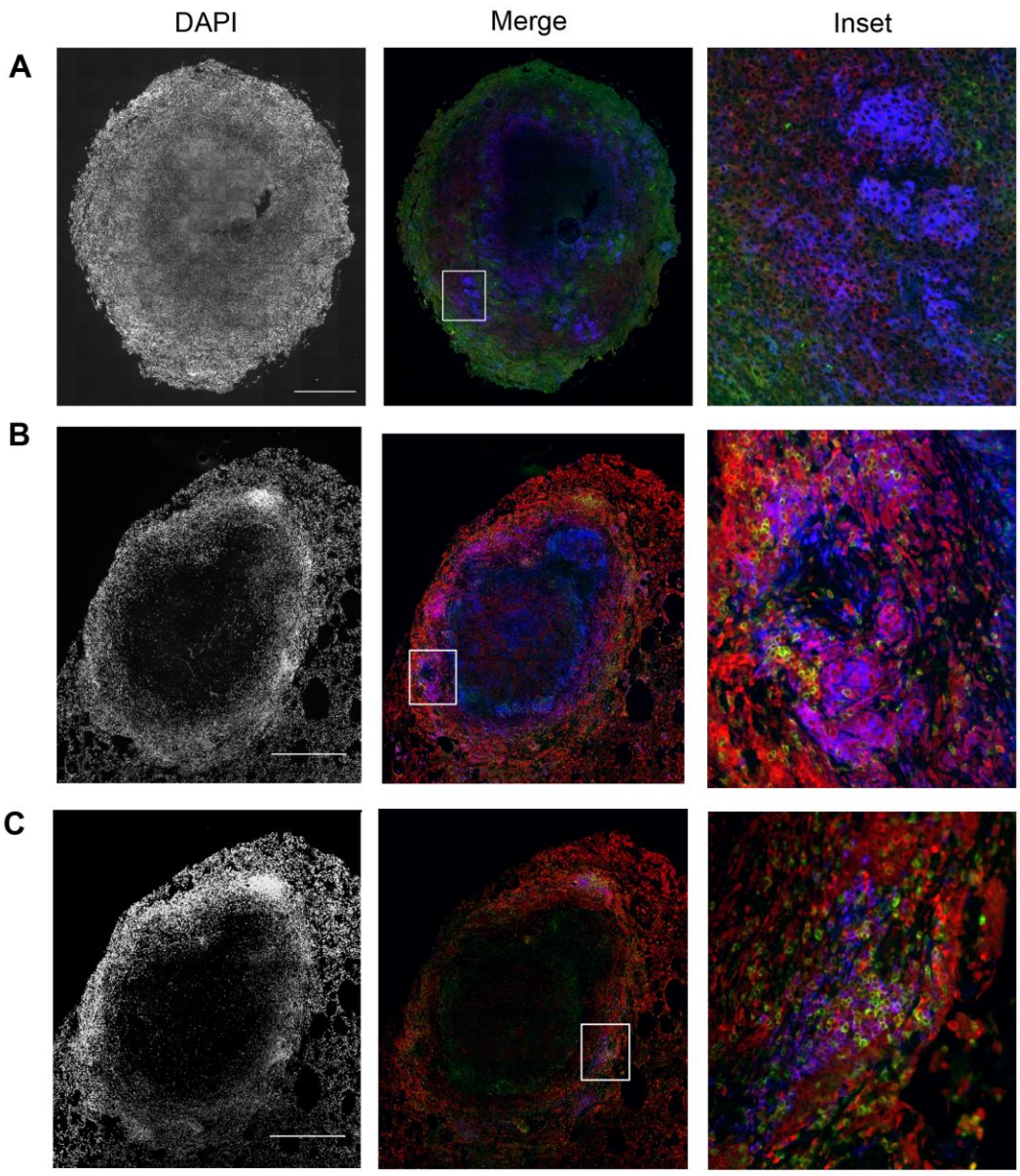

Figure 10. IL-10R co-localizes with non-T cells in TB granulomas.

(A) A representative granuloma from 4 weeks of Mtb infection has more co-localization of IL-10R (red) with CD11c-expressing cells (blue) than CD3-expressing cells (green). (B) A representative granuloma from 8 weeks of Mtb infection also has more IL-10R (red) co-localization with CD11c cells (blue) than CD3 cells (green). (C) The same granuloma as in (B)

shows that the B cells (blue) are IL10R-positive (red), along with a few CD3 cells (green) also expressing IL-10R. Scale bar in DAPI indicates 500um.

2.3.7 IL-10 neutralization increases innate cytokine response and fibrosis in lung granulomas

While we did not discern differences in cell populations or their potential frequencies of cytokine response within lung granulomas and clusters of granulomas, total concentrations of certain cytokines in granulomas were different between anti-IL-10 treated and untreated control animals. Cytokines in supernatants of granuloma homogenates were measured using the multiplex immunoassay Luminex. At 4 weeks post-infection, anti-IL-10 treated animals had increased levels of IL-2, IL-13, IL-12p70, and IL-23 compared to granulomas from control animals (Figure 11A). These cytokines are likely produced by innate cells, as well as T cells, but neutralization of IL-10 did not lead to increases in all cytokine responses. Anti-IL-10-treated animals had reduced IL-18 and IL-1beta in their granulomas compared to control granulomas (Figure 11A).

By 8 weeks post-infection, most of the T cell inducing cytokines that were prominent at 4 weeks post-infection were no longer detectable or were no longer significantly different in granulomas of anti-IL-10 and saline treated animals (Figure 11B). Instead, granulomas from anti-IL-10 treated animals had lower levels of total IL-1beta, IL-1RA, IL-6, and IFN-beta compared to granulomas from untreated animals. IL-23, which was significantly increased at 4 weeks post-infection in anti-IL-10 animals, tended to be lower in anti-IL-10 granulomas at 8 weeks post-infection. IL-10 may reduce the innate and adaptive immune response in lung granulomas early

in infection at 4 weeks, but have a differential effect and increase innate cytokine response after 8 weeks of Mtb infection.

These differences in cytokine response in granulomas from anti-IL-10 animals may change the granuloma structure during Mtb infection. Blinded histopathological analysis of granulomas from both treatment groups revealed more evidence of fibrosis in granulomas from animals treated with anti-IL-10 at the time of necropsy compared to control animals (Figure 12A). Nearly half of the granulomas analyzed from anti-IL-10 animals showed signs of fibrosis, which may suggest that IL-10 prevents healing-associated fibrosis in lung granulomas during Mtb infections. It is possible that the fibrosis in lung granulomas contributes to the lower levels of inflammation previously observed at 4 weeks of infection (Figure 5C and 12B), perhaps due to fewer metabolically active immune cells.

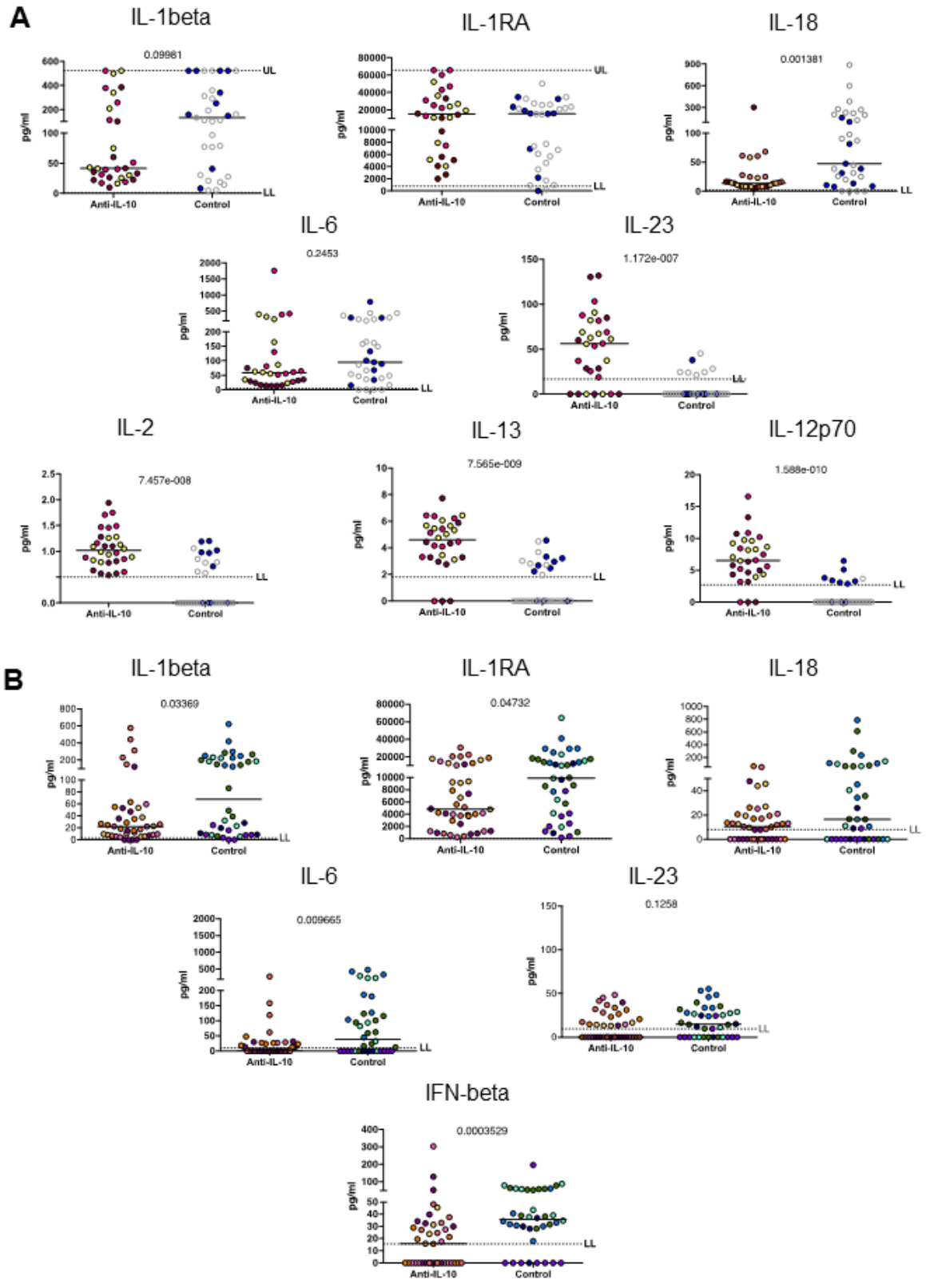

Figure 11. Total cytokine response in lung granulomas and granuloma clusters.

Total cytokine response in lung granulomas and granuloma clusters are higher in anti-IL-10 treated animals (A) at 4 weeks post-infection, but lower (B) at 8 weeks post-infection. Each point represents a lung granuloma or cluster of granulomas, each color is a NHP. Lines are at medians. P-values from Mann-Whitney test.

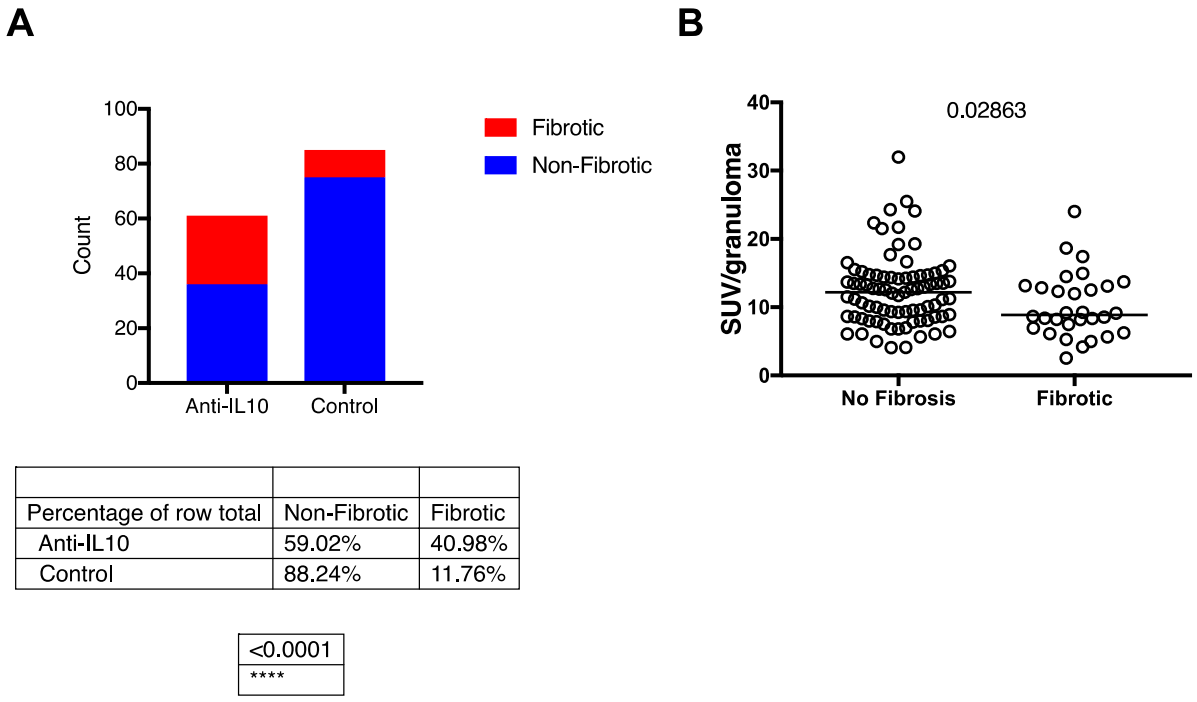

Percentage of row total	Non-Fibrotic	Fibrotic
Anti-IL10	59.02%	40.98%
Control	88.24%	11.76%

<0.0001
****

Figure 12. Fibrosis in lung granulomas.

More fibrotic granulomas from anti-IL-10 treated NHPs compared to untreated controls. (A) Numbers of granulomas with signs of fibrosis compared to non-fibrotic granulomas in the two treatment groups at time of necropsy, anti-IL-10 = 13 NHPs, control = 8 NHPs. P-value from Fisher's exact test. (B) Comparison of ^{18}F[FDG] uptake in lung granulomas at 4 weeks of infection to signs of fibrosis at the time of necropsy. P-value from Mann-Whitney test.

2.3.8 IL-10 inhibits cell recruitment and immune response in lymph nodes

Considering the strong increase in T cell-promoting cytokines, such as IL-2 and IL-12p70, in the absence of IL-10 at 4 weeks post-infection by Luminex, we expected this increase to lead to more T cells or increased T cell function. However, as shown in Figures 8 and 9, there were no differences in frequencies of T cell populations in lung granulomas as assessed by flow cytometry at 4 weeks post-infection. Since thoracic lymph nodes are also infected in macaques, we investigated whether IL-10 neutralization affected the T cell response to Mtb infection in lymph nodes (LNs).

After 4 weeks of infection, the Mtb-infected LNs of anti-IL-10 treated animals had higher levels of bacterial burden compared to control animals (Figure 13A, anti-IL-10 median = 4.98log CFU, control median = 3.4log CFU). Along with the higher bacterial burden, these Mtb-infected LNs had skewed CD4+/CD4- T cell ratios by flow cytometry (Figure 13B). Because of limited space in flow cytometry panels, CD3+CD4- was used as a substitute for CD8 T cells, as previous data had shown that the majority of CD3+CD4- cells were CD3+CD8+ cells. By calculating the numbers of CD3+ T cells in the LNs, at 4 weeks post-infection, there were 4-fold more CD4- (likely CD8+) T cells in LNs of anti-IL-10 treated animals (median = $1.32x10^7$ cells) compared to control animals (median = $3.62x10^6$ cells), while numbers of CD4+ cells were similar between both groups (anti-IL-10 median = $6.35x10^6$ cells, control median = $4.09x10^6$ cells) (Figure 13C and 13D). Similar to the lung granulomas, the total cytokine concentrations in the Mtb-infected LN supernatants of the anti-IL-10 animals had higher levels of T cell-promoting cytokines IL-2 and IL-12p70 compared to LNs of control animals. The Mtb-infected LNs of anti-IL-10 animals also had more IFN-γ and TNF compared to control animals. Interestingly, there were also increased levels of lymphocyte recruiting chemokines in the LNs of anti-IL-10 animals (Figure

13E). This suggests that during Mtb infection, IL-10 may normally prevent T cell proliferation and recruitment in LNs, particularly of CD4- T cells.

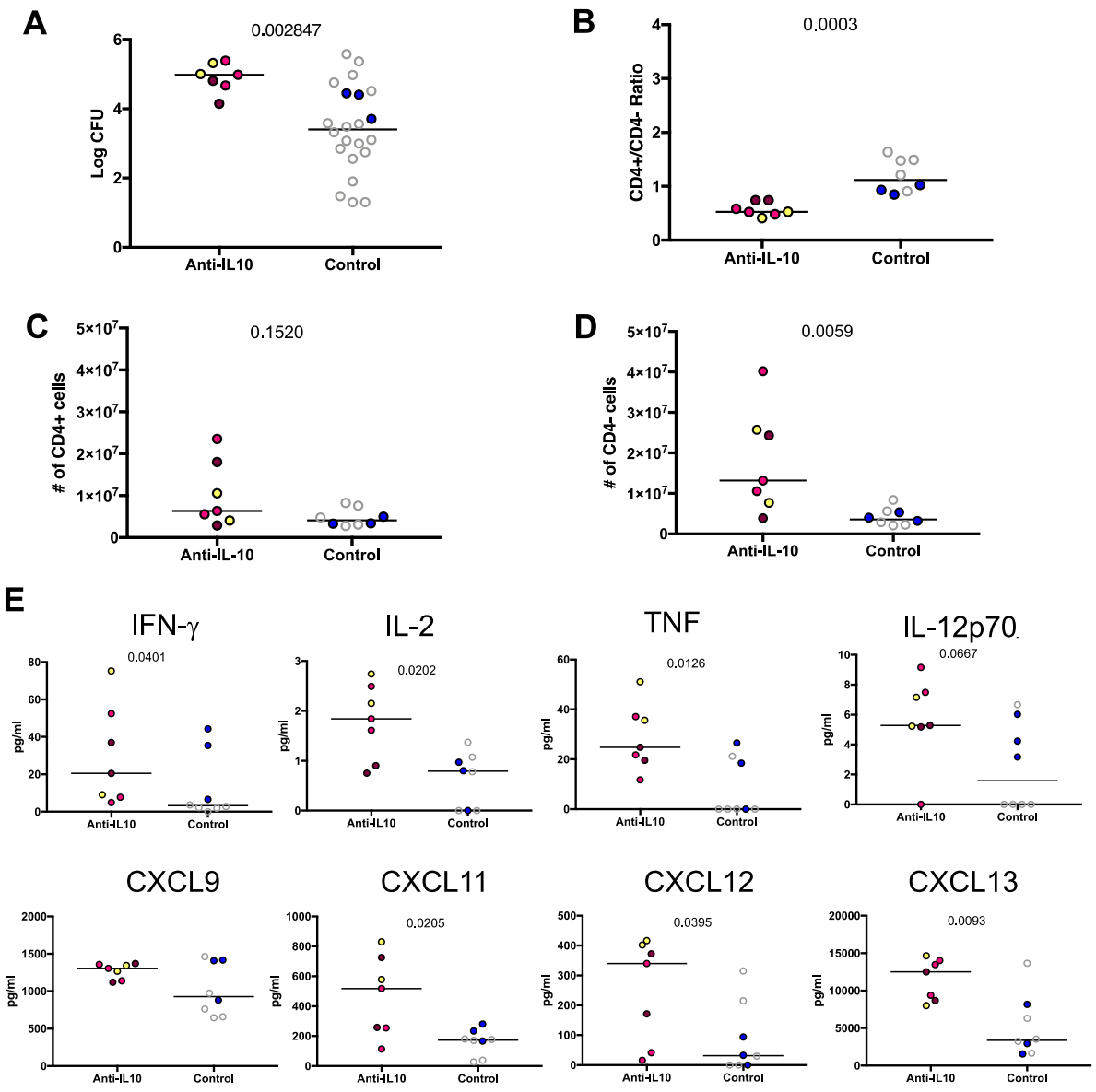

Figure 13. Bacterial burden and immune response in LNs at 4 weeks post-infection.

Neutralization of IL-10 leads to uncontrolled bacterial replication and skewed T cell responses in LNs at 4 weeks post-infection. (A) Bacterial burden is higher in Mtb-infected LNs at 4 weeks post-infection. (B) At 4 weeks post-infection, anti-IL-10 treated animals have skewed CD4/CD4- ratios of CD3+ T cells compared to control animals by flow cytometry. The numbers of CD3+ T cells that are (C) CD4 and (D) CD4- in LNs show that there are more CD4- cells in LNs of anti-

IL-10 treated animals. E) At 4 weeks post-infection, LNs from anti-IL-10 treated animals have higher total cytokine and chemokine responses, particularly lymphocyte-inducing chemokines. Each point is a Mtb-infected LN, each color is a NHP, gray indicates historical control. P-values from Mann-Whitney tests.

However, after an additional 4 weeks of Mtb infection, there was no longer a difference in the bacterial burden in Mtb-infected LNs between the two groups and the ratio of T cell subsets in anti-IL-10 animals reversed, with more CD4+ T cells relative to CD4- T cells (CD4/CD4-ratio median = 1.91) in the IL-10 neutralized group (Figure 14A and 14B). While the number of CD4+ T cells in Mtb-infected LNs were similar at 8 weeks to their numbers at 4 weeks (anti-IL-10 median = $4.2x10^6$ cells, control median = $1.112x10^6$ cells), the elevated numbers of CD4- T cells observed in anti-IL-10 treated animals 4 weeks of Mtb infection greatly decreased by 8 weeks (median = $2.4x10^6$ cells) (Figure 14C and 14D). Thus, after 8 weeks of Mtb infection, the numbers of CD4- T cells in the LNs of anti-IL-10 treated animals decreased, so that not only were there fewer CD4- T cells at 8 weeks relative to CD4+ T cells, but there were also much fewer CD4- T cells at 8 weeks compared to at 4 weeks post-infection. These changes caused the lymph node ratio to then be skewed in the other direction from 4 weeks post-infection.

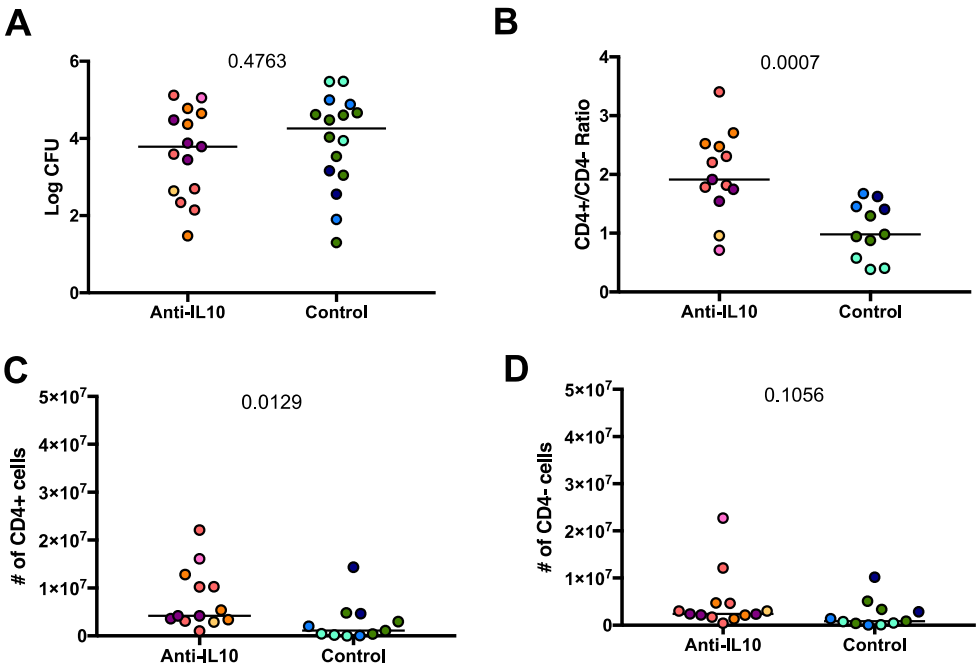

Figure 14. Bacterial burden and immune response in LNs at 8 weeks post-infection. Neutralization of IL-10 leads to skewed T cell responses in LNs at 8 weeks post-infection. (A) Bacterial burden is similar in Mtb-infected LNs from both treatment groups at 8 weeks post-infection. (B) At 8 weeks post-infection, anti-IL-10 treated animals have skewed CD4/CD4- ratios compared to control animals. The numbers of (C) CD4 and (D) CD4- cells in LNs show that there are more CD4- cells in LNs of anti-IL-10 treated animals. Each point is a Mtb-infected LN, each color is a NHP. P-values from Mann-Whitney tests.

The increased bacterial burden, CD4- T cells, T cell-promoting cytokines, and lymphocyte recruiting chemokines at 4 weeks of Mtb infection in the absence of functional IL-10 correlated with an increase in LN effacement (necrosis) compared to control animals (Figure 15A). Along with the effacement, the Mtb-infected LNs from anti-IL-10 treated animals also had increased numbers of total immune cells compared to those from control animals (Figure 15B).

By 8 weeks, however, there are similar numbers of effaced LNs from anti-IL-10 treated and untreated animals, and the Mtb-infected LNs have similar numbers of immune cells (Figure 15C and 15D). Thus, anti-IL-10 treatment may cause earlier effacement of LNs compared to control animals. Taken together, these results suggest that during Mtb infection, IL-10 may help control bacterial growth in LNs, prevent too much T cell proliferation and recruitment, and thus delay LN effacement.

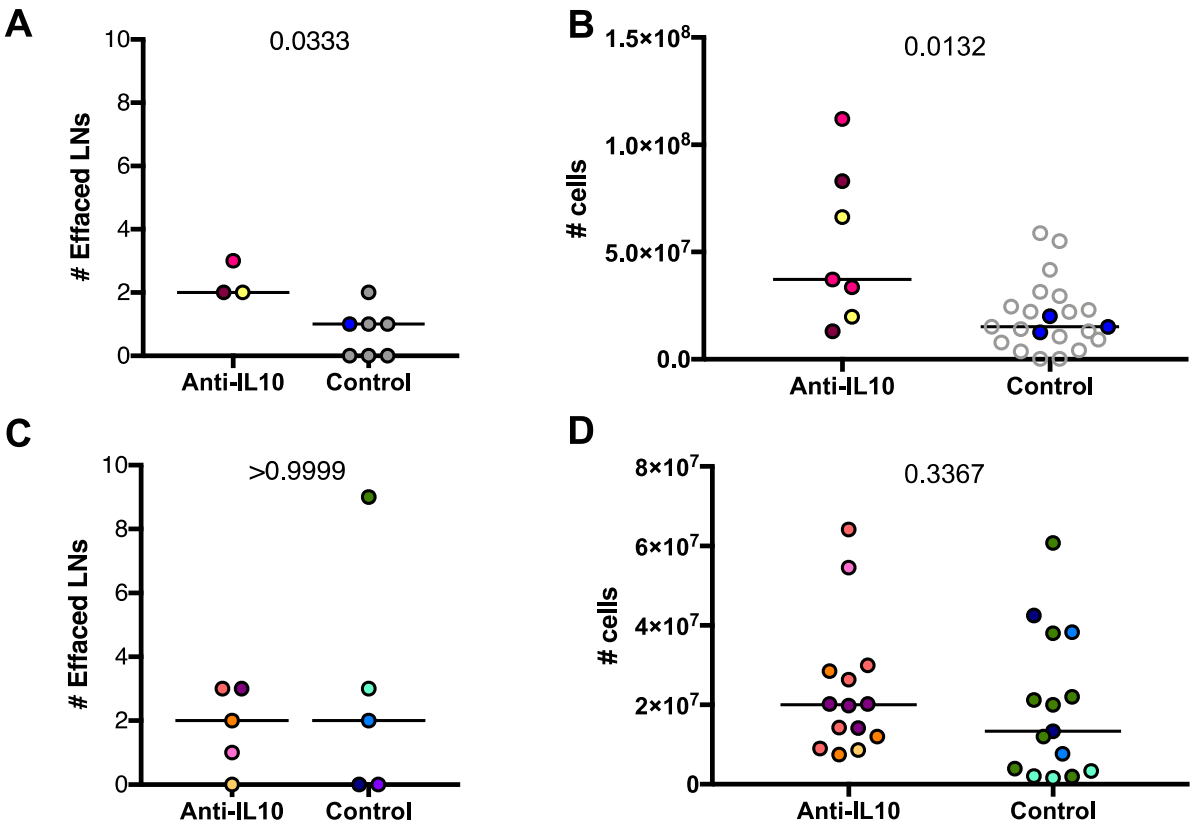

Figure 15. LN effacement at 4 and 8 weeks post-infection.

(A) Anti-IL-10 treatment in animals increases LN effacement early at 4 weeks post-infection, with (B) higher numbers of cells within LNs within anti-IL-10 treated animals. In anti-IL-10 group, number of LNs analyzed per NHP ranged from 7-10. In control group, number of LNs

analyzed per NHP ranged from 7-11. (C) At 8 weeks post-infection, the number of effaced LNs are similar between anti-IL-10 and control animals, with (D) similar numbers of cells in LNs from both experimental groups. In anti-IL-10 group, number of LNs analyzed per NHP ranged from 8-11. In control group, number of LNs analyzed per NHP ranged from 8-12. Each point is a Mtb-infected LN, each color is a NHP, gray indicates historical control. P-values from Mann-Whitney tests.

2.4 DISCUSSION

Nearly a third of the world's population is infected with Mtb, yet the correlates of protection are still unknown. Although pro-inflammatory cytokines have been demonstrated to be necessary to control Mtb replication, the role of anti-inflammatory cytokines to counteract these tissue-damaging cytokines have not been fully elucidated. Previous studies had contradictory conclusions about the beneficial or harmful role of IL-10 during Mtb infection [102, 132-142]. Some studies suggested that IL-10 may have differential roles during Mtb infection depending on stage of infection [134, 136]. We sought to clarify the role of IL-10 within TB lung granulomas using our NHP model of TB and an anti-IL-10 antibody that we demonstrated to neutralize macaque IL-10. Our preliminary *ex vivo* results suggested that IL-10 may downregulate the T cell cytokine response and that not all TB granulomas may be responsive to IL-10. Our *in vivo* study neutralizing the effects of IL-10 in a cohort of NHPs during early Mtb infection (4 and 8 weeks) demonstrated that IL-10 may be downregulating the cytokine response and increasing inflammation in lung granulomas and lymph nodes very early in Mtb infection (4 weeks), but may have fewer effects by 8 weeks of Mtb infection. However, the presence or

absence of IL-10 does not ultimately influence the host control over bacterial burden or disease pathology, at least up to 8 weeks of infection.

The results from this study indicate that IL-10 has the greatest effect on the host immune response to Mtb infection early in infection, within the first 4 weeks of infection. Our peripheral data indicated that the circulating immune cells respond to Mtb by producing IL-10 early on in infection, after 2 weeks of infection, but this response was reduced by 4 weeks of infection. In the absence of IL-10, the peripheral immune cells from the anti-IL-10 treated animals continued to produce significantly higher levels of IL-10 in response to Mtb stimulation. Mtb is a well-documented stimulator of IL-10 production [128, 279], but the neutralization of IL-10 response in anti-IL-10 treated animals seemed to sustain the IL-10 production by Mtb-responsive immune cells longer than control animals. It is possible that the lack of IL-10 prevented downstream mechanisms and downregulation of response to Mtb stimulation, or that lack of active IL-10 interrupted a feedback loop of IL-10 regulation.

The increase in cytokine response in lung granulomas and LNs at 4 weeks after anti-IL-10 treatment was expected, particularly in the pro-inflammatory cytokines IL-23, IL-2, and IL-12p70 in the lungs, and the Th1 cytokines (IFN-γ, IL-2, TNF) and IL-12p70 in the LNs. IL-10 has been demonstrated to be anti-inflammatory, and the blockade or removal of IL-10 from *in vitro* and *in vivo* experimental models increased pro-inflammatory cytokine response, particularly in macrophages and T cells [125-127]. Our initial *ex vivo* experiments indicated that IL-10 neutralization affected the T cell IL-2 response. While our *in vivo* experiments showed increased T cell inducing cytokines and chemokines in the lung granulomas and LNs, we did not observe increased frequencies or numbers of T cells in the absence of functional IL-10. However, increased cytokines and chemokines, particularly in the LNs, may be increasing T cell

priming and functionality. Increased LN responses in the absence of IL-10 during Mtb infection were also observed in previous studies [132, 136]. Interestingly, unlike Redford et al., who observed increased numbers of CD4+ T cells in the draining LNs of IL-10 knock-out mice compared to controls [132], we observed increased numbers of CD4- (presumably CD8+) T cells, particularly at 4 weeks post-infection. Our results were more similar to studies in acute LCMV infection, where blockade of IL-10 during acute LCMV infection increased CD8 T cells, particularly during the priming phase [280, 281]. IL-10 has also been shown to inhibit CD8 T cell responses in other models of infection, such as in listeria and HIV [282, 283]. However, the heightened LN T cell responses and recruitment did not necessarily translate into host control or clearance of Mtb infection, and seemed to only accelerate LN effacement.

Many of the T cell promoting cytokines and chemokines that were produced in anti-IL-10 treated animals are produced by myeloid cells. There were also lower concentrations of macrophage-produced cytokines (IL-1beta, IL-1RA, IL-18, IL-6) in lung granulomas of anti-IL-10 treated animals at 8 weeks. In addition, as we and others have demonstrated, the receptor for IL-10 (IL-10R) is predominantly on non-T cells, especially in TB granulomas [138, 284, 285]. A study investigating overexpression of IL-10 during Mtb infections concluded that macrophage IL-10 was the most crucial aspect of controlling Mtb numbers [138]. Thus, although IL-10 can affect most immune cells, it may primarily affect myeloid cells in the context of Mtb infections. This also corresponds to the change in the immune response in anti-IL-10 treated animals between 4 and 8 weeks of Mtb infection. Since IL-10 may have the most influence on myeloid cells in Mtb infections, it is reasonable that it may cause the most changes during the initial stages of the infection, when the innate immune response dominates in the lungs and in priming, followed by smaller effects after the onset of the adaptive immune response around 6 weeks of

infection [68]. Thus, while we observed greater changes in the cytokine and chemokine response in anti-IL-10 animals after 4 weeks of infection, the adaptive immune response may counteract and minimize the influence of IL-10 by 8 weeks.

The lack of functional IL-10 in this study increased fibrosis in lung granulomas at the time of necropsy (4 or 8 weeks). The role of fibrotic lesions in TB is unclear, but they tend to be associated with containment, drug treatment, and sterility [286, 287]. Fibrosis is a healing response that can result in pathology but can also limit spread of infection, and is not generally observed at early time points in Mtb infection, but is seen more at later time points. Early blockade of IL-10 during Mtb infection also led to fibrotic granuloma formation in the mouse model [136]. Higgins et al. also observed changes in granuloma structure of IL-10 knock-out mice [139]. While we did not observe the same levels of bacterial control in our NHP model, neutralization of IL-10 significantly increased the fibrosis and collagenization of lung granulomas. The significance of fibrosis in granulomas is currently unclear, but the fibrosis in lung granulomas may lead to improved bacterial containment and/or modified lung pathology in the long term beyond the scope of this study.

Surprisingly, a subset of granulomas from the anti-IL-10 treated animals had very low levels of ^{18}F-FDG uptake, a metabolic proxy for inflammation, especially during early Mtb infection. This also contrasted with the higher levels of pro-inflammatory cytokines, such as IL-23, IL-2, IL-12p70 that we measured from lung granulomas. The increased fibrosis in the lung granulomas of anti-IL-10 treated animals could also decrease the amount of metabolically active cells in the granulomas. The measured inflammation could be more influenced by the lower concentrations of pro-inflammatory cytokine IL-18 and higher concentrations of anti-inflammatory cytokine IL-13 we observed. However, because of the non-specificity of ^{18}F-FDG,

other unmeasured factors or indirect effects could be causing the decrease in granuloma inflammation in the absence of functional IL-10.

Although neutralization of IL-10 caused transient increase in cytokine and chemokine response, these increased immune responses did not affect the overall disease pathology or bacterial burden at either of the two time points investigated in this study. The absence of IL-10 during Mtb infection did not decrease the bacterial load in the lungs (or individual granulomas) or lymph nodes as other studies had suggested [132, 134, 136], but it also did not cause increased disease pathology and decreased survival [139]. This could be the result of several possible reasons. First, IL-10 may not have a significant role in the host immune response to Mtb. Some previous studies have found that complete depletion of IL-10 or depletion of the primary T cell producers of IL-10 during Mtb infection had little to no effect on the bacterial load compared to wild-type mice [139-141, 288]. Second, not all granulomas may respond to IL-10 in the same manner. Previous studies from our lab have demonstrated the individuality of each granuloma, even from the same animal [102, 269]. Our *ex vivo* neutralization assays also suggest that granulomas may not all be producing or responding to IL-10 during Mtb infection.

Third, other host factors may compensate for the lack of IL-10. Roach et al. also noticed a transient decrease in bacterial burden of IL-10 knock-out mice after 4 weeks of infection, but by 8 weeks post-infection, there was no difference in bacterial burden compared to wild-type mice [142]. In our study, IL-10 seemed to have the most effect on the host immune response at 4 weeks post-infection. This could be due to the onset of the adaptive immune response by approximately 6 weeks post-infection counteracting the absence of IL-10 [68]. The observed increase in Th2 cytokine IL-13 with anti-IL-10 treatment at 4 weeks may have helped compensate for the lack of IL-10. Although we quantified FOXP3+ regulatory T cells in our

study, we did not measure the anti-inflammatory cytokine TGF-β. Mtb can also stimulate the production of TGF-β, and may compensate for the lack of IL-10 in these animals [285, 289]. Due to the limitations of this study, we may have not quantified the factor(s) that compensated for the actions of IL-10.

Fourth, the role of IL-10 during Mtb infection could be timing-dependent. This study was restricted to look at the earliest time points of Mtb infection, at 4 and 8 weeks, during which we found the greatest peripheral response to Mtb stimulation. Turner et al. observed overexpression of IL-10 in the mouse model of Mtb infection had no effect on the bacterial load until much later in infection, approximately 5 months post-infection [137]. Other studies further dissecting the timing of IL-10 during Mtb infection found that IL-10 had the greatest effect on the host ability to control the bacterial burden starting at least 3 months post-infection [134, 136, 138]. However, computational modeling of IL-10 during the course of Mtb infections indicated that IL-10 prevented clearance of bacteria during early infection [275]. While Moreira-Texeira et al. did not observe decreased bacterial loads within one month of infection, they did have significantly lower bacterial burdens in IL-10-depleted and Mtb-infected mice after two months [135]. Although our study looked at the effects of early neutralization during early Mtb infection only, these early neutralization events may set up the immune response for long-term control of bacterial loads outside the scope of this study, as previously showed by Cyktor et al. [136]. Future studies should further investigate the role of IL-10 during more chronic infections.

In summary, our studies of early Mtb infection in a NHP model in the presence or absence of functional IL-10 indicate that IL-10 primarily affects innate cells, namely macrophages, to downregulate T cell recruitment and proliferation in lung granulomas and draining LNs, to induce LN cell recruitment and effacement, and to decrease inflammation while

promoting fibrosis in lung granulomas. However, with the onset of the adaptive immune response at 6 weeks, many of these changes may be compensated for by other immune cells and host factors by 8 weeks of Mtb infection. Overall, these changes in the immune response without IL-10 do not affect the bacterial load or disease pathology during the first 8 weeks of Mtb infection. This study demonstrates that IL-10 may not have as significant of a role in Mtb infections as previously suggested. IL-10 likely works in more cooperation with other immune cells, and does not appear to be the sole anti-inflammatory response in Mtb to prevent tissue damage, with other cytokines to also compensate [285, 289, 290]. This study further demonstrates the need for a balance of immune responses within the locally affected tissues during Mtb infection, and the need to continue to identify other host factors that may be detrimentally preventing an effective immune response against Mtb.

2.5 MATERIALS AND METHODS

2.5.1 IL-10 neutralization *in vitro* and *ex vivo* assays

D36 mouse mast cells (ATCC, Manassas, VA) were cultured in IMDM media (Sigma, United Kingdom) containing 10% FBS, 1% HEPES, 1mM sodium pyruvate, and 1% L-glutamine in the presence of 1ng/ml IL-3 and 1ng/ml IL-4. Cells were washed in PBS, counted by Trypan Blue exclusion, and resuspended in RPMI media (Sigma, United Kingdom) containing 1% HEPES and 1% L-glutamine before resting for 3 hours at room temperature. Following rest, cells were counted again by Trypan Blue exclusion and aliquoted in sterile 96 well flat bottom plates at 100,000 cells/well in 100μl. Rhesus macaque IL-10 (kindly provided by Dr. Francois Villinger)

was added to appropriate wells at a concentration of 20ng/ml. Macaque-IL-10-specific antibody (IL-10R1-LALA, MassBio, Cambridge, MA) was added to appropriate wells at varying concentrations (1-100 μg/ml). Samples were incubated for 18 hours at 37°C. Tritiated thymidine (PerkinElmer, Waltham, MA) was diluted in AIM V media (Gibco, Gaithersburg, MD) to a concentration of 20 μCi/ml and added to all samples before incubation for another 6 hours at 37°C. Cells were harvested onto glass fiber filters (PerkinElmer, Waltham, MA) before incorporated radioactivity was determined by liquid scintillation counting (TopCount, PerkinElmer, Waltham, MA).

2.5.2 IL-10 neutralization in *ex vivo* assays

Excised lung granulomas from cynomolgus macaques (*Macaca fascicularis*) designated for other studies were homogenized as previously described [267]. Single cell suspensions of lung granulomas were used for flow cytometry, while corresponding supernatants were stored at -80°C until ELISA as described below. Samples were resuspended in assay media (RPMI with 1% HEPES, 1% L-Glutamine, and 10% human AB serum) and divided into 2 wells in a sterile 96 well round bottom plate. Samples were washed with additional assay media. Sample halves designated for anti-IL-10 antibody neutralization treatment were resuspended in media containing anti-IL-10 antibody diluted in assay media for concentration of 10μg/ml (IL-10R1-LALA, MassBio, Cambridge, MA). Corresponding sample halves designated as media controls were resuspended in equal volumes of assay media. Samples were incubated overnight at 37°C. Following overnight incubation, samples were stimulated with peptide pools of Mtb-specific antigens ESAT-6 and CFP-10 (10ug/ml of each peptide) and Brefeldin A (GolgiPlug, BD

Biosciences, San Jose, CA) for 3.5-4 hours at 37°C. Samples were then stained for viability (Invitrogen), cell surface markers, and intracellular cytokine markers. Cells were identified as T cells, with antibodies against CD3 (clone SP34-2), CD4 (clone L200), and CD8 (clone SK1). Following permeabilization using Fixation/Permeabilization solution (BD Biosciences), cytokine and cellular response were identified using antibodies against IFN-g (clone B27), IL-2 (clone MQ1-17H12), TNF (clone MAB11), IL-17 (clone eBio64CAP17), IL-10 (clone JES3-9D7), and Ki67 (clone B56). Data acquisition was performed using a LSRII (BD) and analyzed using FlowJo Software v.9.7 (Treestar Inc, Ashland, OR).

Stored supernatants were thawed and filtered using 0.22μm syringe filter into ~1ml aliquots immediately before assay to prevent freeze-thaw cycles. Concentrations of IL-10 were detected using a NHP-specific IL-10 enzyme-linked immunosorbent assay (ELISA) (U-Cytech, Utrecht, The Netherlands) according to manufacturer's directions. Samples were measured at OD450 on a spectrophotometer (SpectraMax, Molecular Devices, San Jose, CA).

2.5.3 Experimental animals, anti-IL-10 ab infusions, and infections

Fourteen cynomolgus macaques (*Macaca fascicularis*) between 5.7 and 8 years of age, with starting weights of 3.9-6.9 kg (Valley Biosystems, Sacramento, CA) were housed within Biosafety Level 3 (BSL-3) facilities as previously described [57, 88, 291]. Additional historical control animals from a previous study of similar age and weight infected with Mtb and necropsied at 4 weeks were also used in this study.

Starting 1 day prior to Mtb infection, macaques were sedated and given acetaminophen and diphenhydramine ≥ 30 minutes prior to infusion in both anti-IL-10 treatment and saline control groups. Macaques that were randomly designated for the anti-IL-10 treatment group were

then infused with anti-IL-10 antibody (IL-10R1-LALA, MassBio, Cambridge, MA) diluted in saline at 15mg/kg over the course of 20-30 minutes, with pre-dosing, interim, and post-dosing vitals recorded. Following the initial infusion, macaques were infused with 15mg/kg of antibody every 10 days (+/-3 days) using the same procedure methods until necropsy, 4-8 weeks after initial infusion). Macaques randomly designated for the control group were sedated and treated the same as the anti-IL-10 treatment group, except infusions with 50ml of saline over 20-30 minutes. Three macaques were designated for the anti-IL-10 antibody treatment and 1 macaque was designated for the saline control group for the short 4 week study; 4 historical controls were included in the analysis. Five macaques were designated for the anti-IL-10 antibody treatment and 5 macaques were designated for the saline control group for the longer 8 week study.

Animals were infected with 9-19 colony forming units (CFU) of Mtb Erdman strain to the lower lung lobe by bronchoscopic instillation. Infection was confirmed and serial clinical, immunologic, and radiographic examinations were conducted during the course of the study as previously described [57, 61, 267, 269, 270]. Specifically, blood was serially drawn immediately prior to infusions, and TB granuloma formation and progression were tracked by serial ^{18}F-FDG PET-CT imaging, and their relative metabolic activity as a proxy for inflammation measured as ^{18}F-FDG standard uptake values normalized to muscle (SUV).

2.5.4 Whole blood stimulation assay

Blood drawn from NHPs at baseline and at serial intervals was centrifuged to remove plasma and washed with PBS twice. Plasma volume was then replaced with AIM V media and aliquoted in triplicate in flat bottom 96 well plates. Blood was then stimulated with gamma-irradiated Mtb diluted in AIM V media or unstimulated with AIM V media only for 72 hours at 37°C.

Following stimulation, samples were centrifuged and supernatant fluids were collected into clean 96 well round bottom plate, and repeated to minimize cell contamination of supernatant fluids. Samples were stored at -20°C until time of assay. Total cytokine and chemokine levels in thawed samples were measured by multiplex immunoassays specific for NHPs (ProcartaPlex, ThermoFisher Scientific, Waltham, MA) according manufacturer's instructions. Immunoassay results were collected and analyzed using BioRad Bio-Plex 200 (BioRad, Hercules, CA).

2.5.5 Necropsy

After 4 or 8 weeks of infection and infusions, necropsy of study animals was performed as previously described [57, 88, 267, 291, 292]. In summary, 1-3 days prior to necropsy, individual granulomas were identified by ^{18}F-FDG PET-CT scans. At necropsy, NHPs were maximally bled and humanely sacrificed using pentobarbital and phenytoin (Beuthanasia, Schering-Plough, Kenilworth, NJ). Lymph nodes and PET-CT matched granulomas were excised for bacterial burden, immunological studies, and histological analyses. Representative sections were homogenized into single cell suspensions for bacterial quantification, flow cytometry, and multiplex immunoassays. Representative sections were formalin-fixed for immunohistochemistry and histology.

2.5.5.1 Necropsy score

During necropsy, gross disease pathology was quantified by a scoring system of number, size, and pattern of lung granulomas, and extent of disease involvement in lung lobes, mediastinal lymph nodes, and visceral organs, as previously described [57].

2.5.5.2 Bacterial quantification

Bacterial burden in individually excised granulomas, lymph nodes, representative lung lobe tissue, spleen, and liver were quantified by serial plating onto 7H11 medium and colony forming units (CFU) enumerated after 21 days of incubation at 37°C. Total CFU from summation of all plated samples.

2.5.5.3 Flow cytometry

Single cell suspensions of homogenized tissues were incubated in the presence of Brefeldin A (GolgiPlug, BD Biosciences, San Jose, CA) with no additional stimulation for 2.5-3 hours at 37°C. Samples were washed with PBS, and stained for viability (Invitrogen), immune cell subsets, and intracellular cytokine markers. Cells were identified as T cells: CD3 (clone SP34-2), CD4 (clone L200), and CD8 (clone SK1); B cells: CD20 (clone 2H7); and macrophages and neutrophils: CD11b (clone ICRF44), CD163 (clone eBioGH1/61), calprotectin (clone 27E-10). Following permeabilization using FOXP3 staining kit (eBioscience), cytokine and cellular response were identified using antibodies against CD69 (clone TP1.55.3), IFN-g (clone B27), IL-2 (clone MQ1-17H12), TNF (clone MAB11), IL-17 (clone eBio64CAP17), IL-10 (clone JES3-9D7), IL-6 (clone MQ2-6A3) and FOXP3 (clone PCH101). Data acquisition was performed using a LSRII (BD) and analyzed using FlowJo Software v.9.7 (Treestar Inc, Ashland, OR). Only samples with greater than or equal to 100 cells of a population were included in data analysis of cytokine response.

2.5.5.4 Immunohistochemistry of paraffin-embedded granulomas

Formalin-fixed paraffin-embedded tissue sections from animals included in this study were deparaffinized in xylene, 100% ethanol, and 70% ethanol. Tissue sections were then incubated in

a pressure cooker containing Tris-EDTA (pH 9) antigen retrieval buffer for 6 minutes under pressure. Samples were then depressurized and allowed to cool slowly over 30 minutes before washing in PBS. Samples were incubated in blocking buffer (1%BSA in PBS) for 15-30 minutes in a dark humidified chamber before addition of primary antibody cocktails diluted in blocking buffer to sections for overnight incubation at 4°C in a dark humidified chamber. Antibodies were against CD3 (clone CD3-12, 1:200 dilution, Abcam), CD11c (clone 5D11, 1:30 dilution, Leica Microsystems, Buffalo Grove, IL), CD20 (clone L26, 1:100 dilution, Dako), and IL-10Rα (polyclonal, 1:150 dilution, Millipore, Temecula, CA). After incubation with primary antibodies, sections were washed four times in PBS and incubated with secondary antibodies for 1 hour at room temperature in a dark humidified chamber. Secondary antibodies were purchased from Jackson ImmunoResearch Laboratories (West Grove, PA) or Invitrogen (Eugene, OR). Specificity of antibodies for IL-10R were confirmed using no-primary controls using the same staining and imaging protocol on serial sections. After secondary antibody incubation, slides were washed four times in PBS and mounted using ProLong Gold mounting medium with DAPI (Life Technologies, Eugene, OR). Slides were cured at room temperature for at least 24 hours and subsequently stored at -20°C. Slides were imaged using a Nikon immunofluorescent microscope with a scanning stage and saved as TIFF-format images.

2.5.5.5 Multiplex immunoassay

Total cytokine concentrations in lung granulomas and LNs were quantified using multiplex immunoassays. Supernatants from homogenized excised tissues stored at -80°C until time of assay. Supernatants were filtered using a 0.22μm syringe filter into ~1ml aliquots immediately before storage at -80°C or immediately before time of assay to minimize freeze-thaws. Cytokine

and chemokine levels in thawed samples were measured by multiplex immunoassays specific for NHPs (ProcartaPlex, ThermoFisher Scientific, Waltham, MA) according manufacturer's instructions. Immunoassay results were collected and analyzed using BioRad Bio-Plex 200 (BioRad, Hercules, CA).

2.5.5.6 Histopathology of tissues

A subset of tissues excised during necropsy, including lung granulomas and lymph nodes, were fixed in 10% neutral buffered formalin before placing in histology cassettes and paraffin-embedding. Sections of 5μm thick tissues were cut and mounted on SuperFrost Plus slides (ThermoFisher Scientific, Waltham, MA) and stained with hematoxylin and eosin by the University of Pittsburgh's in situ histology laboratory. Structures of lung granulomas and extent of TB disease in LNs were examined and recorded by veterinary pathologist Edwin Klein, VMD, who was blinded to treatment groups. To quantify fibrosis in lung granulomas, granulomas described as containing "collagen", "fibrosis", or "fibroblasts" were scored as fibrotic. Excised lung granulomas that were not described as granulomas Dr. Klein were excluded from the analysis. To quantify LN effacement, LNs described as having "effacement" were scored as effaced. LNs had about 50% or more effacement.

2.5.6 Statistical analysis

Statistical analyses were conducted in GraphPad Prism 7 (GraphPad Software, San Diego, CA). Data were tested for normality by D'Agostino & Pearson Omnibus Normality Test. Since data analyzed in this study were not normally distributed, Mann-Whitney tests were used to compare

two groups. Fisher's exact test was used to analyze contingency tables. P-values ≤ 0.05 were considered significant and noted in individual graphs.

3.0 LOW LEVELS OF T CELL EXHAUSTION IN TUBERCULOUS LUNG GRANULOMAS

3.1 ABSTRACT

The hallmarks of pulmonary *Mycobacterium tuberculosis* infection are lung granulomas. These organized structures are composed of host immune cells whose purpose is to contain or clear infection, creating a complex hub of immune and bacterial cell activity, as well as limiting pathology in the lungs. Yet, given cellular activity and potential for frequent interactions between host immune cells and Mtb infected cells, we observed a surprisingly low quantity of cytokine producing T cells (<10% of granuloma T cells) in our recent study of Mtb infection within non-human primate (NHP) granulomas. Various mechanisms could limit T cell function, and one hypothesis is T cell exhaustion. T cell exhaustion is proposed to result from continual antigen stimulation inducing them to enter a state characterized by low cytokine production, low proliferation and expression of a series of inhibitory receptors – the most common being PD-1, CTLA-4, and LAG-3. In this work, we characterized the expression of inhibitory receptors on T cells and functionality of these cells in TB lung granulomas. These experimental data were then used by our collaborators at the University of Michigan to calibrate and inform an agent-based computational model that captures environmental, cellular, and bacterial dynamics within granulomas in lungs during Mtb infection. Together, the results of the modeling and the

experimental work suggest that T cell exhaustion alone is not responsible for the low quantity of Mtb-responsive T cells observed within TB granulomas, and that the lack of exhaustion is likely an intrinsic property of granuloma structure.

3.2 INTRODUCTION

Tuberculosis (TB), caused by inhalation of the bacterium *Mycobacterium tuberculosis* (Mtb), continues to be a major global health problem. The World Health Organization estimates that more than 10 million people became ill with TB in 2016 alone, and 1.7 million deaths were caused by TB [1]. TB is a chronic pulmonary disease, with organized structures, called granulomas, forming within the lungs and thoracic lymph nodes. Granulomas are formed by the host immune response to Mtb. Due to substantial heterogeneity of granulomas, even within the same host, these structures can contain and kill Mtb but also can be a niche for bacterial survival, replication, and persistence [293]. The host immune cells and Mtb bacilli and antigens interact within the granulomas for the entire course of infection, which, during clinically latent TB, can last the lifetime of the host [27]. Macrophages are the primary host cell for infection, while CD4+ and CD8+ T cells have been shown to be critical for granuloma formation and maintenance through cytokine secretion and activation of other immune cells, including macrophages [294, 295]. Yet, even though the granuloma provides the potential for frequent interactions between host immune cells and Mtb bacilli, our previous data in a macaque model showed that less than 10% of T cells in a granuloma produce cytokines [102]. While various mechanisms could be limiting T cell function, one potential explanation for the low T cell

responses within granulomas is T-cell exhaustion occurring due to chronic antigen stimulation from Mtb-infected cells.

In chronic viral infections and cancer, a subpopulation of T cells has been demonstrated to lose both functionality and proliferation capabilities over time in response to persistent antigen stimulation [143-148]. This subpopulation of T cells enters an "exhausted" state, characterized by low cytokine production, low proliferation, and expression of a series of inhibitory receptors. The most well-studied of these receptors include PD-1, CTLA-4, and LAG-3, which interact with a range of ligands to activate negative regulatory pathways [149, 150]. While these inhibitory receptors may balance an overly activated immune response that could lead to disease pathology, the receptors can also prevent an effective immune response from clearing infections and tumor cells. In cancer and some infectious diseases, blockade of these inhibitory receptors reverses exhaustion and rescues T cell functions [153-158].

Since Mtb causes a chronic bacterial infection confined to a structured environment, it seems obvious that T cell exhaustion would occur within the critical site of granulomas. Not surprisingly, the contribution of T cell exhaustion to TB has been the subject of several studies. Patients with active TB were shown to have significantly higher PD-1 expression on their peripheral blood mononuclear cells (PBMC) compared to healthy controls, and blockade of inhibitory receptors *in vitro* enhanced T cell function [159-161]. Additionally, increased antigen load was associated with decreased T cell responses in patients with high Mtb loads compared to patients with latent Mtb infections [75]. Rhesus macaques with active or reactivated TB expressed more LAG-3 on their CD3+ T cells in their lung tissue compared to clinically latent animals [168]. PD-1 expression significantly correlated with CTLA-4 expression on CD4+ T cells from tissues of Mtb-infected rhesus macaques [179]. Mtb infections in mice increased the

expression of PD-1 and LAG-3 as the infection progressed, and this was associated with increased T cell impairment [180]. However, murine studies also suggested that presence of these inhibitory receptors may be beneficial for overall TB disease pathology and bacterial control, and are necessary to maintain antigen-specific effector T cells during Mtb infections [169, 170], with detrimental outcomes when mice lacking PD-1 were infected with Mtb [171-173]. While these studies examined T cell exhaustion in the periphery (patient studies) or in the whole lung (animal models), the frequency and role of exhausted T cells in individual granulomas is still unstudied and could provide important clues to overall infection dynamics as granulomas are the sites of infection in pulmonary TB. Confounding these data, the relationship between inhibitory markers and functional exhaustion is not abundantly clear. Recent studies have shown that inhibitory receptors can act as activation markers and that T cells can simultaneously express both inhibitory and activation markers [150, 174-177]. Therefore, it becomes difficult to distinguish T cell exhaustion using inhibitory receptors alone.

We hypothesized T cell exhaustion could be contributing to the observed low frequencies of T cells producing cytokines in TB granulomas. We used a non-human primate (NHP) model of TB that recapitulates human granuloma structure and disease to assess the extent of exhausted T cells and their function in lung granulomas [296]. However, contrary to our hypothesis, we found low levels of inhibitory receptor expression, and those T cells expressing inhibitory receptors were often still functional. To further confirm and explore these findings, our collaborators at University of Michigan (Louis Joslyn, under the mentorship of Dr. Denise E. Kirschner) applied a computational modeling approach using *GranSim*, an agent-based model simulator of lung granulomas. The model predicted that the structure of granulomas may prevent T cell exhaustion, and we concluded that this mechanism is likely beneficial for the host because

granulomas can remain functional even after chronic containment of Mtb from months to years. Thus, our data combined with our collaborators' data indicate that T cell exhaustion is limited in most tuberculous granulomas.

3.3 RESULTS

3.3.1 Few T cells in granulomas of Mtb-infected macaques co-express inhibitory receptors

T cells from individual lung granulomas from of Mtb-infected macaques (6-31 weeks post-infection) were characterized for expression of well-documented markers for T-cell exhaustion, namely the inhibitory receptors PD-1, CTLA-4, and LAG-3, using flow cytometry (Figure 16). PD-1 was expressed in higher frequencies (median = 16.55% of the CD3+ T cells), while the majority of the CD3+ T cells expressed very low frequencies of CTLA-4 (median = 2.02%) or LAG-3 (median = 1.53%) in granulomas (Figure 17A). Although exhaustion in CD8 T cells has been more commonly characterized, exhausted CD4 T cells also comprise a critical and distinct population of exhausted T cells [151]. In TB granulomas, inhibitory receptors tended to be expressed more frequently on CD4 T cells than on CD8 T cells, particularly in the expression PD-1 and CTLA-4. (Figure 17B). There was no significant difference in expression of LAG-3 on CD4 and CD8 T cells.

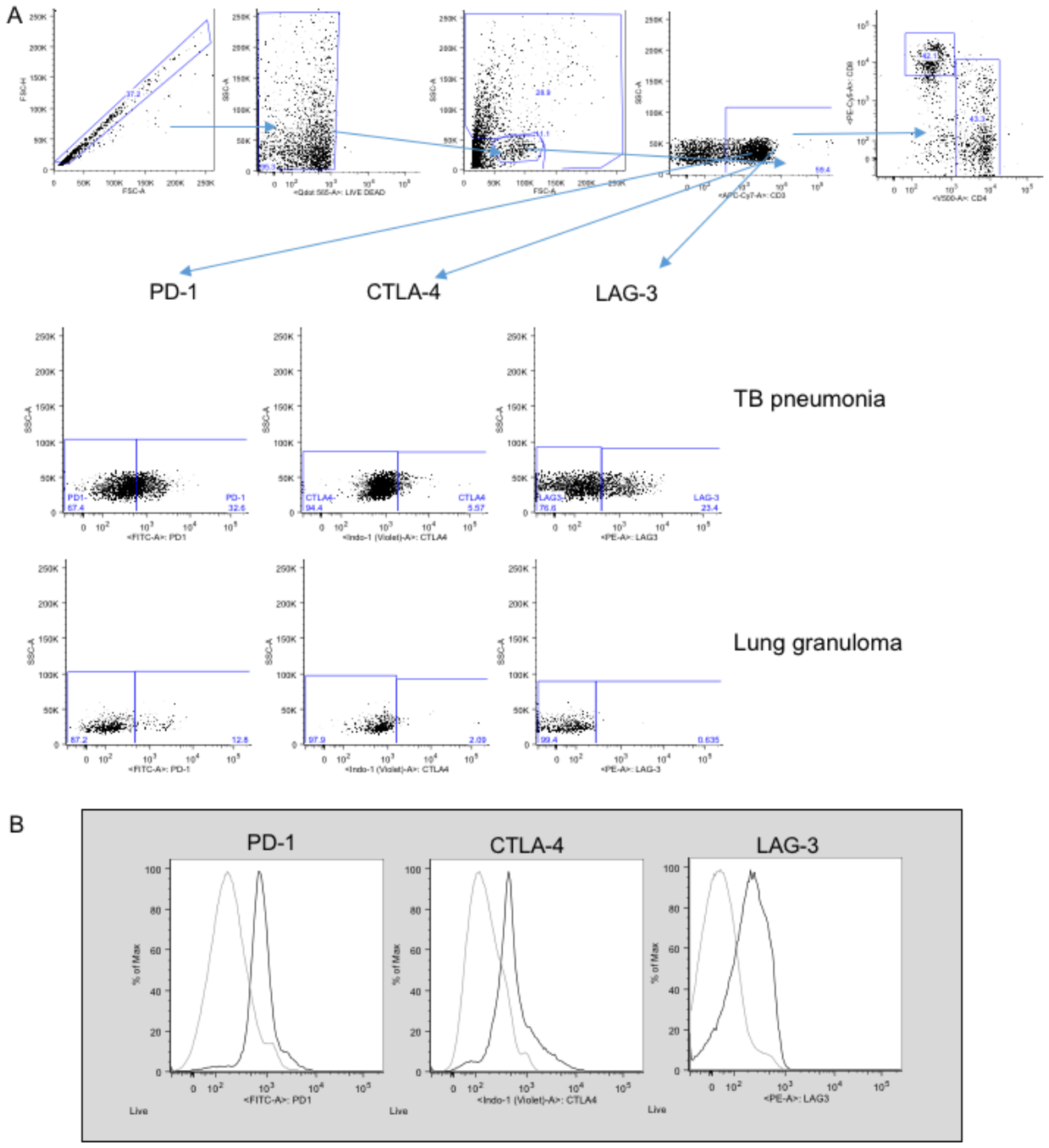

Figure 16. Gating strategy and positive control examples for flow cytometry antibodies against inhibitory receptors in single cell suspensions.

(A) Flow cytometry gating strategy example from TB pneumonia sample excised from Mtb-infected cynomolgus macaque. (B) Testing of flow cytometry antibodies in PBMCs isolated from Mtb-infected cynomolgus macaque stimulated by PDBU & ionomycin for 3 hours at 37°C.

Since these inhibitory receptors also have been characterized as markers of activation on T cells, co-expression of these inhibitory receptors has been demonstrated to be better indicators of exhaustion [178]. By flow cytometry, co-expression of inhibitory receptors on CD3+ T cells in any combination was rare (Figure 17C). There were very few CD3+ T cells that had co-expression of these inhibitory receptors, with the medians less than 1% of CD3+ T cells. PD-1 and CTLA-4 had the highest levels of co-expression in granulomas, but they were still very low (median: 0.6%; range: 0-3.46%). A fraction of granulomas had higher levels of PD-1 and LAG-3 co-expression (0.82-5.51%). Even in more severe forms of disease pathology (i.e., clusters of granulomas and consolidations, where bacterial burden is often higher), expression of inhibitory receptors, including co-expression, was low, similar to that of individual granulomas (Figure 17D). Notably, however, the most severe form of disease, TB pneumonia had the highest expression of LAG-3 and 6.4% of the T cells from the sample co-expressed PD-1 and LAG-3 (diamond, Figure 17D).

Thoracic lymph nodes infected with Mtb also had low levels of inhibitory receptor expression, including PD-1, of total CD3 populations (Figure 18A). Similar to the lung granulomas, there was very few cells co-expressing inhibitory receptors in the lymph nodes (PD-1+CTLA-4+ median = 0.28%, PD-1+LAG-3+ median = 0.171%), suggesting low levels of exhaustion. PBMCs isolated from the blood, which presumably are not chronically stimulated by antigen, had even lower frequencies of inhibitory receptor expression. We found lower

frequencies of PD-1 expression (median = 2.2% vs. 16.55% of CD3 cells in lung granulomas), and similarly low frequencies of CTLA-4 (median = 0.888% vs. 2.02% of CD3 cells in lung granulomas) and LAG-3 (median = 0.442% vs. 1.53% of CD3 cells in lung granulomas) (Figure 18B). Co-expression of these inhibitory receptors on CD3 cells in PBMCs were negligible.

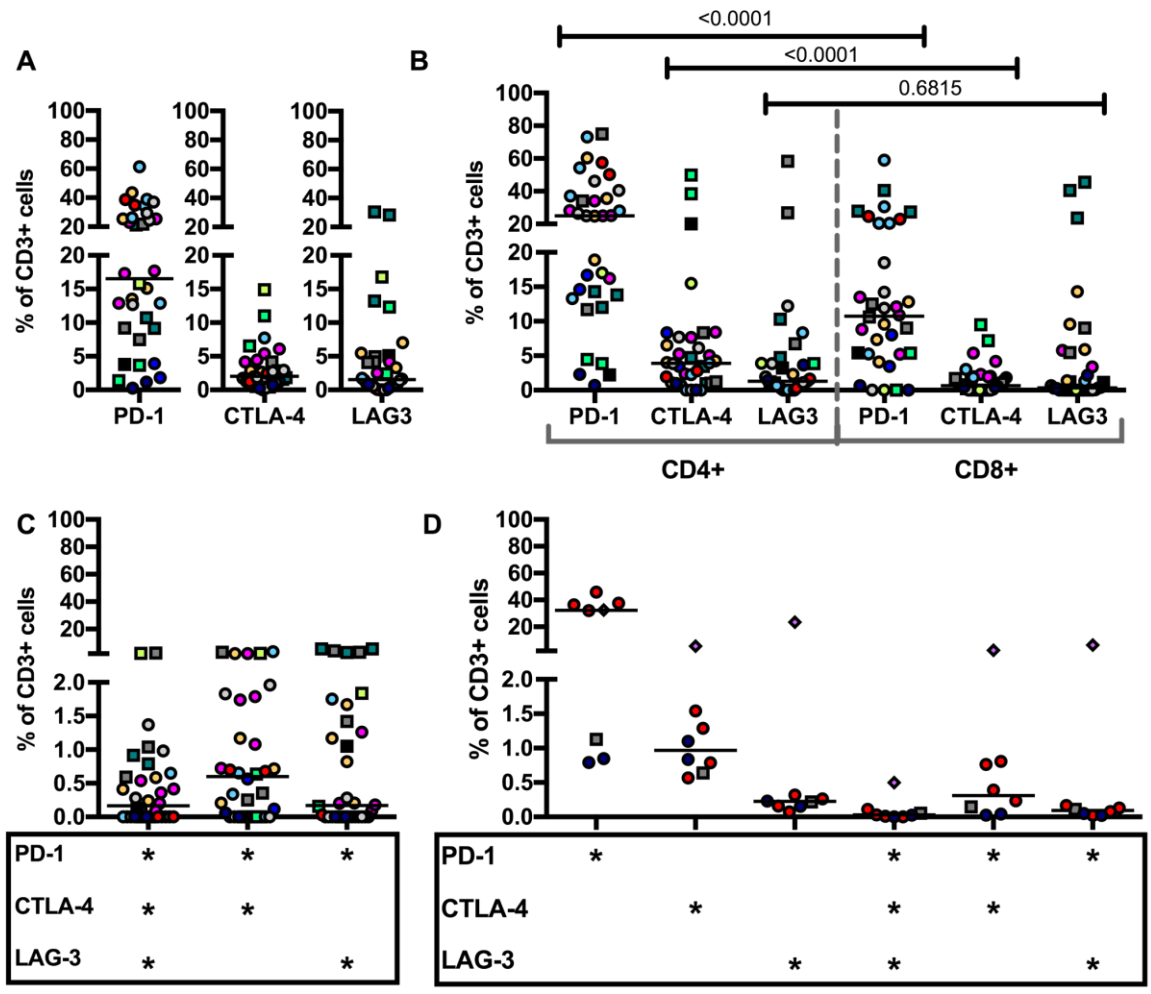

Figure 17. Few T cells in granulomas of Mtb-infected macaques co-express inhibitory receptors.

(A) Frequency of cells expressing inhibitory receptors PD-1, CTLA-4, or LAG-3 in individual granulomas from Mtb-infected cynomolgus or rhesus macaques. (B) CD4 T cells express PD-1 and CTLA-4 significantly more frequently than CD8 T cells. P-values indicated on figure, Wilcoxon matched-pairs signed rank test. (C) Frequency of co-expression of inhibitory receptors in granulomas. Each point indicates a granuloma (N = 34), each color corresponds to a NHP (12 NHPs), circles indicate cynomolgus macaques, squares indicate rhesus macaques. (D) Clusters of

granulomas and TB pneumonia have similarly low frequencies of CTLA-4 and LAG3, and similarly high frequencies of PD-1 alone. There is low co-expression of inhibitory receptors in clusters of granulomas. Each point indicates a cluster, consolidation, or pneumonia lung sample (N = 8), each color corresponds to a NHP (6 NHPs), circles indicate cynomolgus macaque, squares indicate rhesus macaque, diamond indicates TB pneumonia. Lines at medians.

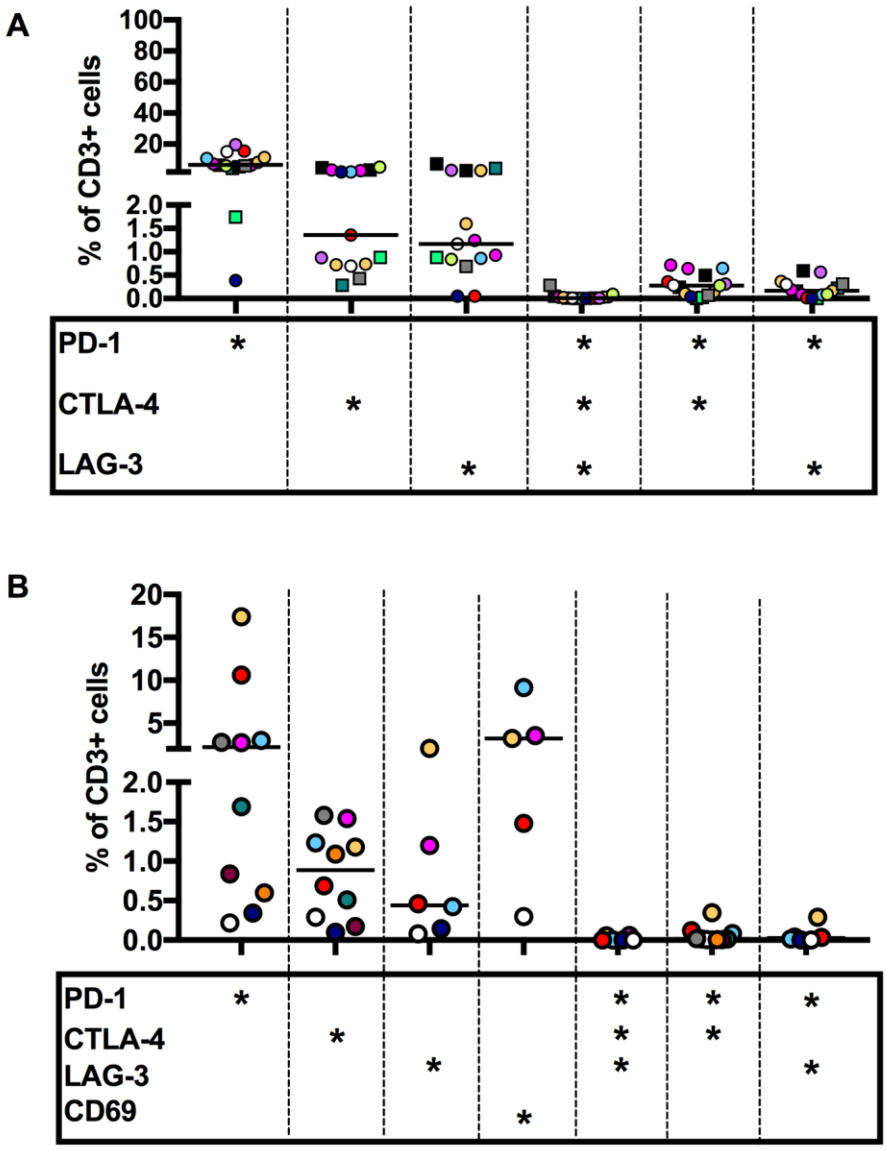

Figure 18. Frequency of inhibitory receptor expression in thoracic lymph nodes infected with Mtb and PBMCs of Mtb-infected NHPs.

(A) Mtb-infected lymph nodes defined as having positive CFU and/or granulomas present in histopathology at time of necropsy. Frequencies of expression of inhibitory receptors on CD3+ T cells from Mtb-infected lymph nodes. Each point indicates a lymph node (N = 15), each color corresponds to a NHP (12 NHPs), circles indicate cynomolgus macaque, squares indicate rhesus

macaques. Lines at medians. (B) Frequencies of expression of inhibitory receptor on PBMCs isolated from Mtb-infected NHPs at time of necropsy. Each point and color indicates a NHP (10 NHPs), all are cynomolgus macaques. Lines at medians.

3.3.2 Inhibitory receptors tend to be expressed on other immune cells in the granuloma

To further characterize T cell exhaustion in TB granulomas, we used immunohistochemistry to identify the spatial location of the few T cells co-expressing inhibitory receptors (Figure 19). Granulomas from early in infection (6 weeks of Mtb infection) had an infiltration of T cells throughout the granuloma, with concentrated clusters of T cells in the outer periphery of the granuloma, and limited but present caseous necrosis. Cell populations in immunohistochemistry images were quantified using CellProfiler™. LAG-3+ CD3+ cells (4.348% of CD3+ cells) were identified close to the periphery of the granuloma, but the majority of LAG-3+ cells were not CD3+. Similarly, there were few PD-1+CD3+ T cells identified in this particular section of granuloma (approximately 1.0%) (Figure 19A-J). In contrast, granulomas from later in infection ($\geq$12 weeks of Mtb infection) were more organized structures, with a region of necrosis in the middle (caseum), and fewer T cells spread throughout the granuloma, mostly concentrated in the lymphocyte cuff away from the region of caseum. Despite differences in organization compared to early granulomas, later granulomas also had very few LAG-3+ CD3+ cells (1.191% of CD3+ cells), but a higher frequency of PD-1+ CD3+ cells than at 6 weeks (4.94% of CD3+ cells). The few PD-1+ CD3+ or LAG-3+ CD3+ cells were localized in the periphery of the granuloma (Figure 19K-T).

In granulomas from both early and late stages in infection, most of the T cells in the granuloma had very little co-expression of CD3 with PD-1 or LAG-3, supporting our results observed by flow cytometry. Instead, most of the expression of these inhibitory receptors tended to be on other immune cells in the granuloma. While PD-1 co-localized with some of the CD3+ cells in the granuloma, LAG-3 was more often expressed on other cells in the granuloma than on T cells. For example, in the samples at 6 and 20 weeks post-infection, 82.9% and 78.2% of the LAG-3+ cells were CD3-, respectively. While we were unable to confirm the identity of the LAG-3+ cells, other immune cell types can express LAG-3, including NK cells, B cells, macrophages, and plasmacytoid dendritic cells [297-300]. Of the CD3+ cells expressing an inhibitory receptor, these cells tended to be in the periphery of the granuloma, further away from the necrotic center of the granuloma, where the Mtb bacilli are located.

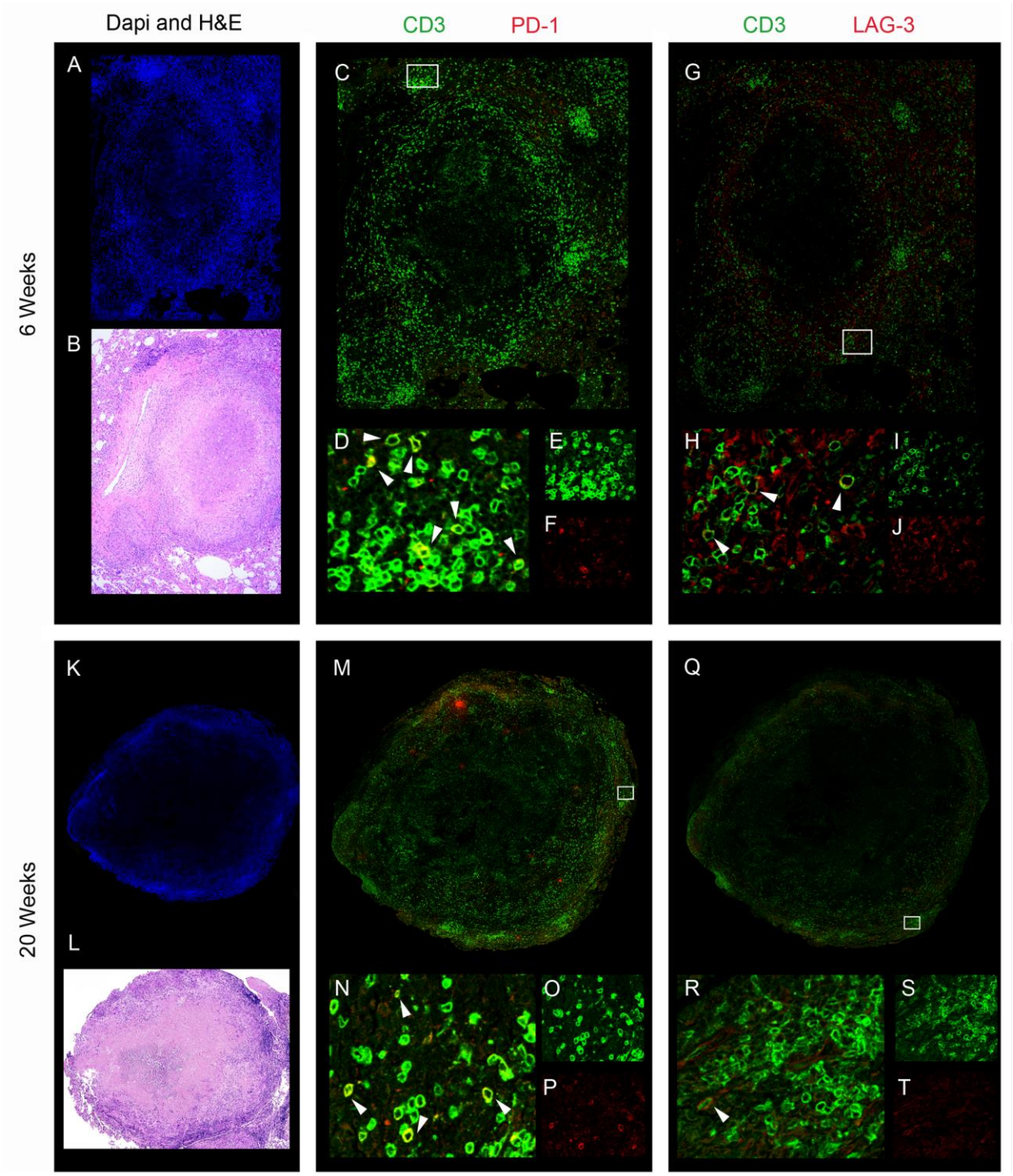

Figure 19. Example spatial organization of inhibitory receptors on T cells within TB granulomas.

Few T cells in lung granulomas express PD-1 or LAG-3 inhibitory receptors, most of the expression of these inhibitory receptors are on other CD3-negative cells. The rare CD3+ and PD-1+ or LAG-3+ co-expressing cells are localized in the periphery of the granuloma, away from the necrotic caseous center. Granulomas isolated at 6 weeks (A-J) and 20 weeks (K-T) were stained using antibodies against CD3, PD-1, and LAG-3 (see methods for details). (A,K) DAPI staining of nuclei (B,L) Hematoxylin and eosin (H&E) staining (C,M) Merged image of CD3 (green) and PD-1 (red). (D,N) Magnified region of interest (ROI) as indicated by white box in C or M, where arrowheads indicate PD-1+CD3+ cells. (E,O) Magnified ROI showing green channel only (CD3). (F,P) Magnified ROI showing red channel only (PD-1). (G, Q) Merged image of CD3 (green) and LAG-3 (red). (H,R) Magnified ROI as indicated by white box in G or Q, where arrowheads indicate LAG-3+CD3+ cells. (I,S) Magnified ROI showing green channel only (CD3). (J,T) Magnified ROI of red channel only (LAG-3). Figure courtesy of Nicole L. Grant, University of Pittsburgh.

3.3.3 T cells expressing inhibitory receptors are not functionally exhausted

Although few T cells in TB granulomas expressed inhibitory receptors, we investigated whether these rare cells were functionally exhausted. Exhausted T cells are characterized by hierarchical defects in function, beginning with decreased proliferation and IL-2 production, followed by decreased TNF production, and finally decreased IFN-γ production [301]. We examined the cytokine production by T cells expressing inhibitory receptors, and found that some of these cells continued to express Ki67 (proliferation marker), and produce IL-2, TNF, and IFN-γ (Figure 20). Overall, the functionality of T cells expressing inhibitory receptors were

mostly not significantly different from the corresponding T cells not expressing inhibitory receptors.

While only about 3% of CD3+T cells expressing PD-1 produced at least one of the cytokines usually lost in exhausted T cells, namely IL-2, TNF, and IFN-γ (Figure 20A), production was comparable to the cytokine response of CD3+T cells not expressing PD-1 (median = 2.12%). Significantly more CD3+PD-1+ cells were expressing Ki67 (median = 2.54%) and IFN-γ (median = 1.43%) than CD3+PD-1- cells (Ki-67 median = 0.04%, IFN-γ median = 1.03%), indicating ongoing, and perhaps increased proliferation in cells expressing PD-1 (Figure 20A). CD3+CTLA-4+ cells and CD3+LAG-3+ cells had a wide range of cytokine responses, but still expressed Ki67 or cytokines at comparable frequencies to CD3+ cells negative for inhibitory receptors (Figure 20B and 20C). The median Ki67 expression and cytokine response was low for CD3+CTLA-4+ cells, especially the significantly lower IFN-γ response compared to CD3+CTLA-4- cells (median = 0.13% vs. median = 1.32%) (Figure 20B). Some CD3+CTLA-4+ cells produced cytokines at high frequencies, causing more spread in the interquartile ranges (IFN-γ: 0 – 10.02%, TNF = 0 – 7.678%, and Any cytokine = 0 – 17.1%). About one-tenth of LAG-3-expressing CD3+ T cells still produced at least one of the cytokines, particularly IFN-γ, but cells seemed to be split between cells not producing any cytokines or proliferation marker and those that continue to function (Figure 20C). Although there were large ranges in cytokine production in CD3+LAG-3+ cells, there was significantly more frequencies of cells producing IFN-γ (median = 4.35, interquartile range = 0 – 14.30%) and Any cytokine (median = 10%, interquartile range = 0 – 17.74%) compared to CD3+LAG-3- cells (IFN-γ: median = 1.31%, interquartile range = 0.42 – 3.81%; Any: median = 2.76%, interquartile range = 0.87 – 6.15%). The T cells expressing inhibitory receptors in the most severe form of TB disease

pathology, TB pneumonia, still show signs of proliferation and cytokine production (diamond, Figure 20A-C). With the exception of frequency of CD3+CTLA-4+ cells producing IFN-γ, CD3+ T cells that also expressed an inhibitory receptor had similar or even higher frequencies of cytokine production or proliferation than CD3+ T cells without inhibitory receptors.

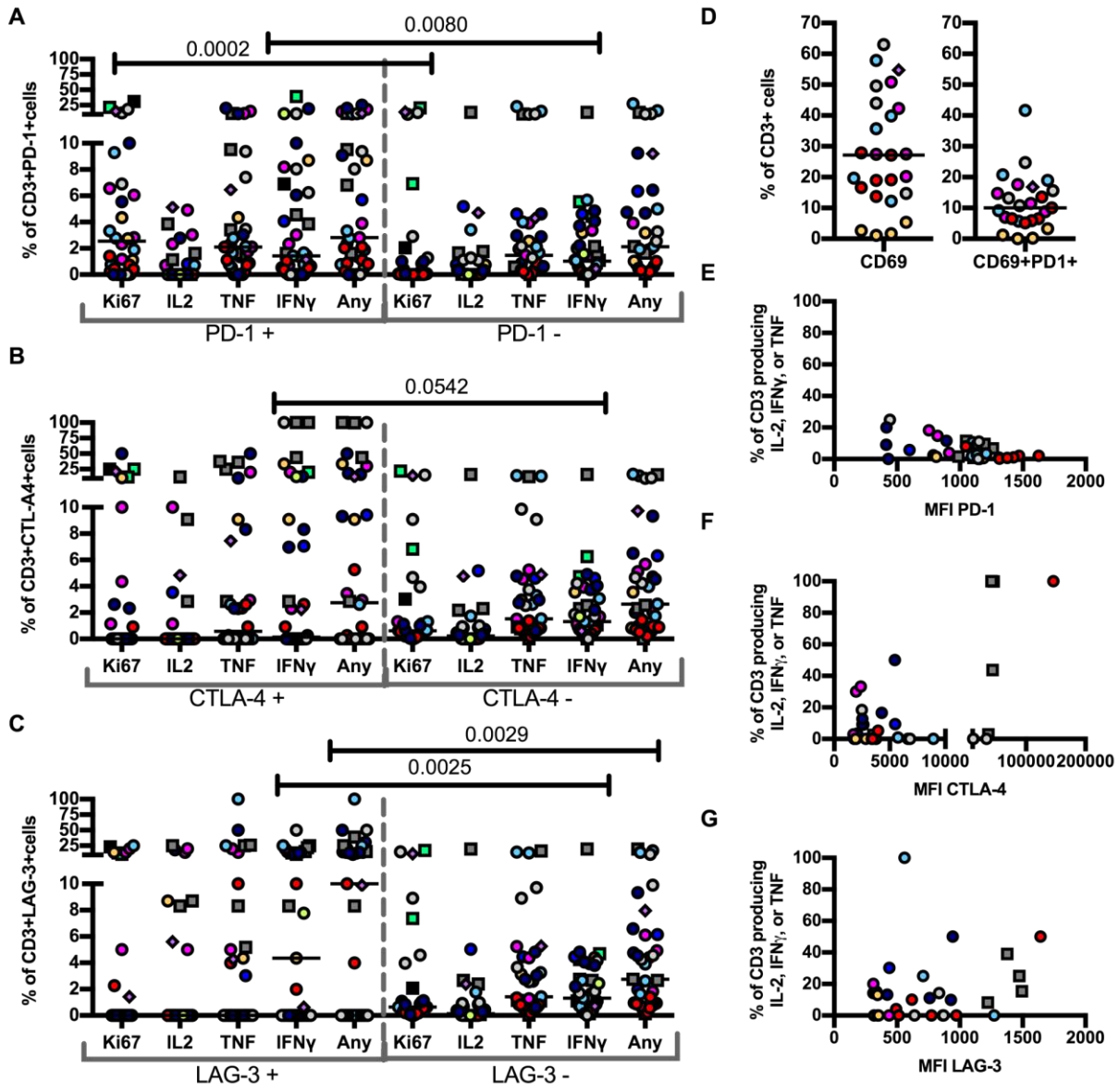

Figure 20. T cells from 2 species of NHP expressing inhibitory receptors in lung granulomas, granuloma clusters, and TB pneumonia remain functional.

Cytokine and Ki67 (proliferation) expression from 2 NHP species were compared between (A) CD3+PD-1+ cells and CD3+PD-1- cells, (B) CD3+CTLA-4+ cells and CD3+CTLA-4- cells, (C) CD3+LAG3+ cells and CD3+LAG3- cells. Each point indicates a lung sample (granuloma, granuloma cluster, or pneumonia) (N = 29), each color corresponds to a NHP (12 NHPs), circles

indicate cynomolgus macaques, squares indicate rhesus macaques, diamond indicates TB pneumonia. P-values from Wilcoxon matched-pairs signed rank test. (D) Frequency of CD69 expression on T cells in the granuloma, and co-expression with PD-1 on T cells in the granuloma. Each point indicates a lung sample (granuloma or granuloma cluster) (N = 25), each color corresponds to a NHP (6 NHPs), diamond indicates TB pneumonia. Lines at the medians. (E) Median Fluorescence Intensity (MFI) of expression of PD-1 (Spearman $\rho = -0.43$, $p = 0.01$) on CD3 T cells negatively correlates with cytokine production. In contrast, MFI of (F) CTLA-4 (Spearman $\rho = 0.16$, $p = 0.37$), and (G) LAG-3 (Spearman $\rho = 0.13$, $p = 0.47$) on CD3 T cells does not correlate with cytokine production. Each point indicates a lung sample (granuloma, granuloma cluster, or pneumonia) (N = 33), each color corresponds to a NHP (12 NHPs), circles indicate cynomolgus macaques, squares indicate rhesus macaques, spearman ρ correlations.

As many of the cells with inhibitory receptors are still proliferating or producing cytokines, they are unlikely to be exhausted. In fact, it may be that these markers, at least when expressed singly, are actually identifying activated T cells within granulomas. Co-expression of PD-1 and CD69 on 10% of the T cells in the granulomas suggests that at least a portion of the few cells expressing inhibitory receptors in the granulomas are activated, and not exhausted (Figure 20D). Likewise, low cytokine response and proliferation activity of CD3+ T cells in Mtb-infected lymph nodes expressing inhibitory receptors likely results from the abundance of naïve T cells, rather than T cell exhaustion present in the lymph nodes (Figure 21). The intensity of PD-1 expression, as measured by median fluorescence intensity, on the T cells of the granulomas did negatively correlate with production of cytokines, suggesting granulomas with stronger expression of PD-1 may be more exhausted, although the correlation was moderate

(Spearman ρ = -0.43, p = 0.01) (Figure 20E). There was no correlation between intensity of CTLA-4 or LAG-3 expression and cytokine production, indicating that higher expression of CTLA-4 or LAG-3 on T cells does not correlate with less cytokine production (Figure 20F and 20G).

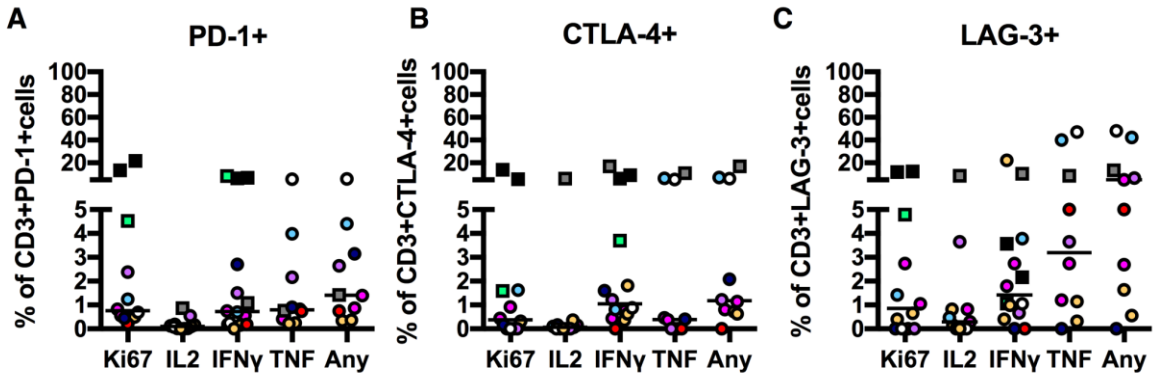

Figure 21. Frequency of cytokine expression in inhibitory receptor-positive T cells in Mtb-infected thoracic LNs.

Frequencies of cytokine or proliferation marker expression in CD3+ cells from Mtb-infected lymph nodes also expressing (B) PD-1, (C) CTLA-4, or (D) LAG-3. Each point indicates an Mtb-infected lymph node (N = 14), each color corresponds to a NHP (12 NHPs), circles indicate cynomolgus macaque, squares indicate rhesus macaques. Lines at medians.

To test whether the T cell cytokine response could be enhanced by blocking PD-1 as had been done with clinical samples [159], we incubated Mtb-infected samples *ex vivo* with anti-PD-1 and PD-L1 antibodies, compared to matched media controls of the same samples. While blocking PD-1 indeed significantly reduced PD-1 expression on T cells, samples with blocked did not lead to markedly increased cytokine response or proliferation (Figure 22), supporting that

PD-1 expression on T cells in Mtb does not necessarily indicate exhaustion or inhibited T cell responses. Together with the continued functionality of these cells (proliferation and cytokine production), these data suggest that the vast majority of T cells in the granuloma are not exhausted.

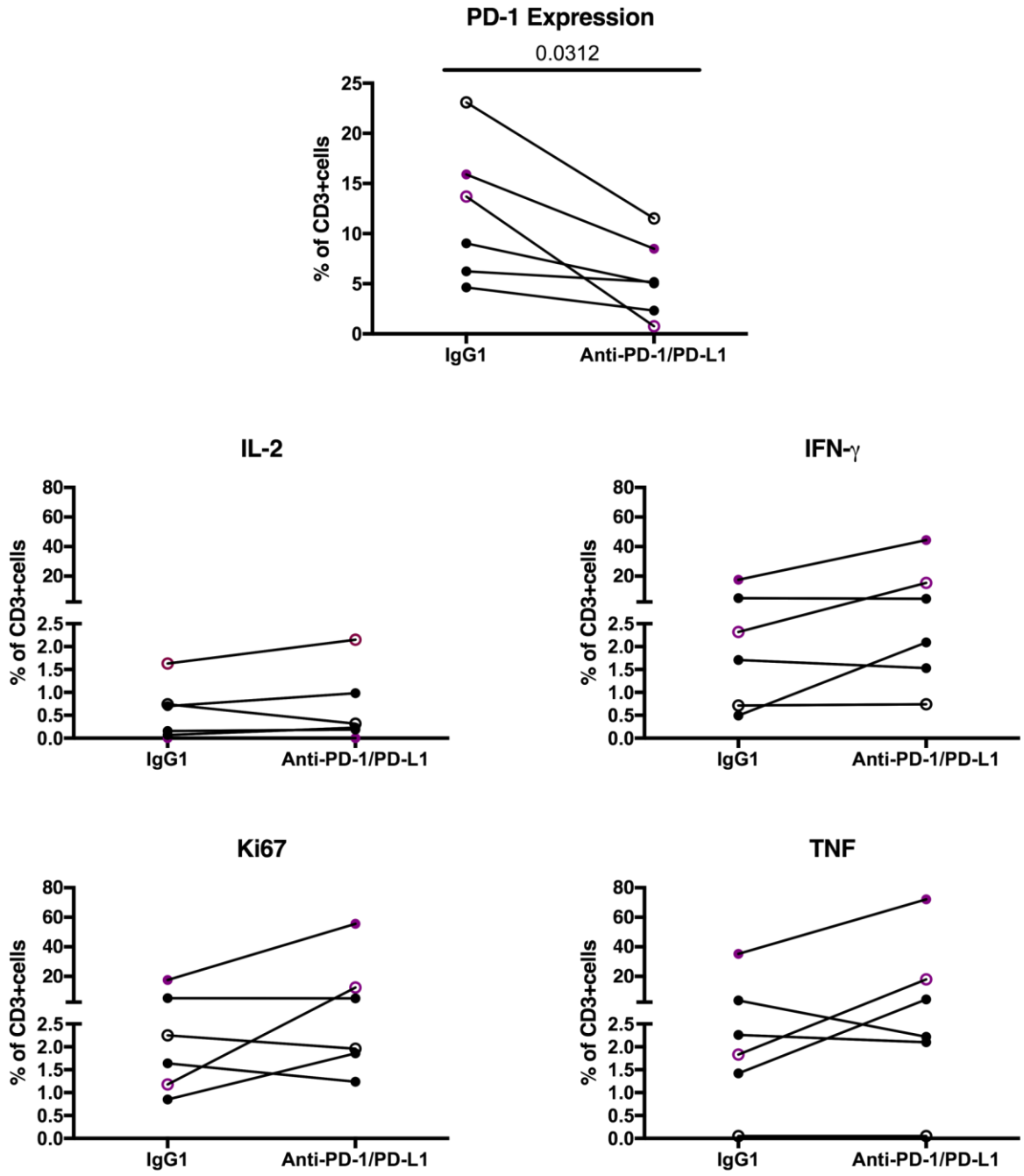

Figure 22. Neutralization of PD-1 and PD-L1 do not always increase cytokine response in tissue or blood.

PD-1 in lung samples and PBMCs from Mtb-infected macaques can be significantly blocked by anti-PD-1 and anti-PD-L1 antibodies, but cytokine and proliferation frequencies do not increase

in response to decreased PD-1 levels. Lines connect matched IgG isotype controls and anti-PD-1/anti-PD-L1 treated samples (N = 6), each color corresponds to a NHP (2 NHPs), filled circles indicate lung sample, open circles indicate PBMC sample.

3.3.4 Expression of inhibitory receptors on T cells in TB granulomas is not correlated with bacterial burden

To determine whether the presence of potentially exhausted T cells in the TB granulomas was related to higher bacterial burden or an inability to control infection, we tested the correlation of inhibitory receptor expression to the colony forming units (CFU) of each individual granuloma. There was no correlation between frequency of CD3+PD-1+, CD3+CTLA-4+, or CD3+LAG-3+ cells with the bacterial burden of each granuloma (Figure 23A-C). Frequencies of T cells co-expressing PD-1 and CTLA-4 or PD-1 and LAG-3 also did not correlate with bacterial burden of the granuloma (Figure 23D and 23E).

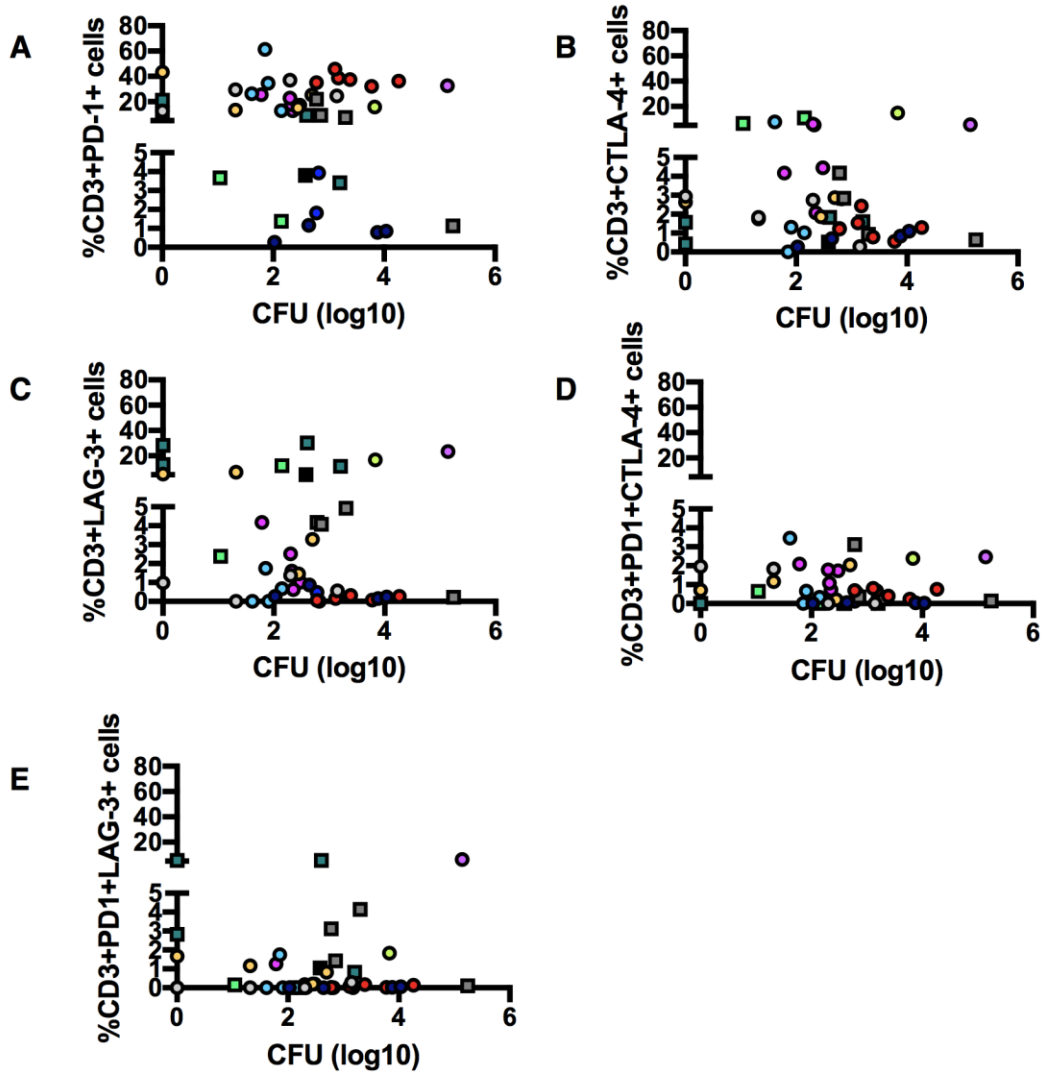

Figure 23. Expression of inhibitory receptors on T cells in TB granulomas and clusters is not correlated with bacterial burden.

Frequency of (A) CD3+PD-1+ cells (Spearman ρ = -0.093, p = 0.55), (B) CD3+CTLA-4+ cells (Spearman ρ = -0.19, p = 0.21), (C) CD3+LAG3+ cells (Spearman ρ = -0.21, p = 0.16), (D) CD3+PD-1+CTLA4+ cells (Spearman ρ = -0.040, p = 0.79), or (E) CD3+PD-1+LAG3+ cells (Spearman ρ = 0.077, p = 0.62) from TB granulomas and clusters do not correlate with their bacterial burdens, measured by colony forming units (CFU). Each point indicates a lung sample

(granuloma, granuloma cluster, or pneumonia) (N = 42), each color corresponds to a NHP (8 NHPs), circles indicate cynomolgus macaques, squares indicate rhesus macaques, nonparametric Spearman correlation.

3.3.5 Granuloma structure may prevent T cell exhaustion

Our *in vivo* data did not support wide-spread T cell exhaustion within granulomas. Further, *in vivo* data could not answer the following questions about T cell exhaustion: 1) What are the temporal dynamics of exhaustion in the granuloma? 2) Within the granuloma, are there areas where a T cell has greater likelihood of becoming exhausted? 3) Can we generally explain the presence of only low quantities of exhausted T cells? These questions required a technique that could address the spatial and temporal dynamics intrinsic to development of a T cell exhaustion phenotype. To further explore the relationship between T cell exhaustion and granuloma function, our computational biologist collaborators at University of Michigan (Louis Joslyn and Denise E. Kirschner) used their existing computational model, *GranSim* [275, 285, 302-305]. Using the uncertainty analysis technique of Latin Hypercube Sampling, we explored the parameter space of granuloma formation and simulated a wide range of granuloma outcomes [306]. We also incorporated varying levels of exhausted T cell phenotypes to ascertain the effects on granuloma outcomes. Finally, we evaluated T cell dynamics in both a temporal and spatial manner, with the aim of developing a hypothesis to explain the low levels of exhaustion observed in the NHP studies herein.

After creating an *in silico* biorepository of 4,500 granulomas (see Methods), we found that every macaque granuloma sample has at least one corresponding simulation match. We

selected three individual granuloma simulations that best matched bacterial burden and CD3+ T cell counts of the three NHP granuloma samples 2016_LLL GR B, 9515_RLL GR 20, 4017_LLL TB pneumonia to investigate the potential roles of exhaustion in granulomas. These were chosen to represent a spectrum of granuloma outcomes: sterile, median bacterial load, and high bacterial load samples, respectively. We directly compared these three NHP samples and their corresponding simulations from *GranSim* (Figure 24). The leftmost column represents a sample that was sterile at the time of necropsy (112 days post-infection with 0 CFU), the middle column shows a sample with median bacterial burden during the time of necropsy (84 days post-infection with 600 CFU), and the far-right column displays a high burden sample (70 days post-infection, with 138000 CFU). The first row displays the H&E of sections, while the second row displays the PD-1 and CD3 expression in the matched granulomas. The third row displays an *in silico* snapshot taken at day 100 for each corresponding granuloma simulation (near time of necropsy of the NHPs). The fourth row represents a prediction: each figure is an *in silico* snapshot of the granuloma simulation at day 200. These comparisons support that the simulated granulomas both temporally and spatially capture the characteristics of the macaque granulomas.

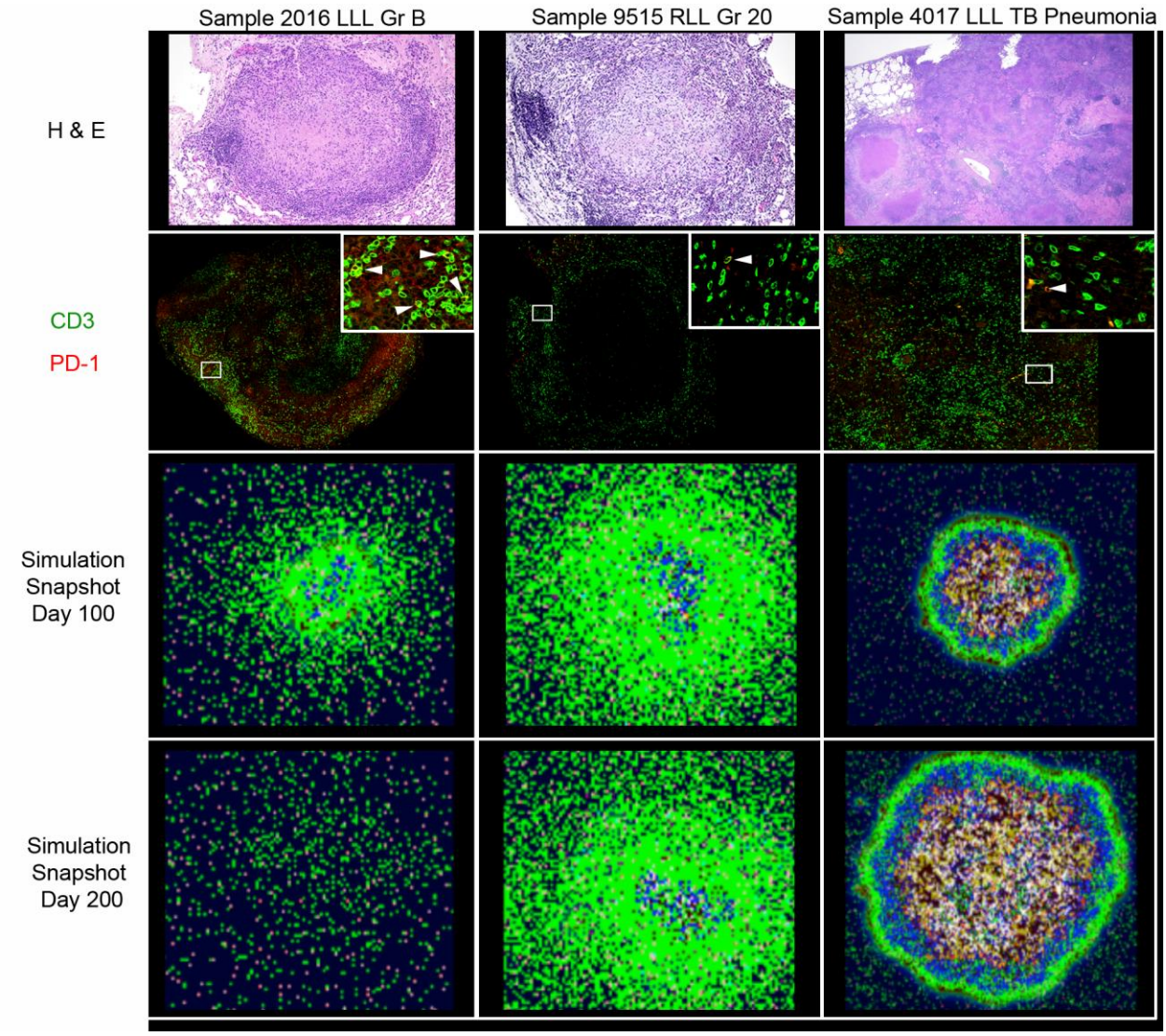

Figure 24. Comparison of macaque and simulated granulomas with varying levels of bacterial burden.

Row 1: H&E sections from granulomas excised from NHPs. Row 2: IHC staining showing spatial organization of PD-1 and CD3 expressing cells in lung granulomas excised from NHPs, green = CD3, red = PD1. Inset is a magnification of the region of interest (indicated by white box), where arrowheads indicate PD-1+CD3+ cells. Row 3: Simulated granuloma snapshots at day 100 (near the matching time of necropsy). Row 4: A snapshot prediction of the granuloma outcome if each simulation is continued until day 200. In both Rows 3 and 4, green - resting

macrophages, blue - activated macrophages, orange - infected macrophages, red - chronically infected macrophages, brown - extracellular bacteria, pink - gamma-producing T cells, purple - cytotoxic T cells, aqua - regulatory T cells, and white crosshatched – caseated. Figure courtesy of Edwin Klein (University of Pittsburgh), Nicole L. Grant (University of Pittsburgh), and Louis Joslyn (University of Michigan).

Under the assumption that T cell exhaustion occurs upon repeated exposure to antigen, we defined an Exposure Event (EE) as the interaction between a T cell and an antigen exposed macrophage in the granuloma. The range of EE across the 2945 simulations that matched the 44 macaque granuloma samples was 205 to 9199, with a median of 5236. Therefore, a threshold of 5236 EE was set as a conservative estimate of our exhaustion threshold, as 5000 interactions across the average life of a T cell (~ 3 days) equates to approximately 1 APC-T cell interaction per minute. We created a new biorepository of 4500 granulomas, using this EE threshold for exhaustion. Using the same three granulomas as in Figure 24, we performed a spatial and temporal analysis (out to 200 days) to investigate the location of exhausted T cells within granulomas (Figure 25). Row 1 displays the spatial location and magnitude of EE throughout the sterile (Figure 25A), median CFU (Figure 25B), and TB pneumonia (Figure 25C) simulations, where dark blue represents high density EE areas and white represents areas within the simulation that lack EE. Row 2 reveals the spatial location of T cells as they exceed the EE threshold and become labeled with an exhaustion phenotype. Each simulation (sterile – Figure 25D, median CFU – Figure 25E, TB pneumonia – Figure 25F) has its own scale ranging from white to dark blue, thus comparison from one EE map to another simulation's EE map should not be performed. Row 3 (Figure 25G-I) displays a plot of the level of overall exhaustion, across

time, as a cumulative percentage of all T cells that were activated in the granuloma simulation. As these simulations show, many granulomas show little cumulative exhaustion throughout the simulation. T cells only become exhausted when they enter the center of the granuloma, where they can accrue sufficient EE. Further the cumulative exhaustion plots reveal that, across time, exhaustion accumulates faster in early time points (between days 25 and 50) than later time points (between days 100 and 200). As the granuloma matures and organizes, T cell exposure events decline, and the rate of exhaustion lowers or stabilizes.

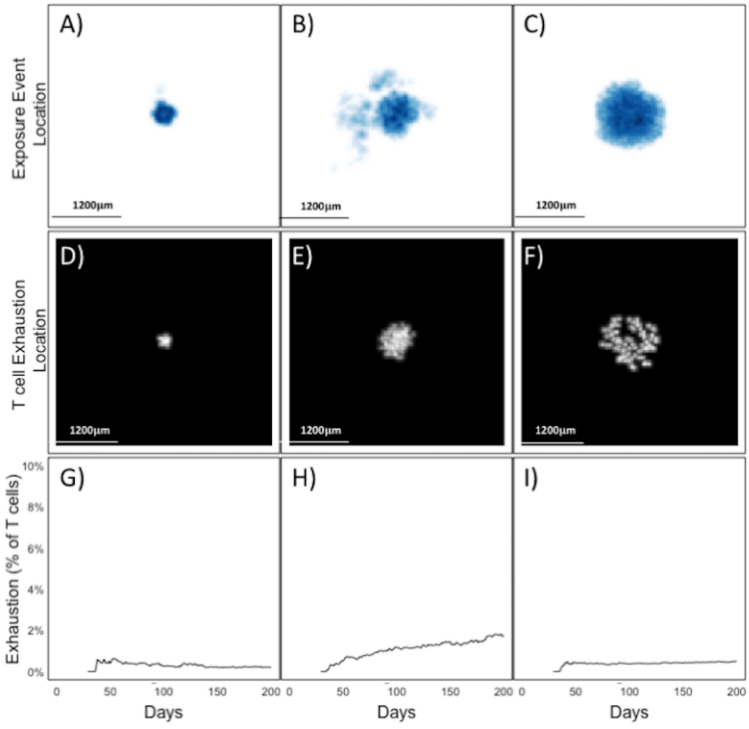

Figure 25. T cell location within granulomas prevents T cell exhaustion by reducing exposure events.

Row 1 (A, B, C): Cloud Maps showing the location of every EE in sterile, medium CFU, and TB pneumonia simulations. Dark blue represents areas of high numbers of EE and white

represents a lack of EE. Row 2 (D, E, F): Heatmap location where T-cells (cytotoxic or IFN-γproducers) became exhausted. White represents the location of T cell at time of exhaustion. Row 3 (G, H, I): Time series graphs that display cumulative levels of exhaustion (as a percentage of total cytotoxic and IFN-γ producers) within corresponding simulations to Rows 1 and 2. Figure courtesy of Louis Joslyn, University of Michigan.

Based on the location of exhausted T cells in the simulations, it appears that cells are more likely to become exhausted as they penetrate deeper into the granuloma. As previously shown, Mtb bacilli are primarily located in the inner core of macrophages and within the necrotic center [268]. As the structure becomes more organized, fewer T cells appear in this region. Thus, *GranSim* predicts that identifying large quantities of a T-cell exhaustion phenotype is unlikely after granuloma formation.

Using our biorepository of nearly 3000 simulated granulomas that matched to all 45 NHP granulomas, we compared observed levels of exhaustion (NHP granulomas) versus those obtained from simulations (Figure 26A). Note that we did not calibrate to the exhaustion levels found in NHP data, but instead calibrated the model to the NHP CFU and CD3+ T cell counts, and then compared exhaustion levels within these simulations to those obtained from NHP studies. The average difference between pairs in these two populations was not significant. That is, overall, our model was able to recapitulate the observed levels of exhaustion.

Computational modeling allows us to artificially inflate the levels of T cell exhaustion in granulomas, to test the impact of widespread T-cell exhaustion on granuloma outcome. We selected the median bacterial burden simulation (Panel B from Fig 25) and re-simulated that same granuloma under hypothetical condition of decreasing EE threshold. We reasoned that a

lower EE threshold would result in a larger number of T cells becoming exhausted, and a decreased ability of the granuloma to contain bacterial growth. We observe that inflated levels of exhaustion in the simulation lead to unfeasible granuloma outcomes, particularly in those granulomas whose EE threshold was less than 200 (Figure 26B). The previous simulation with an EE threshold of 5236 has a bacterial burden of about 288 CFU by day 200 (Figure 26C) and the simulation with an EE of 1 has 115,192,400 CFU (Figure 26D). To our knowledge and in our experience with macaque granulomas [307], these bacterial burdens are biologically unreasonable and can only be attained computationally when exhaustion levels are extremely high, well beyond the NHP findings. We conclude that T-cell exhaustion alone cannot explain the low-frequency of Mtb-responsive T cells in the granuloma, as the vast majority of T cells do not encounter stimulation by antigen sufficiently frequently to become exhausted.

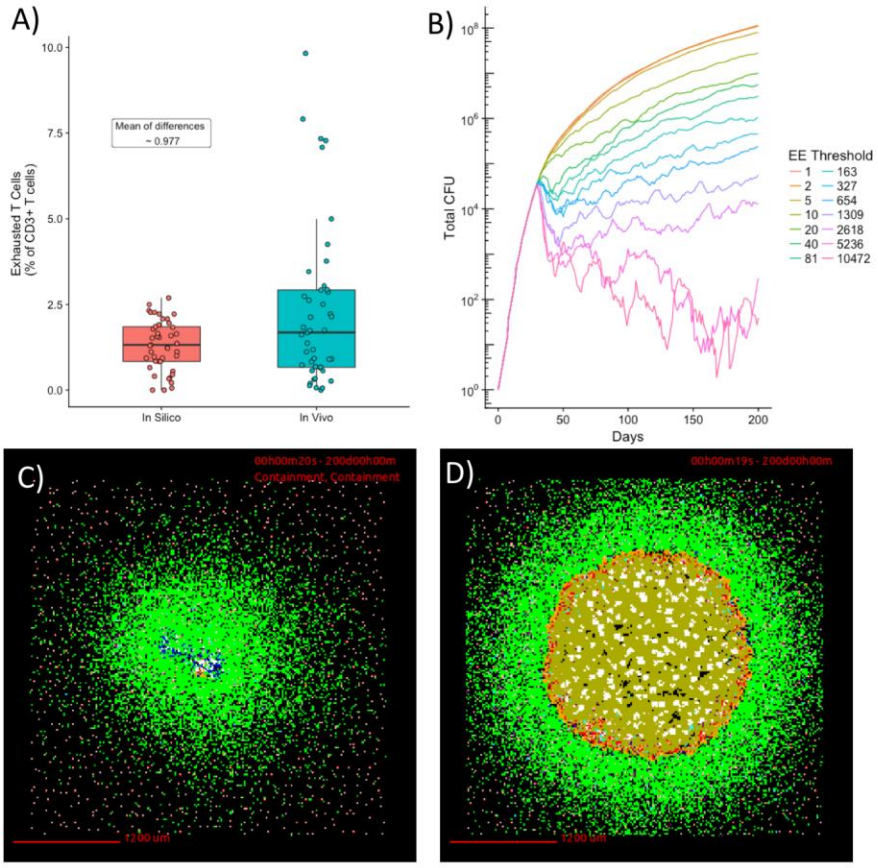

Figure 26. Artificially increasing T cell exhaustion levels result in bacterial burdens that are not observed experimentally.

(A) A box and whisker plot demonstrating the distribution of exhaustion levels from NHP studies versus those obtained via simulation in the 45 macaque granulomas (blue) and the simulations that matched (red). (B) Graph of CFU vs time at varying EE thresholds. (C) Snapshot of granuloma with an EE threshold of 5236 taken at day 200. This granuloma epresents a biologically feasible outcome, and had a bacterial burden of 288 CFU. (D) Snapshot of granuloma with an EE threshold of 1 taken at day 200. This granuloma had a bacterial burden of 115192400 CFU. Figure courtesy of Louis Joslyn, University of Michigan.

3.4 DISCUSSION

The presence and effect of T cell exhaustion has been studied in many chronic diseases. The chronic nature of Mtb infection and continued presence of bacterial antigens in granulomas seemed to be an obvious scenario for development of exhausted T cells, which could explain the inability of some granulomas to completely eliminate the organisms. However, in NHP models of TB, both rhesus and cynomolgus macaques, we detected only limited apparent exhaustion of T cells within granulomas, based on the expression of inhibitory receptors. In fact, the small number of granuloma T cells expressing inhibitory receptors were apparently still functional and producing cytokines or proliferating at similar or higher frequencies as T cells not expressing inhibitory receptors. We observed a moderate negative correlation between the intensity of PD-1 expression (MFI) compared to T cell cytokine expression, suggesting that T cells that express more PD-1 may be more likely to be exhausted, but there may be few T cells strongly expressing PD-1 in TB granulomas. To further investigate the lack of apparent exhaustion in granulomas, we turned to our computational (agent-based) model of a granuloma, GranSim. We demonstrated that GranSim can match macaque granuloma data, and then explored the extent of exhaustion in the simulated granulomas. Again, we found low levels of exhausted T cells in most granulomas. GranSim revealed that T cells could not readily penetrate into the macrophage or caseous layers of the granulomas, where most bacilli exist. Thus, the organized structure of the granuloma precludes widespread T cell exhaustion, in that macrophages and Mtb bacilli tend to be in the center of the granuloma, while T cells are concentrated in the lymphocyte cuff on the periphery of the granuloma. In fact, in cases of less organized pathology (TB pneumonia), we did observe, experimentally and computationally, somewhat higher levels of exhaustion, although still relatively low. Finally, we used our computational model to artificially inflate the level of T cell

exhaustion in granulomas (by decreasing the threshold of T cell-APC interactions), and found that this would lead to exceptionally high bacterial burdens in granulomas. Such high bacterial burdens in individual granulomas are rarely seen in macaque models, even including those with substantial amounts of disease. Thus, we conclude that limited T cell exhaustion in granulomas is due to the relative infrequency of T cells contacting Mtb infected macrophages (or APCs carrying Mtb antigens), which is a key feature of the organized structure of granulomas.

The most frequent inhibitory receptor expressed in granulomas was PD-1, but like the other inhibitory receptors, PD-1 is both an activation and exhaustion marker. There was very little co-expression of multiple inhibitory receptors, with more co-expression of PD-1 with CD69, further suggesting that PD-1 expressing T cells in the granulomas are activated, not exhausted. Thus, we conjecture that the low levels of "inhibitory" receptor expression on granuloma derived T cells actually represent activation markers. This alternative role of inhibitory receptors as markers for proliferating activated cells has been previously explored in Mtb infection and SIV infection. A study of PD-1+ T cells in mice during Mtb infection showed that these cells proliferated, and actually were necessary for maintaining effector cells [169]. Hong et al. also found a similar role for PD-1+ T cells during chronic SIV infections [176]. The necessity of PD-1+ T cells for protection during Mtb infection was further highlighted by studies in PD-1 knockout mice that had higher bacterial burden and extreme inflammation [171, 172] compared to wildtype infected mice.

Although some of our data contradict other studies of T cell exhaustion in TB, we also observed some similar findings. Like the mouse model of TB, PD-1 was one of the most frequently expressed inhibitory markers on T cells [180]. Unfortunately, we were unable to confirm the presence of TIM-3 on granuloma T cells because of lack of a reliable antibody for

NHPs. Although Phillips et al. showed higher LAG-3 expression on T cells from the lungs of Mtb-infected rhesus macaques, we saw much lower levels in individual granulomas from Mtb-infected cynomolgus and rhesus macaques, closer to the levels they observed in clinically latent animals [168]. However, similar to Phillips et al., we observed high frequencies of LAG-3+ cells that were also not CD3+. Some of these discrepancies could be due to differences in the animal models used to investigate exhaustion in Mtb granulomas. Mtb infections in mice do not create the same structured organization in granulomas as observed in humans and NHPs, and therefore T cells may have more interactions with the Mtb bacilli, creating more opportunities for exhausted T cells. We primarily, although not exclusively, used samples from cynomolgus macaques in this study, which tend to have less severe disease than rhesus macaques, thus we may have observed slightly lower expression of LAG-3 in lung granulomas than published studies on lung tissue from Mtb-infected rhesus macaques. There were also differences in timing. In the current study, we examined longer, more chronic infections than was done in previous mouse or rhesus studies, although our samples from early infections also had few T cells expressing inhibitory receptors. Most of the data in Mtb-infected patients is from peripheral blood, so we were unable to confirm our T-cell exhaustion observations at the lung granuloma level to peripheral human data; however, we have previously shown that peripheral immune responses do not reflect local (granuloma) immune responses [102].

Our data support that the lack of T cell exhaustion in a chronic disease like TB is likely a result of the unique characteristic of the disease – containment of the Mtb bacilli within a well-structured granuloma. While the close proximity of bacterial antigens to the host immune cells seemed to be an obvious environment for T cell exhaustion, the structure and spatial arrangement of the immune cells in the granuloma may be responsible for the low levels of T cell exhaustion.

T cells infiltrate the granulomas early in infection, but during chronic infection (>3 months), the vast majority of T cells are on the outer periphery of the granuloma, away from bacteria and exposed macrophages in the center of the granuloma, thus preventing low levels of Mtb-T cell interactions, as also previously suggested by Kauffman et al. [179]. Likewise, we and Phillips et al. observed T cells that express the inhibitory receptors tend to be on the outer edges of the granuloma (Figure 19)[168].

An alternative hypothesis to T cell exhaustion that could explain the low levels of cytokine production by T cells in the granuloma is that many granuloma T cells that are not specific for Mtb antigens. Unfortunately, tetramers for cynomolgus macaques currently do not exist, and we did not use tetramers for the rhesus samples included in this study. Thus, we were unable to quantify the number of Mtb-specific T cells in the granuloma and determine the frequency of T cell exhaustion within Mtb-specific T cells in this current study. In addition, production of immunomodulatory cytokines, such as IL-10 or TGF-β, or inflammation or oxygen or nitric oxide species in granulomas, may regulate T cell function. The low frequency of cytokine producing T cells may be a beneficial characteristic of lung granulomas. Sakai et al. suggested that in a mouse model of Mtb infection, increasing the IFN-γ production by CD4 T cells in lung tissue by reducing PD-1 inhibition exacerbated the bacterial burden within the lungs, worsening TB disease and shortening host lifespan [170]. Our data from macaque granulomas and our computational modeling indicate that a balance of anti-inflammatory (e.g. IL-10) and pro-inflammatory cytokines (TNF, IL-2) within a granuloma is correlated with lower bacterial burdens or sterilization [102, 275, 285]. Studies to examine the T cell cytokine response relative to antigen specificity are underway.

Together, these data support and extend the notion that a balance of cytokine responses and T cell functionality are necessary for control of Mtb within granulomas, and that due to the spatial organization of the granuloma, T cell exhaustion is likely not a major contributor to this balance at the local granuloma level.

3.5 METHODS

3.5.1 Experimental animals

Samples from eleven cynomolgus macaques (*Macaca fascicularis*) between 6.4 and 9.2 years of age, with starting weights of 5-7.8kg (Valley Biosystems, Sacramento, CA), and four rhesus macaques (*Macaca mulatta*) between 5.1 and 14.8 years of age, with starting weights of 5.4-7.9kg (Vaccine Research Center, NIH) were assessed in this study. Animal care was in accordance with institutional guidelines, and all experimental manipulations, protocols, and care of the animals were approved by the University of Pittsburgh School of Medicine Institutional Animal Care and Use Committee (IACUC). Animals were examined while in quarantine as previously described to ensure animals were in good physical health with no previous *M. tuberculosis* infection [57, 291]. Samples were obtained for this study from NHPs from other studies, and infected with 3-31 colony forming units (CFUs) of the virulent Erdman strain of Mtb by bronchoscopic instillation to the lower lung lobe, as previously described [267].

3.5.2 Necropsy procedures, bacterial burden, and staining for flow cytometry

Necropsy was performed as previously described [57, 291]. In summary, NHPs were humanely sacrificed by terminal bleed, and granulomas in lungs identified by PET-CT or at necropsy were individually excised, with half of the granuloma homogenized into single cell suspension for bacterial burden and immunological assays, and the other half for histological analysis, size permitting. To determine the bacterial burden, each granuloma homogenate was plated in serial dilutions on 7H11 medium and incubated at 37°C/5% CO_2 for 21 days before CFU enumeration.

Excised and homogenized granulomas were analyzed for immunological response by surface and intracellular staining and flow cytometry. For each granuloma, cells were resuspended in 1ml of RPMI-1640 containing 1% HEPES, 1% L-glutamine, 10% human AB serum, and 0.1% Brefeldin A (Golgiplug: BD Biosciences), and incubated for 2-3 hours at 37°C/5% CO_2 after homogenization to capture cytokine response. Our previous data indicate that additional *ex vivo* stimulation with Mtb antigens does not increase cytokine production, and can lead to decreased cell recovery. In excised granulomas, Mtb and Mtb antigens are present and likely are restimulating T cells in the homogenized samples. After incubation, granuloma cells were washed with 1xPBS and stained for viability (Invitrogen). Granuloma cells were stained for surface markers, inhibitory receptors, and cytokines in the presence of 1%FBS in PBS. Antibodies for cell surface markers included: CD3 (clone SP34-2, BD Biosciences), CD4 (clone L200, BD Biosciences), CD8 (clone RPA-T8, BD Biosciences), and PD-1 (clone EH12.1, BD Biosciences). Cells were fixed and permeabilized (BD Biosciences). Intracellular staining of inhibitory receptors, activation and proliferation markers, and cytokines included: LAG-3 (clone FAB23193P, R&D Biosystems), CTLA-4 (clone BNI3, BD Biosciences), CD69 (clone TP1.55.3, Beckman Coulter), Ki67 (clone B56, BD Biosciences), IFN-γ (clone B27, BD

Biosciences), IL-2 (clone MQ1-17H12, BD Biosciences), and TNF (clone MAB11, BD Biosciences). Cells were fixed in 1% paraformaldehyde. Data acquisition was performed using a LSR II flow cytometer (BD Biosciences) and analyzed using FlowJo Software v.9.7 (Treestar Inc.).

For the PD-1 and PD-L1 neutralization assay, a subset of lung granulomas and TB pneumonia from two cynomolgus macaques were excised and homogenized as described above. PBMCs were also isolated at the time of necropsy as previously described [291]. Single cell suspensions were divided and each half of the sample incubated *ex vivo*: (1) with 10ug/ml goat polyclonal anti-human-PD-1 antibody (R&D Biosystems) and 10ug/ml goat polyclonal anti-human-PD-L1 antibody (R&D Biosystems), or (2) with polyclonal goat IgG isotype (R&D Biosystems) in 150μl of RPMI-1640 containing 1% HEPES, 1% L-glutamine, 10% human AB serum for 1.5-2.5 hours at 37°C/5% CO_2. After the initial incubation, additional Mtb peptide pools (ESAT-6 and CFP-10, 2ug/ml) were added to the samples to stimulate Mtb-specific cytokine response in the presence of Brefeldin A (Golgiplug: BD Biosystems) and incubated at 37°C/5% CO_2 for an additional 2.5 hours. Samples were then stained for viability, surface markers, inhibitory receptors, and cytokines, then collected and analyzed as described above.

3.5.3 Immunofluorescence of paraffin-embedded samples

Immunofluorescence of paraffin-embedded samples was performed by Nicole L. Grant, University of Pittsburgh. Portions of granulomas excised during necropsy were formalin-fixed, paraffin-embedded, and consecutively cut in 5um sections for histological analysis. For immunofluorescent assays, slides with two consecutive tissue sections were de-paraffinized by xylene, followed by washes in 95% and 70% ethanol before antigen retrieval in Tris-EDTA (pH

9) under heat and pressure. Slides were cooled, washed with PBS, and blocked using 1% BSA in PBS, before incubation overnight at 4°C or 1 hour at room temperature with primary antibodies against CD3 (clone CD3-12, Abcam; DAKO), PD-1 (clone NAT105, Abcam) and LAG-3 (clone EPR4392, Abcam). Antibodies were tested in lymph node samples (S2 Fig). After washing with PBS, slides were stained with secondary anti-mouse, anti-rat, and anti-rabbit antibodies (Jackson Laboratories and Invitrogen) for 1 hour at room temperature and coverslips mounted with ProLong Gold with DAPI (Invitrogen). Confocal microscopy was performed using an Olympus microscope equipped with three lasers. Images were collected using a 20x objective at 1024x1024 size, then compiled using Adobe Photoshop before quantification. Individual cell numbers were identified using the open source image analysis software CellProfiler™. To analyze larger granulomas, small regions of interest were selected and CellProfiler settings were modulated based on image quality so that relevant cell types were accurately quantified. Once pipelines were determined per image, both isotype (secondary only staining) and stained image were analyzed using the same parameters. Isotype image numbers were subtracted from stained images, resulting in an adjusted number representing the cells identified per tissue section.

3.5.4 Computational modeling with *GranSim*

All computational modeling was conducted by Louis Joslyn, University of Michigan. All simulations utilize a 2D hybrid, agent-based model (ABM) called *GranSim* that captures environmental, cellular, and bacterial dynamics across molecular, cellular, and tissue scale events [302, 304, 308, 309]. As an established model, *GranSim* has been calibrated extensively to data from a non-human primate model of TB [302-304, 308-313]. At the molecular scale, *GranSim* incorporates cytokine and chemokine diffusion, secretion and degradation. *GranSim*

also tracks individual immune cells on a 2D simulation grid of micro-compartments, including four macrophage states (resting, activated, infected, and chronically infected) and T-cell types (cytotoxic, IFN-γ producing, and regulatory). Granuloma formation at the tissue level is an emergent behavior of *GranSim*. See http://malthus.micro.med.umich.edu/GranSim for full model details and an executable file. The following methods provide detail on added mechanisms to *GranSim* so that we can use *GranSim* as a tool to study exhaustion in granulomas.

3.5.4.1 Model definitions, assumptions, and justifications.

A great advantage of our *in silico* representation is that we can track cellular movement, behavior, and interaction across time. In *GranSim*, we define an interaction between a T cell and macrophage by the occurrence of a macrophage entering the double Moore neighborhood of a T cell [314-316] (i.e. Moore neighborhood is defined as all micro-compartments on the grid immediately adjacent to the one the cell is in; double Moore includes the next outer ring of micro-compartments). In particular, as we evaluate the possibility of T-cell exhaustion influencing the pathology of granuloma formation, we become solely interested in *Exposure Events (EE*), defined as the interactions between a T cell and an antigen "exposed" macrophage.

In previous model versions, we defined an exposed macrophage according to three criteria: 1) If the cell contained any intracellular Mtb, 2) If, within the single Moore neighborhood of the macrophage, there exists any live or dead extracellular Mtb, and 3) If, within the single Moore neighborhood of the macrophage, there is another macrophage that was determined to be exposed during a previous timestep. Additionally, once a macrophage becomes exposed, it remains exposed for the entirety of its lifespan [275].

As noted in the Introduction, chronic antigenic stimulation is sufficient to develop exhaustion within a T-cell population. Based on current literature, we model antigenic

stimulation via EE [317-319]. We use EE as a standard of stimulation across a T-cell's lifetime to evaluate various analytical measures about T-cell exhaustion, including: individual T-cell exposure to antigens, average EE across T-cell populations, and determination of whether only a few T cells out of the entire population accrue the majority burden of EE.

Finally, we created a new parameter within *GranSim* to introduce an exhausted T-cell phenotype (this parameter was aptly named 'ExhaustionThreshold'). If the EE of an IFN-γ producing T cell or a cytotoxic T cell exceeds this preset threshold, then a T cell is marked as 'exhausted'. Once labeled, it loses all effector function, but continues to move around the grid until it dies from its natural lifespan (we do not assume there is an enhanced death rate for exhausted cells). Because we explore the possible role of exhaustion within granuloma formation, we crafted this parameter to represent the worst-case scenario: if a T cell exceeds the threshold, it immediately ceases effector function rather than for example, exhibiting a progressive loss of function. Other formulations are possible, but we have considered this case as an upper bound for quantifying exhaustion levels (yielding the worst case scenario).

Computational Platform and Post-Run Analysis

GranSim is constructed through use of the C++ programming language, Boost libraries (distributed under the Boost Software License – www.boost.org), and the Qt framework for visualization (distributed under GPL – www.qt.digia.com). The ABM is cross-platform (Macintosh, Windows, Unix) and runs with or without visualization software. *GranSim* model simulations were performed locally and also on the XSEDE's OSG Condor pool resources.

We relied on uncertainty analysis (UA) techniques to explore model parameter space. In particular, we used Latin Hypercube Sampling (LHS, reviewed in [306]) for UA. The LHS algorithm is a stratified Monte Carlo sampling method without replacement [306] and was used

to generate 1,500 unique parameter sets, which were simulated in replication 3 times (a total of 4,500 *in silico* simulations) for 200 days. When we matched our simulations to NHP granulomas, often the size of the high and median bacterial burden samples necessitated the use of a 200 by 200 micro-compartment simulation space, whereas the simulation space for sterile samples could be performed within 100 by 100 micro-compartments.

Analysis of statistical data derived on EE from simulations was performed using smoothScatter, ggplot2 and base packages in R [320] and Matlab [321]. Additional analysis was conducted on more general data concerning granuloma-scale infection outcomes, granuloma formation, and concentration values of various effector molecules and CFU within the simulations.

3.5.4.2 Model calibration and defining exhaustion.

Once the model was updated, we re-calibrated *GranSim* with respect to i) CFU totals, ii) CD3 totals, and iii) time based on 45 separate NHP granuloma sample data. Table 1 outlines a portion of the comprehensive analysis we performed to compare T-cell exhaustion *in silico* versus the data derived on T-cell exhaustion *in vivo.* Table 2 shows the parameter ranges we used to generate an *in silico* bio-repository of 4,500 granulomas.

Table 1. Example analysis of *in silico* versus *in vivo* T cell exhaustion data.

Table 1.3 displays the direct comparison between exhaustion in our matching simulations and the level of observed exhaustion in NHP samples. Tables 1.1 and 1.2 explain our method of matching and aggregating data. Table 1.1 displays 1 of the 44 granuloma NHP samples that we used for calibration. The right-most column shows the number of simulations that matched to the NHP sample CFU values and CD3 Count. Each simulation could match the criteria across several time points. Table 1.2 shows each of the 5 simulations that calibrated to NHP sample 13516_RLL 17_20 cluster and the average percentage of exhausted T cells across the simulation timepoints that matched NHP sample criteria. Finally, we aggregated the data to display an overall sense of model fit by selecting the "median of the means" for each matching simulation. Thus, for NHP sample 13516_RLL 17_20 cluster, the median percent of exhaustion across all samples that matched was 0.0%. Flow cytometry data shows that this sample had 0.66% of T cells that showed two or more exhaustion markers.

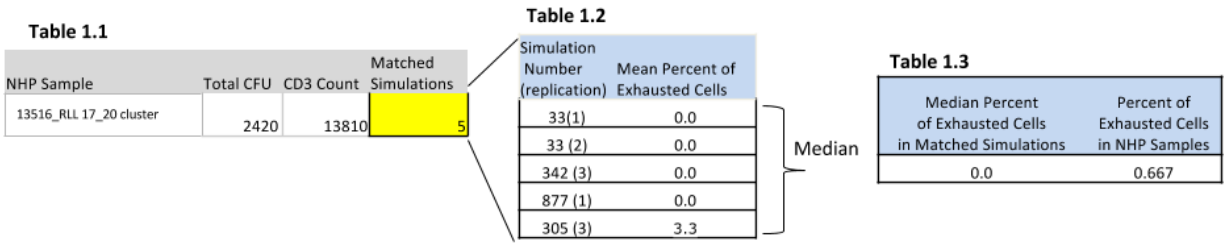

Since the exact roles of individual inhibitory receptors as markers in the progression of T-cell exhaustion is unclear [175], we assume that a T cell is only truly exhausted if it co-expresses any *two or more* inhibitory receptors. Thus, when we compared T-cell exhaustion levels and markers *in vivo* against T-cell exhaustion *in silico*, the *in vivo* percentage of T-cells that are "exhausted" are actually the percent of T-cells that expressed 2 or more inhibitory receptors.

Out of the 4,500 granulomas in our *in silico* bio-repository, we matched simulations to samples according to our criteria, as shown in Table 1.1 of Table 1. As an example, if we examine NHP Sample 13516_RLL 17_20, we were able to select 5 unique simulations that matched CFU and CD3 values across various simulation time points. For each of the 5 simulations, across every time point that matched the NHP sample's CFU and CD3+ T cell levels, we found the average percent of exhausted T cells (Table 1.2). For example, the first replication of simulation no. 33 matched CFU and CD3 counts across 5 different time points over the 200-day simulation. We averaged the exhausted T cells across each of the 5 days and found that the mean percentage of exhausted T cells when this simulation matched our criteria, was 0.0%.

Finally, we aggregated the data to provide a sense of overall model fit for each of the 45 NHP samples. Table 1.3 displays the median value across all the mean percentages of exhausted T cells for each sample's matching simulations. Thus, for Sample 13516_RLL 17_20, the median percent of exhaustion across all the samples that matched was 0.0%. Flow cytometry data shows that this sample had 0.66% of T cells that displayed 2 or more inhibitory markers.

Table 2. Table of parameter ranges used to create both biorepositories of 4500 unique granulomas.

All ranges, with the exception of exhaustionThreshold, were performed within the ranges outlined by previous versions of GranSim. See methods text for details on how the ranges were assigned for exhaustionThreshold.

Parameter Name	Description	Range	Units	Reference
growthExtMtbBound	Upper bound of number of external Mtb used in growth function	[180,240]	Number of bacteria	[275, 285, 302-305]
growthRateIntMtb	Fractional growth rate of intracellular bacteria	[0.001,0.005]	Unitless	[275, 285, 302-305]
growthRateExtMtb	Fractional growth rate of extracellular bacteria	[0.001,0.003]	Unitless	[275, 285, 302-305]
deathRateExtMtbCaseated	Upper bound on the number of external Mtb used in growth function	[1,2]	Number of bacteria	[275, 285, 302-305]
Core				
estBoundFactorTNF	Adjustment for coarse grained internalized fraction estimate	[0.4,0.5]	Unitless	[275, 285, 302-305]
estBoundFactorIL10	Adjustment for coarse grained internalized fraction estimate	[0.4,0.6]	Unitless	[275, 285, 302-305]
estConsRateTNF	Scaling Factor for coarse grained TNF dynamics	[5e-4,9e-4]	Unitless	[275, 285, 302-305]
estConsRateIL10	Scaling Factor for coarse grained IL10 dynamics	[2e-4,6e-4]	Unitless	[275, 285, 302-305]
estIntPartitionTNF	Scaling Factor for coarse grained internalization of bound TNFR1	[9,13]	Unitless	[275, 285, 302-305]
nrKillingCaseation	Number of killings for a compartment to become caseated	[7,13]	Number	[275, 285, 302-305]
caseationHealingTime	Time it takes for a caseated compartment to heal	[1700,2600]	Timesteps	[275, 285, 302-305]

Table 2 (continued)				
sourceDensity	Density of vascular sources on the gridspace	[0.002,0.05]	Unitless	[275, 285, 302-305]
diffusivityTNF	TNF diffusivity	[4e-08, 6e-08]	Cm^2/second	[275, 285, 302-305]
diffusivityChemokines	Chemokine diffusivity	[4e-08,6e-08]	Cm^2/second	[275, 285, 302-305]
diffusivityIL10	IL10 diffusivity	[4e-08,6e-08]	Cm^2/second	[275, 285, 302-305]
ChemokinekDeg	Chemokine degradation rate constant	[0.0005,0.005]	1/second	[275, 285, 302-305]
kDeg	TNF degradation rate constant	[0.0005,0.005]	1/second	[275, 285, 302-305]
Ikdeg	Degradation rate constant for IL10	[0.0003,0.003]	1/second	[275, 285, 302-305]
IC50ChemokineIL10	IC50 of IL10 inhibition of chemokine secretion	[1,10]	Molecules/mL	[275, 285, 302-305]
thresholdApoptosisTNF	TNF threshold for TNF-induced apoptosis	[1000, 5000]	Unitless	[275, 285, 302-305]
kApoptosis	Rate of apoptosis happening	[1e-07, 2e-6]	1/second	[275, 285, 302-305]
saturationApoptosisTNF	Signal saturation of number of internal bound TNFR1 Molecules	[5000, 9000]	Molecules	[275, 285, 302-305]
minChemotaxis	Minimum of Chemotaxis sensitivity range	[1, 50]	Molecules	[275, 285, 302-305]
maxChemotaxis	Maximum of Chemotaxis sensitivity range	[100,1000]	Molecules	[275, 285, 302-305]
maxIL10Inhibition	Coarse grained TNF/IL10 dose dependence parameter beta	[0.05, 0.3]	Log10(ng/mL)	[275, 285, 302-305]
Mac				
initDensity	Initial density of macrophages on the gridspace	[0.005,0.03]	Unitless	[275, 285, 302-305]
movementRest	Time required for a resting macrophage to move one micro-compartment	[1,10]	Timesteps	[275, 285, 302-305]
movementAct	Time required for an activated macrophage to move one micro-compartment	[10,50]	Timesteps	[275, 285, 302-305]

Table 2 (continued)				
movementInf	Time required for an infected macrophage to move one micro-compartment	[100,200]	Timesteps	[275, 285, 302-305]
dTNF	Secretion rate of TNF by a macrophage	[1.3,1.7]	Molecules/second	[275, 285, 302-305]
dCCL2	Secretion rate of CCL2 by a macrophage	[4,8]	Molecules/second	[275, 285, 302-305]
dCCL5	Secretion rate of CCL5 by a macrophage	[4,8]	Molecules/second	[275, 285, 302-305]
dIL10Act	Secretion rate of IL10 by an activated macrophage	[0.2, 0.4]	Molecules/second	[275, 285, 302-305]
halfSatIL10	Half saturation for TNF induction of IL10 in an activated macrophage	[170,210]	Number/cell	[275, 285, 302-305]
thresholdNFkBTNF	TNF threshold for NFkB activation	[75,115]	Molecules	[275, 285, 302-305]
kNFkB	Rate of NFkB activation	[0.7e-5, 1e-5]	Fraction	[275, 285, 302-305]
probKillExtMtbRest	Probability of a resting macrophage to kill extracellular bacteria	[0.05, 0.3]	Unitless	[275, 285, 302-305]
fKillExtMtbRest	Fractional increase of a resting macrophage to kill extracellular bacteria when STAT1 or NFkB pathways are on	[0.3,0.5]	Unitless	[275, 285, 302-305]
nrExtMtbNFkB	Number of extracellular bacteria for NFkB activation in an infected macrophage	[150, 250]	Bacteria	[275, 285, 302-305]
nrIntMtbCInf	Number of intracellular bacteria necessary for an infected macrophage to become chronically infected	[8,12]	Bacteria	[275, 285, 302-305]
nrIntMtbBurstCInf	Number of intracellular bacteria necessary for a chronically infected macrophage to burst	[13,20]	Bacteria	[275, 285, 302-305]

Table 2 (continued)				
nrExtMtbUptakeAct	Number of extracellular bacteria an activated macrophage can uptake and kill	[3,7]	Bacteria	[275, 285, 302-305]
Stat1ActivationTime	Time a macrophage is Stat1 activated	[400,460]	Timesteps	[275, 285, 302-305]
nfkbActivationTime	Time a macrophage is NFkB activated	[13,17]	Timesteps	[275, 285, 302-305]
Stat3ActivationTime	Time a macrophage is Stat3 activated	[75,125]	Timesteps	[275, 285, 302-305]
thresholdSTAT3IL10	Threshold of IL10 to IL10R1 for STAT3 signaling	[5,15]	Unitless	[275, 285, 302-305]
kSTAT3IL10	Rate constant of bound IL10 to IL10R1 for STAT3 signaling	[5e-4, 1.5e-3]	Unitless	[275, 285, 302-305]
probHealCaseation	Rate constant for wound healing	[0.005, 0.05]	Unitless	[275, 285, 302-305]
T cell				
maxAge	Maximum age of a T cell	[400,460]	Timesteps	[275, 285, 302-305]
exhaustionThreshold	Threshold of Exposure Events for an individual T cell before it becomes exhausted	[200, 10000] (5236 during generation of 2nd biorepository)	Count	Estimated
probMoveToMac	Probability of a T cell moving into a compartment already containing a macrophage	[0.01, 0.2]	Unitless	[275, 285, 302-305]
probMoveToTcell	Probability of a T cell moving into a compartment already containing another T cell	[0.01, 0.2]	Unitless	[275, 285, 302-305]
maxDivisions	Maximum number of times a T cell can create a daughter cell	[3,5]	Timesteps	[275, 285, 302-305]
γ-producing T cells				
dTNF	Secretion rate of TNF by γ-producing T cell	[0.1, 0.2]	Molecules/second	[275, 285, 302-305]
maxTimeReg	Time span during which a γ producing T cell remains down-regulated	[30,40]	Timesteps	[275, 285, 302-305]

Table 2 (continued)				
probApoptosisFasFasL	Probability of Fas/FasL induced apoptosis by a γ-producing T cell	[0.01,0.03]	Unitless	[275, 285, 302-305]
probTNFProducer	Probability that a γ-producing T cell can produce TNF	[0.04, 0.1]	Unitless	[275, 285, 302-305]
probIFNProducer	Probability that a γ-producing T cell can produce IFNγ	[0.3, 0.4]	Unitless	[275, 285, 302-305]
probIFNMooreExtend	Probability a macrophage will be IFNγ/STAT1 activated in the extended Moore Neighborhood.	[0.2, 0.3]	Unitless	[275, 285, 302-305]
Cytotoxic T cells				
dTNF	Secretion rate of TNF by a cytotoxic T cell	[0.01, 0.02]	Molecules/second	[275, 285, 302-305]
maxTimeReg	Time span during which a cytotoxic T cell remains down-regulated	[30,40]	Timesteps	[275, 285, 302-305]
probKillMac	Probability of a cytotoxic T cell killing a chronically infected mac	[0.005, 0.015]	Unitless	[275, 285, 302-305]
probKillMacCleanly	Probability of a cytotoxic T cell killing a chronically infected mac cleanly	[0.6, 0.9]	Unitless	[275, 285, 302-305]
probTNFProducer	Probability that a cytotoxic T cell is producing TNF	[0.05, 0.09]	Unitless	[275, 285, 302-305]
Regulatory T cells				
dIL10	Secretion of IL10 by a regulatory T cell	[0.7, 0.8]	Molecules/second	[275, 285, 302-305]
probTregDeactivate	Probability of successful downregulation by a regulatory T cell	[0.01, 0.02]	Unitless	[275, 285, 302-305]
factorDeactIL10	Factor when a regulatory T cell is making IL10 to scale probTregDeactivate	[1,3]	Unitless	[275, 285, 302-305]

3.5.4.3 EE threshold selection.

Initially, we created a biorepository of 4500 granulomas using the LHS technique. Within this biorepository, the EE threshold for T cell exhaustion ranged from 200 to 10000. We calculated the upper bound of 10000 interactions of the EE threshold as a T cell that has every location in a T cell double Moore Neighborhood occupied by an exposed macrophage throughout the entirety of its life (average of 3 days in our simulation), will accrue 10500 interactions. We selected 200 interactions as the lower level of EE because a T cell with 200 interactions has encountered exposed macrophages less than 2% of the time it has been alive – certainly, a sufficient EE threshold for a phenotype that is caused by chronic stimulation.

Figures 25 and 26 were produced from a second biorepository of 4500 granulomas. This biorepository was created with the exact same parameter ranges as in Table 2, but the EE threshold was set to 5236, the median of all simulations that matched the macaque granulomas. A threshold of 5236 EE seems reasonable, as 4320 interactions equals 1 interaction per minute through the average lifespan of a T cell.

3.5.5 Statistical Analyses

Statistical analyses were conducted in GraphPad Prism 7 (GraphPad Software, San Diego, CA). Data were tested for normality by D'Agostino & Pearson Omnibus Normality Test. Since data analyzed in this study were not normally distributed but were paired, Wilcoxon matched-pair signed rank tests were used to compare two groups for multiple comparisons, with no multiple comparison adjustments to p-values. Correlations were calculated by nonparametric Spearman rho tests. P-values ≤ 0.05 were considered significant and noted in individual graphs.

4.0 VACCINATION CAN MODULATE IMMUNE RESPONSES IN TB GRANULOMAS

4.1 ABSTRACT

Despite the availability of the Bacille Calmette-Guérin (BCG) vaccine against TB for the past century, tuberculosis (TB) remains a major threat to global health. Although BCG can protect infants from disseminated disease, its efficacy against adult pulmonary TB is much more variable. Several TB vaccines are currently in various stages of development and clinical trials to replace, boost, or improve the only currently licensed vaccine BCG. We tested combinations of novel TB subunit vaccines and adjuvants via different strategies for their ability to induce immune response and protection against TB using a non-human primate (NHP) model in a two-part study. In the initial study, we vaccinated cynomolgus macaques with a recombinant protein vaccine (H56) admixed with a novel adjuvant (CAF09) by three routes—intranasal, subcutaneous, and aerosol to assess the immunological and protective effects of different vaccination routes. Frequencies of T cells producing pro-inflammatory cytokines increased in the blood and BAL following vaccinations in all groups, but NHPs vaccinated by aerosol had a rapid and transient recall of T cells to the airways after the third vaccination. After *M. tuberculosis* (Mtb) challenge, aerosol vaccinated NHPs had less inflammation by PET-CT compared to other vaccinated groups and unvaccinated controls, although they had little to no improvement in disease pathology or total bacterial burden compared to controls at necropsy. Although

vaccination in this initial study did not lead to protection of NHPs, the aerosol vaccinated animals appeared to have slightly improved disease outcomes after Mtb challenge. Following the reduction of inflammation and improved T cell recruitment to the airways, we further examined aerosol vaccination in the second part of this study, with all vaccines used as a "boost" in the context of BCG vaccination. We examined a novel recombinant fusion protein vaccine, H74, but because of adverse reactions during the first part of the study, we switched from CAF09 to CAF01 in the secondary study. Based on previous studies that suggested BCG could act as an adjuvant, and particularly could have synergistic effects on the immune response and protection with a fusion protein vaccine, we also tested whether simultaneous injection of BCG and H56/H74-CAF01 could improve protection. While we induced peripheral immune responses to vaccination and altered the granuloma cytokine response after Mtb challenge, these vaccination strategies did not improve disease pathology or bacterial loads in NHPs compared to BCG vaccination alone. Among the vaccination groups, BCG followed by intramuscular H74 boost vaccinations had some improved disease parameters, while simultaneous BCG&H74 vaccination, with intramuscular and H74 boosts seemed to worsen TB disease compared to BCG alone. This study did not support that these new vaccination strategies improved upon the currently used BCG vaccination, but demonstrates the difficulty in optimizing the immune response within granulomas to prevent TB. The results from this study may help inform future vaccine studies and research on vaccination strategies.

4.2 INTRODUCTION

Mycobacterium tuberculosis (Mtb), the causative agent of tuberculosis (TB), continues to be a top cause of death by infectious disease worldwide. According to the World Health Organization, 1.7 million people died from TB in 2016 [1]. A live attenuated vaccine against TB, Bacille Calmette-Guérin (BCG), has been widely used over the past century, but has little efficacy in preventing the pulmonary TB commonly seen in adolescents and adults [322]. Although BCG can protect infants from more severe forms of disseminated TB disease, a more effective vaccine or vaccination method to prevent development of active TB disease or reactivation of latent infection is needed [323, 324]. BCG is traditionally administered intradermally, while most other vaccines are administered intramuscularly, orally, or subcutaneously [325]. Recently, vaccines that target the site of infection for mucosal pathogens have garnered increased interest [262]. In particular, a vaccination route that targets the airways has been suggested to increase the efficacy of TB vaccine protection from pulmonary disease [258-261]. Additionally, studies have shown that booster vaccines given simultaneously with BCG target the same draining lymph node and can boost immune responses [264].

Several vaccine candidates employing different vaccination strategies for TB are in various stages of development, including multiple fusion protein vaccines, which combine a variety of Mtb immunogenic proteins to induce an immune response. Our collaborators led by Dr. Peter Andersen at Statens Serum Institut (SSI) recently developed two fusion protein vaccine candidates, H56 and H74. H56 is a fusion of the Mtb immunogenic antigens, Ag85B and ESAT-6, as well as the latency-associated protein Rv2660c [326]. Administered with different adjuvants, H56 has been shown to induce vaccine-specific immune responses in mice, non-human primates (NHPs), and humans [229, 326, 327]. H56 reduces bacterial burden after Mtb

challenge in mice and reduces disease and prevents reactivation in NHPs [326, 327]. H74 is composed of the Mtb antigens ESAT-6, Rv3881c (EspB), Rv3614c (EspD), Rv3615c (EspC), Rv3616c (EspA), and Rv3849 (EspR). These antigens are strongly immunogenic and co-regulated and secreted through the ESX-1 secretion system of Mtb. Unlike classical vaccines that primarily emphasize the immune response to mycobacterial antigens only produced early in infection, such as Ag85B, these novel vaccines from SSI include immunogenic proteins that continue to be produced throughout the course of Mtb infection [231-241]. H74 has been demonstrated to cause strong immunogenic response and reduce bacterial burden in the mouse model of Mtb infection (data from Dr. Peter Andersen, not published).

Protein vaccines require adjuvants for proper vaccine delivery and induction of immune responses. A series of novel liposome-based cationic adjuvant formulations (CAF) were developed by our collaborators at SSI to enhance the T cell responses during vaccination [242]. CD4 T cell (Th1 and Th17) responses are important for controlling Mtb replication and disease pathology, as shown in knock-out mouse models and patients with genetic defects in Th1 IFN-γ/IL-12 signaling pathways [71-73, 86, 328]. CD8 T cells in Mtb infections have been shown to be crucial for protection from TB, as mutations in the MHC I pathway in mice and CD8 depletion in NHPs resulted in increased lung pathology and decreased control of Mtb [94-96]. Two of these liposomal delivery systems are CAF09 and CAF01. CAF09 was designed to enhance the CD4 and CD8 T cell response against vaccine antigens. CAF09 is composed of dimethyldioctadecyltammonium (DDA)-liposomes and monomycoloyl glycerol (MMG)-1, a synthetic analogue of a mycobacterial cell wall lipid, and Poly(I:C), a synthetic dsRNA and TLR3 agonist. Targeting TLR3 can enhance cross-priming and improve antigen presentation to CD8 T cells, while MMG induces Th1/Th17 immune responses and stimulates DCs. In mice,

CAF09 delivered with various antigens from HIV, Mtb, and HPV increased antigen-specific CD8 T cell responses [244]. CAF09 used as an adjuvant for another TB protein vaccine in mouse and guinea pig models induced a strong pro-inflammatory (IFN-γ, TNF, IL-2) CD4 T cell response, and reduced bacterial burdens in vaccinated animals compared to unvaccinated controls [243]. Similar to CAF09, CAF01 is also composed of DDA liposomes, but with trehalose 6,6-dibehenate (TDB) glycolipids, a synthetic variant of a mycobacterial cell wall cord factor, as a stabilizer and immunomodulator. In different animal models and humans, CAF01 with TB protein vaccines has been demonstrated to promote long-lasting Th1 and Th17 immune responses [242, 245-248]. Targeting particular T cell responses by vaccination may help with protection against Mtb challenge.

While fusion protein vaccines H56 and H74, along with liposomal adjuvants CAF01 and CAF09, have shown encouraging vaccine-specific immune response in the mouse model and, in the case of H56, in NHP models [221, 222, 229, 230, 242-245], different vaccination strategies using these promising TB vaccine candidates in NHPs has not yet been thoroughly investigated. Using a low-dose Mtb infection of cynomolgus macaques (*M. fasicularis*), we can recapitulate the spectrum of human Mtb infection in both disease progression and pathology [77, 267]. Initially, we investigated whether targeting the mucosal airways by intranasal or aerosol administration, or targeting the lymphatic system by subcutaneous administration would increase the efficacy of vaccination. Thus, we conducted an *in vivo* immunogenicity study using H56 admixed with CAF09 and administered by different routes – intranasal, subcutaneous, aerosol – and then assessed the protection conferred by vaccination after Mtb challenge in a NHP model. Following the somewhat encouraging aerosol results of our initial study but noting adverse reactions in NHPs to CAF09, we further investigated the protection conferred by H56 or H74

admixed with CAF01 boosts followed by aerosolized vaccination of H56 or H74. Additionally, based on previously published results of the synergistic immunogenic response of simultaneous vaccination of protein vaccines and BCG [264], we tested whether simultaneous vaccination of H74-CAF01 and BCG would improve protection from Mtb challenge. Although the entire study is not yet complete, from the first two cohorts of NHPs we can infer that boosting BCG vaccination with H74-CAF01 or H56-CAF01 by aerosol vaccination, intramuscular injection, or simultaneous administration did not increase protection against Mtb infection or disease over BCG vaccination alone.

4.3 RESULTS

4.3.1 Vaccination with H56 and CAF09 can induce adverse inflammatory responses

To first determine whether vaccination route influenced immune responses or protection, cynomolgus macaques were randomly assigned to three vaccination cohorts, and vaccinated with H56 admixed with CAF09 adjuvant three times each as indicated in Table 3. Each cohort received their vaccinations by different administrations routes – intranasal, subcutaneous, aerosol. The subcutaneous cohort received a pegylated form of CAF09 injected directly above an axillary lymph node to increase the depot effect.

Table 3. Vaccination cohorts for H56-CAF09 vaccination routes.

Nine NHPs were randomized to receive vaccination by different routes. Each group received 3 vaccinations of the same dose of H56 vaccine (50ug) in CAF09 adjuvant, with 4-5 weeks between each vaccination, except for the aerosol group, which received H56 alone for the third vaccination.

Vaccination Route	N	Vaccination 1 (Week 0)	Vaccination 2 (Week 4)	Vaccination 3 (Week 9)
Intranasal	3	H56-CAF09	H56-CAF09	H56-CAF09
Subcutaneous (over LN)	3	H56-CAF09	H56-CAF09	H56-CAF09
Aerosol	3	H56-CAF09	H56-CAF09	H56

The intranasal group received their vaccinations with no notable side effects or inflammation, but the subcutaneous and aerosol groups had some adverse reactions to vaccination. Four weeks after their initial vaccination, animals in the subcutaneous group had small minor lesions in the injection region. Two days after the second injection, the right axillary lymph node became swollen in all three macaques, ranging from 5-15 mm by 10-13 mm. The lymph nodes remained enlarged through the course of vaccinations, and small ulcerations at the sites of injections appeared after the third vaccination. The aerosol group was resistant to the aerosolization mask despite sedation during the first vaccination. Thirty seconds into their second vaccination, animals in the aerosol group began to hyperventilate and their mucus membranes turned bright red. To prevent repeat adverse effects during the third vaccination, the aerosol group received the last vaccination without CAF09 (H56 protein only), and received a small dose of Benadryl and Tylenol prior to third vaccination.

4.3.2 T cells are pulled into the airways after H56-CAF09 vaccination

After the third and last vaccination, there was an increase in CD3+ T cells in the airways, as measured in bronchoalveolar lavage (BAL), in all of the cohorts (Figure 27). The aerosol cohort that received a third, protein-only "pull" vaccination had an immediate but transient increase in CD3+ T cells in airways, with numbers of T cells peaking one day after the third vaccination, and decreasing by one week after the third vaccination. In both intranasal and subcutaneous groups, T cell numbers in the BAL increased 1 week after the third vaccination, although the immediate response 1 day after third vaccination was not measured.

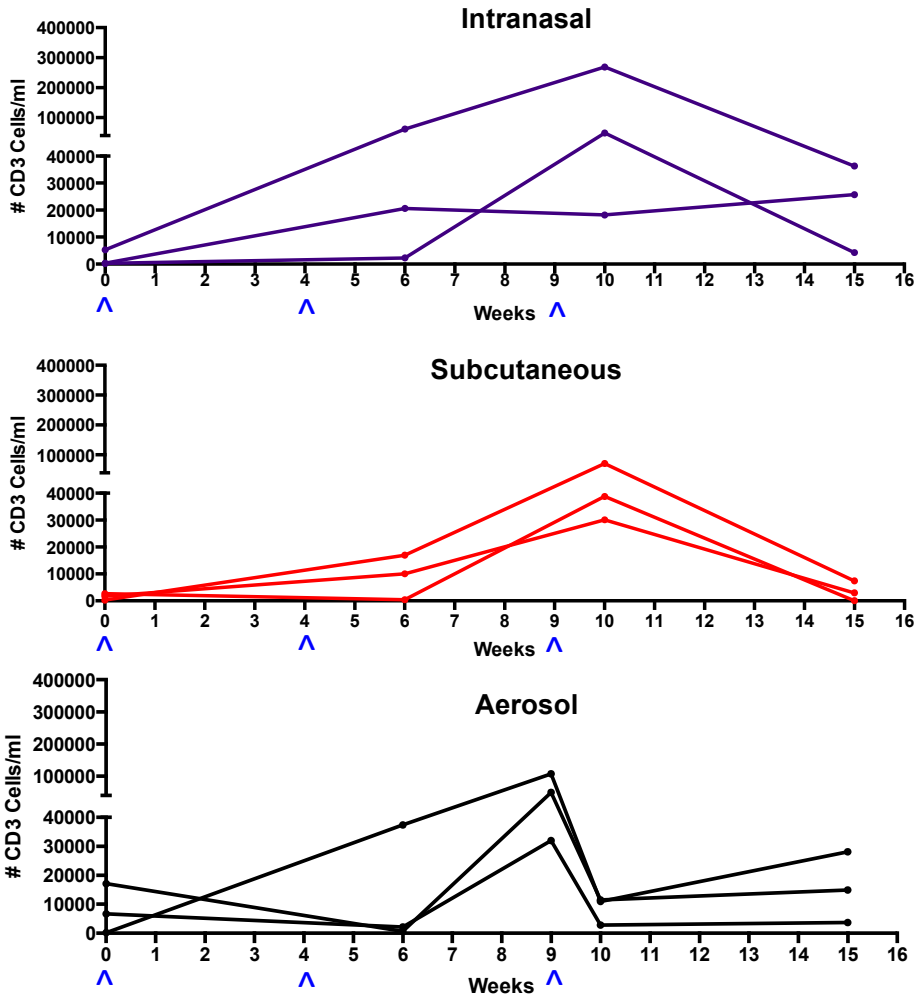

Figure 27. T cell are drawn to the airways (BAL).

Numbers of CD3+ T cells per ml in BAL in each vaccination cohort. T cells are pulled to the lungs 1 day after third H56 only vaccination in aerosol cohort, while intranasal and subcutaneous cohorts have increase in T cells 1 week after third vaccination. Blue arrowheads indicate vaccination times. N = 3 NHPs in each cohort.

4.3.3 Immune response to H56-CAF09 vaccinations in the airways and blood

We investigated the immune response in the BAL to vaccination by intracellular staining and flow cytometry. NHPs in all cohorts had a detectable T cell cytokine response in the BAL following the third vaccination. The increase in concentrations of CD4+ and CD8+ T cells producing IFN-γ, TNF, IL-17, or IL-2 corresponded to the peak in numbers of T cells in the BAL (i.e., 1 week after third vaccination for intranasal and subcutaneous, 1 day after third vaccination for aerosol) (Figure 28A). The transient increase and decrease in T cells after the last vaccination in the aerosol group (Figure 27) also corresponded to the cytokine response in CD4+ and CD8+T cells in the BAL.

Some patterns of CD4 T cell functionality were observed in the BAL. The CD4 T cells in the BAL of NHPs vaccinated by the intranasal and subcutaneous routes at the time points with highest T cell response (1 week after third vaccination) had similar T cell cytokine patterns, with more polyfunctional CD4 T cells producing different cytokines (intranasal median = 1.47% CD4 T cells, and subcutaneous median = 1.13% of CD4 T cells making three or more cytokines). In contrast, the cytokine profile of CD4 T cells of aerosol vaccinated NHPs was dominated by single cytokine producers, particularly TNF-only T cells 1 day and 1 week after third vaccination (Figure 28B). Aerosol vaccinated animals had median polyfunctional CD4 T cell (three or more cytokines) response of 0.24% and 0.36% 1 day and 1 week after third vaccination, respectively. This suggests that the third boosting vaccination with the protein alone directly to the lung by aerosol may rapidly increase CD3+ T cells in the airways and induce a strong TNF-producing response with fewer polyfunctional T cells, compared to administering the vaccine with the liposomal adjuvant CAF09 intranasally or subcutaneously.

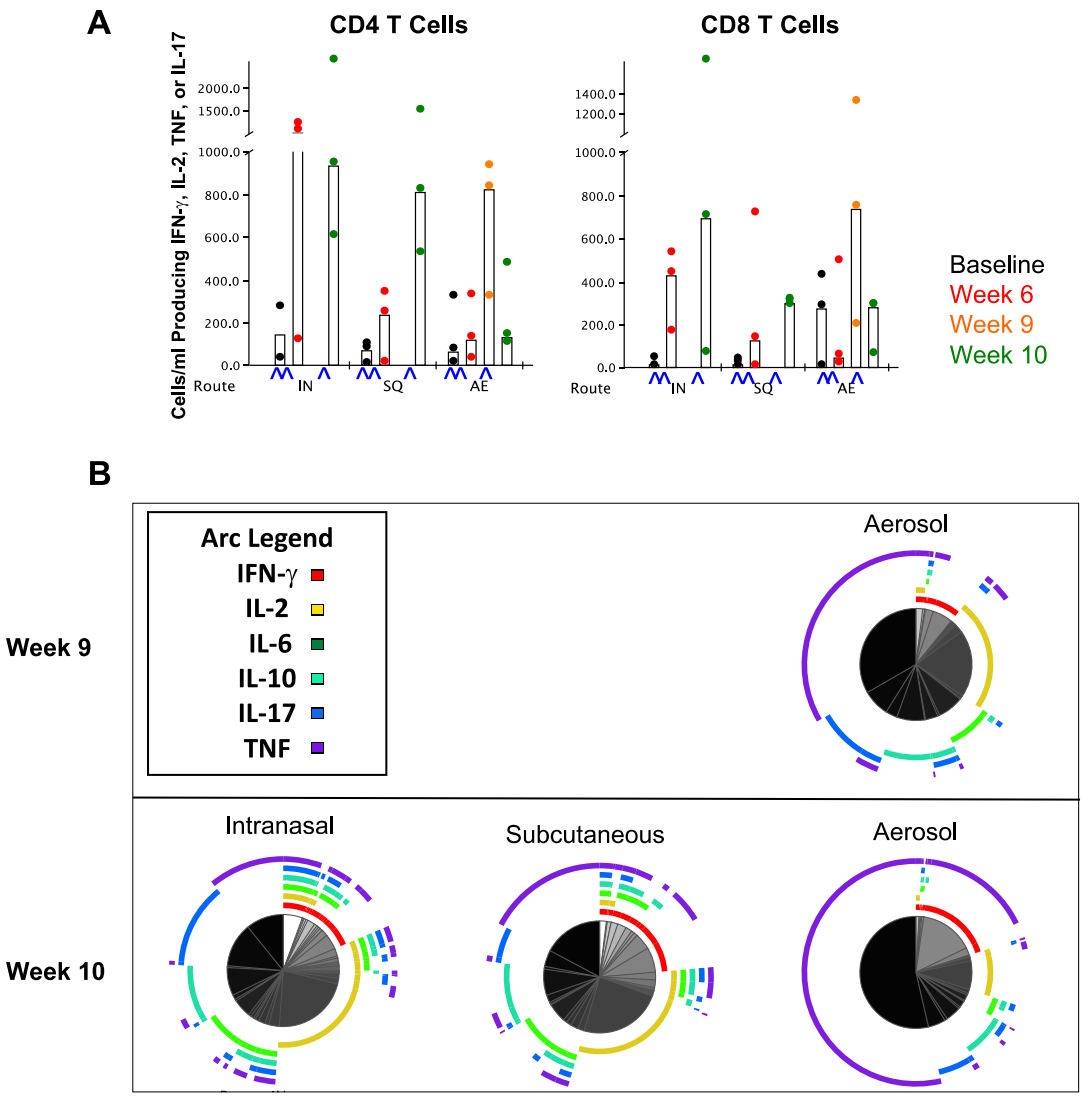

Figure 28. T cell cytokine responses in the airways to H56-CAF09 vaccination.

(A) Numbers of BAL CD4 or CD8 T cells producing IFN-γ, IL-2, TNF, or IL-17 cytokines per mL of BAL fluid after vaccinations (marked by blue arrowheads). Slight increase in intranasal group after first two vaccinations (Week 6), with majority of response from all groups after the third vaccination (Week 9/10). BAL cells were unstimulated with Brefeldin A for 12 hours. Lines at medians. IN = Intranasal, SQ = Subcutaneous, AE = Aerosol (B) Polyfunctional CD4 T cell cytokine response in BAL at times of peak T cell response. Intranasal and subcutaneous

groups have more polyfunctional T cells at Week 10 compared to aerosol group at either Week 9 or Week 10 (i.e., more overlapping lines for intranasal and subcutaneous groups compared to aerosol group). Pie charts are of unstimulated CD4 T cells from BAL.

The BAL fluid was used to assess antibody responses using ELISAs. Only aerosol and subcutaneous vaccinated animals had H56-specific antibody responses in their BAL (Figure 29A). Levels of H56-specific IgG peaked 1 week after the third vaccination in the BAL of aerosol animals (black lines), decreasing to minimal levels again 5 weeks later. H56-specific IgG also increased 1 week after the third vaccination in subcutaneous animals, but this group showed increased or maintained levels of IgG after another 5 weeks. Only one animal from the aerosol group had measurable levels of H56-specific IgA in its BAL (Figure 29B).

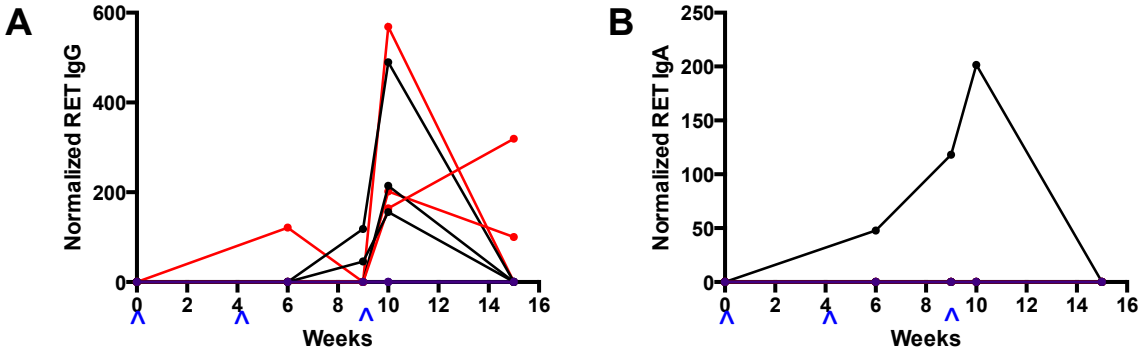

Figure 29. Antibody response in the airways to H56-CAF09 vaccination.

H56-specific (A) IgG and (B) IgA antibody responses in the BAL fluid of vaccinated animals during the course of vaccination. Intranasal = purple, subcutaneous = red, aerosol = black. Vaccinations in all graphs marked by blue arrowheads.

The immune response to vaccination in PBMCs was more variable than in the BAL. The frequency of CD4+ and CD8+ T cells producing pro-inflammatory cytokines in the PBMCs increased following the vaccinations, but the response was variable within groups, and typically transient (Figure 30A). However, the subcutaneous group had higher levels of H56-specific IgG in their plasma than the other two vaccination groups, particularly after their second and third vaccinations (Figure 30B).

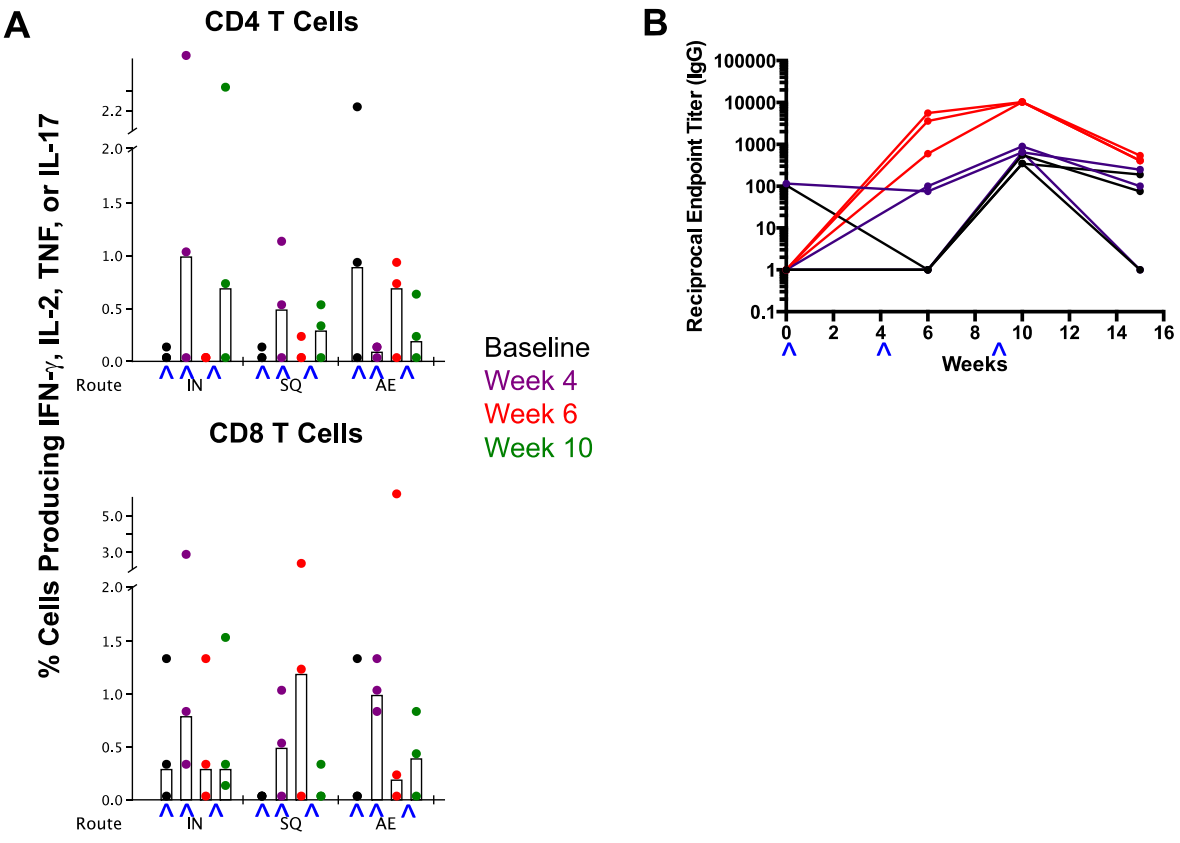

Figure 30. Peripheral blood response to vaccinations with H56-CAF09.

(A) PBMC T cell cytokine response after vaccinations (marked by blue arrowheads). Variable PBMC response between cohorts, with some increase after vaccinations. PBMC cells were stimulated with peptide pools of Ag85B for 6 hours (5 hours with Brefeldin A), and cytokine

frequencies were media-subtracted. Lines at medians. IN = Intranasal, SQ = Subcutaneous, AE = Aerosol (B) H56-specific IgG in plasma of vaccinated animals during the course of vaccination. Intranasal = purple, subcutaneous = red, aerosol = black. Vaccinations in all graphs marked by blue arrowheads.

4.3.4 Aerosol vaccinated NHPs have less inflammation and dissemination after Mtb challenge

We then investigated whether the differences in immune response after vaccination would translate to different levels of protection of NHPs following Mtb challenge. NHPs were intrabronchially challenged with a low dose of Mtb Erdman (12-21 CFU). Inflammation in NHP lungs was quantified by total ^{18}F-FDG activity in lung on PET-CT scans over the course of infection as described [329]. Total FDG activity has been previously shown by our group to correlate with bacterial burden in lungs [61]. Aerosol vaccinated NHPs had lower total FDG activity than other vaccinated cohorts and unvaccinated controls (black lines, Figure 31A). Intranasal and subcutaneous vaccinated NHPs rapidly increased in inflammation 3 weeks after challenge, with inflammation levels similar to or above those seen in unvaccinated control NHPs (green lines). Although two of the aerosol vaccinated NHPs had increased inflammation early in infection, this decreased over the course of infection. In contrast, the other vaccination cohorts tended to stabilize at high levels of inflammation. By necropsy, two of the three aerosol vaccinated NHPs had less inflammation than the unvaccinated controls. Although not significant due to low numbers of animals in this pilot study, the results were intriguing.

We also tracked granuloma numbers in the lungs during the course of infection by PET-CT scans. The aerosol vaccinated NHPs tended to have less change in granuloma numbers between 3 and 6 weeks after infection compared to the other vaccinated groups, but similar to the unvaccinated controls (Figure 31B). Stable numbers of granulomas suggest less dissemination in the lungs.

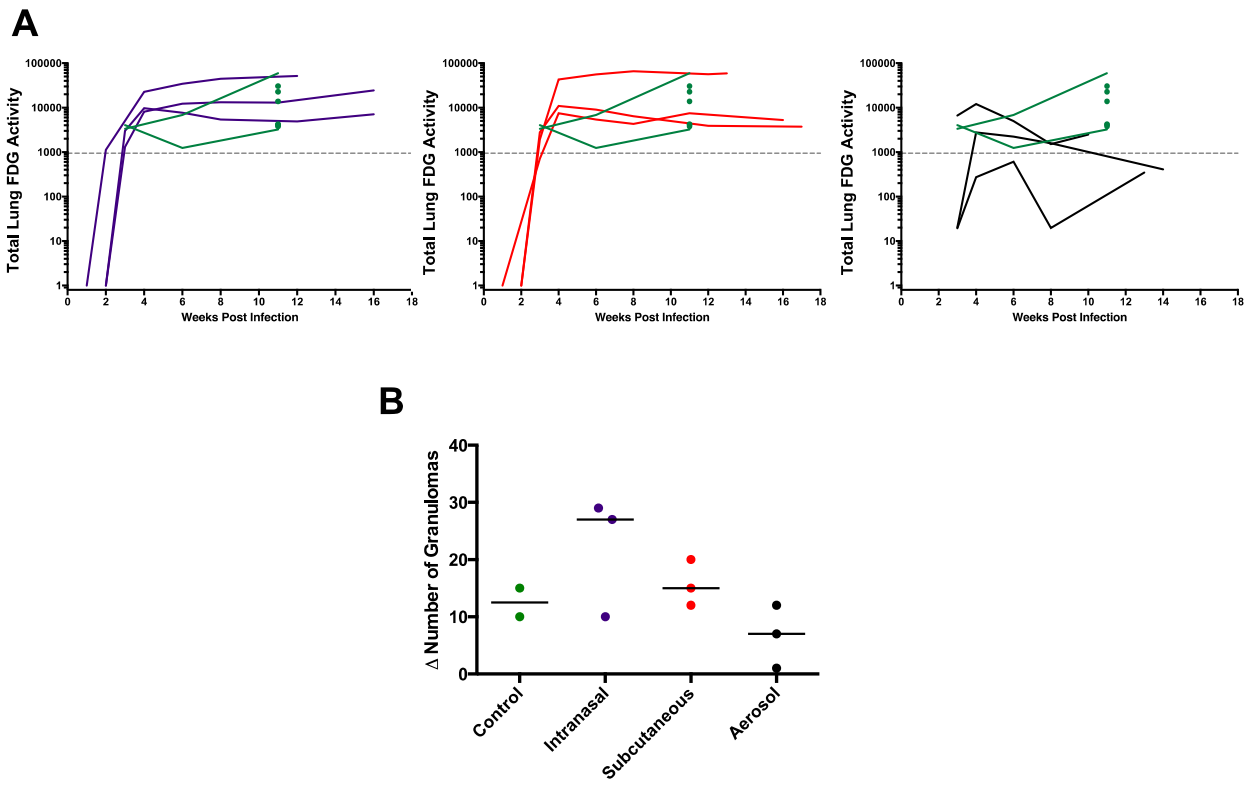

Figure 31. Inflammation and granuloma dissemination in lungs of H56-CAF09 vaccinated after Mtb challenge.

(A) Inflammation in lungs, as measured by the summation of ^{18}F-FDG uptake in the lungs by PET-CT scans. Intranasal (purple) and subcutaneous (red) cohorts have similarly high levels of inflammation as unvaccinated control monkeys (green) after Mtb challenge. In contrast, aerosol

vaccinated monkeys (black) have less inflammation compared to other vaccinated cohorts and unvaccinated controls. Dotted line represents PET Hot of 947.2, which we have found to be the cutoff for high risk of reactivation in latent TB macaques (i.e., PET Hot below 947.2 has low risk of reactivation) [330]. (B) Change in numbers of granulomas in the lungs during infection, from first scan at 3 weeks post-infection to 6 weeks, quantified by PET-CT scans. Aerosol vaccinated monkeys have the least change in granulomas numbers in the lungs, indicating more stable granulomas.

4.3.5 Vaccination with H56-CAF09 did not substantially improve disease pathology and bacterial burden

Although vaccinated NHPs, particularly the aerosol vaccinated cohort, had indicators of less disease by PET-CT during the course of infection, the overall disease pathology and bacterial burden at necropsy was not significantly different from unvaccinated controls; again, there were a small number of animals in this pilot study. The total disease pathology (lung, lymph node, extrapulmonary) quantified at necropsy in vaccinated NHPs was similar to unvaccinated controls (Figure 32A). The aerosol cohort, which had the least inflammation after Mtb challenge, had slightly less disease pathology, but was still within the range of the unvaccinated controls. The aerosol vaccinated macaques had less extrapulmonary disease than intranasal and subcutaneous groups, but it was not less than the unvaccinated controls (Figure 32B). Overall, the aerosol cohort had slightly less disease pathology than other groups, but still within the range of the unvaccinated controls. In this model, approximately half of unvaccinated controls will develop latent infection, while the other half develops active TB, thus the range of infection outcomes in control macaques is not unexpected.

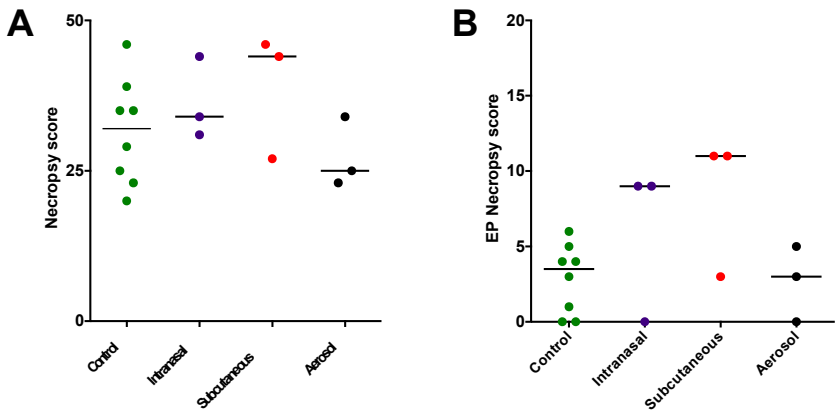

Figure 32. Disease pathology of vaccinated animals and controls at the end of challenge. (A) At necropsy, aerosol vaccinated has slightly less disease pathology than other vaccinated cohorts, but within the range of unvaccinated control monkeys. (B) Less disease in extrapulmonary tissues of aerosol vaccinated monkeys, comparable to controls. Necropsy scores are tabulated based on spread and extent of disease at time of necropsy. Lines at medians. Each point is a NHP.

An important outcome measure of vaccine protection is bacterial burden and dissemination of disease. The total bacterial burden (thoracic cavity) of the vaccinated NHPs at necropsy was similar to the unvaccinated controls. The aerosol cohort had slightly less total bacterial burden in lymph nodes than other groups, but similar bacterial burden within lungs (Figure 33A). Bacterial burden by individual granulomas shows that granulomas from all vaccinated animals have fewer bacteria than unvaccinated, which is reflected in a higher frequency of sterile granulomas in vaccinated compared to unvaccinated (Figure 33B). The aerosol group has slightly higher frequency of sterile granulomas than other vaccination groups, but with overlapping variability (Figure 33C). The bacterial burdens in individual thoracic lymph

nodes of vaccinated and unvaccinated macaques are similar, as well as the frequency of sterile lymph nodes between the cohorts (Figure 33D and 33E). Generally, all groups poorly controlled bacterial replication and had high lung and lymph node bacterial burdens, but the aerosol cohort had slightly higher frequencies of sterile granulomas, suggesting slightly better clearance of bacteria.

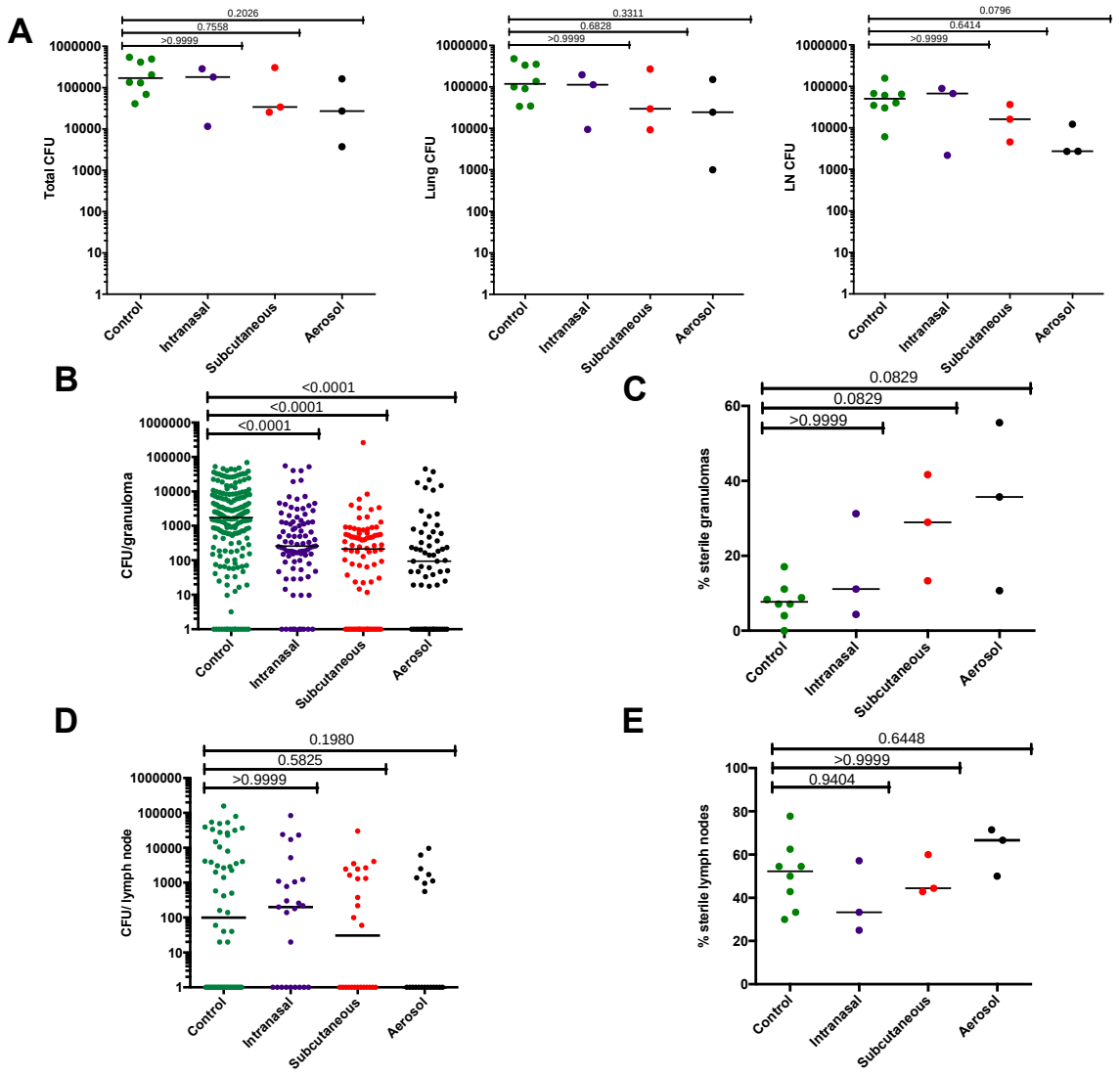

Figure 33. Bacterial burden in total, lung, and lymph nodes after challenge.

(A) Vaccinated monkeys have bacterial burdens within the range of unvaccinated controls, although aerosol vaccinated monkeys have slightly less CFU in the LN than the other groups. Each point is a NHP. (B) Bacterial burden in excised granulomas at necropsy. Vaccinated groups have significantly less bacterial burden in granulomas compared to unvaccinated controls. Each point is a granuloma. (C) Vaccinated animals also have slightly higher frequencies of sterile granulomas, particularly in the aerosol cohort. Each point is a NHP. (D) Bacterial burden in lymph nodes at necropsy. Vaccinated and unvaccinated animals have similar bacterial burden in

lymph nodes. Each point is a LN. (E) Vaccinated groups have similar frequencies of sterile lymph nodes as unvaccinated controls. Each point is a NHP. All tests for significance compared experimental groups to control groups by Dunn's multiple comparisons tests. Lines at medians.

4.3.6 Variable cytokine response in lymph nodes and granulomas after H56-CAF09 vaccination

To investigate the local immune response, individual lymph nodes and granulomas were excised from NHPs and stained for cell surface markers and intracellular cytokines for flow cytometry. The peripheral lymph node immune response, specifically the right axillary lymph nodes draining the subcutaneous vaccine site, were of interest because of their particularly large size after vaccination. At necropsy, the subcutaneous group had higher IFN-γ responses in their peripheral lymph nodes compared to other groups (Figure 34). However, there was no difference between the right axillary lymph node and the unrelated inguinal lymph node (stars vs. dots in Figure 34). It is likely that vaccination over the lymph node had a local effect on immune responses in the lymph node, but that over time, this effect spread to other peripheral lymph nodes, resulting in higher T cell responses.

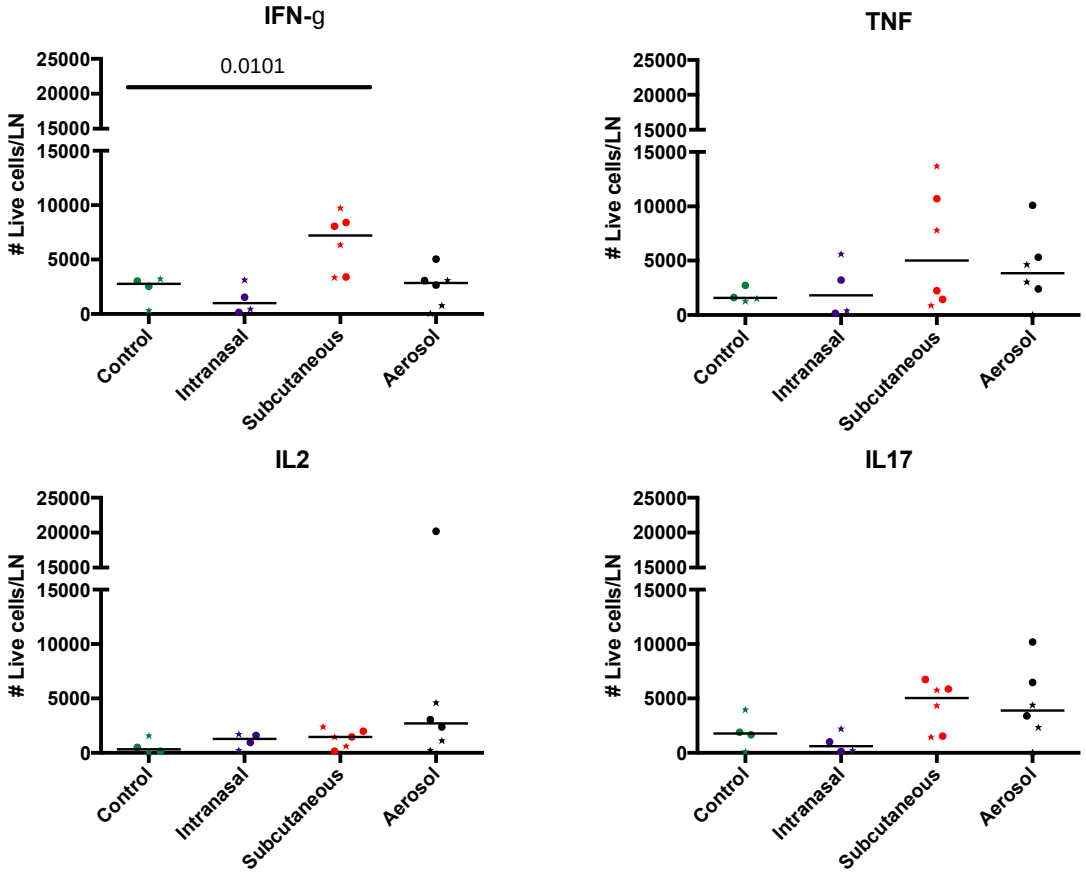

Figure 34. Cytokine response in peripheral (axillary/inguinal) lymph nodes after Mtb challenge.

Subcutaneous vaccination above right axillary LN (indicated by stars in figure) increases IFN-γ response in peripheral LNs compared to other vaccinated cohorts, but other cytokine responses similar to other vaccinated cohorts. Dunn's multiple comparisons test for significance. Lines at medians. Each point is a LN, stars mark R axillary LN.

The lung granulomas also had diverse cytokine responses as previously reported [102] (Figure 35). Aerosol vaccinated macaques had higher frequencies of IFN-γ producing granuloma T cells compared to the unvaccinated controls. The intranasal cohort had higher frequencies of

IFN-γ and TNF producing T cells, but lower frequencies of IL17 producing T cells compared to unvaccinated controls. Subcutaneously vaccinated NHPs had lower frequencies of IL17 producing T cells compared to the unvaccinated. All groups had similar frequencies of T cells producing IL2. These differences in T cell cytokine responses within the granulomas may contribute to the slight differences in local granuloma outcome and ability to control the bacterial burden.

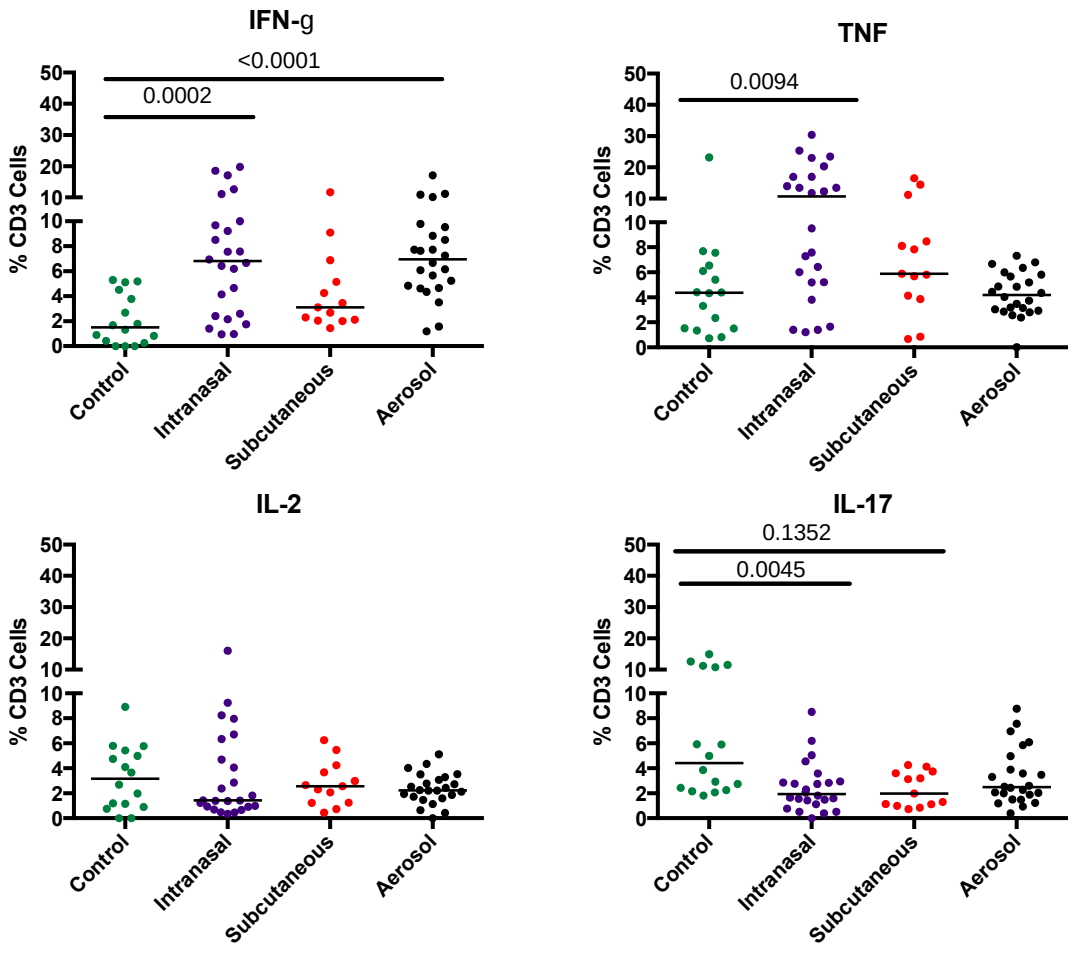

Figure 35. Local T cell cytokine response in lung granulomas after Mtb challenge.

Intranasal group has significantly higher IFN-γ and TNF, and lower IL-17 response compared to the unvaccinated monkeys, while other vaccinated cohorts had fewer differences in granuloma T

cell response relative to unvaccinated monkeys. Aerosol vaccinated monkeys had significantly higher IFN-γ response compared to the unvaccinated. Dunn's multiple comparisons for significance. Lines at medians. Each point is a granuloma.

4.3.7 Experimental boost of BCG responses by aerosolization of protein vaccines

Based on the H56-CAF09 results, aerosolization of the vaccine seemed to draw T cells to the airways, decrease inflammation, and alter the T cell response within granulomas, although it did not decrease total bacterial burden. Since H56 was optimized as a booster vaccine to BCG, to further investigate the efficacy of aerosolizing TB vaccines, we designed another *in vivo* NHP study to determine whether there were benefits to aerosolizing the protein fusion vaccine in the context of a BCG vaccination. We also wanted to test whether simultaneous administration of a protein vaccine and BCG had synergistic immunogenic effects in the NHP model as it did in mouse studies [264]. At the same time, we decided to investigate a newer fusion protein vaccine, H74, which had shown protection in mouse studies. Finally, since CAF09 caused adverse effects in the initial study, we chose to continue our study using an adjuvant that we knew worked well in NHPs, CAF01. The different experimental groups to encompass these vaccines, adjuvants, and vaccination routes are listed in Table 4.

Table 4. Vaccination cohorts for H56/H74-CAF01 vaccination routes.

Thirty-six NHPs were randomized to receive vaccination by different routes. Each group received BCG intradermally (ID), with or without simultaneous booster vaccine (H56-CAF01 or H74-CAF01) intramuscularly in the same region on the right quadriceps to ensure drainage to the same LN. Fourteen weeks after the initial priming vaccination, most groups except for BCG only group received H56/H74-CAF01. After 6 weeks, NHPs received a second boost of H74-CAF0 intramuscularly or H56 or H74 without adjuvant. While the majority of the cohorts are completed, not all outcome data has been collected yet, numbers are denoted as "In Progress."

Vaccination Name	Prime (Week 0)	Boost 1 (Week 14)	Boost 2 (Week 20)	Completed N	In Progress N
BCG	BCG (ID)			3	1
BCG&H74 IMx2	BCG (ID) & H74-CAF01 (IM)	H74-CAF01 (IM)	H74-CAF01 (IM)	6	2
BCG&H74 IM AE	BCG (ID) & H74-CAF01 (IM)	H74-CAF01 (IM)	H74 (AE)	5	3
BCG, H74 IMx2	BCG (ID)	H74-CAF01 (IM)	H74-CAF01 (IM)	5	3
BCG&H56 IMx2	BCG (ID) & H56-CAF01 (IM)	H56-CAF01 (IM)	H56 (AE)	6	2

For statistical analyses, we compared vaccine-boosted animals to BCG only animals (Table 4, Figure 36) using unpaired non-parametric ANOVA (Kruskal-Wallis) and post-hoc analysis Dunn's multiple comparisons test. All NHPs were vaccinated at the same time with the initial priming intradermal BCG vaccination, with some receiving simultaneous intramuscular

vaccinations with H56-CAF01 or H74-CAF01. All groups, except the BCG only group, received additional 2 booster vaccinations, 6 weeks apart to compare aerosolization and intramuscular administration of booster vaccines. No adverse effects of vaccination were observed in any experimental animals. Eight to 10 weeks after final vaccination, NHPs were challenged with a low dose (4-25 CFU) to determine efficacy of vaccination. Throughout the course of vaccination and challenge, we assessed vaccine-specific peripheral and airway immune responses. After challenge, we monitored inflammation and disease progression by ^{18}F-FDG PET-CT scans before quantifying final disease outcomes (pathology and bacterial burden) at necropsy.

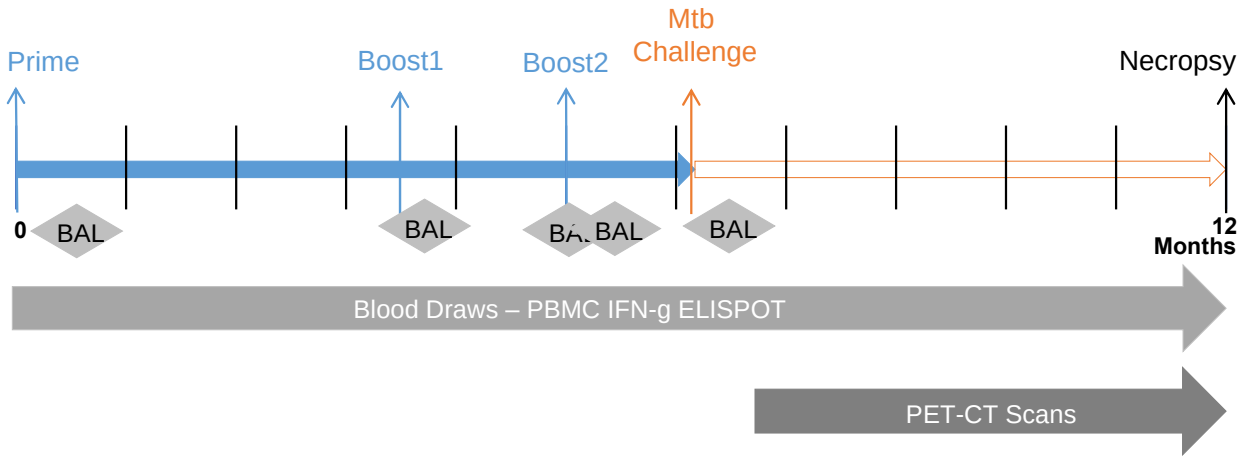

Figure 36. Experimental timeline of H56/H74-CAF01 vaccination route study.

Day 0 = day of BCG prime vaccination, followed by two boost vaccinations at weeks 14 and 20. Eight to 10 weeks following final vaccination (28-30 weeks post-BCG), NHPs were challenged with a low dose (4-25 CFU) and the course of infection followed for 5 months.

4.3.8 T cells are not pulled to the airways during H56/H74-CAF01 aerosol vaccination

Vaccinated animals had different T cell airway responses during vaccination and immediately after challenge (Figure 37). The BCG-only animals had fairly stable concentrations of T cells in the airway through vaccinations, increasing only after Mtb challenge. The two groups of animals that received their vaccinations by intramuscular administrations (BCG&H74-CAF01, IMx2 and BCG, H74-CAF01. IMx2) had some variable responses throughout infection, and a slight increase in numbers of T cells in the airway 1 week after the second boost (Week 21), compared to 1 day after the second boost (Week 20). With the exception of one or two animals, the two intramuscular vaccination groups did not have an influx of T cells in the airway 2 weeks after challenge. We were most interested to see if the aerosol vaccination increased the T cell response in the airways (BCG&H74-CAF01, IM AE and BCG&H56-CAF01, IM AE). Unlike with H56-CAF09 vaccination animals, we did not observe much T cell pull to the airways after aerosolization of the boosting fusion protein vaccines, even in the group that received the same H56 protein aerosol vaccine as in the previous study (BCG&H56-CAF01, IM AE). We had expected to observe a similar increase in concentration in T cells in the BAL, especially immediately after the aerosol vaccination at the second boost, but we only saw modest changes in some of the animals between 1 day and 1 week after the second boost (Week 20 and Week 21), instead of a peak 1 day after the second boost (Figures 27 and 37). Interestingly, there was a slight increase in T cell concentrations in the BAL of the BCG&H74-CAF01, IM AE group after the first boost, which was given by aerosol. Some of the animals in the two aerosol groups also had increased T cell concentrations 2 weeks after Mtb challenge.

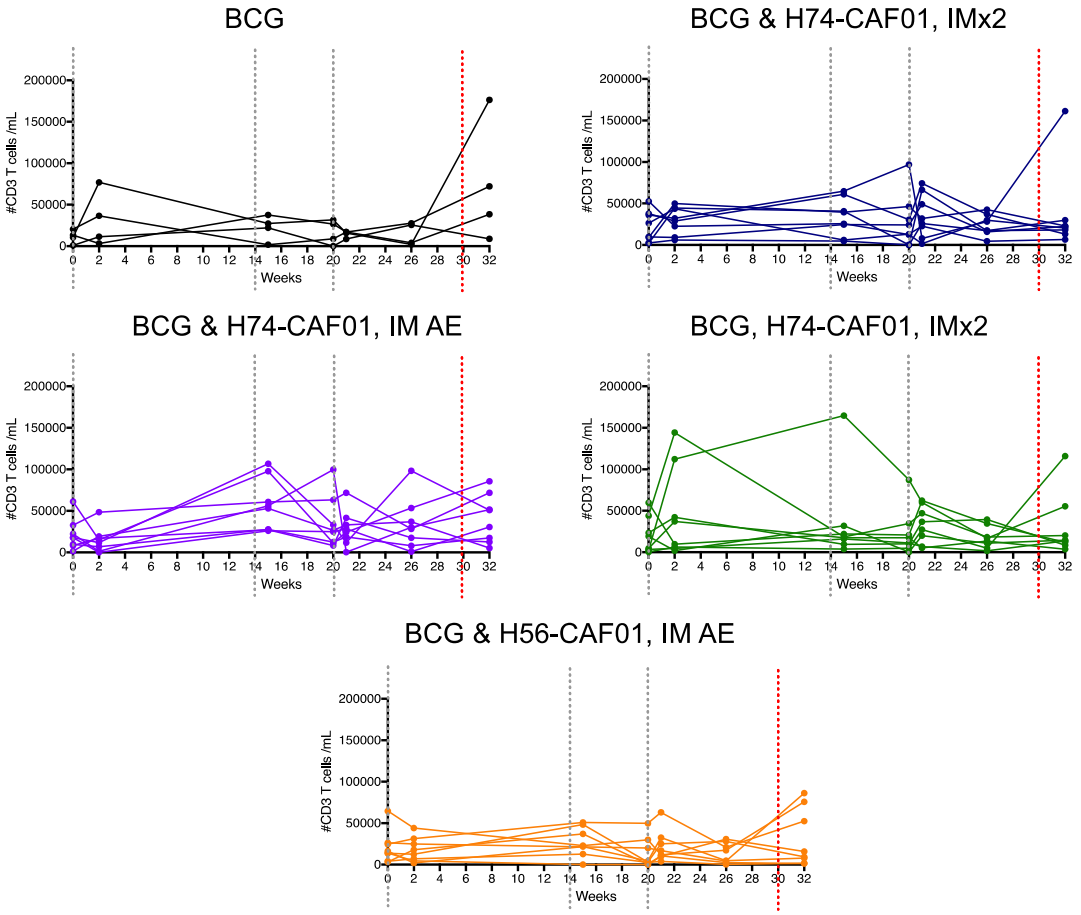

Figure 37. T cells are not drawn to the airways after H56/H74-CAF01 vaccinations.

Concentrations of CD3+ T cells/mL of BAL fluid recovered from the airways of vaccinated animals over the course of vaccination and initially after Mtb challenge. IM = intramuscular vaccination, AE = aerosol vaccination. Gray dotted lines mark vaccination time points, red dotted lines mark Mtb challenge. Each line is a NHP. BCG, N = 4 NHPs; BCG&H74-CAF01, IMx2, N = 8 NHPs; BCG&H74-CAF01, IM AE, N = 8 NHPs; BCG, H74-CAF01, IMx2, N = 8 NHPs; BCG&H56-CAF01, IM AE, N = 8 NHPs.

Although the numbers of T cells did not increase in the airways, the vaccine boosts may affect the functionality of the T cells in the airways. Some of the H56/H74-CAF01 animals had an increase in the concentrations of vaccine-specific CD4 T cells producing any of pro-inflammatory cytokines (IFN-γ, IL-2, TNF, or IL-17) after the first or second boost (Figure 38). However, aerosolization of the H56 or H74 did not appear to further draw functional cells to the airways, as intramuscularly boosted animals also had an increase in their vaccine-specific CD4 T cells. The vaccine-specific CD8 T cell response appeared to be more variable, with the BAL cells from one BCG-vaccinated animal surprisingly stimulated by H74 throughout vaccination, and some early (2 week) high responses before the boost vaccinations (Figure 39). There were particularly low vaccine-specific CD8 T cell responses in H56-CAF01 vaccinated animals, especially responses after aerosol vaccination (week 20) compared to H56-CAF09 animals from the initial study (Figure 28A).

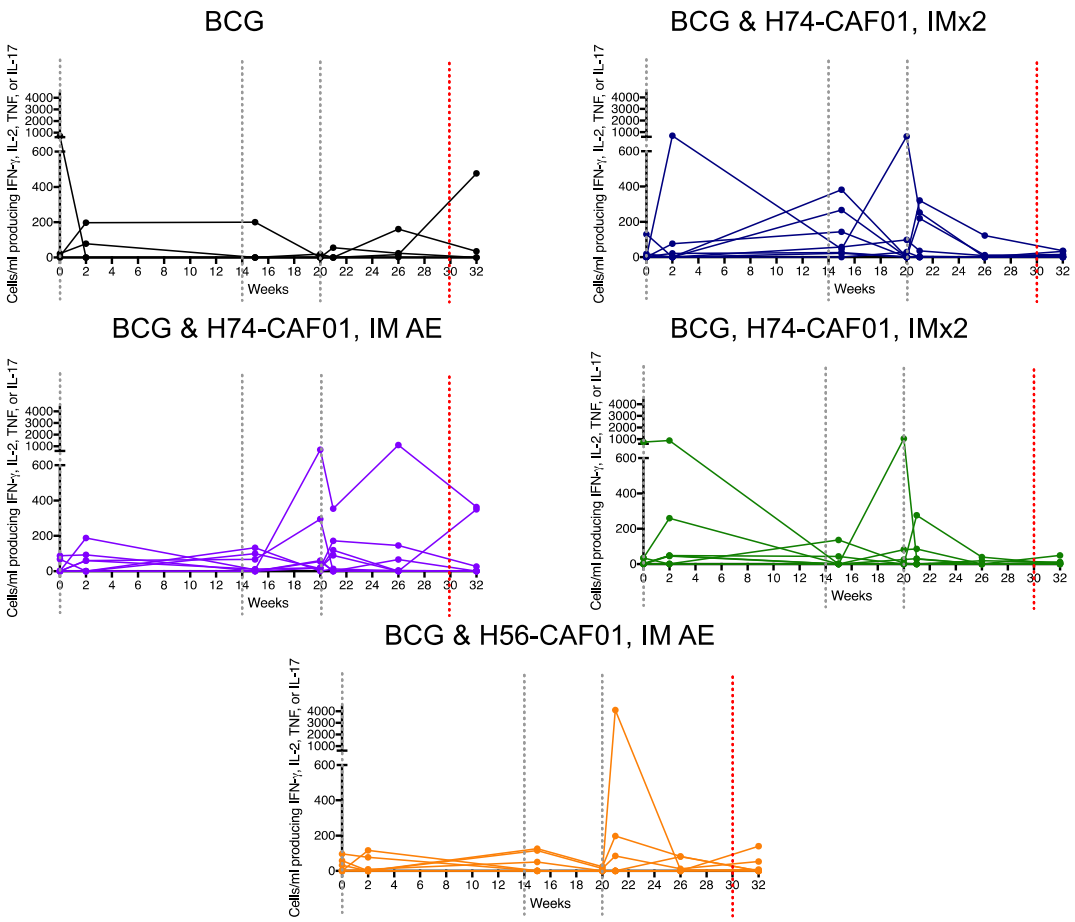

Figure 38. CD4 T cell response in the airways to H56/H74-CAF01 vaccinations.

BAL cells were stimulated with H74 or H56 peptide pools for 14 hours, and background media only responses were subtracted. H56/H74-CAF01 boosted NHPs have more cytokine response in their CD4 T cells after boosts. IM = intramuscular vaccination, AE = aerosol vaccination. Gray dotted lines mark vaccination time points, red dotted lines mark Mtb challenge. Each line is a NHP. BCG, N = 4 NHPs; BCG&H74-CAF01, IMx2, N = 8 NHPs; BCG&H74-CAF01, IM AE, N = 8 NHPs; BCG, H74-CAF01, IMx2, N = 8 NHPs; BCG&H56-CAF01, IM AE, N = 8 NHPs.

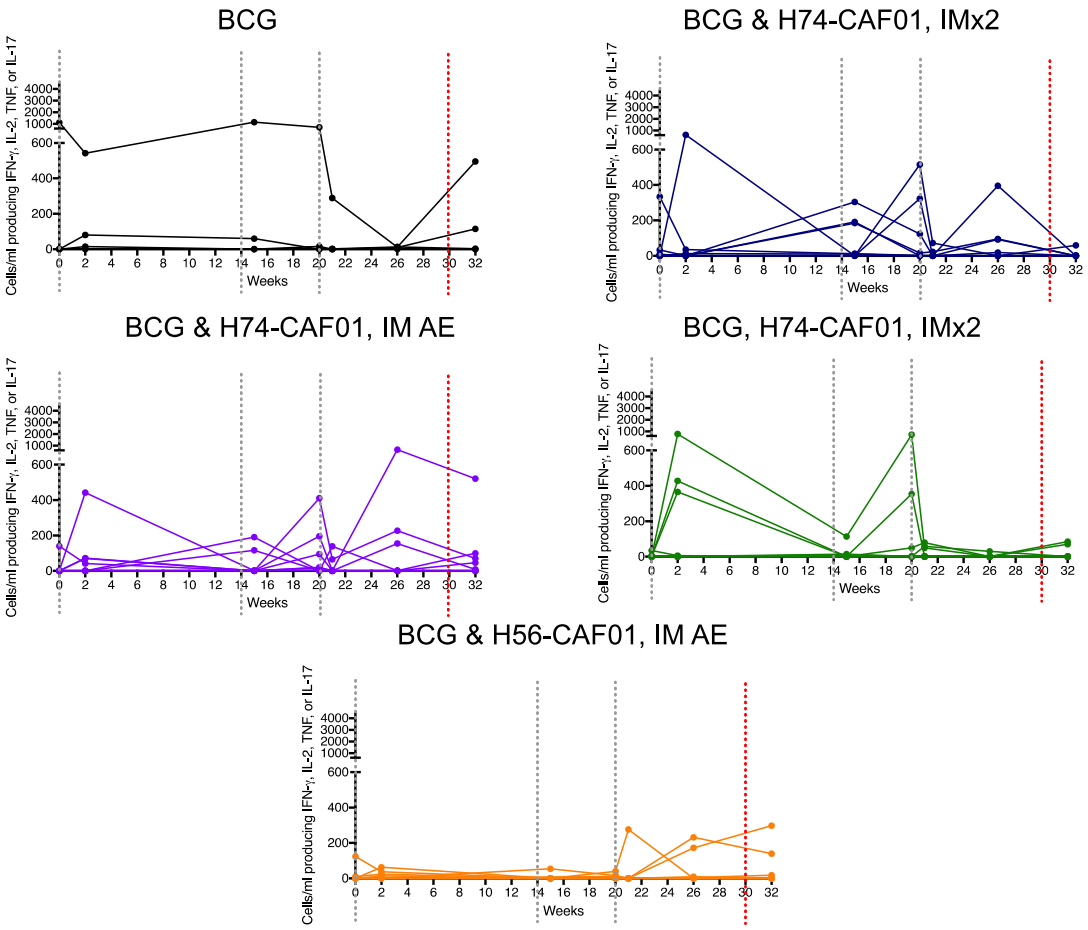

Figure 39. CD8 T cell response in the airways to H56/H74-CAF01 vaccinations.

BAL cells were stimulated with H74 or H56 peptide pools for 14 hours, and background media only responses were subtracted. IM = intramuscular vaccination, AE = aerosol vaccination. Gray dotted lines mark vaccination time points, red dotted lines mark Mtb challenge. Each line is a NHP. BCG, N = 4 NHPs; BCG&H74-CAF01, IMx2, N = 8 NHPs; BCG&H74-CAF01, IM AE, N = 8 NHPs; BCG, H74-CAF01, IMx2, N = 8 NHPs; BCG&H56-CAF01, IM AE, N = 8 NHPs.

4.3.9 Peripheral immune response in the blood during H56/H74-CAF01 vaccination

To monitor the immune response throughout the study, we quantified the PBMC response to vaccine-specific peptide pools and general mycobacterial antigens in culture filtrate protein (CFP). The response to culture filtrate protein (CFP), a mixture of proteins secreted from Mtb, was strong and immediate, continuing through vaccination and Mtb challenge, which is expected since all of the animals were vaccinated with BCG, and proteins in BCG are also in CFP (Figure 40). In contrast, there was little IFN-γ response to H74-specific peptides in BCG only animals (Figure 41). The greatest PBMC response to vaccination was in the H74-vaccinated animals, with slightly higher response in the intramuscularly vaccinated animals compared to the aerosol animals. There was a stronger response earlier in animals given BCG and H74 simultaneously (blue lines, Figure 41). H56-vaccinated animals had slight reaction to H74 peptides, probably because both vaccines contain Mtb-specific, immunogenic protein ESAT-6.

All vaccination groups had some IFN-γ response to H56-specific peptide pools, including BCG only animals (Figure 42). Since H56 contains Ag85B, an immunogenic protein that is also in BCG, it is not surprising that all of the groups have some response to the peptide pools of H56. The majority of the response in H74-vaccinated animals was observed after vaccination boosts, when they may be responding to both Ag85B and ESAT-6 or other vaccine proteins. Interestingly, in each of the vaccination groups, including BCG only, only a subset of animals had stronger IFN-γ response to H56-specific peptide stimulation, and the responses were usually delayed until after the boosts.

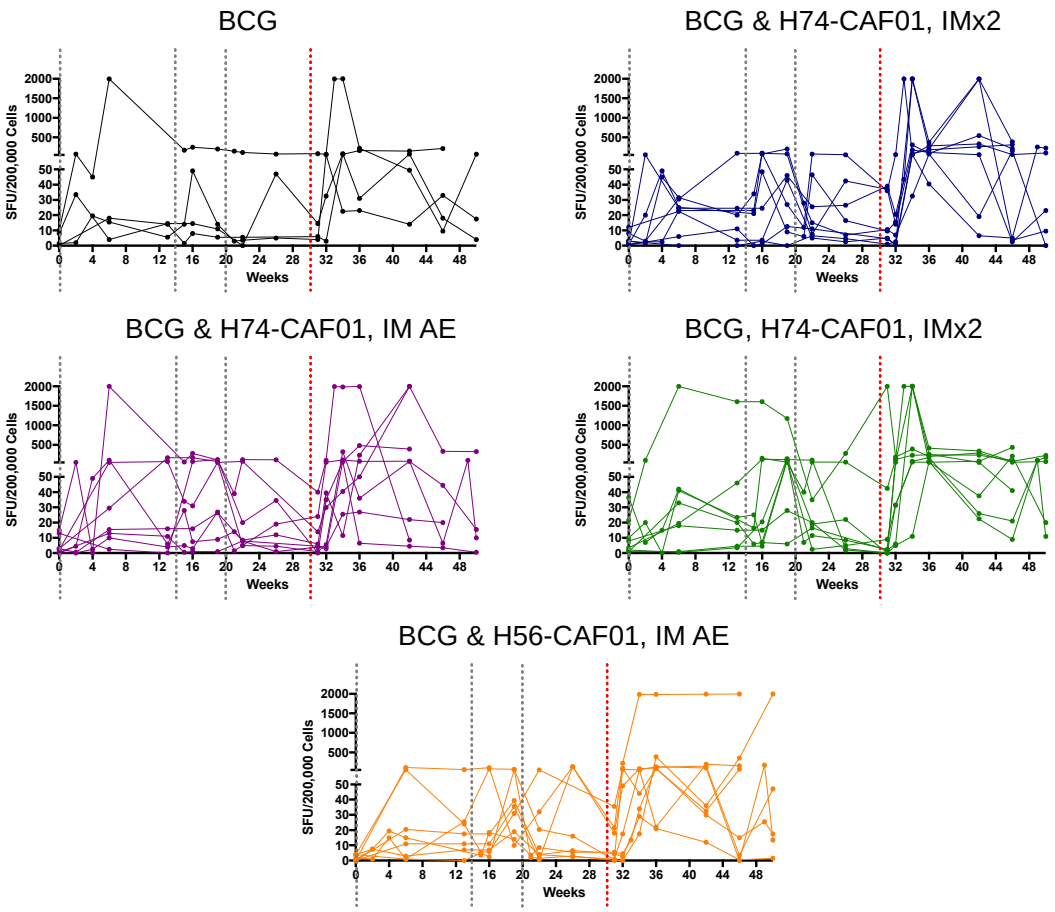

Figure 40. PBMC IFN-γ response to Mtb culture filtrate protein (CFP) during vaccination and Mtb challenge.

Strong responses in all vaccination groups to CFP throughout vaccination and challenge. All points are background response (media) subtracted. Gray dotted lines mark vaccination time points, red dotted lines mark Mtb challenge. Each line is a NHP. BCG, N = 4 NHPs; BCG&H74-CAF01, IMx2, N = 8 NHPs; BCG&H74-CAF01, IM AE, N = 8 NHPs; BCG, H74-CAF01, IMx2, N = 8 NHPs; BCG&H56-CAF01, IM AE, N = 8 NHPs.

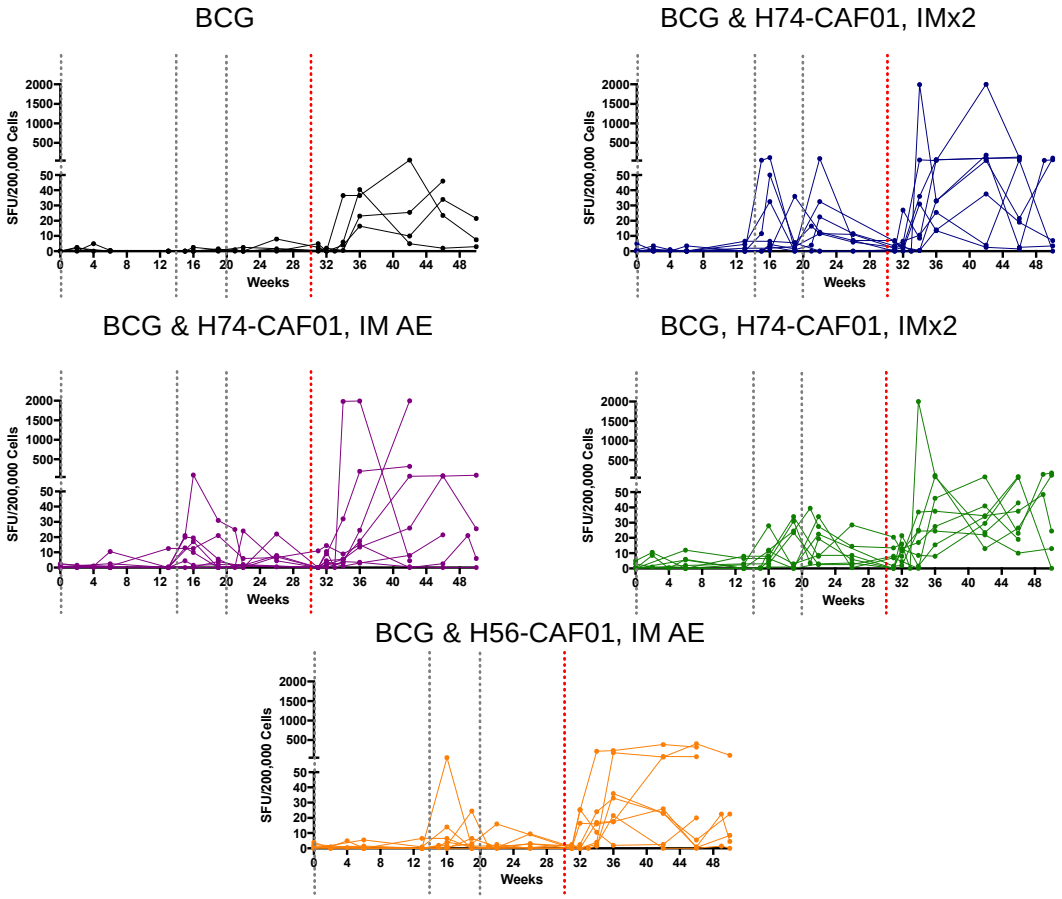

Figure 41. PBMC IFN-γ response to H74 vaccine peptides (ESAT-6, Rv3881c, Rv3614c, Rv3615c, Rv3616c, and Rv3849) during vaccination and Mtb challenge.

All points are background response (media) subtracted. Gray dotted lines mark vaccination time points, red dotted lines mark Mtb challenge. Each line is a NHP. BCG, N = 4 NHPs; BCG&H74-CAF01, IMx2, N = 8 NHPs; BCG&H74-CAF01, IM AE, N = 8 NHPs; BCG, H74-CAF01, IMx2, N = 8 NHPs; BCG&H56-CAF01, IM AE, N = 8 NHPs.

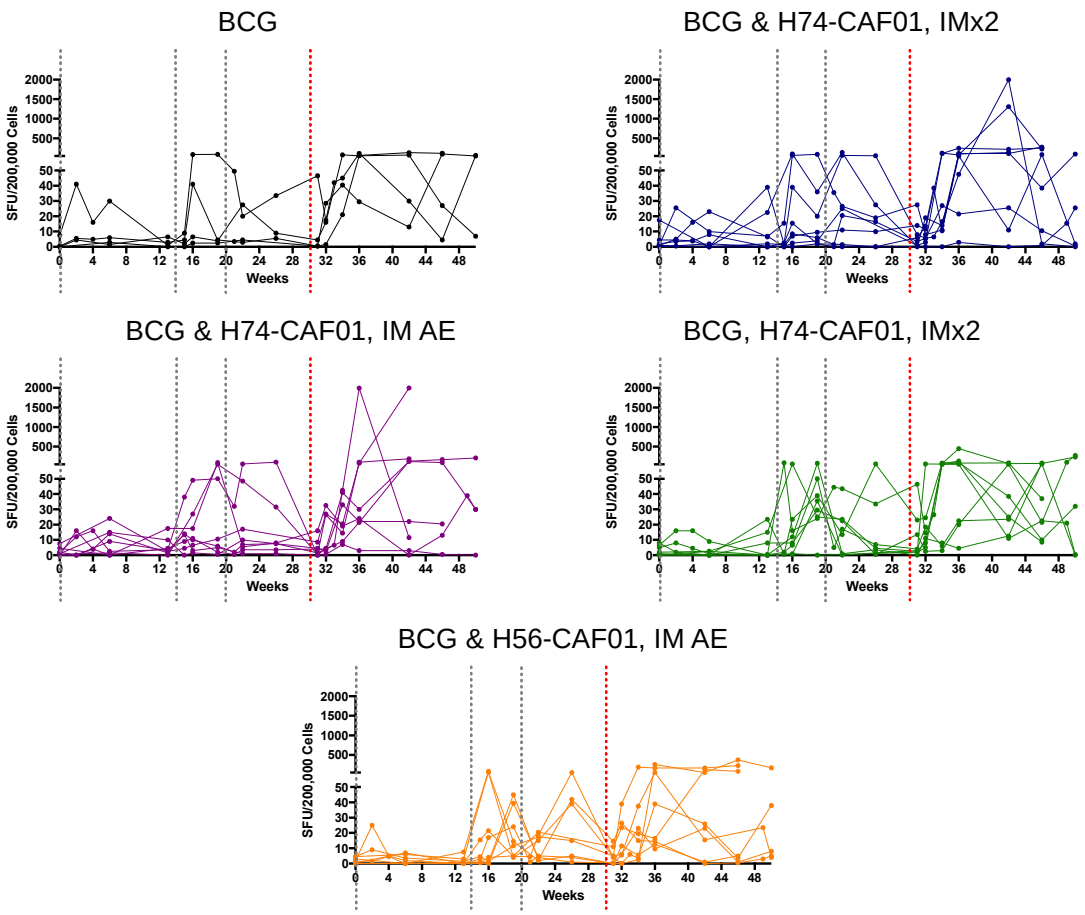

Figure 42. PBMC IFN-γ response to H56 vaccine peptides (ESAT-6, Ag85B, and Rv2660c) during vaccination and Mtb challenge.

All points are background response (media) subtracted. Gray dotted lines mark vaccination time points, red dotted lines mark Mtb challenge. Each line is a NHP over course of infection. Each line is a NHP. BCG, N = 4 NHPs; BCG&H74-CAF01, IMx2, N = 8 NHPs; BCG&H74-CAF01, IM AE, N = 8 NHPs; BCG, H74-CAF01, IMx2, N = 8 NHPs; BCG&H56-CAF01, IM AE, N = 8 NHPs.

4.3.10 Vaccination with H56/H74-CAF01 does not prevent granuloma formation

Similar to our earlier study of H56-CAF09, we tracked disease progression by serial PET-CT scans after Mtb challenge, using ^{18}F-FDG to quantify total inflammation in the lungs and as a proxy of bacterial burden [61]. However, none of H56/H74-CAF01 boost-vaccinated animals had less inflammation or disease progression in their lungs compared to animals that had received BCG only (Figure 43A). There was variability in the inflammation in all of the vaccination groups, with some animals controlling infection early and continually throughout the course of infection. NHPs with total lung ^{18}F-FDG activity below 947.2 (gray dotted line, Figure 43A) tend to do better and have less of a chance of reactivation if latent [330]. However, each vaccination group had at least one NHP with total lung ^{18}F-FDG activity above that level during course of infection, indicating a poor outcome and high bacterial burden. Additionally, four animals reached their humane endpoint before their experimental endpoint and were from the two vaccination groups that received H74-CAF01 at the same time as BCG (BCG&H74-CAF01, IMx2 and BCG&H74-CAF01 IM AE, Figure 43A). Besides the BCG only animals, the only vaccination group with only one animal with a bad prognosis was the group that received H74-CAF01 twice by intramuscular injections subsequent to their BCG vaccinations (BCG, H74-CAF01, IMx2, Figure 43A). This suggests that concurrent vaccination of H74-CAF01 and BCG may cause increased inflammation and disease during Mtb challenge.

We also enumerated granuloma numbers by PET-CT throughout infection. Our lab has previously shown that the change in the number of granulomas between early time points post-infection can help predict disease outcome, with increase in number of granulomas associated with more disease and dissemination [270]. While the BCG and H56/H74-CAF01 concurrently vaccinated animals had new granulomas form between 4 and 8 weeks of infection, the

vaccination group that received H74-CAF01 subsequent to BCG had stable or decreased numbers of granulomas at the same time points (Figure 43B). Most of the BCG only animals had stable numbers of granulomas, with few new granulomas formed between 4 and 8 weeks of infection, although 2 animals formed more granulomas. Thus, by these disease parameters, H56/H74-CAF01 boosting the NHPs did not prevent infection dissemination any more than BCG alone.

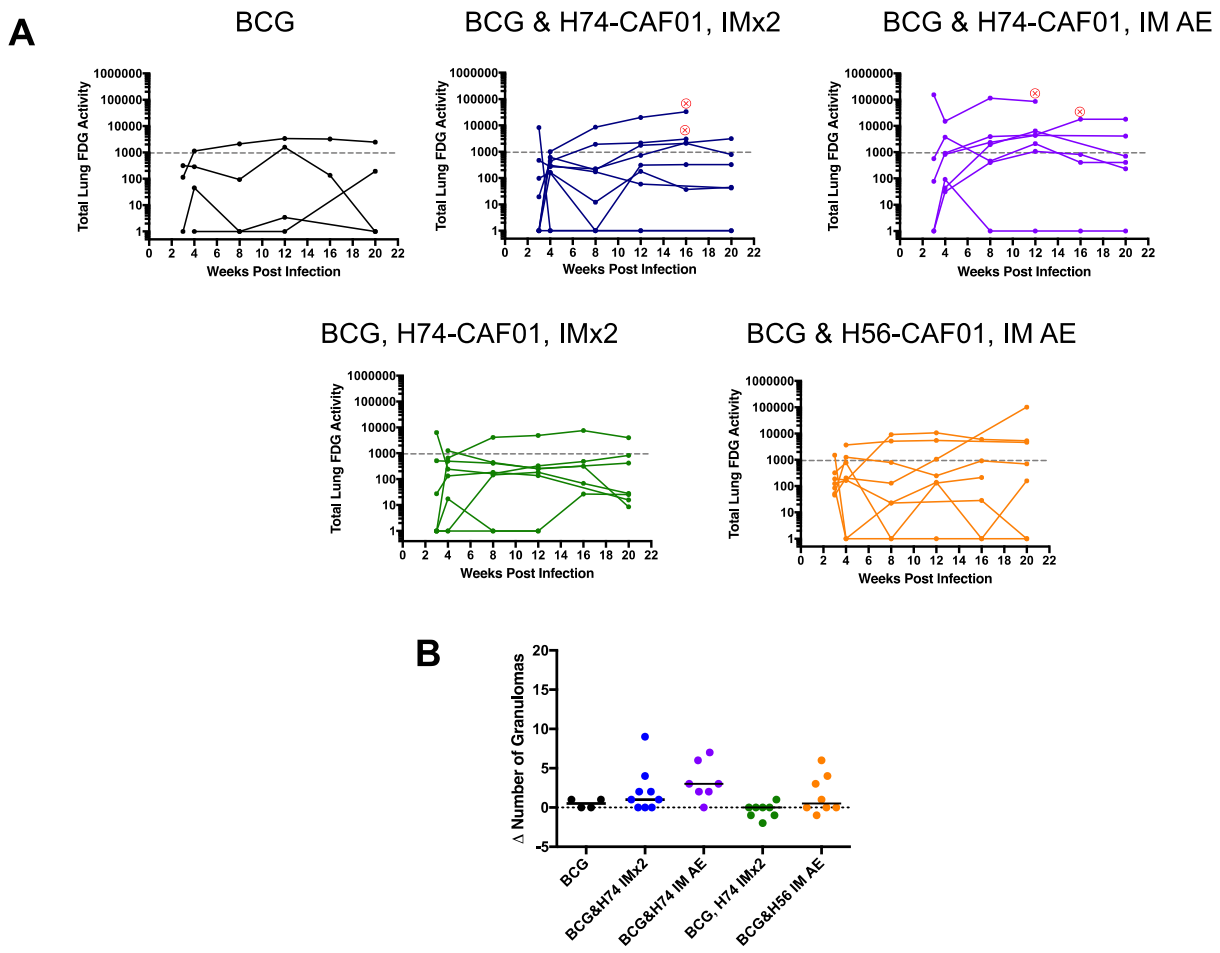

Figure 43. Inflammation and granuloma dissemination in lungs after Mtb challenge.

(A) Inflammation in lungs, quantified by summed ^{18}F-FDG uptake from PET-CT scans for each of the vaccination groups. Gray dotted line represents PET Hot of 947.2, which we have found to be the cutoff for high risk of reactivation (i.e., PET Hot below 947.2 has low risk of reactivation) [330]. Each vaccination group has spectrum of NHPs with more or less lung inflammation, although BCG, H74-CAF01, IMx2 (green) has only one animal with higher total lung FDG activity. BCG&H74-CAF01, IMx2 (blue) and BCG&H74-CAF01, IM AE (purple) have a few more animals with higher total lung FDG activity during course of infection, and each group had two animals that reached humane endpoint early (marked by red circles). Each line is a NHP. (B)

Change in numbers of granulomas in the lungs during infection between 4 and 8 weeks of infection, quantified by PET-CT scans. BCG, H74 IMx2 (green) has the least change or decrease in lung granulomas, indicating less dissemination. Each point is a NHP. BCG, N = 4 NHPs; BCG&H74-CAF01, IMx2, N = 8 NHPs; BCG&H74-CAF01, IM AE, N = 8 NHPs; BCG, H74-CAF01, IMx2, N = 8 NHPs; BCG&H56-CAF01, IM AE, N = 8 NHPs.

4.3.11 H56/H74-CAF01 vaccine boost does not greatly improve disease outcomes after Mtb challenge

At necropsy, the extent of gross disease pathology in the lungs, LNs, and extrapulmonary sites was also quantified into a score (Figure 44A). There were no significant differences in disease pathology between the different vaccination groups, although BCG only and BCG, H74 IMx2 animals seemed to have slightly lower median necropsy scores with less variability between animals. In order to assess the protection conferred from the addition of H56/H74-CAF01 boost vaccines, we quantified the bacterial load in each of the NHPs at necropsy 5 months after Mtb challenge (Figure 44B). Vaccination with H74-CAF01 intramuscularly after BCG vaccination (BCG, H74 IMx2) had a lower median of total and lung CFU compared to the other vaccination groups, including BCG only animals (Figure 44B). However, the variability within that experimental group was still within the range of BCG animals. Additionally, most animals in the boosted vaccine groups had at least some CFU+ LNs at the time of necropsy, but the BCG only animals had no involved LNs.

Two of the H74-CAF01 vaccinated groups (BCG&H74 IMx2 and BCG, H74 IMx2) had significantly lower median CFU in their individual granulomas compared to BCG only animals

(Figure 44C), likely because of larger numbers of sterile granulomas. Indeed, BCG&H74-CAF01 IMx2 animals had lower median CFU/granuloma and higher frequencies of sterile granulomas compared to other vaccinated groups, including BCG only animals (Figure 44C and 44D). BCG only animals tended to have lower frequencies of sterile granulomas compared to all vaccinated groups. Even though their lung CFU were similar to vaccinated groups, nearly all lung granulomas from BCG only animals had viable Mtb. In contrast, some of the H74-CAF01 boost vaccinated animals were able to clear the bacteria within their lung granulomas, even though their total CFU remained high. In summary, the BCG only vaccinated animals had the best overall disease outcomes, compared to boost-vaccinated animals, with lower bacterial loads, low necropsy scores and no LN involvement.

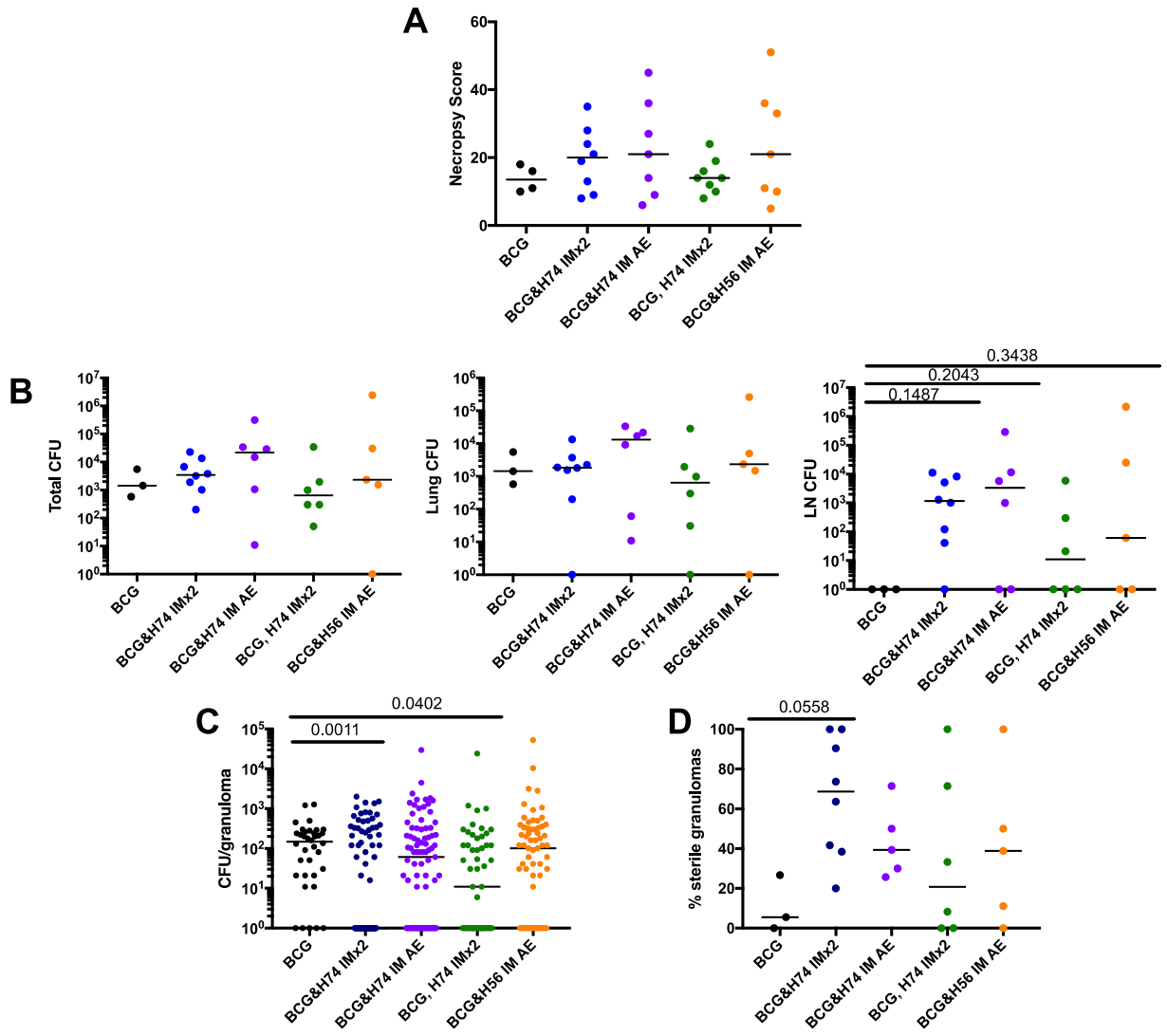

Figure 44. Bacterial burden and disease pathology in vaccinated animals at necropsy 5 months after Mtb challenge.

(A) All vaccinated animals have similar disease pathology at the time of necropsy, quantified as necropsy scores. Necropsy scores are tabulated based on spread and extent of disease at time of necropsy. Each point is a NHP. BCG, N = 4 NHPs; BCG&H74-CAF01, IMx2, N = 8 NHPs; BCG&H74-CAF01, IM AE, N = 7 NHPs; BCG, H74-CAF01, IMx2, N = 8 NHPs; BCG&H56-CAF01, IM AE, N = 7 NHPs. (B) Total, lung, and LN CFU of vaccinated animals are similar,

except BCG only animals do not have viable bacteria in their LNs. Each point is a NHP. (C) Bacterial burden of individual excised granulomas at necropsy. BCG&H74 IMx2 and BCG, H74 IMx2 boost vaccinated animals have significantly less bacterial burden in granulomas compared to BCG only animals. Each point is a granuloma. Dunn's Multiple Comparisons for significance. (D) Vaccinated animals, especially BCG&H74 IMx2, also have slightly higher frequencies of sterile granulomas. Each point is a NHP. Lines at medians. BCG, N = 3 NHPs; BCG&H74-CAF01, IMx2, N = 8 NHPs; BCG&H74-CAF01, IM AE, N = 6 NHPs; BCG, H74-CAF01, IMx2, N = 6 NHPs; BCG&H56-CAF01, IM AE, N = 5 NHPs.

4.3.12 Airway T cell response during vaccination does not correlate with bacterial burden

There was substantial variability in both immune responses and protection in all the animals. We investigated whether the quality and quantity of immune responses in airways provided insight into protection in this vaccine study. Thus, we compared peak CD4 and CD8 T cell cytokine responses during vaccination after boost vaccinations with H56/H74-CAF01 with outcome of infection (total thoracic bacterial burden) to determine whether there were correlations (Figure 45). As expected, Th1/Th17 responses in CD4 and CD8 T cells in the BAL after boosting vaccinations were higher than in BCG only animals, although some animals in BCG&H74 IMx2 and BCG&H56 IM AE had low Th1/Th17 responses (Figure 45A and 45C). However, these BAL responses did not correlate with total bacterial load after Mtb challenge, even in the two aerosol vaccination groups (BCG&H74-CAF01 IM, AE and BCG&H56-CAF01 IM, AE) (Figure 45B and 45D). This suggests that these H56/H74-CAF01 vaccines to boost the airway responses, particularly the aerosolized vaccines, did not confer any additional protection or reduce bacterial burden in NHPs after Mtb challenge.

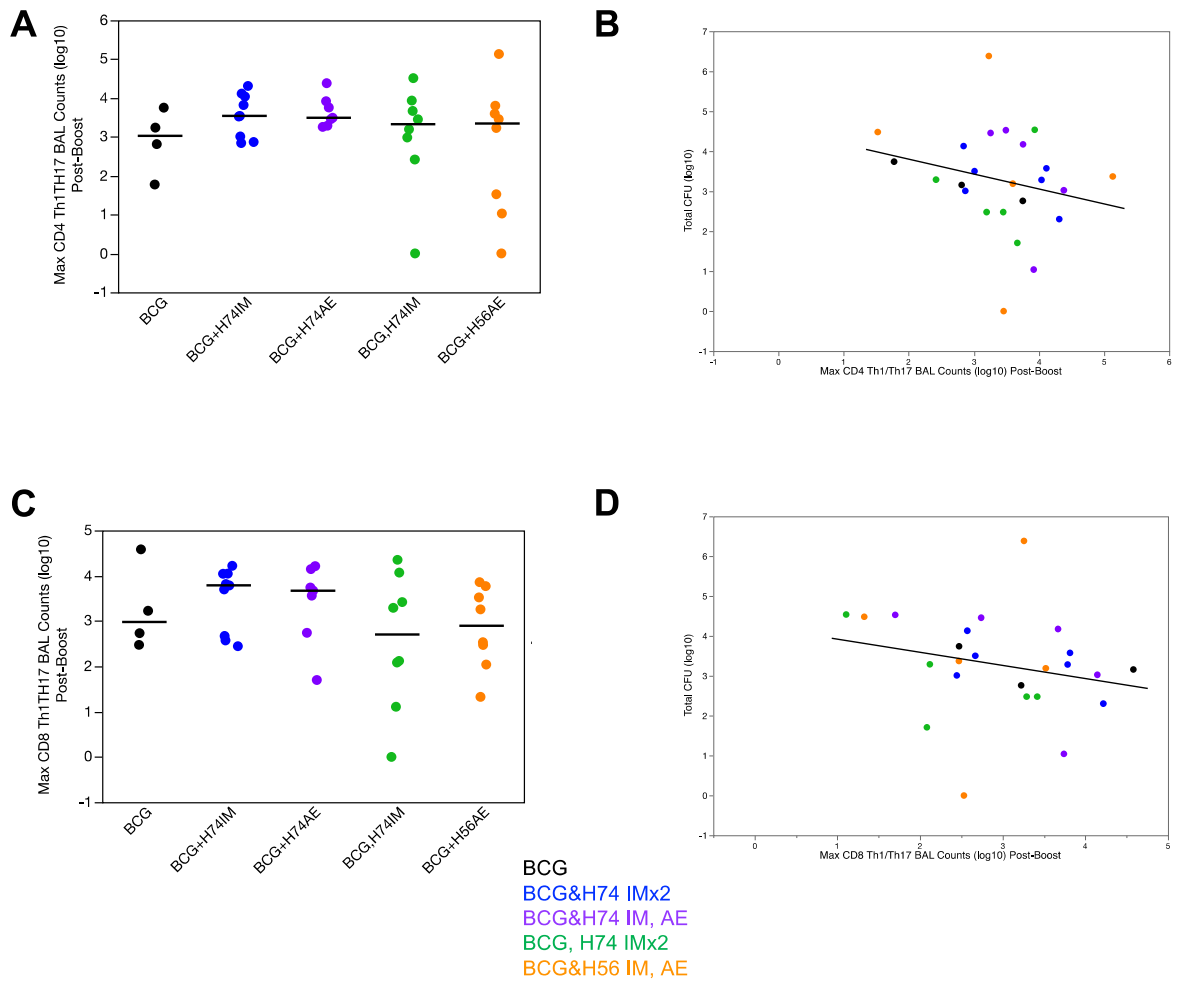

Figure 45. Maximum Th1/Th17 BAL responses after boost vaccinations do not correlate with bacterial burden.

Maximum (A) CD4 and (C) CD8 Th1/Th17 (IFN-γ, IL-2, TNF, IL-17) responses after boost vaccinations for each vaccination group. Each point is a NHP, lines at medians. Post-boost vaccination and pre-challenge (B) CD4 and (D) CD8 Th1/Th17 BAL responses did not correlate with bacterial burden (CFU) at time of necropsy. Line represents linear regression, (B) r^2 = 0.05394, p-value = 0.2748 (D) r^2 = 0.05445, p-value = 0.2725. Each point is a NHP. CFU correlations: BCG, N = 3 NHPs; BCG&H74-CAF01, IMx2, N = 6 NHPs; BCG&H74-CAF01,

IM AE, N = 5 NHPs; BCG, H74-CAF01, IMx2, N = 6 NHPs; BCG&H56-CAF01, IM AE, N = 5 NHPs.

4.3.13 Different vaccination strategies alter T cell cytokine response in lung granulomas

Although H56/H74-CAF01 boost vaccinations did not appear to significantly enhance the protection conferred by BCG alone, we wanted to understand if the boost vaccinations could alter the local granuloma cytokine environment and to further investigate correlates of protection for Mtb infections. The H56/H74-CAF01 vaccinated animals overall were similar to BCG animals in terms of infection outcome, but BCG&H74 IM AE animals seemed to have the worst disease parameters and outcomes, with higher total lung inflammation, more granulomas formed, and slightly higher bacterial burden and necropsy scores compared to other vaccination groups, as well as 2 of the 8 animals reaching their endpoints early. In contrast, BCG, H74 IMx2 animals seemed to have the best disease parameters and outcomes of the vaccinated groups, with lower total lung inflammation, fewer granulomas formed, slightly lower bacterial burden, and lower necropsy scores compared to other H56/H74-CAF01 boost vaccinated animals.

To first understand why BCG&H74 IM AE animals seemed to have worse outcomes than BCG animals and other boost vaccinated animals, we quantified the T cell responses in lung granulomas. Surprisingly, lung granulomas from BCG&H74 IM AE animals had significantly lower frequencies of T cells producing several cytokines compared to granulomas from BCG animals (Figure 46). Lung granulomas from BCG&H74 IM AE had particularly low frequencies of T cells producing total Th1 cytokines, IL-2, IFN-γ, or IFN-γ+IL-2+ co-expressing T cells. Additionally, there were significantly lower frequencies of T cells producing IL-17 or anti-inflammatory cytokine IL-10 in the same lung granulomas compared to lung granulomas from

BCG animals. Interestingly, the other aerosol vaccinated group, BCG&H56 IM AE also had significantly lower frequencies of IFN-γ+IL-2+ co-expressing T cells in their lung granulomas compared to BCG animals. Otherwise, the other H74-CAF01 vaccinated groups had similar frequencies of cytokine response in their T cells compared to BCG animals.

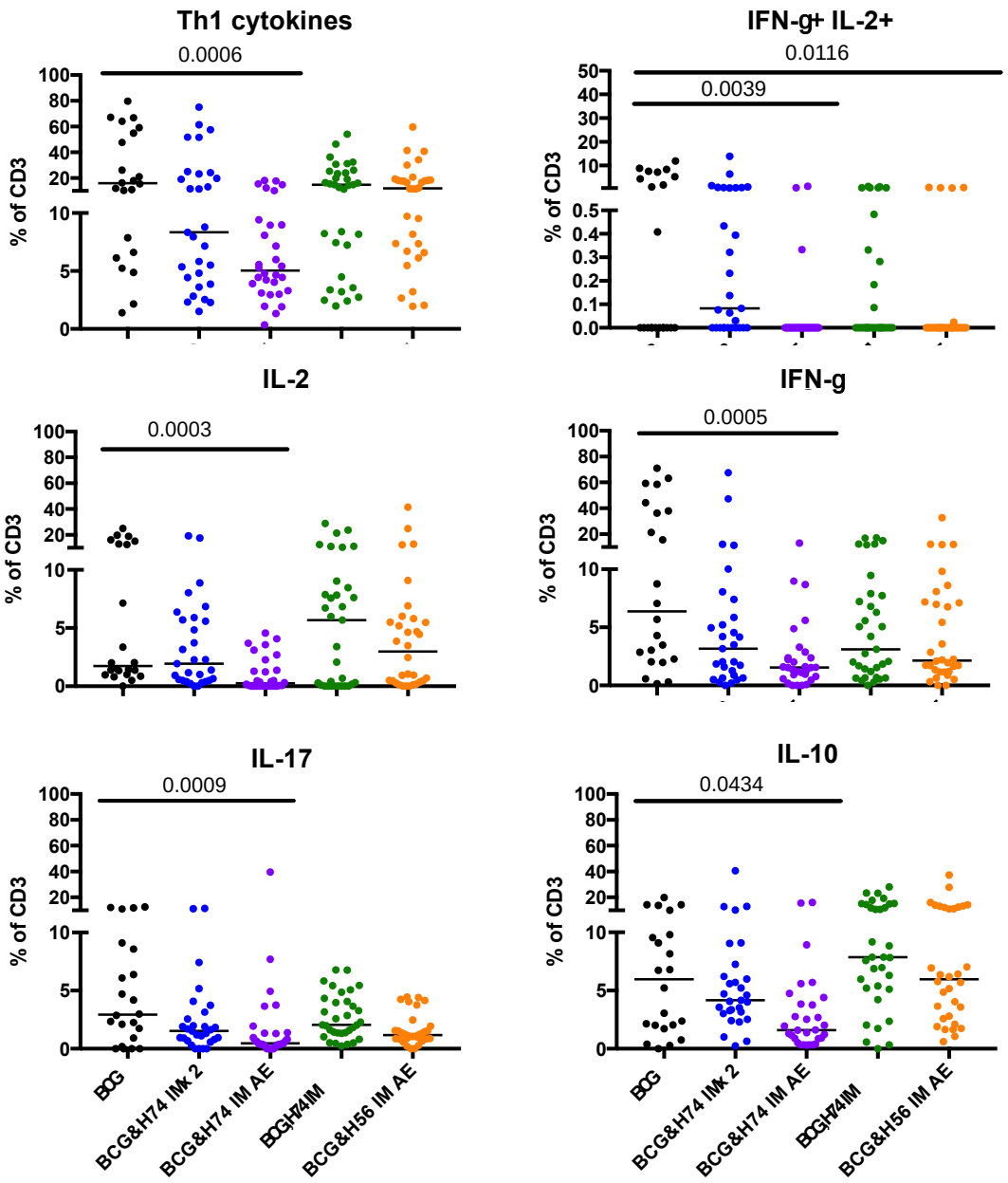

Figure 46. Lower cytokine response in lung granulomas of BCG&H74 IM AE vaccinated animals compared to BCG only animals.

Frequency of cytokine response in CD3+ T cells for each vaccination group, as labeled. Each point is a granuloma, lines at medians. Dunn's multiple comparisons test for significance. BCG,

N = 3 NHPs; BCG&H74-CAF01, IMx2, N = 6 NHPs; BCG&H74-CAF01, IM AE, N = 5 NHPs; BCG, H74-CAF01, IMx2, N = 6 NHPs; BCG&H56-CAF01, IM AE, N = 5 NHPs.

At the other end of the spectrum, BCG, H74 IMx2 animals did relatively better than other vaccination groups, and similar or better than BCG animals in granuloma stabilization and sterilization. Within the lung granulomas of BCG, H74 IMx2 animals, there were higher frequencies of T cells producing TNF and IL-2+TNF+ together compared to BCG animals (Figure 47). Additionally, the T cells of BCG, H74 IMx2 animals had higher frequencies of Ki67, a proliferation marker, but lower frequencies of CD69, an early activation marker, compared to BCG only animals. Perhaps having one or more of these factors helped lung granulomas in BCG, H74 IMx2 animals to prevent further dissemination and to increase sterilization.

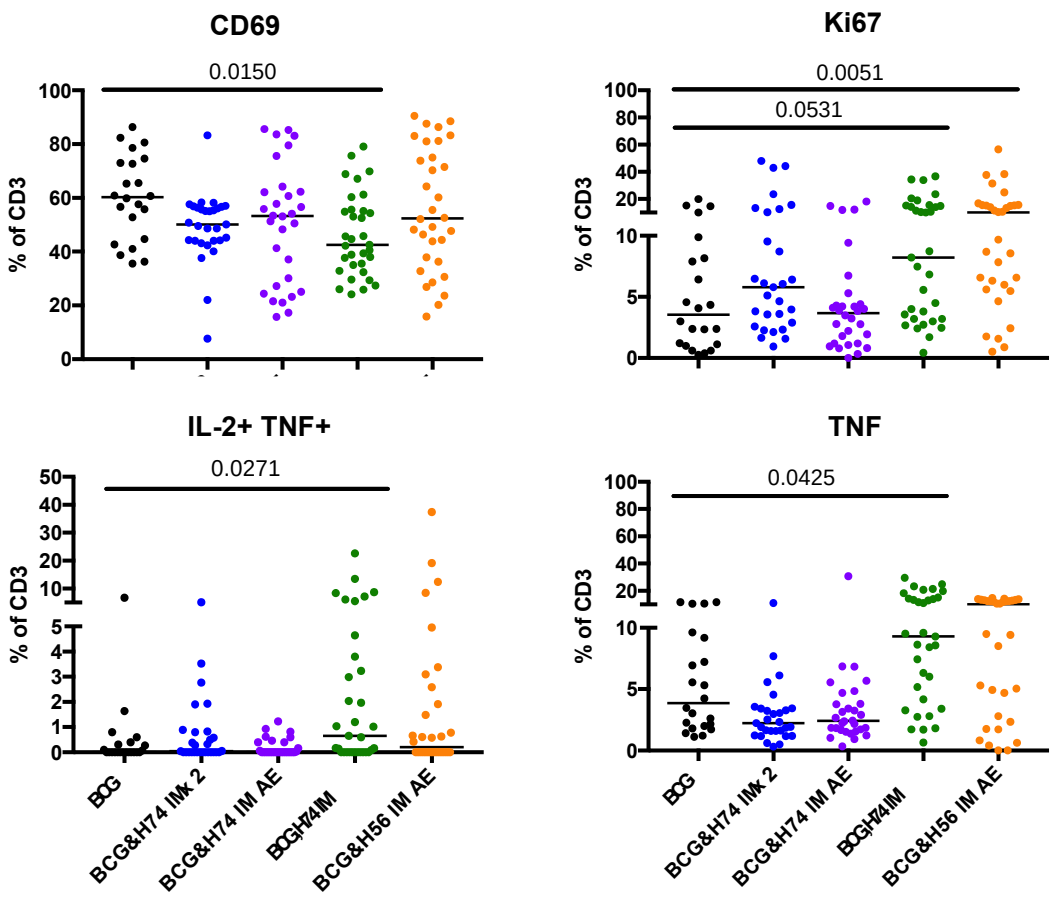

Figure 47. Frequency of T cell proliferation and inflammatory cytokine response is higher in BCG, IMx2 animals compared to BCG only.

Frequencies of CD3 T cell activation (CD69), proliferation (Ki67), and inflammatory cytokine response (IL-2+TNF+ and TNF). Each point is a granuloma, lines at medians. Dunn's multiple comparisons test for significance. BCG, N = 3 NHPs; BCG&H74-CAF01, IMx2, N = 6 NHPs; BCG&H74-CAF01, IM AE, N = 5 NHPs; BCG, H74-CAF01, IMx2, N = 6 NHPs; BCG&H56-CAF01, IM AE, N = 5NHPs.

We then investigated the differences in CD4 and CD8 T cell responses within lung granulomas of the vaccinated animals (Figure 48). CD4 and CD8 T cells had similar frequencies of Th1 cytokine responses between vaccinated and BCG animals, except BCG&H74 IM AE had lower Th1 response in CD4 T cells and BCG&H74 IMx2 had lower Th1 response in CD8 T cells compared to BCG animals. However, three of the vaccination groups had lower frequencies of IL-17 CD8 T cells in their lung granulomas compared to BCG animals. Since BCG, H74 IMx2 animals did similar or better than BCG only animals, and also had similar levels of IL-17-producing CD8 T cells, while the other vaccination groups had worse disease parameters and outcomes with fewer IL-17 CD8 T cells, this may suggest that CD8 T cell IL-17 response may be a factor worsening the protection from BCG.

In summary, many of the T cell responses were similar between lung granulomas of vaccination groups and BCG animals. However, of the vaccination groups that had slightly worse and slightly better disease outcomes, particular cytokine responses in their lung granulomas could differentiate them from BCG animals. Additionally, decreased CD8 T cell IL-17 response may decrease the protection conferred from BCG alone.

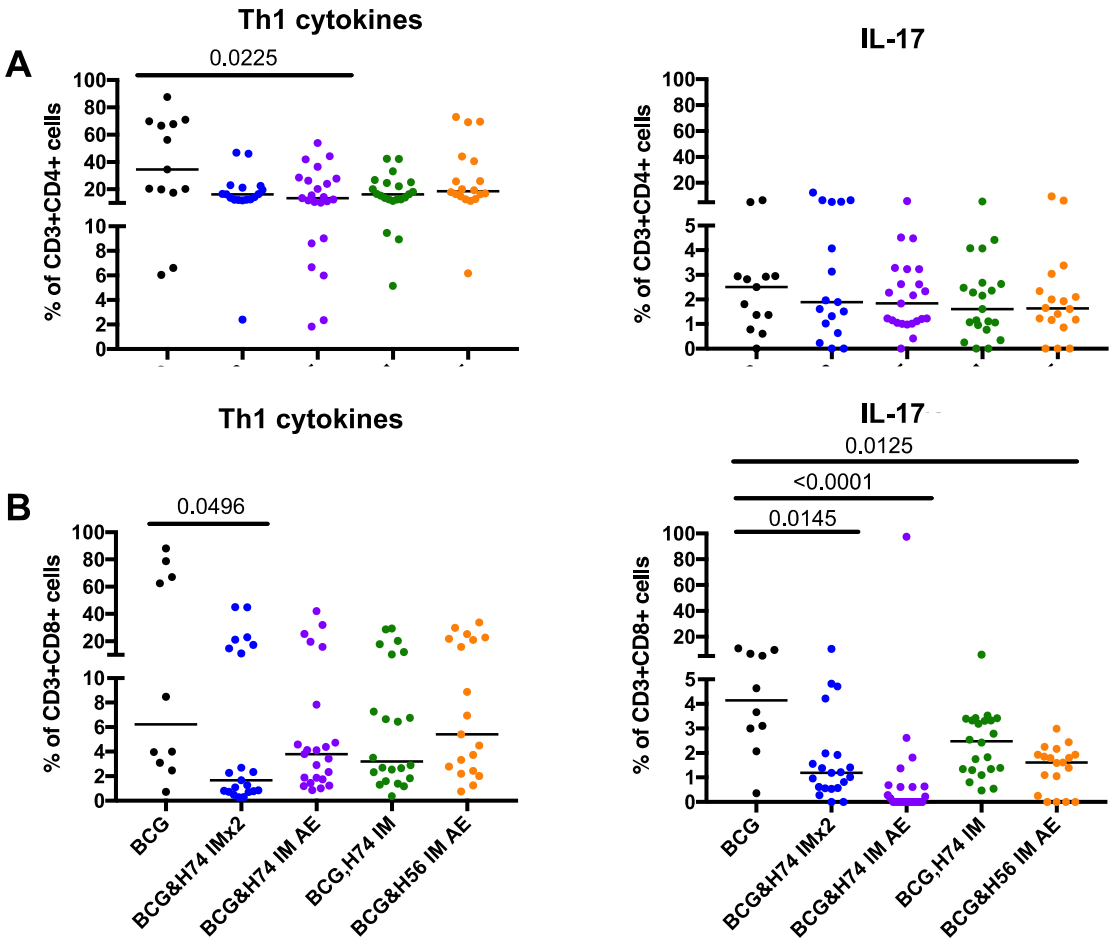

Figure 48. CD4 and CD8 T cells responses in granulomas of vaccinated animals.

Frequencies of (A) CD3+CD4+ and (B) CD3+CD8+ T cells producing Th1 cytokines (IFN-γ, IL-2, or TNF) and IL-17. Each point is a granuloma, lines at medians. Dunn's multiple comparisons test for significance, compared to BCG only animals. BCG, N = 3 NHPs; BCG&H74-CAF01, IMx2, N = 6 NHPs; BCG&H74-CAF01, IM AE, N = 5 NHPs; BCG, H74-CAF01, IMx2, N = 6 NHPs; BCG&H56-CAF01, IM AE, N = 5 NHPs.

4.3.14 Similar LN responses to different vaccination strategies

In addition to testing aerosolization of the boost vaccines, this study also investigated the benefits of simultaneous injection of the boost vaccine with BCG in the same area for increased LN response. Since we administered the vaccines in the right quadriceps of each NHP, we excised their right inguinal LN at necropsy, assuming that it was the primary vaccine draining LN. For comparison, we also excised the left axillary LN as a distant peripheral LN. We compared the cytokine response in the distant left axillary LN to the draining right inguinal LN for each NHP (Figure 49). In general, the immune response did not differ between the two LNs for all of the vaccination groups. There was more variable TNF response in T cells from the LNs, with some right inguinal LNs having higher frequencies of TNF compared to the left axillary LN T cell response. However, not all LNs had higher T cell TNF response in their right inguinal LNs compared to their left axillary LN. The simultaneous vaccination into the same draining LN did not appear to greatly increase the cytokine response in the draining LN compared to a distant LN.

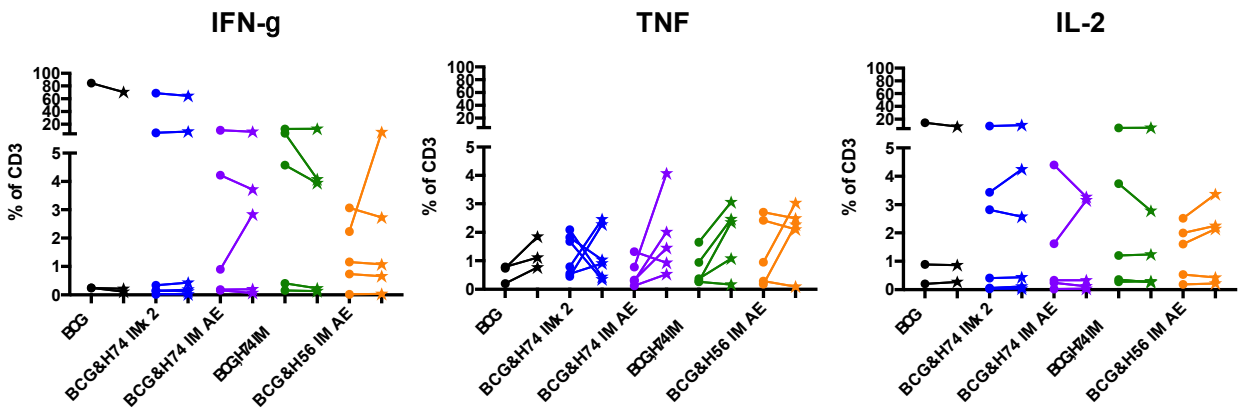

Figure 49. Cytokine responses in draining lymph nodes of vaccinated animals.

Simultaneous administration of BCG and H56/H74-CAF01 boosting vaccine does not enhance immune response in draining LN compared to distant LN. Distant, left axillary LN represented by dot on the left connected to corresponding vaccine draining right inguinal LN represented by star on the right for each NHP. All samples were excised at necropsy and unstimulated. BCG, N = 3 NHPs; BCG&H74-CAF01, IMx2, N = 6 NHPs; BCG&H74-CAF01, IM AE, N = 5 NHPs; BCG, H74-CAF01, IMx2, N = 6 NHPs; BCG&H56-CAF01, IM AE, N = 5 NHPs.

The BCG animals in this study did not have any LN involvement after Mtb challenge. We quantified the cytokine response in the thoracic LNs of the different vaccination groups to see if there were particular cytokines that may help prevent LN infection (Figure 50). Of the parameters we measured, there were few cytokines that differed between vaccination groups and BCG. Only LNs from BCG&H74 IM AE animals had significantly lower TNF compared to BCG animals. We could not discern any cytokine response in the LN that may prevent infection or dissemination.

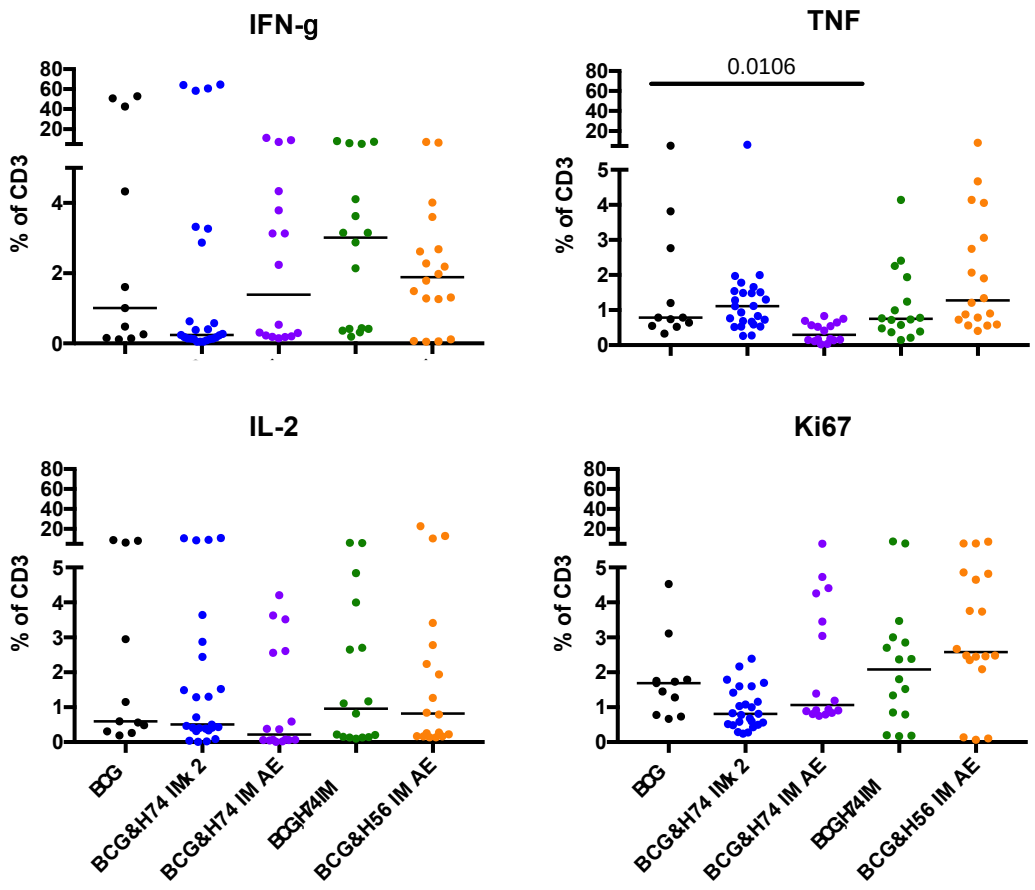

Figure 50. Frequencies of cytokine responses in thoracic LNs of vaccinated animals.

Only BCG&H74 IM AE vaccinated animals had lower frequencies of T cells producing TNF in thoracic LNs compared to BCG only animals. Each point is a thoracic LN, lines at medians. Dunn's multiple comparisons test for significance. BCG, N = 3 NHPs; BCG&H74-CAF01, IMx2, N = 6 NHPs; BCG&H74-CAF01, IM AE, N = 5 NHPs; BCG, H74-CAF01, IMx2, N = 6 NHPs; BCG&H56-CAF01, IM AE, N = 5 NHPs.

4.4 DISCUSSION

H56 fusion protein vaccine has been shown to be a promising TB vaccine candidate, boosting the protection against pulmonary TB when used in conjunction with BCG vaccination in mouse and NHP models [326, 327]. Previous NHP studies testing H56 admixed with the adjuvants IC31 and CAF01 intramuscularly, in macaques first vaccinated with BCG, showed that the boosting vaccination could help boost some aspects of BCG protection [327] (DiFazio et al, in preparation). H74 fusion protein vaccine has shown promising protective effects in mouse models (SSI, unpublished data). The adjuvant CAF09 was designed to boost both CD4 Th1/Th17 and CD8 T cell responses, while CAF01 induces Th1/Th17 responses [242, 244-247]. In this study, we investigated multiple vaccination strategies, first testing vaccine delivery route (intranasal, subcutaneous, and aerosol) with fusion protein vaccine and the novel liposomal adjuvant CAF09 against Mtb challenge. Given the slightly decreased inflammation and improved disease outcomes of aerosol vaccinated animals compared to the other vaccination routes and unvaccinated controls, we further investigated the benefits of heterologous prime-boost aerosol vaccination using BCG, followed by H56 or H74 and liposomal adjuvant CAF01, demonstrating that aerosolized boost vaccinations led to similar or slightly worse disease outcomes and bacterial load compared to BCG only vaccinated animals. Additionally, we probed the benefits of simultaneous vaccination of H56/H74-CAF01 and BCG into the same draining LN, but found no increased protection or immune response from simultaneously vaccinated animals. Instead, BCG, H74 IMx2 had slightly improved outcomes compared to other experimental vaccination groups and in some respects compared to BCG only animals. However, overall animals that received H56/H74-CAF01 boosts had little increased protection from Mtb challenge compared to BCG alone, although vaccination altered the T cell immune responses within granulomas.

The initial adverse effects seen in giving H56 with CAF09 by aerosol suggest that CAF09 is not an ideal adjuvant for delivering a vaccine against TB. The subcutaneously vaccinated NHPs also had substantial swelling at the site of injection with H56 and CAF09, implying a possibly robust and immediate local immune response to one of the components of the vaccine. When we did not use CAF09 adjuvant in the third vaccination of the aerosol cohort, only aerosolizing the H56 protein vaccine, we observed considerably less adverse response after vaccination, indicating the adjuvant CAF09 as the cause of the immediate response. Additionally, the intranasal and subcutaneous vaccination NHPs had strikingly high inflammation in their lungs soon after Mtb challenge, even compared to unvaccinated controls. The inclusion of Poly(I:C), a double-stranded RNA virus mimic, in the CAF09 liposomes may be the cause of this poor response in the case of TB, as Poly(I:C) has been shown to exacerbate TB disease [331]. In mouse studies, Poly(I:C) can induce a Type I IFN response, causing a rapid influx of neutrophils and monocytes to the lung tissue parenchyma of Poly(I:C) treated mice [331, 332]. For TB, induction of Type I IFNs, whether artificially generated by Poly-IC or triggered by a particular strain of Mtb, is detrimental, causing increased bacterial loads and decreased survival [331, 333]. We did not detect any measurable amounts of IFN-β from the BAL fluid after vaccination, but we may have missed the critical, early time period of a rapid Type I IFN response (data not shown). Although apparently unfavorable for TB, the induction of Type I IFNs by CAF09 may be beneficial for other diseases. Although CAF01 did not cause any of the immediate adverse effects observed with CAF09, the vaccination of CAF01 with H56 and H74 did not significantly improve the protection conferred by BCG alone.

The reduced inflammation and slightly improved disease outcomes after Mtb challenge in aerosol vaccinated compared to other vaccination cohorts suggested that administration of the

same vaccine by different routes can cause divergent outcomes, particularly in inflammation. The aerosol vaccinated cohort had less inflammation, granuloma dissemination, or extrapulmonary disease, and slightly higher frequency of sterile granulomas compared to the other cohorts. The marginally better outcomes of the aerosol cohort could be due to the route of vaccination (directly to the lungs as an aerosol), or the "prime and pull" during vaccination, where the NHPs were initially immunologically "primed" with H56 protein vaccine and CAF09 adjuvant for the first two vaccinations, then the response "pulled" back to the lungs by the third vaccination with H56 protein vaccine only, or by a combination of both factors.

Aerosol BCG vaccination in the guinea pig model has demonstrated the potential benefits of directly administering TB vaccines to the site of infection [261]. The promising effects of a prime and pull vaccination strategy were first shown against genital herpes simplex virus 2, using a parenteral vaccination to prime, followed by a local topical application of chemokines to pull in a local response [334]. Additional studies have had variable success with the prime and pull strategy, suggesting the need for optimization of combination of disease model, vaccine, and adjuvant [335-337]. In this study, we saw an influx of T cells immediately to the airways after the "pull" vaccination in the aerosol cohort, suggesting that prime and pull vaccination may be an important factor in improving the aerosol cohort's response to Mtb challenge. Unfortunately, when we conducted further studies to enhance the effects of aerosolizing TB vaccines, we no longer saw any protective effects of the vaccine or the "pull" to the mucosal sites of infection. In the later study, we vaccinated using a heterologous prime-boost strategy, priming with intradermal vaccination of BCG and boosting with intramuscular vaccination of H56/H74-CAF01, before a second boost aerosol vaccination of H56/H74. Since the previous study had administered H56-CAF09 by aerosol twice before the final aerosol administration pulled T cells

to the airway, perhaps the results differed between the two studies because of the different routes of the initial two vaccinations. The intradermal/intramuscular administration of priming vaccine may not be sufficient to pull immune responses to the airway in the context of Mtb.

Previously, BCG has been shown to be a strong adjuvant in the context of other infections and in cancer treatments [338-340]. Our collaborators at SSI had shown that simultaneous administration of BCG and boost vaccines led to synergistic immune responses and reduced bacterial burden after Mtb challenge [264]. However, our results from this study showed no added benefit to simultaneous injection of BCG and boost vaccines. Although there were clear peripheral immune responses to vaccination, there was also increased inflammation, low immune response in the draining lymph node, and little improvement in bacterial burden or disease outcome above BCG alone. There were slightly higher frequencies of sterile granulomas in BCG&H74 IMx2 animals, but two of the eight animals in the vaccination group also met their humane endpoints early. Instead, animals that did not receive the boost vaccine at the same time as BCG (BCG, H74 IMx2) had slightly better outcomes, with slightly less inflammation, more stable granuloma numbers, and low bacterial load and disease pathology, comparable to BCG alone vaccinated animals. This suggests that if H74-CAF01 boost vaccination can confer any additional protection to BCG vaccination during Mtb vaccination, it may not be ideal to concurrently administer BCG with H74-CAF01. To our knowledge, no other studies have investigated simultaneous heterologous prime-boost vaccination in TB. However, in a study of cytomegalovirus (CMV)-based TB vaccines, rhesus macaques that were vaccinated with BCG 6 weeks before boost CMV vaccination had less protection during Mtb challenge than those that were only vaccinated with the CMV-based vaccine, suggesting that BCG may have interfered with the immune response and protection of their vaccine [341]. Additionally, in the context of

tumor treatment with BCG, Yu et al. found that simultaneous injection of BCG and a VEGF inhibitor was worse at reducing tumors in a mouse model than administering BCG or VEGF independently [342]. Thus, simultaneous vaccination of BCG with boost vaccines may not always confer additional protection, and may interfere with BCG immune effects rather than serve as an adjuvant.

The ideal combinations of local cytokine response for reducing bacterial burden in the granuloma are not known [68, 102]. The different vaccination groups from both parts of this study resulted in slightly different granuloma T cell cytokine profiles. In the first part of the study, the aerosol group, which had the least inflammation and disease among the H56-CAF09 vaccinated groups, had higher frequencies of IFN-γ-producing T cells compared to granulomas from unvaccinated controls. Moreover, although the intranasal and subcutaneous cohorts had similar disease outcomes, their local cytokine responses were different compared to the unvaccinated cohort. The intranasal group had higher frequencies of IFN-γ and TNF, and lower frequencies of IL-17, while the subcutaneous group only had significantly lower frequencies of IL-17 compared to the unvaccinated controls. In the later study with H56/H74-CAF01 vaccination, the vaccination group with the relatively best disease parameters, BCG, H74 IMx2, had significantly higher proliferation, IL-2+TNF+ and TNF cytokine response and lower activation of T cells compared to BCG alone. In contrast, the vaccination group with the relatively worst disease parameters and outcomes, BCG&H74 IM AE, had significantly lower frequencies of pro-inflammatory cytokines (Any Th1 cytokine, IFN-γ+IL-2+, IL-2, IFN-γ, IL-17) and anti-inflammatory cytokine IL-10. The consistently lower frequencies of CD3 T cells producing IL-17 in lung granulomas of vaccinated animals with worse disease outcomes (intranasal and subcutaneous groups from the initial study, BCG&H74 IM AE from the later

study) is consistent with previous studies showing the necessity of a strong IL-17 response for bacterial control and may warrant further investigation [92, 93, 102]. The peripheral BAL and PBMC cytokine response during vaccination from both parts of this study did not predict the differences of the local granuloma T cell response or bacterial loads between the vaccinated groups.

In summary, this study has demonstrated that the different vaccination strategies using subunit fusion proteins and adjuvants tested in this study are not protective against Mtb challenge. We can conclude that many potential vaccination strategies may not work in the context of Mtb in a NHP model. First, H56-CAF09, particularly without initial BCG priming vaccination, is not an ideal strategy for TB vaccinations, leading to adverse effects and high levels of inflammation after Mtb challenge. Second, aerosol vaccination of boosting vaccines may pull T cells to the desired mucosal site, but may need multiple administrations of aerosolized vaccinations to be successful. When we vaccinated NHPs with aerosol vaccinations multiple times of H56-CAF09, we observed a T cell influx to the airways after boost vaccination. However, when we primed NHPs by intradermal/intramuscular vaccination, we did not observe any additional influx of immune cells to the airways. Third, simultaneous vaccination of BCG and H56/H74-CAF01 does not seem to significantly boost immune responses or protective effects. Finally, although H56, H74, CAF01, and CAF09 in different combinations had demonstrated some protective effects in mouse and NHP models and in human studies, these particular combinations using these vaccination strategies did not significantly increase protection above BCG vaccination alone. While this study failed to produce any viable vaccines or vaccination strategies for TB, it demonstrated that beyond preparing and influencing the peripheral responses, vaccines can also alter the T cell responses at the site of infection, in TB

granulomas. These results may better inform the potential correlates of protection for TB vaccines and better inform our vaccination strategies for TB.

4.5 METHODS

4.5.1 Experimental animals

For the initial H56-CAF09 study, nine cynomolgus macaques (*Macaca fascicularis*) between 7 and 8 years of age, with starting weights of 6-8kg were used (Valley Biosystems, Sacramento, CA). For the subsequent H56/H74-CAF01 study, 36 cynomolgus macaques (*Macaca fascicularis*) between 5 and 10.5 years of age, with starting weights of 3.1-8kg were used (Valley Biosystems, Sacramento, CA). Animal care was in accordance with institutional guidelines, and all experimental manipulations, protocols, and care of the animals were approved by the University of Pittsburgh School of Medicine Institutional Animal Care and Use Committee (IACUC). Animals were examined while in quarantine as previously described to ensure animals were in good physical health with no previous *M. tuberculosis* infection [57, 291].

4.5.2 Experimental vaccines

Recombinant H56 protein vaccine (Ag85B-ESAT6-Rv2660c) and recombinant H74 protein vaccine (Rv3881c-ESAT-6-Rv3614c-Rv3615c-Rv3616c-Rv3849) were purified from *Escherichia coli* [326]. CAF01 liposomes were formulated by incorporating the glycolipid α,α'-trehalose 6,6'-dibehenate (TDB) into dimethyldioctadeclyammonium (DDA) liposomal vesicles

suspended in 10mM Tris-buffer, pH7.4 as previously described [343]. CAF09 liposomes were prepared with DDA, monomycoloyl glycerol (MMG)-1, and Poly(I:C) and suspended in 10mM Tris-buffer, pH7.4 [244]. CAF09PEG2000, a pegylated form of CAF09, was created for subcutaneous vaccinations. Doses used for H56-CAF09 study were 50ug H56 protein vaccine and 625ug CAF09 adjuvant in 0.3ml for intranasal or subcutaneous delivery, and 1ml for aerosol delivery, diluted in filter-sterilized 10mM Tris-buffer, pH7.4. Doses used for H56/H74-CAF01 study were 15ug H56 protein vaccine or 15ug H74 protein vaccine and 625ug CAF09 adjuvant in 1ml for intramuscular delivery, diluted with 10mM Tris-buffer, pH7.4. For aerosolized delivery of H56 or H74 during H56/H74-CAF01 study, 50ug of H56 protein vaccine or 50ug of H74 protein vaccine were resuspended in 1ml of filter-sterile 10mM Tris-buffer, pH7.4.

4.5.3 Vaccinations

For the H56-CAF09 study, NHPs were vaccinated with H56 protein and CAF09 adjuvant by three routes – intranasal, subcutaneous, and aerosol, with each animal receiving 3 vaccinations every 4-5 weeks (Table 1). As this was a pilot study, each vaccine group consisted of 3 macaques. The intranasal group received H56 and CAF09 by intranasal mucosal atomization device in the right nare (Teleflex, Morrisville, NC). The subcutaneous group was injected with H56 and CAF09PEG2000 (pegylated CAF09) subcutaneously above the right axillary lymph node. The aerosol group received H56 and CAF09 by the Investigational e-Flow Nebulizer System (PARI Pharma, Munich, Germany), an electronic nebulizer with vibrating membranes that generates aerosolized droplets of 2-8um, together with a pediatric face mask to deliver the aerosolized droplets to the animals. The aerosol group received only H56 protein for their third

vaccination because of observed adverse effects when H56 and CAF09 were administered by aerosol for the first two vaccinations.

For the H56/H74-CAF01 study, NHPs were vaccinated with BCG and H56-CAF01 or H74-CAF01 in different combinations, with all animals receiving an initial BCG vaccination at Week 0, followed by boost vaccinations for animals in experimental boost vaccine groups at Week 14 and Week 20 (Table 2). BCG Danish (courtesy of Statens Serum Institut, Copenhagen, Denmark) was administered according to manufacturer's directions by intradermal injection on the right quadriceps. Resuspended BCG vaccine was also plated on 7H11 agar plates to confirm bacterial growth was within range of manufacturer's standards. During simultaneous vaccinations, H56-CAF01 or H74-CAF01 were injected intramuscularly adjacent to site of BCG injection. At subsequent boost vaccinations, H56-CAF01 and H74-CAF01 was injected on the right quadriceps adjacent to original BCG injection. The vaccine groups that received aerosol vaccinations had H56 or H74 aerosolized using the Investigational e-Flow Nebulizer System (PARI Pharma, Munich, Germany) as described above.

4.5.4 Intracellular cytokine staining and flow cytometry

Blood samples were collected over the course of vaccination and after infection, and peripheral blood mononuclear cells (PBMCs) were isolated as previously described [344]. In the H56-CAF09 study, for each NHP, $1x10^6$ PBMCs were stimulated with individual peptide pools of Mtb proteins ESAT-6, Ag85B, and Rv2660c, whole protein H56, and PDBU and ionomycin for 1 hour at 37°C/5% CO_2, then for an additional 5 hours in the presence of Brefeldin A (Golgiplug: BD Biosciences) at 37°C/5% CO_2. PBMCs and stimulators were diluted in RPMI-1640 containing 1% HEPES, 1% L-glutamine, and 10% human AB serum. Peptide pools and

protein were diluted to 10ug/ml. After stimulation, PBMCs were washed with 1xPBS and 1% Fetal Bovine Serum and stained as described below.

Bronchoalveolar lavage (BAL) was also collected as previously described [344], centrifuged to obtain the immune cells, and live immune cells quantified by trypan blue exclusion. In the H56-CAF09 study, BAL cells were stimulated with individual peptide pools of H56 vaccine-specific proteins ESAT-6, Ag85B, and Rv2660c for 2 hours at 37°C/5% CO_2, then for an additional 12 hours at 37°C/5% CO_2. Peptide pools were diluted to 1ug/ml. PDBU and ionomycin was used as a positive control for stimulation whenever additional cells were available. After stimulation, BAL cells were washed with 1xPBS and stained as described below.

Similarly, in the H56/H74-CAF01 study, after BAL cells were isolated, they were stimulated with peptide pools/proteins of H56 vaccine-specific proteins ESAT-6, Ag85B, and Rv2660c, or H74 vaccine-specific proteins ESAT-6, Rv3881c, Rv3614c, Rv3615c, Rv3616c, and Rv3849, for 2 hours at 37°C/5% CO_2, then for an additional 12 hours at 37°C/5% CO_2. Peptide pools were diluted to 1ug/ml. PDBU and ionomycin was used as a positive control for stimulation whenever additional cells were available, and BAL cell responses were media-subtracted to approximate vaccine-specific responses. After stimulation, BAL cells were washed with 1xPBS and stained as described below.

After stimulation and wash, BAL cells were stained for viability (Invitrogen). BAL cells and PBMCs were stained for surface and intracellular cytokine markers. Antibodies for cell surface markers included: CD3 (clone SP34-2, BD Biosciences), CD4 (clone L200, BD Biosciences), CD8 (RPA-T8, BD Biosciences), CD45Ra (clone 5H9, BD Biosciences), CD27 (clone 0323, eBiosciences). Cells were fixed and permeabilized (BD Biosciences). Intracellular staining of cytokines and other cellular markers included: CD69 (clone TP1.55.3, Beckman

Coulter), IFN-γ (clone B27, BD Biosciences), IL-2 (clone MQ1-17H12, BD Biosciences), TNF (clone MAB11, BD Biosciences), IL-10 (clone JES3-9D7), Ki67 (clone B56, BD Biosciences), and IL-17 (clone eBio64CAP17, eBiosciences). Cells were fixed in 1% paraformaldehyde. Data acquisition was performed using a LSR II flow cytometer (BD Biosciences) and analyzed using FlowJo Software v.9.7 or v.9.9 (Treestar Inc.). BAL cytokine responses were normalized to live cell counts and mL of fluid obtained.

4.5.5 PBMC ELISPOTs

Isolated PBMCs were serially stimulated over the course of vaccination and infection with vaccine-specific peptides, and IFN-γ production captured by NHP-specific IFN-γ ELISPOTs (Mabtech) according to manufacturer's instructions. Briefly, white membrane ELISPOT plates (Millipore) were coated with IFN-γ specific capture antibody (MT162L, Mabtech) and blocked with ELISPOT media (RPMI+1% L-glutamine+1% HEPES+10% human AB serum). 2ug/ml peptide pools of H56 proteins (ESAT-6, Ag85B, and Rv2660c) and H74 proteins (ESAT-6, Rv3881c, Rv3614c, Rv3615c, Rv3616c, and Rv3849), and 2ug/ml Mtb culture filtrate protein (CFP) were added to $2x10^5$ PBMCs in duplicate and incubated at 37°C/5% CO_2 for 40-50 hours. Cells were then washed, and IFN-γ detection antibody (7B6-biotin) was added for 2 hours at 37°C or overnight at 4°C. After washing, streptavidin-HRP was incubated for 45 minutes at 37°C, and ELISPOT plates were developed using AEC substrate solution. After development and drying, IFN-γ spots were enumerated by ImmunoSpot program, and results normalized by spot forming units per $2x10^5$ cells.

4.5.6 ELISAs

Reciprocal endpoint titer ELISAs were used to measure the H56 vaccine-specific response in the BAL and plasma. IgG responses were detected using a pan-monkey antibody (clone: 1B3-HRP, NIH NHP Resources, Mass Biologics) and IgA responses were detected using a rhesus antibody (clone: 10F12, NIH NHP Resources, Mass Biologics). Results were measured at OD450 on a spectrophotometer (SpectraMax). Antibody levels were measured by serial sample dilutions, and calculated using the average OD450 + 2 standard deviations of the highest dilution of the negative control as a cutoff. All BAL results were normalized by plasma and BAL urea levels.

4.5.7 Animal infection

Animals in H56-CAF01 study were infected with 12-21 colony forming units (CFUs) of Mtb virulent Erdman strain per monkey by bronchoscopic instillation to the lower lung lobe, as previously described [267]. Similarly, animals in H56/H74-CAF01 study were infected with 4-25 CFUs of Mtb virulent Erdman strain per monkey. To reduce numbers of macaques used, 6 unvaccinated controls for the H56-CAF01 study were from another published study [106].

4.5.8 PET/CT scans

After Mtb challenge, serial ^{18}F-fluorodeoxyglucose (FDG) PET-CT scans were performed in a biosafety level 3 imaging suite as previously described [269]. Scan analyses were conducted using OsiriX viewer as described elsewhere, with quantification of granulomas on scans and

summation of total 18F-FDG uptake in lungs [329]. Six of the eight unvaccinated controls only had a single PET CT scan prior to necropsy, while two had serial scans.

4.5.9 Necropsy procedures, pathology scores, and bacterial burden

Necropsy was performed as previously described [57, 291]. In summary, NHPs were humanely sacrificed by terminal bleed, and lesions in lungs and thoracic lymph nodes identified by PET-CT or at necropsy were individually excised for histological analysis, and homogenized into single cell suspension for bacterial burden and immunological assays. Extent of disease was quantified using a disease pathology score that incorporates the number, size, and pattern of granulomas in each lung lobe, mediastinal lymph nodes, peripheral lymph nodes, and extrapulmonary organs, modified from our previously described version [57]. To determine the bacterial burden, each granuloma homogenate was plated in serial dilutions on 7H11 medium and incubated at 37°C/5% CO_2 for 21 days before CFU enumeration. Total CFU was calculated from a summation of plated samples. Excised and homogenized granulomas were also analyzed for immunological response by intracellular staining and flow cytometry as described above after 2.5-3.5 hours in the presence of Brefeldin A (GolgiPlug, BD Biosciences) to capture cytokine response.

4.5.10 Statistical analysis

Statistical analyses were performed using GraphPad Prism v6 and v7 (Graphpad Software). Kruskal-Wallis test was used with post hoc analysis Dunn's multiple test comparisons to

compare vaccinated groups to unvaccinated controls. P values less than 0.05 were considered significant. Linear regressions were performed using JMP Pro 13.

5.0 SUMMARY AND IMPLICATIONS

5.1 IL-10 AND T CELL EXHAUSTION ARE NOT SIGNIFICANT MODULATORS OF T CELL CYTOKINE RESPONSE IN TB GRANULOMAS

The goal of this dissertation was to determine the contributions of the immunomodulators IL-10 and exhausted T cells on T cell cytokine response in TB granulomas. Studies in the mouse model of Mtb infection and other infectious disease models suggested that IL-10 may be dampening protective T cell cytokine responses [132-137, 345-347]. While the absence of functional IL-10 in Mtb-infected NHPs had transient effects on the inflammation, cytokine response, and structure in a subset of lung granulomas, it did not affect the overall disease outcome or bacterial burden of the NHPs (**Chapter 2**). The changes in the lungs and lymph nodes in NHPs with IL-10 neutralization were mostly nullified or reversed by 8 weeks of Mtb infection. Since the Mtb-specific adaptive immune response is typically induced 4-6 weeks after Mtb infection in NHPs, the differences observed at 4 weeks may have been counteracted by the adaptive response by 8 weeks of infection [57]. As some of the previous murine studies of Mtb infection in the absence of IL-10 suggested, IL-10 alone may not have a significant role in modulating the immune response during Mtb infection, and may be compensated by other, currently unidentified, immune factors [139-142]. These results also suggested that some but not all lung granulomas

may be modulated by IL-10. Thus, although IL-10 may modulate some of the cell responses during Mtb infection, it is not the only or the major contributor.

A major limitation of this study is the short timeframe of Mtb infection. We had wanted to capture the effect of IL-10 during the transition from innate- to adaptive-dominated immune response in granulomas, thus only investigated two early, critical time points of Mtb infection. Administration of antibodies for long periods of time is challenging in non-human primates. However, in restricting our time frame, we may have missed the long-term effects of IL-10 during Mtb infection. A previous study in Mtb infection in mice found that lack of IL-10 did not make a difference in the granuloma structure or bacterial burden until after at least 2 months of infection [136]. Additionally, neutralizing IL-10 only within the first 3 weeks of infection set the Mtb-infected mice up for similar granuloma structure and bacterial control during chronic disease compared to mice completely lacking IL-10 during the entire infection. This suggests that IL-10 may be critical during the first month of Mtb infection, and the changes that we observed after 4 weeks of IL-10 neutralization may have set the stage for increased long-term bacterial control that we simply did not observe because we did not extend our study long enough. It also confirms that blockade of IL-10 beyond the first month of Mtb infection did not further increase the protection. Interestingly, as in the mouse study, we also observed increased signs of fibrosis in the granulomas in the absence of IL-10, further suggesting that these fibrotic granulomas may have better chronic control of Mtb, which supports previous studies associating fibrotic granulomas with containment, drug treatment, and sterility [286, 287]. The timing of the greater effects of the IL-10 neutralization, increasing cytokine and chemokine responses and decreasing inflammation at 4 weeks post-infection also suggests a stronger effect of IL-10 on the innate immune response during Mtb infection, before a robust adaptive immune response begins

around 6 weeks post-infection. By 8 weeks post-infection, during the establishment of the adaptive immune response, Furthermore, many of the changes in cytokine response during anti-IL-10 treatment were cytokines typically produced by innate immune cells. Thus, IL-10 may be more critical for innate cell response, rather than on T cells, as previously hypothesized.

Our observations that IL-10 is not critical for bacterial control during the first two months of infection settles the discordant mouse studies about the role of IL-10 during early Mtb infection. Additionally, the absence of IL-10 does not significantly affect the T cell response. Thus, while therapeutics to supplement or block IL-10 have been suggested for other autoimmune or infectious diseases, therapeutics to reduce IL-10 and boost immune responses may not be prudent [348-350]. Although the research in this dissertation strongly suggests that IL-10 alone may not significantly affect disease outcomes early in Mtb infections, further research into the effects of IL-10 later on in infection should be conducted. Understanding the role of IL-10 during later stages of Mtb infection is especially critical because human Mtb infections are typically not diagnosed until months to years later. IL-10 may have a different role during Mtb infections by the time patients are diagnosed. Regulatory T cells, other immunomodulatory cytokines, such as TGF-β, currently unidentified factors, or IL-10 in conjunction with another factor may be more critical to modulating the T cell response in TB granulomas.

This dissertation also aimed to investigate whether exhaustion of T cells during Mtb infection influenced the T cell responses in TB granulomas. T cell exhaustion is a major contributor to T cell dysfunction in many chronic viral diseases and cancer [143-148]. Using our NHP model of TB, we did not find evidence that T cells in TB granulomas across infection time or pathology were definitively exhausted (**Chapter 3**). There were low frequencies of T cells

expressing the inhibitory receptors PD-1, CTLA-4, or LAG-3, and those expressing these inhibitory receptors still had similar or even more cytokine functionality and proliferation capability than those without inhibitory receptors. Our collaborators further demonstrated that when they manipulated levels of T cell exhaustion in a computational model of TB granulomas, there were much higher levels of bacterial load than observed *in vivo*. The low levels of T cell exhaustion we observed contrast with previous studies in humans, mice, and NHPs. However, many of those studies characterized T cell exhaustion by the expression of a single inhibitory receptor [159-161]. Additionally, the presence of an inhibitory marker (PD-1 or CTLA-4) in some studies seemed to mark T cells as activated rather than exhausted [115, 169, 179]. Thus, although TB is a chronic disease where Mtb and its antigens can persist in granulomas for extended periods of time, the T cells do not appear to be exhausted. Our collaborators' computational model and observations of the compartmentalization of activated cells in granulomas support our hypotheses that the low levels of T cell exhaustion may be a virtue of the highly organized structure of granulomas preventing T cells from encountering Mtb antigens [179, 268, 351].

Due to limited reliable reagents available for NHPs, our study focused only on 3 main inhibitory receptors, PD-1, CTLA-4, and LAG-3, as markers of T cell exhaustion. However, these inhibitory receptors are also the ones with blocking therapies furthest in development. Drugs targeting inhibitory receptors have been used in cancer immunotherapy, with anti-PD-1 and anti-CTLA-4 drugs FDA-approved since 2014 and 2011, respectively [352]. Immunotherapies to block LAG-3 are also in development to treat cancer [353]. The success of these therapies depend on the presence of these inhibitory receptors on the T cells in the tumors [352]. With low levels of these inhibitory receptors on T cells in TB granulomas, these therapies

would not be beneficial during TB treatment. The contrast between T cell exhaustion in TB granulomas and tumor microenvironments, although similar in their congregations of immune cells, highlights the unique spatialization and organization within TB granulomas that prevent the chronic antigen presentation necessary for T cell exhaustion.

IL-10 and T cell exhaustion have been long suggested as potential reasons for the low T cell responses and lack of bacterial control during Mtb infections. The results from this dissertation demonstrate that IL-10 and T cell exhaustion individually are not significant contributors to the modulation of T cell responses at the local site of Mtb infection, in TB granulomas. Understanding that IL-10 and T cell exhaustion are not immunological correlates of TB protection helps push TB research into different directions, so that hopefully other more significant contributing factors may be found.

5.2 VACCINATION STRATEGY CAN ALTER IMMUNE RESPONSE

By testing different vaccination strategies, this dissertation sought to alter the T cell response in the TB granulomas and engender greater protection than the current TB vaccine, BCG, with protein subunit vaccines. Although we were able to alter the immune response, and interestingly did so by only changing the routes or timing of vaccination, the vaccine strategies that we tested did not significantly improve protection above traditional BCG vaccination (**Chapter 4**). Initial results of homologous subunit vaccination suggested targeting the mucosal airways by aerosol vaccination may recruit lymphocytes to the airways and lead to less inflammation after Mtb challenge. However, when NHPs were vaccinated by BCG prime and heterologous aerosol subunit boosts, there were few protective benefits, with slightly increased inflammation, bacterial

loads, and disease pathology in aerosol boost-vaccinated NHPs compared to BCG-vaccinated NHPs. Additional testing of a novel vaccination strategy of simultaneous priming with BCG and a subunit vaccine before further subunit boosting demonstrated few benefits of simultaneous prime vaccinations. Instead, the NHPs that received BCG-only prime followed by subunit boosts did the best among the experimental vaccination groups. These NHPs also had similar to slightly improved protection compared to BCG-vaccinated NHPs, with slightly less inflammation, more stable lung granuloma numbers, and slightly lower lung bacterial burdens. Ultimately, these different vaccination strategies suggested that the subunit vaccines H56 and H74 with the liposomal adjuvants we tested, CAF01 and CAF09, did not boost much immune protection beyond BCG alone, although the granuloma T cell responses were different depending on the vaccination strategy.

Additional boost vaccination could have resulted in minimal additional protection for a variety of reasons. The vaccination routes tested may not have been effective. We primarily targeted the lymph node priming by the simultaneous BCG-subunit vaccination and the mucosal airways by aerosol vaccination, but other vaccination strategies may be more effective, such as intravenous administration, which has shown increased protection of BCG [252-254]. The combination of subunit vaccine and adjuvant may not have been optimal, and may have not targeted the "right" immune response for protection. Current strategies design vaccines to elicit T cell responses, but because the correlates of protection for TB have not yet been identified, these T cell responses may not be sufficient to create a protective immune response to TB. Likewise, subunit vaccines may not be creating memory T cell responses to the necessary Mtb antigens [209].

Although this dissertation did not identify a vaccination strategy that could improve the current BCG vaccine, it challenges the benefits of aerosol vaccination and simultaneous priming of BCG with a subunit vaccine. It has demonstrated the difficulty in designing and optimizing an effective subunit vaccine for TB, and the complexity in improving BCG despite its deficiencies. More positively, the differential T cell responses under various vaccination strategies establishes that vaccinations can alter the immune response in TB granulomas, and may eventually improve understanding of the protective T cell responses necessary in the local environment of Mtb.

5.3 FUTURE DIRECTIONS IN TB RESEARCH

This dissertation highlighted the difficulty in pinpointing a single modulator of T cell responses or correlate of protection within TB granulomas. TB is an intricate disease with many moving parts, and TB granulomas are dynamic structures that involve many different cell types and are heterogeneous in nature. Studying granulomas within NHPs, which are heterogeneous with complex immune systems, further complicate matters. However, because of their similarity to human disease, the ability to track TB disease from the moment of infection, and the ability to analyze the individual granulomas, NHPs are an accessible and accurate representation of the elaborate local response to Mtb in humans. Beyond the complexities of the host immune response to Mtb, the bacteria can also exert its own pressures on the immune response. Understanding the interactions between Mtb and host will continue to be a pressing question. The results from this dissertation confirm that the protective immune response to Mtb infection is not simple and likely cannot be reduced to a single factor.

How can we build upon the results presented in this dissertation? Although these data demonstrated IL-10 does not have a significant role in the outcome of pathology and bacterial load early in Mtb infection, it had transient effects on the immune response in the granulomas. To understand the role of IL-10 during the course of Mtb infection, future studies should investigate whether the role of IL-10 may change depending on the stage of Mtb infection and whether the observed early effects of IL-10 may change disease outcome during longer infections. This work has also described the low frequencies of T cell exhaustion in TB granulomas. Although there may be conditions in which T cell exhaustion may occur during Mtb infections, these data suggest that it is not a common or critical component of TB granuloma outcomes. Until further evidence of high levels of functionally exhausted T cells in the granulomas of TB patients, it may be reasonable to consider alternate modulators of T cell responses in TB granulomas. Namely, the inhibitory cytokine TGF-β was outside of the scope of this dissertation, but as a main mechanism of regulatory T cells to modulate immune responses, it may have additional regulatory effects on the immune response in TB granulomas. In this study, another anti-inflammatory cytokine, IL-13, was also observed to increase TB granulomas in the absence of IL-10, which may contribute to the observed increased fibrosis and warrants further investigation. Other factors that may modulate other immune cells in addition to T cells, such as mesenchymal stem cells and myeloid-derived suppressor cells, may also be critical in the immune response during Mtb infections.

Furthermore, this study investigated the roles of IL-10 and T cell exhaustion within Mtb infection separately. However, IL-10 and T cell exhaustion have been shown to be associated in other disease models, and concurrent targeting during experimental immunotherapies are increasingly recognized to have synergistic effects. As previously mentioned, the host response

to TB is complex, and the modulation of the immune response is not likely by a single modulator. Thus, despite the results of this dissertation suggesting the low individual contributions of IL-10 and T cell exhaustion to the control of TB, future studies should still investigate the synergistic effects of these factors, and of the other previously suggested immune modulators. While the research in this dissertation indicates few benefits of treating with anti-IL-10 or anti-inhibitory receptor therapies, it does not eliminate the potential of combinatorial therapies to enhance the effects of antibiotic treatments.

Finally, the absence of protection observed after testing multiple vaccination strategies using subunit proteins as a boost to BCG reminds us that producing a vaccine or vaccination strategy for a complicated disease like TB, which has evolved with the human immune system for millennia, will take much more research and innovation. Besides designing a vaccine to better elicit a protective immune response, future vaccination research will also need to optimize delivery strategies and consider vaccine/adjuvant combinations, prime/boost combinations, and routes of vaccination. The results of this study also demonstrated that despite the problems with BCG, it continues to confer some level of protection, supporting its continued use as improvements are researched. Boosting BCG with a protein subunit vaccine in a liposomal adjuvant such as those tested in this dissertation may not provide sufficient lasting immune responses to protect from Mtb challenge. Although the liposomal adjuvant was designed and tested to create a vaccine depot, slower clearance of a live vaccine, such as BCG or a viral vector, may be necessary to create a sustained or larger immune response against Mtb. However, since these experimental boost vaccination strategies were able to increase the T cell cytokine response within TB granulomas without improving the granuloma or overall disease outcomes, this suggests that more research into understanding the correlates of protection for TB is still

needed. The cytokines classically associated with improved disease outcomes, such as IFN-γ and TNF, may continue to be critical for control of Mtb, but are likely not sufficient for complete protection from Mtb. In order to identify these factors that may improve host outcomes during Mtb infection, future studies should continue to dissect the immune responses of hosts protected vs. unprotected from Mtb and granulomas that are sterile vs. nonsterile. With improvements in techniques for multi-parameter immune research down to even a single cell from a TB granuloma, the identification of the correlates of protection and protective balance of Mtb-specific immune response may be possible in future research.

Much work remains to be done, but I expect that the results of this dissertation will help move the field of TB research forward by focusing the understanding of potential significant modulators of T cell response in TB granulomas away from IL-10 or T cell exhaustion. This study also establishes the ability of vaccination routes and strategies to affect the local immune response during Mtb challenge, suggesting important considerations during future TB vaccine studies. I am confident that these dissertation results, when combined with the results of the many ongoing TB studies around the world, will help to one day identify the correlates of protection for a fully protective vaccine and eradication of TB.

APPENDIX A

PUBLICATION LIST

Wong EA*, L Joslyn*, NL Grant, E Klein, PL Lin, DE Kirschner, JL Flynn (2018). Low levels of T cell exhaustion in tuberculous lung granulomas. Infection and Immunity, accepted
*co-first authors

Cadena AM, FF Hopkins, P Maiello, AF Carey, **EA Wong**, CJ Martin, RM DiFazio, PL Lin, SM Fortune, JL Flynn (2018). Primary infection with Mycobacterium tuberculosis confers robust protection against secondary infection in macaques. Nature Medicine, submitted and under review

DiFazio RM, JT Mattila, EC Klein, LR Cirrincione, M Howard, **EA Wong** and JL Flynn (2016). Active transforming growth factor-b is associated with phenotypic changes in granulomas after drug treatment in pulmonary tuberculosis. Fibrogenesis & Tissue Repair 9:6.

Phuah JY, **EA Wong**, HP Gideon, P Maiello, MT Coleman, MR Hendricks, R Ruden, L Cirrincione, J Chan, PL Lin, and JL Flynn (2016). Effects of B cell depletion on early *Mycobacterium tuberculosis* infection in cynomolgus macaques. Infection and Immunity 84(5):1301-11.

BIBLIOGRAPHY

1. WHO. *Tuberculosis Fact Sheet*. January 2018 [cited 2018 Febuary 6]; No 104:[Available from: http://www.who.int/mediacentre/factsheets/fs104/en/.
2. CDC, *Reported Tuberculosis in the United States*. 2016, U.S. Department of Health and Human Services, CDC: Atlanta, GA.
3. Gideon, H.P. and J.L. Flynn, *Latent tuberculosis: what the host "sees"?* Immunologic research, 2011. **50**(2-3): p. 202-212.
4. Vynnycky, E. and P. Fine, *The natural history of tuberculosis: the implications of age-dependent risks of disease and the role of reinfection.* Epidemiology & Infection, 1997. **119**(2): p. 183-201.
5. Koul, A., et al., *The challenge of new drug discovery for tuberculosis.* Nature, 2011. **469**(7331): p. 483-490.
6. Comstock, G.W., V.T. LIVESAY, and S.F. WOOLPERT, *The prognosis of a positive tuberculin reaction in childhood and adolescence.* American journal of epidemiology, 1974. **99**(2): p. 131-138.
7. Vynnycky, E. and P.E. Fine, *Lifetime risks, incubation period, and serial interval of tuberculosis.* American journal of epidemiology, 2000. **152**(3): p. 247-263.
8. Luca, S. and T. Mihaescu, *History of BCG Vaccine.* Maedica, 2013. **8**(1): p. 53-58.
9. Barberis, I., et al., *The history of tuberculosis: from the first historical records to the isolation of Koch's bacillus.* Journal of preventive medicine and hygiene, 2017. **58**(1): p. E9.
10. Cambau, E. and M. Drancourt, *Steps towards the discovery of Mycobacterium tuberculosis by Robert Koch, 1882.* Clinical Microbiology and Infection, 2014. **20**(3): p. 196-201.
11. Comas, I., et al., *Out-of-Africa migration and Neolithic coexpansion of Mycobacterium tuberculosis with modern humans.* Nature genetics, 2013. **45**(10): p. 1176.
12. Bos, K.I., et al., *Pre-Columbian mycobacterial genomes reveal seals as a source of New World human tuberculosis.* Nature, 2014. **514**(7523): p. 494.
13. Daniel, T.M., *The history of tuberculosis.* Respiratory medicine, 2006. **100**(11): p. 1862-1870.
14. Organization, W.H., *Global tuberculosis report 2017*. 2017: World Health Organization.
15. Riley, R., et al., *Air Hygiene in Tuberculosis: Quantitative Studies of Infectivity and Control in a Pilot Ward. A Cooperative Study between the Veterans Administration, the Johns Hopkins University School of Hygiene and Public Health, and the Maryland Tuberculosis Association.* American Review of Tuberculosis and Pulmonary Diseases, 1957. **75**(3): p. 420-31.

16. Riley, R., et al., *Aerial dissemination of pulmonary tuberculosis. A two-year study of contagion in a tuberculosis ward.* American Journal of Hygiene, 1959. **70**(2): p. 185-96.
17. Riley, R., et al., *Infectiousness of air from a tuberculosis ward: ultraviolet irradiation of infected air: comparative infectiousness of different patients.* American Review of Respiratory Disease, 1962. **85**(4): p. 511-525.
18. Fennelly, K.P., et al., *Cough-generated aerosols of Mycobacterium tuberculosis: a new method to study infectiousness.* American journal of respiratory and critical care medicine, 2004. **169**(5): p. 604-609.
19. Fox, G.J., et al., *Contact investigation for tuberculosis: a systematic review and meta-analysis.* European Respiratory Journal, 2013. **41**(1): p. 140-156.
20. Beyers, N., et al., *A prospective evaluation of children under the age of 5 years living in the same household as adults with recently diagnosed pulmonary tuberculosis.* The International Journal of Tuberculosis and Lung Disease, 1997. **1**(1): p. 38-43.
21. Martinez, L., et al., *Transmission of Mycobacterium tuberculosis in households and the community: a systematic review and meta-analysis.* American journal of epidemiology, 2017. **185**(12): p. 1327-1339.
22. Andrews, J.R., et al., *Integrating social contact and environmental data in evaluating tuberculosis transmission in a South African township.* The Journal of infectious diseases, 2014. **210**(4): p. 597-603.
23. Yates, T.A., et al., *The transmission of Mycobacterium tuberculosis in high burden settings.* The Lancet infectious diseases, 2016. **16**(2): p. 227-238.
24. Andrews, J.R., C. Morrow, and R. Wood, *Modeling the role of public transportation in sustaining tuberculosis transmission in South Africa.* American journal of epidemiology, 2013. **177**(6): p. 556-561.
25. Pai, M., et al., *Tuberculosis.* Nat Rev Dis Primers, 2016. **2**: p. 16076.
26. Barry 3rd, C.E., et al., *The spectrum of latent tuberculosis: rethinking the biology and intervention strategies.* Nature Reviews Microbiology, 2009. **7**(12): p. 845.
27. Lin, P.L. and J.L. Flynn, *Understanding latent tuberculosis: a moving target.* The Journal of Immunology, 2010. **185**(1): p. 15-22.
28. Tiemersma, E.W., et al., *Natural history of tuberculosis: duration and fatality of untreated pulmonary tuberculosis in HIV negative patients: a systematic review.* PloS one, 2011. **6**(4): p. e17601.
29. Dowdy, D.W., S. Basu, and J.R. Andrews, *Is passive diagnosis enough? The impact of subclinical disease on diagnostic strategies for tuberculosis.* American journal of respiratory and critical care medicine, 2013. **187**(5): p. 543-551.
30. Andrews, J.R., et al., *Risk of progression to active tuberculosis following reinfection with Mycobacterium tuberculosis.* Clinical infectious diseases, 2012. **54**(6): p. 784-791.
31. Boehme, C.C., et al., *Feasibility, diagnostic accuracy, and effectiveness of decentralised use of the Xpert MTB/RIF test for diagnosis of tuberculosis and multidrug resistance: a multicentre implementation study.* The lancet, 2011. **377**(9776): p. 1495-1505.
32. Organization, W.H., *Policy statement: automated real-time nucleic acid amplification technology for rapid and simultaneous detection of tuberculosis and rifampicin resistance: Xpert MTB/RIF system.* Policy statement: automated real-time nucleic acid amplification technology for rapid and simultaneous detection of tuberculosis and rifampicin resistance: Xpert MTB/RIF system., 2011.

33. Zak, D.E., et al., *A blood RNA signature for tuberculosis disease risk: a prospective cohort study.* The Lancet, 2016. **387**(10035): p. 2312-2322.
34. Suliman, S., et al., *Four-gene Pan-African Blood Signature Predicts Progression to Tuberculosis.* American journal of respiratory and critical care medicine, 2018(ja).
35. Lawn, S.D. and A.I. Zumla, *Tuberculosis.* The Lancet, 2011. **378**(9785): p. 57-72.
36. Brosch, R., et al., *A new evolutionary scenario for the Mycobacterium tuberculosis complex.* Proceedings of the national academy of Sciences, 2002. **99**(6): p. 3684-3689.
37. Gagneux, S., et al., *Variable host–pathogen compatibility in Mycobacterium tuberculosis.* Proceedings of the National academy of Sciences of the United States of America, 2006. **103**(8): p. 2869-2873.
38. Parwati, I., R. van Crevel, and D. van Soolingen, *Possible underlying mechanisms for successful emergence of the Mycobacterium tuberculosis Beijing genotype strains.* The Lancet infectious diseases, 2010. **10**(2): p. 103-111.
39. Cole, S., et al., *Deciphering the biology of Mycobacterium tuberculosis from the complete genome sequence.* Nature, 1998. **393**(6685): p. 537.
40. Sonnenberg, M.G. and J.T. Belisle, *Definition of Mycobacterium tuberculosis culture filtrate proteins by two-dimensional polyacrylamide gel electrophoresis, N-terminal amino acid sequencing, and electrospray mass spectrometry.* Infection and immunity, 1997. **65**(11): p. 4515-4524.
41. Arend, S.M., et al., *Detection of active tuberculosis infection by T cell responses to early-secreted antigenic target 6-kDa protein and culture filtrate protein 10.* The Journal of infectious diseases, 2000. **181**(5): p. 1850-1854.
42. Roberts, A., et al., *Characteristics of protective immunity engendered by vaccination of mice with purified culture filtrate protein antigens of Mycobacterium tuberculosis.* Immunology, 1995. **85**(3): p. 502.
43. Simeone, R., D. Bottai, and R. Brosch, *ESX/type VII secretion systems and their role in host–pathogen interaction.* Current opinion in microbiology, 2009. **12**(1): p. 4-10.
44. Lewis, K.N., et al., *Deletion of RD1 from Mycobacterium tuberculosis mimics bacille Calmette-Guerin attenuation.* The Journal of infectious diseases, 2003. **187**(1): p. 117-123.
45. Pym, A.S., et al., *Loss of RD1 contributed to the attenuation of the live tuberculosis vaccines Mycobacterium bovis BCG and Mycobacterium microti.* Molecular microbiology, 2002. **46**(3): p. 709-717.
46. Pathak, S.K., et al., *Direct extracellular interaction between the early secreted antigen ESAT-6 of Mycobacterium tuberculosis and TLR2 inhibits TLR signaling in macrophages.* Nature immunology, 2007. **8**(6): p. 610.
47. Smith, J., et al., *Evidence for pore formation in host cell membranes by ESX-1-secreted ESAT-6 and its role in Mycobacterium marinum escape from the vacuole.* Infection and immunity, 2008. **76**(12): p. 5478-5487.
48. Kinhikar, A.G., et al., *Potential role for ESAT6 in dissemination of M. tuberculosis via human lung epithelial cells.* Molecular microbiology, 2010. **75**(1): p. 92-106.
49. Smith, I., *Mycobacterium tuberculosis pathogenesis and molecular determinants of virulence.* Clinical microbiology reviews, 2003. **16**(3): p. 463-496.
50. Russell, D.G., et al., *Foamy macrophages and the progression of the human tuberculosis granuloma.* Nature immunology, 2009. **10**(9): p. 943.

51. Tsai, M.C., et al., *Characterization of the tuberculous granuloma in murine and human lungs: cellular composition and relative tissue oxygen tension.* Cellular microbiology, 2006. **8**(2): p. 218-232.
52. Srivastava, S., J.D. Ernst, and L. Desvignes, *Beyond macrophages: the diversity of mononuclear cells in tuberculosis.* Immunological reviews, 2014. **262**(1): p. 179-192.
53. Wolf, A.J., et al., *Mycobacterium tuberculosis infects dendritic cells with high frequency and impairs their function in vivo.* The Journal of Immunology, 2007. **179**(4): p. 2509-2519.
54. Clay, H., et al., *Dichotomous role of the macrophage in early Mycobacterium marinum infection of the zebrafish.* Cell host & microbe, 2007. **2**(1): p. 29-39.
55. Wolf, A.J., et al., *Initiation of the adaptive immune response to Mycobacterium tuberculosis depends on antigen production in the local lymph node, not the lungs.* Journal of Experimental Medicine, 2008. **205**(1): p. 105-115.
56. Poulsen, A., *Some clinical features of tuberculosis. 1. Incubation period.* Acta tuberculosea Scandinavica, 1950. **24**(3-4): p. 311.
57. Lin, P.L., et al., *Quantitative comparison of active and latent tuberculosis in the cynomolgus macaque model.* Infect Immun, 2009. **77**(10): p. 4631-42.
58. Russell, D.G., C.E. Barry, and J.L. Flynn, *Tuberculosis: what we don't know can, and does, hurt us.* Science, 2010. **328**(5980): p. 852-856.
59. Ramakrishnan, L., *Revisiting the role of the granuloma in tuberculosis.* Nature Reviews Immunology, 2012. **12**(5): p. 352-366.
60. O'Garra, A., et al., *The immune response in tuberculosis.* Annual review of immunology, 2013. **31**: p. 475-527.
61. Lin, P.L., et al., *Sterilization of granulomas is common in active and latent tuberculosis despite within-host variability in bacterial killing.* Nature medicine, 2013.
62. Davis, J.M. and L. Ramakrishnan, *The role of the granuloma in expansion and dissemination of early tuberculous infection.* Cell, 2009. **136**(1): p. 37-49.
63. Vergne, I., et al., *Cell biology of Mycobacterium tuberculosis phagosome.* Annu. Rev. Cell Dev. Biol., 2004. **20**: p. 367-394.
64. Gutierrez, M.G., et al., *Autophagy is a defense mechanism inhibiting BCG and Mycobacterium tuberculosis survival in infected macrophages.* Cell, 2004. **119**(6): p. 753-766.
65. Divangahi, M., et al., *Eicosanoid pathways regulate adaptive immunity to Mycobacterium tuberculosis.* Nature immunology, 2010. **11**(8): p. 751.
66. Hanekom, W.A., et al., *Mycobacterium tuberculosis inhibits maturation of human monocyte-derived dendritic cells in vitro.* The Journal of infectious diseases, 2003. **188**(2): p. 257-266.
67. Shafiani, S., et al., *Pathogen-specific regulatory T cells delay the arrival of effector T cells in the lung during early tuberculosis.* Journal of Experimental Medicine, 2010. **207**(7): p. 1409-1420.
68. Cadena, A.M., J.L. Flynn, and S.M. Fortune, *The importance of first impressions: early events in mycobacterium tuberculosis infection influence outcome.* MBio, 2016. **7**(2): p. e00342-16.
69. Lin, P.L. and J.L. Flynn, *Nonhuman Primates in Biomedical Research: Diseases*, C.R.M. Abee, K.; Tardif, S.; Morris, T., Editor. 2012, Elsevier Inc. Academic Press. p. 173-196.

70. Saunders, B.M. and W.J. Britton, *Life and death in the granuloma: immunopathology of tuberculosis.* Immunology and cell biology, 2007. **85**(2): p. 103-111.
71. Casanova, J.-L. and L. Abel, *Genetic dissection of immunity to mycobacteria: the human model.* Annual review of immunology, 2002. **20**(1): p. 581-620.
72. Flynn, J.L., et al., *An essential role for interferon gamma in resistance to Mycobacterium tuberculosis infection.* The Journal of experimental medicine, 1993. **178**(6): p. 2249-2254.
73. Flynn, J.L., et al., *Tumor necrosis factor-α is required in the protective immune response against Mycobacterium tuberculosis in mice.* Immunity, 1995. **2**(6): p. 561-572.
74. Zhang, M., et al., *T-cell cytokine responses in human infection with Mycobacterium tuberculosis.* Infection and immunity, 1995. **63**(8): p. 3231-3234.
75. Day, C.L., et al., *Functional capacity of Mycobacterium tuberculosis-specific T cell responses in humans is associated with mycobacterial load.* The Journal of Immunology, 2011. **187**(5): p. 2222-2232.
76. Harari, A., et al., *Dominant TNF-[alpha]+ Mycobacterium tuberculosis-specific CD4+ T cell responses discriminate between latent infection and active disease.* Nature medicine, 2011. **17**(3): p. 372-376.
77. Lin, P.L., et al., *Quantitative comparison of active and latent tuberculosis in the cynomolgus macaque model.* Infection and immunity, 2009. **77**(10): p. 4631-4642.
78. Flynn, J.L., et al., *Immunology studies in non-human primate models of tuberculosis.* Immunological reviews, 2015. **264**(1): p. 60-73.
79. Flynn, J.L., *Immunology of tuberculosis and implications in vaccine development.* Tuberculosis, 2004. **84**(1): p. 93-101.
80. Oliver, B.G., et al., *Mediators of innate and adaptive immune responses differentially affect immune restoration disease associated with Mycobacterium tuberculosis in HIV patients beginning antiretroviral therapy.* Journal of Infectious Diseases, 2010. **202**(11): p. 1728-1737.
81. Sharma, S., A. Mohan, and T. Kadhiravan, *HIV-TB co-infection: epidemiology, diagnosis & management.* Indian Journal of Medical Research, 2005. **121**(4): p. 550-567.
82. Scanga, C.A., et al., *The inducible nitric oxide synthase locus confers protection against aerogenic challenge of both clinical and laboratory strains of Mycobacterium tuberculosis in mice.* Infection and immunity, 2001. **69**(12): p. 7711-7717.
83. Green, A.M., R. DiFazio, and J.L. Flynn, *IFN-γ from CD4 T cells is essential for host survival and enhances CD8 T cell function during Mycobacterium tuberculosis infection.* The Journal of Immunology, 2013. **190**(1): p. 270-277.
84. Lin, P.L., et al., *CD4 T cell depletion exacerbates acute Mycobacterium tuberculosis while reactivation of latent infection is dependent on severity of tissue depletion in cynomolgus macaques.* AIDS research and human retroviruses, 2012. **28**(12): p. 1693-1702.
85. Flynn, J.L. and J. Chan, *Immunology of tuberculosis.* Annual review of immunology, 2001. **19**(1): p. 93-129.
86. Cooper, A.M., et al., *Disseminated tuberculosis in interferon gamma gene-disrupted mice.* The Journal of experimental medicine, 1993. **178**(6): p. 2243-2247.
87. Dixon, W., et al., *Drug-specific risk of tuberculosis in patients with rheumatoid arthritis treated with anti-TNF therapy: results from the British Society for Rheumatology Biologics Register (BSRBR).* Annals of the rheumatic diseases, 2010. **69**(3): p. 522-528.

88. Lin, P.L., et al., *Tumor necrosis factor neutralization results in disseminated disease in acute and latent Mycobacterium tuberculosis infection with normal granuloma structure in a cynomolgus macaque model.* Arthritis & Rheumatism, 2010. **62**(2): p. 340-350.
89. Toossi, Z., M.E. Kleinhenz, and J.J. Ellner, *Defective interleukin 2 production and responsiveness in human pulmonary tuberculosis.* The Journal of experimental medicine, 1986. **163**(5): p. 1162-1172.
90. Millington, K.A., et al., *Dynamic relationship between IFN-γ and IL-2 profile of Mycobacterium tuberculosis-specific T cells and antigen load.* The Journal of Immunology, 2007. **178**(8): p. 5217-5226.
91. Lockhart, E., A.M. Green, and J.L. Flynn, *IL-17 production is dominated by γδ T cells rather than CD4 T cells during Mycobacterium tuberculosis infection.* The Journal of Immunology, 2006. **177**(7): p. 4662-4669.
92. Scriba, T.J., et al., *Distinct, specific IL-17-and IL-22-producing CD4+ T cell subsets contribute to the human anti-mycobacterial immune response.* The Journal of Immunology, 2008. **180**(3): p. 1962-1970.
93. Khader, S.A., et al., *IL-23 and IL-17 in the establishment of protective pulmonary CD4+ T cell responses after vaccination and during Mycobacterium tuberculosis challenge.* Nature immunology, 2007. **8**(4): p. 369-377.
94. Chen, C.Y., et al., *A critical role for CD8 T cells in a nonhuman primate model of tuberculosis.* PLoS pathogens, 2009. **5**(4): p. e1000392.
95. Flynn, J.L., et al., *Major histocompatibility complex class I-restricted T cells are required for resistance to Mycobacterium tuberculosis infection.* Proceedings of the National Academy of Sciences, 1992. **89**(24): p. 12013-12017.
96. Behar, S.M., et al., *Susceptibility of mice deficient in CD1D or TAP1 to infection with Mycobacterium tuberculosis.* The Journal of experimental medicine, 1999. **189**(12): p. 1973-1980.
97. Lawn, S.D., S.T. Butera, and T.M. Shinnick, *Tuberculosis unleashed: the impact of human immunodeficiency virus infection on the host granulomatous response to< i> Mycobacterium tuberculosis</i>*. Microbes and Infection, 2002. **4**(6): p. 635-646.
98. Lin, P.L., et al. *Tumor necrosis factor and tuberculosis*. in *Journal of Investigative Dermatology Symposium Proceedings*. 2007. Elsevier.
99. Saunders, B.M., et al., *Transmembrane TNF is sufficient to initiate cell migration and granuloma formation and provide acute, but not long-term, control of Mycobacterium tuberculosis infection.* The Journal of Immunology, 2005. **174**(8): p. 4852-4859.
100. Bean, A.G., et al., *Structural deficiencies in granuloma formation in TNF gene-targeted mice underlie the heightened susceptibility to aerosol Mycobacterium tuberculosis infection, which is not compensated for by lymphotoxin.* The Journal of Immunology, 1999. **162**(6): p. 3504-3511.
101. Roach, D.R., et al., *TNF regulates chemokine induction essential for cell recruitment, granuloma formation, and clearance of mycobacterial infection.* The Journal of immunology, 2002. **168**(9): p. 4620-4627.
102. Gideon, H.P., et al., *Variability in tuberculosis granuloma T cell responses exists, but a balance of pro- and anti-inflammatory cytokines is associated with sterilization.* PLoS Pathog, 2015. **11**(1): p. e1004603.

103. Phuah, J.Y., et al., *Activated B cells in the granulomas of nonhuman primates infected with Mycobacterium tuberculosis.* The American journal of pathology, 2012. **181**(2): p. 508-514.
104. Slight, S.R., et al., *CXCR5+ T helper cells mediate protective immunity against tuberculosis.* The Journal of clinical investigation, 2013. **123**(2).
105. Lu, L.L., et al., *A functional role for antibodies in tuberculosis.* Cell, 2016. **167**(2): p. 433-443. e14.
106. Phuah, J., et al., *The Effects of B cell Depletion on early Mycobacterium tuberculosis infection in Cynomolgus Macaques.* Infect Immun, 2016.
107. Achkar, J.M., J. Chan, and A. Casadevall, *B cells and antibodies in the defense against Mycobacterium tuberculosis infection.* Immunological reviews, 2015. **264**(1): p. 167-181.
108. Scott-Browne, J.P., et al., *Expansion and function of Foxp3-expressing T regulatory cells during tuberculosis.* The Journal of experimental medicine, 2007. **204**(9): p. 2159-2169.
109. Green, A.M., et al., *CD4+ regulatory T cells in a cynomolgus macaque model of Mycobacterium tuberculosis infection.* Journal of Infectious Diseases, 2010. **202**(4): p. 533-541.
110. Burl, S., et al., *FOXP3 gene expression in a tuberculosis case contact study.* Clinical & Experimental Immunology, 2007. **149**(1): p. 117-122.
111. Periasamy, S., et al., *Programmed death 1 and cytokine inducible SH2-containing protein dependent expansion of regulatory T cells upon stimulation With Mycobacterium tuberculosis.* Journal of Infectious Diseases, 2011. **203**(9): p. 1256-1263.
112. Vignali, D.A., L.W. Collison, and C.J. Workman, *How regulatory T cells work.* Nature Reviews Immunology, 2008. **8**(7): p. 523.
113. Lowther, D.E., et al., *PD-1 marks dysfunctional regulatory T cells in malignant gliomas.* JCI insight, 2016. **1**(5).
114. Park, H.J., et al., *PD-1 upregulated on regulatory T cells during chronic virus infection enhances the suppression of CD8+ T cell immune response via the interaction with PD-L1 expressed on CD8+ T cells.* The Journal of Immunology, 2015. **194**(12): p. 5801-5811.
115. Gong, J.-H., et al., *Interleukin-10 downregulates Mycobacterium tuberculosis-induced Th1 responses and CTLA-4 expression.* Infection and immunity, 1996. **64**(3): p. 913-918.
116. Gerosa, F., et al., *CD4< sup>+</sup> T Cell Clones Producing both Interferon-γ and Interleukin-10 Predominate in Bronchoalveolar Lavages of Active Pulmonary Tuberculosis Patients.* Clinical Immunology, 1999. **92**(3): p. 224-234.
117. Othieno, C., et al., *Interaction of Mycobacterium tuberculosis-induced transforming growth factor β1 and interleukin-10.* Infection and immunity, 1999. **67**(11): p. 5730-5735.
118. Toossi, Z., et al., *Enhanced production of TGF-beta by blood monocytes from patients with active tuberculosis and presence of TGF-beta in tuberculous granulomatous lung lesions.* The journal of Immunology, 1995. **154**(1): p. 465-473.
119. Dai, G. and D. McMurray, *Effects of modulating TGF-beta; 1 on immune responses to mycobacterial infection in guinea pigs.* Tubercle and Lung Disease, 1999. **79**(4): p. 207-214.
120. Marshall, B.G., et al., *Enhanced Antimycobacterial Response to RecombinantMycobacterium bovis BCG Expressing Latency-Associated Peptide.* Infection and immunity, 2001. **69**(11): p. 6676-6682.

121. Hirsch, C.S., et al., *Cross-modulation by transforming growth factor beta in human tuberculosis: suppression of antigen-driven blastogenesis and interferon gamma production.* Proceedings of the National Academy of Sciences, 1996. **93**(8): p. 3193-3198.
122. Sabat, R., et al., *Biology of interleukin-10.* Cytokine & Growth Factor Reviews, 2010. **21**(5): p. 331-344.
123. Fiorentino, D.F., et al., *IL-10 inhibits cytokine production by activated macrophages.* The Journal of Immunology, 1991. **147**(11): p. 3815-3822.
124. Fiorentino, D.F., et al., *IL-10 acts on the antigen-presenting cell to inhibit cytokine production by Th1 cells.* The Journal of Immunology, 1991. **146**(10): p. 3444-3451.
125. Moore, K.W., et al., *Interleukin-10 and the interleukin-10 receptor.* Annual review of immunology, 2001. **19**(1): p. 683-765.
126. Couper, K.N., D.G. Blount, and E.M. Riley, *IL-10: the master regulator of immunity to infection.* The Journal of Immunology, 2008. **180**(9): p. 5771-5777.
127. Iyer, S.S. and G. Cheng, *Role of interleukin 10 transcriptional regulation in inflammation and autoimmune disease.* Critical Reviews™ in Immunology, 2012. **32**(1).
128. Barnes, P., et al., *Cytokine production at the site of disease in human tuberculosis.* Infection and immunity, 1993. **61**(8): p. 3482-3489.
129. Almeida, A.S., et al., *Tuberculosis is associated with a down-modulatory lung immune response that impairs Th1-type immunity.* The Journal of Immunology, 2009. **183**(1): p. 718-731.
130. Bonecini-Almeida, M.G., et al., *Down-modulation of lung immune responses by interleukin-10 and transforming growth factor β (TGF-β) and analysis of TGF-β receptors I and II in active tuberculosis.* Infection and immunity, 2004. **72**(5): p. 2628-2634.
131. Verbon, A., et al., *Serum concentrations of cytokines in patients with active tuberculosis (TB) and after treatment.* Clinical and experimental immunology, 1999. **115**(1): p. 110.
132. Redford, P.S., et al., *Enhanced protection to Mycobacterium tuberculosis infection in IL-10-deficient mice is accompanied by early and enhanced Th1 responses in the lung.* European journal of immunology, 2010. **40**(8): p. 2200-2210.
133. Pitt, J.M., et al., *Blockade of IL-10 signaling during BCG vaccination enhances and sustains Th1, Th17, and innate lymphoid IFN-γ and IL-17 responses and increases protection to Mycobacterium tuberculosis infection.* Journal of immunology (Baltimore, Md.: 1950), 2012. **189**(8): p. 4079.
134. Beamer, G.L., et al., *Interleukin-10 promotes Mycobacterium tuberculosis disease progression in CBA/J mice.* The Journal of Immunology, 2008. **181**(8): p. 5545-5550.
135. Moreira-Teixeira, L., et al., *T Cell–Derived IL-10 Impairs Host Resistance to Mycobacterium tuberculosis Infection.* The Journal of Immunology, 2017. **199**(2): p. 613-623.
136. Cyktor, J.C., et al., *IL-10 inhibits mature fibrotic granuloma formation during Mycobacterium tuberculosis infection.* The Journal of Immunology, 2013. **190**(6): p. 2778-2790.
137. Turner, J., et al., *In vivo IL-10 production reactivates chronic pulmonary tuberculosis in C57BL/6 mice.* The Journal of Immunology, 2002. **169**(11): p. 6343-6351.

138. Schreiber, T., et al., *Autocrine IL-10 induces hallmarks of alternative activation in macrophages and suppresses antituberculosis effector mechanisms without compromising T cell immunity*. The Journal of Immunology, 2009. **183**(2): p. 1301-1312.
139. Higgins, D.M., et al., *Lack of IL-10 alters inflammatory and immune responses during pulmonary< i> Mycobacterium tuberculosis</i> infection.* Tuberculosis, 2009. **89**(2): p. 149-157.
140. Jung, Y.J., et al., *Increased interleukin-10 expression is not responsible for failure of T helper 1 immunity to resolve airborne Mycobacterium tuberculosis infection in mice.* Immunology, 2003. **109**(2): p. 295-299.
141. North, R., *Mice incapable of making IL-4 or IL-10 display normal resistance to infection with Mycobacterium tuberculosis.* Clinical & Experimental Immunology, 1998. **113**(1): p. 55-58.
142. Roach, D., et al., *Endogenous Inhibition of Antimycobacterial Immunity by IL-10 Varies between Mycobacterial Species.* Scandinavian journal of immunology, 2001. **54**(1-2): p. 163-170.
143. Zajac, A.J., et al., *Viral immune evasion due to persistence of activated T cells without effector function.* Journal of Experimental Medicine, 1998. **188**(12): p. 2205-2213.
144. Jiang, Y., Y. Li, and B. Zhu, *T-cell exhaustion in the tumor microenvironment.* Cell death & disease, 2015. **6**(6): p. e1792.
145. Boni, C., et al., *Characterization of hepatitis B virus (HBV)-specific T-cell dysfunction in chronic HBV infection.* Journal of virology, 2007. **81**(8): p. 4215-4225.
146. Urbani, S., et al., *PD-1 expression in acute hepatitis C virus (HCV) infection is associated with HCV-specific CD8 exhaustion.* Journal of virology, 2006. **80**(22): p. 11398-11403.
147. D'Souza, M., et al., *Programmed death 1 expression on HIV-specific CD4+ T cells is driven by viral replication and associated with T cell dysfunction.* The Journal of Immunology, 2007. **179**(3): p. 1979-1987.
148. Day, C.L., et al., *PD-1 expression on HIV-specific T cells is associated with T-cell exhaustion and disease progression.* Nature, 2006. **443**(7109): p. 350.
149. Wherry, E.J., *T cell exhaustion.* Nature immunology, 2011. **12**(6): p. 492-499.
150. Buggert, M., et al., *CD4+ T cells with an activated and exhausted phenotype distinguish immunodeficiency during aviremic HIV-2 infection.* AIDS (London, England), 2016. **30**(16): p. 2415.
151. Crawford, A., et al., *Molecular and transcriptional basis of CD4+ T cell dysfunction during chronic infection.* Immunity, 2014. **40**(2): p. 289-302.
152. Wherry, E.J., et al., *Molecular signature of CD8+ T cell exhaustion during chronic viral infection.* Immunity, 2007. **27**(4): p. 670-684.
153. Pardoll, D.M., *The blockade of immune checkpoints in cancer immunotherapy.* Nature Reviews Cancer, 2012. **12**(4): p. 252-264.
154. Ngiow, S.F., et al., *Anti-TIM3 antibody promotes T cell IFN-γ–mediated antitumor immunity and suppresses established tumors.* Cancer research, 2011. **71**(10): p. 3540-3551.
155. Velu, V., et al., *Enhancing SIV-specific immunity in vivo by PD-1 blockade.* Nature, 2009. **458**(7235): p. 206-210.
156. Barber, D.L., et al., *Restoring function in exhausted CD8 T cells during chronic viral infection.* nature, 2006. **439**(7077): p. 682-687.

157. Trautmann, L., et al., *Upregulation of PD-1 expression on HIV-specific CD8+ T cells leads to reversible immune dysfunction.* Nature medicine, 2006. **12**(10): p. 1198.
158. Pardoll, D.M., *The blockade of immune checkpoints in cancer immunotherapy.* Nature reviews. Cancer, 2012. **12**(4): p. 252.
159. Singh, A., et al., *Inhibiting PD-1 Pathway rescues M. tuberculosis specific IFN-g producing T cells from apoptosis in tuberculosis patients.* Journal of Infectious Diseases, 2013. **208**(4): p. 603-15.
160. Shen, L., et al., *PD-1/PD-L pathway inhibits M.tb-specific CD4(+) T-cell functions and phagocytosis of macrophages in active tuberculosis.* Scientific Reports, 2016. **6**: p. 38362.
161. Jurado, J.O., et al., *Programmed death (PD)-1: PD-ligand 1/PD-ligand 2 pathway inhibits T cell effector functions during human tuberculosis.* The Journal of Immunology, 2008. **181**(1): p. 116-125.
162. Einarsdottir, T., E. Lockhart, and J.L. Flynn, *Cytotoxicity and secretion of gamma interferon are carried out by distinct CD8 T cells during Mycobacterium tuberculosis infection.* Infection and immunity, 2009. **77**(10): p. 4621-4630.
163. McNab, F.W., et al., *Programmed death ligand 1 is over-expressed by neutrophils in the blood of patients with active tuberculosis.* European journal of immunology, 2011. **41**(7): p. 1941-1947.
164. Schreiber, H.A., et al., *Dendritic cells in chronic mycobacterial granulomas restrict local anti-bacterial T cell response in a murine model.* PloS one, 2010. **5**(7): p. e11453.
165. Thye, T., et al., *CTLA4 autoimmunity-associated genotype contributes to severe pulmonary tuberculosis in an african population.* PloS one, 2009. **4**(7): p. e6307.
166. Wang, C., et al., *Association of CTLA4 Gene Polymorphisms with Susceptibility and Pathology Correlation to Pulmonary Tuberculosis in Southern Han Chinese.* International Journal of Biological Sciences, 2012. **8**(7): p. 945-952.
167. Kirman, J., et al., *CTLA-4 blockade enhances the immune response induced by mycobacterial infection but does not lead to increased protection.* Infection and immunity, 1999. **67**(8): p. 3786-3792.
168. Phillips, B.L., et al., *LAG3 expression in active Mycobacterium tuberculosis infections.* The American journal of pathology, 2015. **185**(3): p. 820-833.
169. Reiley, W.W., et al., *Distinct functions of antigen-specific CD4 T cells during murine Mycobacterium tuberculosis infection.* Proceedings of the National Academy of Sciences, 2010. **107**(45): p. 19408-19413.
170. Sakai, S., et al., *CD4 T cell-derived IFN-γ plays a minimal role in control of pulmonary Mycobacterium tuberculosis infection and must be actively repressed by PD-1 to prevent lethal disease.* PLoS pathogens, 2016. **12**(5): p. e1005667.
171. Barber, D.L., et al., *CD4 T cells promote rather than control tuberculosis in the absence of PD-1–mediated inhibition.* The Journal of Immunology, 2011. **186**(3): p. 1598-1607.
172. Lázár-Molnár, E., et al., *Programmed death-1 (PD-1)–deficient mice are extraordinarily sensitive to tuberculosis.* Proceedings of the National Academy of Sciences, 2010. **107**(30): p. 13402-13407.
173. Tousif, S., et al., *T cells from Programmed Death-1 deficient mice respond poorly to Mycobacterium tuberculosis infection.* PloS one, 2011. **6**(5): p. e19864.
174. Larbi, A. and T. Fulop, *From "truly naïve" to "exhausted senescent" T cells: when markers predict functionality.* Cytometry Part A, 2014. **85**(1): p. 25-35.

175. Yi, J.S., M.A. Cox, and A.J. Zajac, *T-cell exhaustion: characteristics, causes and conversion.* Immunology, 2010. **129**(4): p. 474-481.
176. Hong, J.J., et al., *Re-evaluation of PD-1 expression by T cells as a marker for immune exhaustion during SIV infection.* PloS one, 2013. **8**(3): p. e60186.
177. Hokey, D.A., et al., *Activation drives PD-1 expression during vaccine-specific proliferation and following lentiviral infection in macaques.* European journal of immunology, 2008. **38**(5): p. 1435-1445.
178. Blackburn, S.D., et al., *Coregulation of CD8+ T cell exhaustion by multiple inhibitory receptors during chronic viral infection.* Nature immunology, 2009. **10**(1): p. 29-37.
179. Kauffman, K., et al., *Defective positioning in granulomas but not lung-homing limits CD4 T-cell interactions with Mycobacterium tuberculosis-infected macrophages in rhesus macaques.* Mucosal immunology, 2017.
180. Jayaraman, P., et al., *TIM3 mediates T cell exhaustion during Mycobacterium tuberculosis infection.* PLoS Pathog, 2016. **12**(3): p. e1005490.
181. Daniel, T., *Leon Charles Albert Calmette and BCG vaccine [Founders of Our Knowledge]*. The international journal of tuberculosis and lung disease, 2005. **9**(9): p. 944-945.
182. Sakula, A., *BCG: who were Calmette and Guérin?* Thorax, 1983. **38**(11): p. 806.
183. Greenwood, M., *Professor Calmette's statistical study of BCG vaccination.* British Medical Journal, 1928. **1**(3514): p. 793.
184. Comstock, G.W., *The International Tuberculosis Campaign: a pioneering venture in mass vaccination and research.* Clinical infectious diseases, 1994. **19**(3): p. 528-540.
185. *B.C.G. Vaccination in the U.S.A.* British Medical Journal, 1957. **2**(5051): p. 989-990.
186. Anderson, A.S., et al., *The case against BCG.* British Medical Journal, 1959. **1**(5135): p. 1423.
187. Rodrigues, L.C., V.K. Diwan, and J.G. Wheeler, *Protective effect of BCG against tuberculous meningitis and miliary tuberculosis: a meta-analysis.* International journal of epidemiology, 1993. **22**(6): p. 1154-1158.
188. Mangtani, P., et al., *Protection by BCG vaccine against tuberculosis: a systematic review of randomized controlled trials.* Clinical infectious diseases, 2013. **58**(4): p. 470-480.
189. Roy, A., et al., *Effect of BCG vaccination against Mycobacterium tuberculosis infection in children: systematic review and meta-analysis.* Bmj, 2014. **349**: p. g4643.
190. Colditz, G.A., et al., *Efficacy of BCG vaccine in the prevention of tuberculosis: meta-analysis of the published literature.* Jama, 1994. **271**(9): p. 698-702.
191. Fine, P.E., *The BCG story: lessons from the past and implications for the future.* Reviews of infectious diseases, 1989. **11**(Supplement_2): p. S353-S359.
192. Tuberculosis Prevention Trial, M., *Trial of BCG vaccines in South India for tuberculosis prevention.* Indian journal of medical research, 1980. **72**(Jul): p. 1-74.
193. Hart, P.D.A. and I. Sutherland, *BCG and vole bacillus vaccines in the prevention of tuberculosis in adolescence and early adult life.* Br Med J, 1977. **2**(6082): p. 293-295.
194. Fine, P.E., *Variation in protection by BCG: implications of and for heterologous immunity.* The Lancet, 1995. **346**(8986): p. 1339-1345.
195. Brosch, R., et al., *Genome plasticity of BCG and impact on vaccine efficacy.* Proceedings of the National Academy of Sciences, 2007. **104**(13): p. 5596-5601.
196. Roth, A., et al., *Bacillus Calmette-Guerin vaccination and infant mortality.* Expert review of vaccines, 2006. **5**(2): p. 277-293.

197. Behr, M., et al., *Comparative genomics of BCG vaccines by whole-genome DNA microarray.* Science, 1999. **284**(5419): p. 1520-1523.
198. Copin, R., et al., *Impact of in vitro evolution on antigenic diversity of Mycobacterium bovis bacillus Calmette-Guerin (BCG).* Vaccine, 2014. **32**(45): p. 5998-6004.
199. Murray, R.A., et al., *Bacillus Calmette Guerin vaccination of human newborns induces a specific, functional CD8+ T cell response.* The Journal of Immunology, 2006. **177**(8): p. 5647-5651.
200. Soares, A.P., et al., *Bacillus Calmette-Guerin vaccination of human newborns induces T cells with complex cytokine and phenotypic profiles.* The Journal of Immunology, 2008. **180**(5): p. 3569-3577.
201. Marchant, A., et al., *Newborns develop a Th1-type immune response to Mycobacterium bovis bacillus Calmette-Guerin vaccination.* The Journal of Immunology, 1999. **163**(4): p. 2249-2255.
202. Soares, A.P., et al., *Longitudinal changes in CD4+ T-cell memory responses induced by BCG vaccination of newborns.* The Journal of infectious diseases, 2013. **207**(7): p. 1084-1094.
203. Lindenstrøm, T., et al., *Control of chronic Mycobacterium tuberculosis infection by CD4 KLRG1− IL-2–secreting central memory cells.* The Journal of Immunology, 2013. **190**(12): p. 6311-6319.
204. Fletcher, H.A., et al., *Human newborn bacille Calmette–Guérin vaccination and risk of tuberculosis disease: a case-control study.* BMC medicine, 2016. **14**(1): p. 76.
205. Kagina, B.M., et al., *Specific T cell frequency and cytokine expression profile do not correlate with protection against tuberculosis after bacillus Calmette-Guerin vaccination of newborns.* American journal of respiratory and critical care medicine, 2010. **182**(8): p. 1073-1079.
206. Rodrigues, L.C., et al., *Effect of BCG revaccination on incidence of tuberculosis in school-aged children in Brazil: the BCG-REVAC cluster-randomised trial.* The Lancet, 2005. **366**(9493): p. 1290-1295.
207. Barreto, M.L., et al., *Evidence of an effect of BCG revaccination on incidence of tuberculosis in school-aged children in Brazil: second report of the BCG-REVAC cluster-randomised trial.* Vaccine, 2011. **29**(31): p. 4875-4877.
208. Barreto, M.L., et al., *Causes of variation in BCG vaccine efficacy: examining evidence from the BCG REVAC cluster randomized trial to explore the masking and the blocking hypotheses.* Vaccine, 2014. **32**(30): p. 3759-3764.
209. Kaufmann, S.H., G. Hussey, and P.-H. Lambert, *New vaccines for tuberculosis.* The Lancet, 2010. **375**(9731): p. 2110-2119.
210. Kaufmann, S.H., J. Weiner, and C.F. von Reyn, *Novel approaches to tuberculosis vaccine development.* International Journal of Infectious Diseases, 2017. **56**: p. 263-267.
211. Marinova, D., et al., *MTBVAC from discovery to clinical trials in tuberculosis-endemic countries.* Expert review of vaccines, 2017. **16**(6): p. 565-576.
212. Nieuwenhuizen, N.E., et al., *The Recombinant Bacille Calmette–Guérin Vaccine VPM1002: Ready for Clinical Efficacy Testing.* Frontiers in immunology, 2017. **8**: p. 1147.
213. Vilaplana, C., et al., *Double-blind, randomized, placebo-controlled Phase I Clinical Trial of the therapeutical antituberculous vaccine RUTI®.* Vaccine, 2010. **28**(4): p. 1106-1116.

214. Abou-Zeid, C., et al., *Induction of a type 1 immune response to a recombinant antigen from Mycobacterium tuberculosis expressed in Mycobacterium vaccae.* Infection and immunity, 1997. **65**(5): p. 1856-1862.
215. Lahey, T., et al., *Immunogenicity and protective efficacy of the DAR-901 booster vaccine in a murine model of tuberculosis.* PloS one, 2016. **11**(12): p. e0168521.
216. McShane, H., et al., *Protective immunity against Mycobacterium tuberculosis induced by dendritic cells pulsed with both CD8+-and CD4+-T-cell epitopes from antigen 85A.* Infection and immunity, 2002. **70**(3): p. 1623-1626.
217. Tameris, M.D., et al., *Safety and efficacy of MVA85A, a new tuberculosis vaccine, in infants previously vaccinated with BCG: a randomised, placebo-controlled phase 2b trial.* The Lancet, 2013. **381**(9871): p. 1021-1028.
218. Bertholet, S., et al., *A defined tuberculosis vaccine candidate boosts BCG and protects against multidrug-resistant Mycobacterium tuberculosis.* Science translational medicine, 2010. **2**(53): p. 53ra74-53ra74.
219. Leroux-Roels, I., et al., *Improved CD4+ T cell responses to Mycobacterium tuberculosis in PPD-negative adults by M72/AS01 as compared to the M72/AS02 and Mtb72F/AS02 tuberculosis candidate vaccine formulations: a randomized trial.* Vaccine, 2013. **31**(17): p. 2196-2206.
220. Schellack, C., et al., *IC31, a novel adjuvant signaling via TLR9, induces potent cellular and humoral immune responses.* Vaccine, 2006. **24**(26): p. 5461-5472.
221. Aagaard, C., et al., *A multistage tuberculosis vaccine that confers efficient protection before and after exposure.* Nature medicine, 2011. **17**(2): p. 189-194.
222. Lin, P.L., et al., *The multistage vaccine H56 boosts the effects of BCG to protect cynomolgus macaques against active tuberculosis and reactivation of latent< i> Mycobacterium tuberculosis</i> infection.* The Journal of clinical investigation, 2012. **122**(122 (1)): p. 303-314.
223. Dietrich, J., et al., *Exchanging ESAT6 with TB10. 4 in an Ag85B fusion molecule-based tuberculosis subunit vaccine: efficient protection and ESAT6-based sensitive monitoring of vaccine efficacy.* The Journal of Immunology, 2005. **174**(10): p. 6332-6339.
224. Lozes, E., et al., *Immunogenicity and efficacy of a tuberculosis DNA vaccine encoding the components of the secreted antigen 85 complex.* Vaccine, 1997. **15**(8): p. 830-833.
225. Mustafa, A.S., et al., *Identification and HLA Restriction of Naturally Derived Th1-Cell Epitopes from the Secreted Mycobacterium tuberculosisAntigen 85B Recognized by Antigen-Specific Human CD4+ T-Cell Lines.* Infection and immunity, 2000. **68**(7): p. 3933-3940.
226. Skjøt, R.L.V., et al., *Epitope mapping of the immunodominant antigen TB10. 4 and the two homologous proteins TB10. 3 and TB12. 9, which constitute a subfamily of the esat-6 gene family.* Infection and immunity, 2002. **70**(10): p. 5446-5453.
227. Houghton, J., et al., *A small RNA encoded in the Rv2660c locus of Mycobacterium tuberculosis is induced during starvation and infection.* PloS one, 2013. **8**(12): p. e80047.
228. Harboe, M., et al., *Evidence for occurrence of the ESAT-6 protein in Mycobacterium tuberculosis and virulent Mycobacterium bovis and for its absence in Mycobacterium bovis BCG.* Infection and immunity, 1996. **64**(1): p. 16-22.
229. Luabeya, A.K., et al., *First-in-human trial of the post-exposure tuberculosis vaccine H56:IC31 in Mycobacterium tuberculosis infected and non-infected healthy adults.* Vaccine, 2015. **33**(33): p. 4130-40.

230. Billeskov, R., et al., *Testing the H56 vaccine delivered in 4 different adjuvants as a BCG-booster in a non-human primate model of tuberculosis.* PloS one, 2016. **11**(8): p. e0161217.
231. Bold, T.D., et al., *Suboptimal activation of antigen-specific CD4+ effector cells enables persistence of M. tuberculosis in vivo.* PLoS pathogens, 2011. **7**(5): p. e1002063.
232. Brodin, P., et al., *Dissection of ESAT-6 system 1 of Mycobacterium tuberculosis and impact on immunogenicity and virulence.* Infection and immunity, 2006. **74**(1): p. 88-98.
233. Chen, J.M., et al., *EspD is critical for the virulence-mediating ESX-1 secretion system in Mycobacterium tuberculosis.* Journal of bacteriology, 2012. **194**(4): p. 884-893.
234. Fortune, S., et al., *Mutually dependent secretion of proteins required for mycobacterial virulence.* Proceedings of the National Academy of Sciences of the United States of America, 2005. **102**(30): p. 10676-10681.
235. MacGurn, J.A., et al., *A non-RD1 gene cluster is required for Snm secretion in Mycobacterium tuberculosis.* Molecular microbiology, 2005. **57**(6): p. 1653-1663.
236. Millington, K.A., et al., *Rv3615c is a highly immunodominant RD1 (Region of Difference 1)-dependent secreted antigen specific for Mycobacterium tuberculosis infection.* Proceedings of the National Academy of Sciences, 2011. **108**(14): p. 5730-5735.
237. Pym, A.S., et al., *Recombinant BCG exporting ESAT-6 confers enhanced protection against tuberculosis.* Nature medicine, 2003. **9**(5): p. 533.
238. Raghavan, S., et al., *Secreted transcription factor controls Mycobacterium tuberculosis virulence.* Nature, 2008. **454**(7205): p. 717.
239. Garces, A., et al., *EspA acts as a critical mediator of ESX1-dependent virulence in Mycobacterium tuberculosis by affecting bacterial cell wall integrity.* PLoS pathogens, 2010. **6**(6): p. e1000957.
240. McLaughlin, B., et al., *A mycobacterium ESX-1–secreted virulence factor with unique requirements for export.* PLoS pathogens, 2007. **3**(8): p. e105.
241. Xu, J., et al., *A unique Mycobacterium ESX-1 protein co-secretes with CFP-10/ESAT-6 and is necessary for inhibiting phagosome maturation.* Molecular microbiology, 2007. **66**(3): p. 787-800.
242. Christensen, D., et al., *Liposome-based cationic adjuvant formulations (CAF): past, present, and future.* Journal of liposome research, 2009. **19**(1): p. 2-11.
243. Commandeur, S., et al., *The in vivo expressed Mycobacterium tuberculosis (IVE-TB) antigen Rv2034 induces CD4(+) T-cells that protect against pulmonary infection in HLA-DR transgenic mice and guinea pigs.* Vaccine, 2014. **32**(29): p. 3580-8.
244. Korsholm, K.S., et al., *Induction of CD8+ T-cell responses against subunit antigens by the novel cationic liposomal CAF09 adjuvant.* Vaccine, 2014. **32**(31): p. 3927-35.
245. Agger, E.M., et al., *Cationic liposomes formulated with synthetic mycobacterial cordfactor (CAF01): a versatile adjuvant for vaccines with different immunological requirements.* PloS one, 2008. **3**(9): p. e3116.
246. Lindenstrøm, T., et al., *T Cells Primed by Live Mycobacteria Versus a Tuberculosis Subunit Vaccine Exhibit Distinct Functional Properties.* EBioMedicine, 2018. **27**: p. 27-39.
247. van Dissel, J.T., et al., *A novel liposomal adjuvant system, CAF01, promotes long-lived Mycobacterium tuberculosis-specific T-cell responses in human.* Vaccine, 2014. **32**(52): p. 7098-7107.

248. Woodworth, J.S., et al., *Subunit vaccine H56/CAF01 induces a population of circulating CD4 T cells that traffic into the Mycobacterium tuberculosis-infected lung.* Mucosal immunology, 2017. **10**(2): p. 555.
249. Moliva, J.I., J. Turner, and J.B. Torrelles, *Prospects in Mycobacterium bovis Bacille Calmette et Guerin (BCG) vaccine diversity and delivery: why does BCG fail to protect against tuberculosis?* Vaccine, 2015. **33**(39): p. 5035-5041.
250. Lagranderie, M., et al., *BCG-induced protection in guinea pigs vaccinated and challenged via the respiratory route.* Tubercle and Lung disease, 1993. **74**(1): p. 38-46.
251. Mittrücker, H.-W., et al., *Poor correlation between BCG vaccination-induced T cell responses and protection against tuberculosis.* Proceedings of the National Academy of Sciences, 2007. **104**(30): p. 12434-12439.
252. Barclay, W., et al., *Aerosol-induced tuberculosis in subhuman primates and the course of the disease after intravenous BCG vaccination.* Infection and immunity, 1970. **2**(5): p. 574-582.
253. Barclay, W.R., et al., *Protection of monkeys against airborne tuberculosis by aerosol vaccination with bacillus Calmette-Guerin.* American review of respiratory disease, 1973. **107**(3): p. 351-358.
254. Sharpe, S., et al., *Alternative BCG delivery strategies improve protection against Mycobacterium tuberculosis in non-human primates: protection associated with mycobacterial antigen-specific CD4 effector memory T-cell populations.* Tuberculosis, 2016. **101**: p. 174-190.
255. Santosuosso, M., et al., *Intranasal boosting with an adenovirus-vectored vaccine markedly enhances protection by parenteral Mycobacterium bovis BCG immunization against pulmonary tuberculosis.* Infection and immunity, 2006. **74**(8): p. 4634-4643.
256. White, A., et al., *Evaluation of the safety and immunogenicity of a candidate tuberculosis vaccine, MVA85A, delivered by aerosol to the lungs of macaques.* Clinical and Vaccine Immunology, 2013. **20**(5): p. 663-672.
257. Goonetilleke, N.P., et al., *Enhanced immunogenicity and protective efficacy against Mycobacterium tuberculosis of bacille Calmette-Guerin vaccine using mucosal administration and boosting with a recombinant modified vaccinia virus Ankara.* The Journal of Immunology, 2003. **171**(3): p. 1602-1609.
258. White, A., et al., *Evaluation of the immunogenicity of Mycobacterium bovis BCG delivered by aerosol to the lungs of macaques.* Clinical and Vaccine Immunology, 2015. **22**(9): p. 992-1003.
259. Derrick, S.C., et al., *Intranasal administration of Mycobacterium bovis BCG induces superior protection against aerosol infection with Mycobacterium tuberculosis in mice.* Clinical and Vaccine Immunology, 2014. **21**(10): p. 1443-1451.
260. Giri, P.K., et al., *Comparative evaluation of intranasal and subcutaneous route of immunization for development of mucosal vaccine against experimental tuberculosis.* FEMS Immunology & Medical Microbiology, 2005. **45**(1): p. 87-93.
261. Garcia-Contreras, L., et al., *Immunization by a bacterial aerosol.* Proceedings of the National Academy of Sciences, 2008. **105**(12): p. 4656-4660.
262. Belyakov, I.M. and J.D. Ahlers, *What role does the route of immunization play in the generation of protective immunity against mucosal pathogens?* The Journal of Immunology, 2009. **183**(11): p. 6883-6892.

263. Manjaly Thomas, Z.-R. and H. McShane, *Aerosol immunisation for TB: matching route of vaccination to route of infection.* Transactions of The Royal Society of Tropical Medicine and Hygiene, 2015. **109**(3): p. 175-181.
264. Dietrich, J., et al., *Synergistic effect of bacillus calmette guerin and a tuberculosis subunit vaccine in cationic liposomes: increased immunogenicity and protection.* The Journal of Immunology, 2007. **178**(6): p. 3721-3730.
265. McMurray, D.N., *A nonhuman primate model for preclinical testing of new tuberculosis vaccines.* Clinical infectious diseases, 2000. **30**(Supplement_3): p. S210-S212.
266. Gupta, U. and V. Katoch, *Animal models of tuberculosis.* Tuberculosis, 2005. **85**(5): p. 277-293.
267. Capuano, S.V., et al., *Experimental Mycobacterium tuberculosis infection of cynomolgus macaques closely resembles the various manifestations of human M. tuberculosis infection.* Infection and immunity, 2003. **71**(10): p. 5831-5844.
268. Mattila, J.T., et al., *Microenvironments in tuberculous granulomas are delineated by distinct populations of macrophage subsets and expression of nitric oxide synthase and arginase isoforms.* The Journal of Immunology, 2013. **191**(2): p. 773-784.
269. Lin, P.L., et al., *Radiologic responses in cynomolgus macaques for assessing tuberculosis chemotherapy regimens.* Antimicrobial agents and chemotherapy, 2013. **57**(9): p. 4237-4244.
270. Coleman, M.T., et al., *Early Changes by (18)Fluorodeoxyglucose Positron Emission Tomography Coregistered with Computed Tomography Predict Outcome after Mycobacterium tuberculosis Infection in Cynomolgus Macaques.* Infection and Immunity, 2014. **82**(6): p. 2400-2404.
271. Dannenberg Jr, A.M., *Immune mechanisms in the pathogenesis of pulmonary tuberculosis.* Reviews of infectious diseases, 1989. **11**(Supplement_2): p. S369-S378.
272. Flynn, J.L. and J.D. Ernst, *Immune responses in tuberculosis.* Current opinion in immunology, 2000. **12**(4): p. 432-436.
273. Quesniaux, V.F., et al., *TNF in host resistance to tuberculosis infection*, in *TNF Pathophysiology*. 2010, Karger Publishers. p. 157-179.
274. Gerosa, F., et al., *CD4+ T cell clones producing both interferon-γ and interleukin-10 predominate in bronchoalveolar lavages of active pulmonary tuberculosis patients.* Clinical Immunology, 1999. **92**(3): p. 224-234.
275. Cilfone, N.A., et al., *Computational modeling predicts IL-10 control of lesion sterilization by balancing early host immunity–mediated antimicrobial responses with caseation during Mycobacterium tuberculosis infection.* The Journal of Immunology, 2015. **194**(2): p. 664-677.
276. Keubler, L.M., et al., *A Multihit Model: Colitis Lessons from the Interleukin-10–deficient Mouse.* Inflammatory bowel diseases, 2015. **21**(8): p. 1967.
277. Correa, I., et al., *Defective IL-10 production in severe phenotypes of Crohn's disease.* Journal of leukocyte biology, 2009. **85**(5): p. 896-903.
278. Ouyang, W., et al., *Regulation and functions of the IL-10 family of cytokines in inflammation and disease.* Annual review of immunology, 2011. **29**: p. 71-109.
279. Richardson, E.T., et al., *Toll-like receptor 2-dependent extracellular signal-regulated kinase signaling in Mycobacterium tuberculosis-infected macrophages drives anti-inflammatory responses and inhibits Th1 polarization of responding T cells.* Infection and immunity, 2015. **83**(6): p. 2242-2254.

280. Ejrnaes, M., et al., *Resolution of a chronic viral infection after interleukin-10 receptor blockade.* The Journal of Experimental Medicine, 2006. **203**(11): p. 2461-2472.
281. Tian, Y., et al., *IL-10 Regulates Memory T Cell Development and the Balance between Th1 and Follicular Th Cell Responses during an Acute Viral Infection.* The Journal of Immunology, 2016. **197**(4): p. 1308-1321.
282. Biswas, P.S., et al., *Pathogen-specific CD8 T cell responses are directly inhibited by IL-10.* J Immunol, 2007. **179**(7): p. 4520-8.
283. Brockman, M.A., et al., *IL-10 is up-regulated in multiple cell types during viremic HIV infection and reversibly inhibits virus-specific T cells.* Blood, 2009. **114**(2): p. 346-56.
284. Ruffell, B., et al., *Macrophage IL-10 Blocks CD8+ T Cell-Dependent Responses to Chemotherapy by Suppressing IL-12 Expression in Intratumoral Dendritic Cells.* Cancer Cell, 2014. **26**(5): p. 623-637.
285. Warsinske, H.C., et al., *Deletion of TGF-beta1 Increases Bacterial Clearance by Cytotoxic T Cells in a Tuberculosis Granuloma Model.* Front Immunol, 2017. **8**: p. 1843.
286. Lin, P.L., et al., *Metronidazole prevents reactivation of latent Mycobacterium tuberculosis infection in macaques.* Proceedings of the National Academy of Sciences, 2012. **109**(35): p. 14188-14193.
287. DiFazio, R.M., et al., *Active transforming growth factor-β is associated with phenotypic changes in granulomas after drug treatment in pulmonary tuberculosis.* Fibrogenesis & tissue repair, 2016. **9**(1): p. 6.
288. Cyktor, J.C., et al., *Clonal expansions of CD8+ T cells with IL-10 secreting capacity occur during chronic Mycobacterium tuberculosis infection.* PloS one, 2013. **8**(3): p. e58612.
289. Dahl, K.E., et al., *Selective induction of transforming growth factor beta in human monocytes by lipoarabinomannan of Mycobacterium tuberculosis.* Infection and immunity, 1996. **64**(2): p. 399-405.
290. Nandi, B. and S.M. Behar, *Regulation of neutrophils by interferon-γ limits lung inflammation during tuberculosis infection.* Journal of Experimental Medicine, 2011: p. jem. 20110919.
291. Lin, P.L., et al., *Early events in Mycobacterium tuberculosis infection in cynomolgus macaques.* Infection and immunity, 2006. **74**(7): p. 3790-3803.
292. Lin, P.L.e.a., *Radiologic Responses in Cynomolgus Macaques for Assessing Tuberculosis Chemotherapy Regimens.* Antimicrob Agents and Chemotherapy, 2013. **57**(9): p. 8.
293. Ehlers, S. and U.E. Schaible, *The granuloma in tuberculosis: dynamics of a host–pathogen collusion.* Frontiers in immunology, 2013. **3**: p. 411.
294. Russell, D.G., *Who puts the tubercle in tuberculosis?* Nature Reviews Microbiology, 2007. **5**(1): p. 39-47.
295. Flynn, J., J. Chan, and P. Lin, *Macrophages and control of granulomatous inflammation in tuberculosis.* Mucosal immunology, 2011. **4**(3): p. 271.
296. Flynn, J.L.a.K., Edwin, *Pulmonary Tuberculosis in Monkeys*, in *A Color Atlas of Comparative Pathology of Pulmonary Tuberculosis*, F.J. Leong, Dartois, Veronique, Dick, Thomas, Editor. 2011, CRC Press: Boca Raton, FL. p. 83-105.
297. Triebel, F., et al., *LAG-3, a novel lymphocyte activation gene closely related to CD4.* Journal of Experimental Medicine, 1990. **171**(5): p. 1393-1405.
298. Kisielow, M., et al., *Expression of lymphocyte activation gene 3 (LAG-3) on B cells is induced by T cells.* European journal of immunology, 2005. **35**(7): p. 2081-2088.

299. Workman, C.J., et al., *LAG-3 regulates plasmacytoid dendritic cell homeostasis.* The Journal of Immunology, 2009. **182**(4): p. 1885-1891.
300. Becker, M., et al., *Integrated transcriptomics establish macrophage polarization signatures and have potential applications for clinical health and disease.* Scientific reports, 2015. **5**.
301. Wherry, E.J., et al., *Viral persistence alters CD8 T-cell immunodominance and tissue distribution and results in distinct stages of functional impairment.* Journal of virology, 2003. **77**(8): p. 4911-4927.
302. Segovia-Juarez, J.L., S. Ganguli, and D. Kirschner, *Identifying control mechanisms of granuloma formation during M. tuberculosis infection using an agent-based model.* Journal of theoretical biology, 2004. **231**(3): p. 357-376.
303. Ray, J.C.J., J.L. Flynn, and D.E. Kirschner, *Synergy between individual TNF-dependent functions determines granuloma performance for controlling Mycobacterium tuberculosis infection.* The Journal of Immunology, 2009. **182**(6): p. 3706-3717.
304. Fallahi-Sichani, M., et al., *Multiscale computational modeling reveals a critical role for TNF-α receptor 1 dynamics in tuberculosis granuloma formation.* The Journal of Immunology, 2011. **186**(6): p. 3472-3483.
305. Pienaar, E., et al., *A computational tool integrating host immunity with antibiotic dynamics to study tuberculosis treatment.* J Theor Biol, 2015. **367**: p. 166-79.
306. Marino, S., et al., *A methodology for performing global uncertainty and sensitivity analysis in systems biology.* Journal of theoretical biology, 2008. **254**(1): p. 178-196.
307. Maiello, P., et al., *Rhesus macaques are more susceptible to progressive tuberculosis than cynomolgus macaques: A quantitative comparison.* Infection and immunity, 2017: p. IAI. 00505-17.
308. Ray, J.C.J., et al., *The timing of TNF and IFN-γ signaling affects macrophage activation strategies during Mycobacterium tuberculosis infection.* Journal of theoretical biology, 2008. **252**(1): p. 24-38.
309. Cilfone, N.A., et al., *Multi-scale modeling predicts a balance of tumor necrosis factor-α and interleukin-10 controls the granuloma environment during Mycobacterium tuberculosis infection.* PloS one, 2013. **8**(7): p. e68680.
310. Fallahi-Sichani, M., D.E. Kirschner, and J.J. Linderman, *NF-κB signaling dynamics play a key role in infection control in tuberculosis.* Frontiers in physiology, 2012. **3**.
311. Fallahi-Sichani, M., et al., *Identification of key processes that control tumor necrosis factor availability in a tuberculosis granuloma.* PLoS computational biology, 2010. **6**(5): p. e1000778.
312. Fallahi-Sichani, M., et al., *Differential risk of tuberculosis reactivation among anti-TNF therapies is due to drug binding kinetics and permeability.* The Journal of Immunology, 2012. **188**(7): p. 3169-3178.
313. Marino, S., et al., *Differences in reactivation of tuberculosis induced from anti-TNF treatments are based on bioavailability in granulomatous tissue.* PLoS computational biology, 2007. **3**(10): p. e194.
314. Mirsky, H.P., et al., *Systems biology approaches for understanding cellular mechanisms of immunity in lymph nodes during infection.* Journal of theoretical biology, 2011. **287**: p. 160-170.

315. Riggs, T., et al., *A comparison of random vs. chemotaxis-driven contacts of T cells with dendritic cells during repertoire scanning.* Journal of theoretical biology, 2008. **250**(4): p. 732-751.
316. Castellino, F., et al., *Chemokines enhance immunity by guiding naive CD8+ T cells to sites of CD4+ T cell-dendritic cell interaction.* Nature, 2006. **440**(7086): p. 890.
317. Utzschneider, D.T., et al., *High antigen levels induce an exhausted phenotype in a chronic infection without impairing T cell expansion and survival.* Journal of Experimental Medicine, 2016: p. jem. 20150598.
318. Zuniga, E.I. and J.A. Harker, *T-cell exhaustion due to persistent antigen: Quantity not quality?* European journal of immunology, 2012. **42**(9): p. 2285-2289.
319. Bucks, C.M., et al., *Chronic antigen stimulation alone is sufficient to drive CD8+ T cell exhaustion.* The Journal of Immunology, 2009. **182**(11): p. 6697-6708.
320. Team, R.C., *R: A language and environment for statistical computing.* 2016, R Foundation for Statistical Computing: Vienna, Austria.
321. MATLAB. 2011b, The MathWorks, Inc.: Natick, Massachusetts, United States.
322. Tuberculosis Research Center, C., *Fifteen year follow up of trial of BCG vaccines in south India for tuberculosis prevention.* Indian J Med Res, 1999. **110**: p. 4.
323. Trunz, B.B., P.E.M. Fine, and C. Dye, *Effect of BCG vaccination on childhood tuberculous meningitis and miliary tuberculosis worldwide: a meta-analysis and assessment of cost-effectiveness.* The Lancet, 2006. **367**(9517): p. 1173-1180.
324. Roy, A., et al., *Effect of BCG vaccination against Mycobacterium tuberculosis infection in children: systematic review and meta-analysis.* 2014.
325. Lambert, P.H. and P.E. Laurent, *Intradermal vaccine delivery: will new delivery systems transform vaccine administration?* Vaccine, 2008. **26**(26): p. 3197-3208.
326. Aagaard, C., et al., *A multistage tuberculosis vaccine that confers efficient protection before and after exposure.* Nat Med, 2011. **17**(2): p. 189-94.
327. Lin, P.L., et al., *The multistage vaccine H56 boosts the effects of BCG to protect cynomolgus macaques against active tuberculosis and reactivation of latent Mycobacterium tuberculosis infection.* J Clin Invest, 2012. **122**(1): p. 303-14.
328. Gopal, R., et al., *Unexpected role for IL-17 in protective immunity against hypervirulent Mycobacterium tuberculosis HN878 infection.* PLoS Pathog, 2014. **10**(5): p. e1004099.
329. Coleman, M.T.C., Ray Y.; Lee, Myungsun; Lin, Philana Ling; Dodd, Lori E.; Maiello, Pauline; Via, Laura E.; Kim, Youngran; Marriner, Gwendolyn; Dartois, Veronique; Scanga, Charles; Janssen, Christopher; Wang, Jing; Klein, Edwin; Cho, Sang Nae; Barry III, Clifton E.; Flynn, JoAnne L., *PET/CT imaging reveals a therapeutic response to oxazolidinones in macaques and humans with tuberculosis.* Science Translational Medicine, 2014. **6**(265).
330. Lin, P.L., et al., *PET CT identifies reactivation risk in cynomolgus macaques with latent M. tuberculosis.* PLoS pathogens, 2016. **12**(7): p. e1005739.
331. Antonelli, L.R.R., Antonio Gigliotti; Gonclaves, Ricardo; Roffe, Ester; Cheever, Allen W., Bafica, Andre; Salazar, Andres M.; Feng, Carl G.; Sher, Alan, *Intranasal Poly-IC treatment exacerbates tuberculosis in mice through the pulmonary recruitment of a pathogen-permissive monocyte/macrophage population.* The Journal of Clinical Investigation, 2010. **120**(5): p. 9.
332. Sionov, E., et al., *Type I IFN Induction via Poly-ICLC Protects Mice against Cryptococcosis.* PLoS Pathog, 2015. **11**(8): p. e1005040.

333. Manca, C., et al., *Virulence of a Mycobacterium tuberculosis clinical isolate in mice is determined by failure to induce Th1 type immunity and is associated with induction of IFN-alpha /beta.* Proc Natl Acad Sci U S A, 2001. **98**(10): p. 5752-7.
334. Shin, H. and A. Iwasaki, *A vaccine strategy that protects against genital herpes by establishing local memory T cells.* Nature, 2012. **491**(7424): p. 463-7.
335. Bomsel, M., et al., *Immunization with HIV-1 gp41 subunit virosomes induces mucosal antibodies protecting nonhuman primates against vaginal SHIV challenges.* Immunity, 2011. **34**(2): p. 269-80.
336. Britton, G., et al., *Using a prime and pull approach, lentivector vaccines expressing Ag85A induce immunogenicity but fail to induce protection against Mycobacterium bovis bacillus Calmette-Guerin challenge in mice.* Immunology, 2015. **146**(2): p. 264-70.
337. Tregoning, J.S., et al., *A "prime-pull" vaccine strategy has a modest effect on local and systemic antibody responses to HIV gp140 in mice.* PLoS One, 2013. **8**(11): p. e80559.
338. Armijos, R., et al., *Safety, immunogenecity, and efficacy of an autoclaved Leishmania amazonensis vaccine plus BCG adjuvant against New World cutaneous leishmaniasis.* Vaccine, 2004. **22**(9-10): p. 1320-1326.
339. Eilber, F.R., C.M. Townsend, and D.L. Morton, *Results of BCG adjuvant immunotherapy for melanoma of the head and neck.* The American Journal of Surgery, 1976. **132**(4): p. 476-479.
340. BÖhle, A. and S. Brandau, *Immune mechanisms in bacillus Calmette-Guerin immunotherapy for superficial bladder cancer.* The Journal of urology, 2003. **170**(3): p. 964-969.
341. Hansen, S.G., et al., *Prevention of tuberculosis in rhesus macaques by a cytomegalovirus-based vaccine.* Nature medicine, 2018.
342. Yu, D.-S., et al., *The feasibility of BCG and sunitinib combination therapy for transitional cell carcinoma.* Urological Science, 2011. **22**(1): p. 19-27.
343. Davidsen, J., et al., *Characterization of cationic liposomes based on dimethyldioctadecylammonium and synthetic cord factor from M. tuberculosis (trehalose 6, 6'-dibehenate)—a novel adjuvant inducing both strong CMI and antibody responses.* Biochimica et Biophysica Acta (BBA)-Biomembranes, 2005. **1718**(1): p. 22-31.
344. Pawar, S.N., et al., *Comparison of the effects of pathogenic simian human immunodeficiency virus strains SHIV-89.6P and SHIV-KU2 in cynomolgus macaques.* AIDS Res Hum Retroviruses, 2008. **24**(4): p. 643-54.
345. Wilson, E.H., et al., *A critical role for IL-10 in limiting inflammation during toxoplasmic encephalitis.* Journal of neuroimmunology, 2005. **165**(1): p. 63-74.
346. Li, C., I. Corraliza, and J. Langhorne, *A defect in interleukin-10 leads to enhanced malarial disease in Plasmodium chabaudi chabaudi infection in mice.* Infection and immunity, 1999. **67**(9): p. 4435-4442.
347. Hunter, C.A., et al., *IL-10 is required to prevent immune hyperactivity during infection with Trypanosoma cruzi.* The Journal of Immunology, 1997. **158**(7): p. 3311-3316.
348. Asadullah, K., W. Sterry, and H. Volk, *Interleukin-10 therapy—review of a new approach.* Pharmacological reviews, 2003. **55**(2): p. 241-269.
349. Belkaid, Y., et al., *The role of interleukin (IL)-10 in the persistence of Leishmania major in the skin after healing and the therapeutic potential of anti–IL-10 receptor antibody for sterile cure.* Journal of Experimental Medicine, 2001. **194**(10): p. 1497-1506.

350. Llorente, L., et al., *Clinical and biologic effects of anti–interleukin-10 monoclonal antibody administration in systemic lupus erythematosus.* Arthritis & Rheumatology, 2000. **43**(8): p. 1790-1800.
351. Marakalala, M.J., et al., *Inflammatory signaling in human tuberculosis granulomas is spatially organized.* Nature medicine, 2016. **22**(5): p. 531.
352. Ribas, A. and J.D. Wolchok, *Cancer immunotherapy using checkpoint blockade.* Science, 2018. **359**(6382): p. 1350-1355.
353. Ascierto, P.A., et al., *Initial efficacy of anti-lymphocyte activation gene-3 (anti–LAG-3; BMS-986016) in combination with nivolumab (nivo) in pts with melanoma (MEL) previously treated with anti–PD-1/PD-L1 therapy*. 2017, American Society of Clinical Oncology.